The sHsp expression signature in the brain and modulation in models of chronic neurodegeneration

by

Shmma Quraishe BSc (Hons)

A thesis presented for the degree of
Doctor of Philosophy
of the
University of Southampton
in the
Faculty of Medicine, Health and Life Sciences
School of Biological Sciences

April 2010

UNIVERSITY OF SOUTHAMPTON
ABSTRACT
FACULTY OF MEDICINE, HEALTH AND LIFE SCIENCES
SCHOOL OF BIOLOGICAL SCIENCES
<u>Doctor of Philosophy</u>
The sHsp expression signature in the mouse brain and modulation in models of chronic neurodegeneration

Intrinsic protein folding pathways are modulated by molecular chaperones, such as the diverse group of heat shock proteins (Hsps). Among these is the small heat shock protein (sHsp) family which in the mammalian genome consists of 10 low molecular weight (15-30kDa) members. The sHsps have classical chaperone functions but additionally contribute to pathways that protect against cellular stresses, maintain the cytoskeleton, prevent protein aggregation and regulate apoptosis. They contain a characteristic C-terminal α-crystallin domain, which is exclusive to the sHsp family. In addition to their constitutive expression under physiological (non-disease) conditions, they are also induced under conditions of stress/heat shock which is thought to play a role in response to protein misfolding that underpins disease. There are a wide range of diseases in which the sHsps function or are dysfunctional by mutations, such as neurodegenerative disorders, cataract, and desmin related myopathy.

  Each of the 10 sHsps is believed to have a unique expression profile. Seven of the sHsps are expressed in heart and muscle, but little is known about their precise expression and/or physiological role in the CNS. In the present study the expression of the mammalian sHsps in various mouse tissues including the brain was investigated. This provided evidence for the constitutive expression of 4 sHsps in the brain. *In situ* hybridization using naïve adult mice revealed a distinct white matter (oligodendrocyte) specific expression pattern for HspB5 (αB-crystallin). HspB1 (Hsp25) and HspB8 (Hsp22) demonstrated overlapping expression in the lateral and dorsal ventricles of the brain, as well as expression in a distinct set of motor neurons in the ventral horn of the spinal cord. Further, cellular immunostaining and sub-fractionation of brain tissue supports a distinct cellular and subcellular protein expression of HspB1, HspB5, HspB6 (Hsp20) and HspB8 in the brain. Both HspB5 and HspB6 were enriched in the myelin fraction. In view of the potential for induction of these sHsps by stress and modulation in chronic brain diseases we systematically investigated the sHsp signature in two distinct models of intracellular (R6/2) and extracellular (ME7) proteinopathies. These models recapitulate key features of Huntington's and prion disease, respectively.

  Analysis of the sHsps in the R6/2 Huntington's disease (HD) mouse model showed a specific down-regulation of HspB5 in the white matter at all time points analyzed. All other sHsps investigated did not change in this model of HD. Analysis of the sHsps in ME7 prion disease showed up-regulation of HspB1, HspB5 and HspB8 in the hippocampus. For HspB1, this was selective to an anatomically defined sub-population of astrocytes distributed in the stratum radiatum. In contrast, all GFAP positive astrocytes throughout the hippocampus exhibited induced expression of HspB5 and HspB8. Based on QT-PCR data, the changes in expression of the sHsps in either model was not under transcriptional control, suggesting translation/post-translational regulation. The differing results in the two models suggest that the presence of intracellular (R6/2) or extracellular (ME7) aggregates may dictate the sHsp response associated with non-neuronal cells. In view of the emerging significance of non-neuronal cells in chronic diseases the data supports adaptive and differential responses that might contribute to and/or provide a route to therapy of distinct aspects of neurodegeneration.

Contents

List of Figures

List of Tables

Declaration of Authorship

I, Shmma Quraishe declare that the thesis entitled "The sHsp expression signature in the brain and modulation in models of chronic neurodegeneration" and the work presented in the thesis are both my own, and have been generated by me as the result of my own original research. I confirm that:

this work was done wholly or mainly while in candidature for a research degree at this University;

where any part of this thesis has previously been submitted for a degree or any other qualification at this University or any other institution, this has been clearly stated;

where I have consulted the published work of others, this is always clearly attributed;

where I have quoted from the work of others, the source is always given. With the exception of such quotations, this thesis is entirely my own work;

I have acknowledged all main sources of help;

where the thesis is based on work done by myself jointly with others, I have made clear exactly what was done by others and what I have contributed myself;

parts of this work have been published as: (Quraishe et al., 2008)

Signed: …S.Quraishe......…………………………………………………..

Date:…....14th June 2010..…....………………………………………….

Acknowledgments

Abbreviations

ABC	avidin biotin complex
AC	associative commisure
AD	Alzheimer's disease
ALS	Amyotrophic lateral sclerosis
Alv	alveus of the hippocampus
APC	antigen presenting cell
APP	amyloid precursor protein
ATP	adenosine-5'-triphosphate
AxD	Alexander's disease
Aβ	amyloid beta
BLAST	basic local alignment search tool
BSA	bovine serum albumin
BSE	bovine spongiform encephalopathies
Caspr	contactin associated protein
CBP	CREB binding protein
cc	corpus callosum
CC	congenital cataract
cDNA	complementary DNA
CER	cerebellum
cg	cingulate gyrus
CHIP	C-terminus of Hsp70 interacting protein
CI	cerebral infarct
CJD	Creutzfeldt-Jakob disease
CM	cardiomyopathy
CMA	chaperone mediated autophagy
CMT	Charcot-Marie-Tooth disease
CNP	2'-3'-cyclic nucleotide 3'phosphodiesterase
CNS	central nervous system
cpm	count per minute
CRE	cyclic AMP response element
CREB	cyclic AMP response element binding protein
csf	cerebrospinal fluid
Ct	cycle threshold
Cu	copper
d3v	dorsal ventricle
DAB	diaminibenzidine
DAPI	4',6-diamidino-2-phenylindole
DG	dentate gyrus
DHMN	distal hereditary motor neuropathy
DEPC	diethylpyrocarbonate
DIG	dioxigenin
DMEM	Dulbecco's Modified Eagles Medium
DML	dementia with lewy bodies
DMPK	myotonic dystrophy protein kinase

DNA	deoxyribonucleic acid
Dox	doxorubicin
DPX	Dibutyl phthalate - Xylene
DRG	dorsal root ganglia
DRM	desmin related myopathy
DTI	diffuse tensor imaging
E.coli	*Escherichia Coli*
EAE	experimental autoimmune encephalomyelitis
ec	external capsule
ECL	enhanced chemiluminescence
EDTA	Ethylene-diamine-tetra-acetic acid
ER	endoplasmic reticulum
ERK	extracellular related kinase
FBS	fetal bovine serum
FC	frontal cortex
FGF	fibroblast frowth factor
fi	fimbria
fmi	forceps minor of the corpus callosum
fmj	forceps major of the corpus callosum
FTDP	frontotemporal dementia with parkinsonism
GABA	gamma-aminobutyric acid
GAPDH	glyceraldehyde 3-phosphate dehydrogenase
GFAP	glial fibrillary acidic protein
GFP	green fluorescent protein
GR	glucocorticoid receptor
GrDG	granular layer of DG
GSH	glutathione
HAP	huntingtin associated protein
HD	Huntington's disease
HGNC	HUGO Gene Nomenclature Committee
HRP	horse radish peroxidase
Hsps	heat shock proteins
Htt	huntingtin
httEx1	huntingtin exon 1
HUGO	Human genome organisation
i.p.	intraperitoneal
i.v.	intravenous
IB	inclusion body
ic	internal capsule
IHGSC	International human Genome Sequencing Consortium
IL	interleukin
InsP3R	inositol (1,4,5)-tri-phosphate receptor
JNK	c-Jun N-terminal kinase
LAMP	lysosomal associated membrane protein
LBs	lewy bodies
LFB	luxol fast blue

LMol	stratum lacunosum moleculare
lv	lateral ventricle
MAG	myelin associated protein
MAL	myelin and lymphocyte protein
MAP	microtubule associated protein
MAPKAP	mitogen associated protein kinase associated protein
MBP	myelin basic protein
MCAO	middle cerebral artery occlusion
MDL	major dense line
MF	mossy fibers
MJD	Machado-Joseph disease
MKBP	myotonic dystrophy kinase binding protein
MM	myofibrillar myopathy
Mn	manganese
MOBP	myelin associated oligodendrocyte binding protein
MoDG	molecular layer of DG
MOG	myelin oligodendrocyte glycoprotein
MRI	magnetic resonance imaging
mRNA	messenger ribonucleic acid
MS	Multiple sclerosis
MSN	medium spiny neuron
mtHtt	mutant huntingtin
mTOR	mammalian target for rampamycin
NAWM	normal appearing white matter
NBH	normal brain homogenate
NCBI	National Centre for Biotechnology Information
NF	neurofilament
NF155	neurofascin 155
NF-kB	nuclear factor kB
NFTs	neurofibrillary tangles
NMDA	N-methyl-D-aspartate
NMDAR	N-methyl-D-aspartate receptor
NOS	nitric oxide synthase
NP-40	Tergitol-type NP-40
OPC	oligodendrocyte precursor cell
OSP	oligodendrocyte specific protein
PFA	paraformaldehyde
PBS	phosphate buffered saline
PCR	polymerase chain reaction
PD	Parkinson's disease
pi	post injection/inoculation
PI3K	phosphotidyl inositol 3-kinase
PK	protein kinase
PLP	proteolipid protein
PMP22	peripheral myelin protein 22
PNS	peripheral nervous system

PoDG	polymorphic layer of DG
polyQ	polyglutamine
PrP^c	normal cellular prion
PrP^{sc}	scrapie prion
PSD	post-synaptic density
PV	paraventricular thalamic nucleus
QT-PCR	quantitative PCR
RF	Rosenthal fibers
RNA	ribonucleic acid
RNA	ribonucleic acid
ROS	reactive oxygen species
RT	reverse transcription
RTS	RNA transport signal
Sb	subiculum
SC	Schaffer collaterals
SCA	spinocerebellar ataxia
SDS	sodium dodecyl sulphate
SDS-PAGE	SDS polyacrylamide gel electrophoresis
SEM	standard error mean
SGT	small glutamine-rich tetricopeptide repeat domain protein
sHsps	small heat shock proteins
SOD	superoxide dismutase
SOr	stratum oriens
SPs	senile plaques
Spy	stratum pyramidale
SRad	stratum radiatum
St	stria terminalis
STR	striatum
Sub	submedius thalamic nucleus
TAE	tris acetate EDTA
TBS	trizma buffered saline
TEA/AA	Triethanolamine /acetic anhydride
TEMED	N,N,N',N'-tetramethyl-ethylenediamine
Tg	transgenic
TGFβ	transforming growth factor β
TNF	tumour necrosis factor
TPR	tetratricopeptide repeat
TRAIL	TNF-related apoptosis inducing ligand
TSE	transmissible spongiform encephalopathies
Ub	ubiquitin
UPP	ubiquitin proteasome pathway
UTR	untranslated region
Wt	wild type
YAC	yeast artificial chromosome
Zn	zinc

Amino acids

A	Alanine	Ala
C	Cysteine	Cys
D	Aspartate	Asp
E	Glutamate	Glu
F	Phenylalanine	Phe
G	Glycine	Gly
H	Histidine	His
I	Isoleucine	Ile
K	Lysine	Lys
L	Leucine	Leu
M	Methionine	Met
N	Asparagine	Asn
P	Proline	Pro
Q	Glutamine	Gln
R	Arginine	Arg
S	Serine	Ser
T	Threonine	Thr
V	Valine	Val
W	Tryptophan	Trp
Y	Tyrosine	Tyr

Nucleotide bases

A	Adenosine
C	Cytosine
G	Guanine
T	Thymine
U	Uracil

Chapter 1 – Introduction

The functions of proteins rely upon their characteristic native three-dimensional structure (Morange, 2006). The native structure is the most thermodynamically stable state and is adopted via a number of distinct intermediate states (Pande and Rokhsar, 1999). These intermediates transiently expose hydrophobic regions on their surface that have the potential to form inappropriate interactions with themselves or other cellular components leading to protein aggregation (Mogk et al., 2002). Native proteins undergoing conformational changes and proteins that have become unfolded have the potential to form protein aggregates due to exposed hydrophobic surfaces. This potential is further heightened by the high concentrations of macromolecules and proteins that are present in cells (Minton, 1983). However, this is normally regulated and kept under control by molecular chaperones that have evolved to assist proteins to fold efficiently by shielding exposed hydrophobic surfaces and promote refolding of the substrate protein (Ellis, 2001). The many states that a protein can encompass have been exploited by the cell for selective targeting of proteins to relevant cellular compartments (Radford and Dobson, 1999). For example, unfolded and partially folded protein states are known to be important for translocation across membranes, trafficking of proteins and in targeting proteins that are no longer needed, for destruction (Dunker and Obradovic, 2001). In addition to the protein folding machinery involving molecular chaperones, other sophisticated mechanisms of protein quality control exist to monitor whether proteins are correctly folded, and to target them for destruction if they are not. For example, the unfolded protein response (UPR) has evolved to encounter the stresses associated with the endoplasmic reticulum (ER) as a result of misfolded proteins. Folding processes in the ER are assisted by molecular chaperones such as Bip/Grp78. Bip is directly involved in the UPR response as it binds to the ER stress sensors, however when unfolded protein concentrations rise, it preferentially binds unfolded proteins, thus freeing the stress sensors and triggering a cascade of events to either slow protein synthesis, increase chaperone content or increase protein degradation (Sitia and Braakman, 2003, Boot-Handford and Briggs, 2010). The ubiquitin/proteasome degradation system is a complex system involving the ubiquitination of proteins selected for removal, followed by their degradation to peptides in the cytosol by the proteasome (Goldberg, 2003). This process not only regulates the amount of intracellular proteins, but is also involved in their quality control.

Although all the above mentioned mechanisms are in place to prevent protein aggregation, it is inevitable that mistakes can be made leading to the formation and deposition of abnormal protein aggregates and disease. Increasingly a large number of diseases are associated with a misfolding stress. For example, in neurodegenerative diseases such as Alzheimer's disease (AD), normally soluble amyloid β-peptides (Aβ) accumulate in the extracellular compartment as insoluble deposits rich in β-structure (Selkoe, 2003).

Interestingly the ability to form aggregates is not a unique feature of proteins associated with disease but is thought to be a general property of all polypeptide chains (Dobson, 2001). For example, myoglobin, a compact and highly soluble protein with most of its sequence arranged in α-helices is able to form fibrillar structures under conditions that substantially destabilize its native fold (Fandrich et al., 2001). Additionally two normally harmless protein domains, the SH3 domain from bovine phosphatidyl-inositol-3-kinase (PI3-SH3) and the N-terminal ('acylphosphatase-like') domain of the *Escherichia coli* (*E.coli*) HypF protein (HypF-N) are also able to form fibrillar aggregates *in vitro* under appropriate conditions (Guijarro et al., 1998, Chiti et al., 2001).

The key features involved in protein homeostasis as described above include protein folding by molecular chaperones, protein folding in the endoplasmic reticulum pathway and protein degradation pathways. For the purposes of this thesis, molecular chaperones will be discussed more extensively below, followed by a brief description of protein degradation pathways.

1.1.   Molecular Chaperones

Molecular chaperones, including the heat shock proteins (Hsps), are able to bind specifically and non-covalently to interactive protein surfaces that are transiently exposed during cellular processes (Thulasiraman et al., 1999). The controlled binding and release of substrate proteins facilitates the correct fate of the protein in the cell, whether this be correct folding, assembly into oligomers, transport to a specific subcellular compartment, membrane translocation, or even degradation (Saibil, 2000). Molecular chaperones protect the cell against a variety of stresses by preventing abnormal protein aggregation and by keeping proteins in a state competent for either refolding or degradation (Bryantsev et al.,

2007). Some chaperones interact with a variety of polypeptide chains, whereas others act on specific targets via substrate specific binding domains. For example the 70-kDa Hsps recognise hydrophobic protein surfaces or amino acid residues that are generally exposed by non-native proteins and newly synthesized polypeptide chains (Rudiger et al., 1997). An example of the specificity of some molecular chaperones can be illustrated by the ClpX/Hsp100 family. Proteins of this family form ring-like subunit architectures and are able to disassemble multimeric or aggregated forms of certain proteins in an ATP dependent fashion (Schirmer et al., 1996). Two members of this family, (ClpX and ClpA) recognize specific C-terminal sequences on target proteins. This property has been extensively characterized for the interaction between *E.coli* ClpX and the transposase of phage Mu (MuA protein) (Levchenko et al., 1997).

Molecular chaperones were originally termed heat shock proteins (Hsps) due to their initial discovery in *Drosophila melanogaster* cells exposed to elevated temperatures. However, the Hsps are also known to be induced by a wide variety of environmental or metabolic stresses including anoxia, ischemia and viral agents (Whitley et al., 1999, Haak and Kregel, 2008). Hsps can be divided into ATP dependent and ATP independent families as well as being subdivided into families according to molecular weight. The ATP dependent molecular chaperones require ATP hydrolysis to facilitate the folding process (Saibil, 2000). Each of the distinct Hsp (molecular chaperone) families will be described below.

1.1.1. Hsps (molecular chaperone) families

The name of each chaperone family (Table 1.1) is derived from the molecular weight of the main representative protein (Lindquist, 1986, Sghaier et al., 2004). Additionally the nomenclature is based on the systematic gene symbols that have been assigned by the HUGO Gene Nomenclature Committee (HGNC) (Wheeler et al., 2008).

Chaperone family	Structure	ATP	Examples prokaryote	Examples eukaryote	Co-chaperone	Function
Hsp100	6–7-mer	+	ClpB			disaggregation together with Hsp70
			ClpA			proteolysis together with the ClpP protease
				Hsp104		thermotolerance disaggregation together with Hsp70
Hsp90	dimer	+	HtpG			tolerance to extreme heat shock
				Hsp90	Hop, p23, CDC37	stress tolerance control of folding and activity of steroid hormone receptors, protein kinases, etc.
Hsp70	monomer	+	DnaK		DnaJ, GrpE	de novo protein folding prevention of aggregation of heat-denatured proteins solubilization of protein aggregates together with ClpB regulation of the heat shock response
				Hsp70, Hsc70	Hsp40, Bag1, Hip, Chip, Hop, HspBP1	de novo protein folding prevention of aggregation of heat-denatured proteins solubilization of protein aggregates together with Hsp104 regulation of the heat shock response regulation of the activity of folded regulatory proteins (such as transcription factors and kinases)
Hsp60	14-mer, 16-mer	+	GroEL		GroES	de novo protein folding prevention of aggregation of heat-denatured proteins
				CCT/TRiC	prefoldin	de novo folding of actin and tublin
sHsp	8–24-mer		IbpA, IbpB			prevention of aggregation of heat-denatured proteins binding to inclusion bodies
				Hsp25 (crystalline)		prevention of aggregation of heat-denatured proteins component of the lens of the vertebrate eye

Table 1.1. Structure and function of the Hsp families. Only the major Hsp chaperone families are described. Examples of prokaryotic and eukaryotic members are given with brief functional descriptions (Mogk et al., 2002).

Hsp100 (Clp family in *E. coli*). The human genome encodes four Hsp100 genes (Kampinga et al., 2009) which encode a family of proteins with high homology to the Hsp70 family (described below). The primary distinction arises from the existence of a long linker domain between the N-terminal ATPase domain and the C-terminal peptide binding domain (Shaner et al., 2006). This family of Hsps targets and unfolds proteins tagged for degradation and misfolded proteins. Although this family of Hsps is able to function independently, co-operation with the Hsp70 family forms an efficient system to reverse protein aggregation and promote folding (Mogk et al., 2008). Some of the Hsp100 chaperones are associated with peptidases (e.g. ClpP) via a conserved P-element (Neuwald et al., 1999). Protein substrates containing specific degradation tags are unfolded and threaded through the axial channel of the hexameric complex in an ATP dependent

process. The substrate is then threaded into the proteolytic chamber of the peptidase for degradation (Wang et al., 2001). Hsp110 is ubiquitously expressed and is abundant in the brain with the exception of the cerebellum (Hylander et al., 2000).

Hsp90 (HtpG in *E. coli*). The Hsp90 family consisting of 5 members are also ubiquitously expressed, ATP dependent molecular chaperones (Chen et al., 2005, Kampinga et al., 2009), with a molecular weight of approximately 90 kDa. Hsp90 is one of the most abundant proteins in eukaryotic cells accounting for 1-2% of all cellular proteins (Csermely et al., 1998). Isoforms of Hsp90 are found in the cytosol (Hsp90-α, inducible and Hsp90-β, constitutive), endoplasmic reticulum (ER) (Grp48) and mitochondria (TRAP) (Csermely et al., 1998, Krishna and Gloor, 2001). This family of chaperones is involved in signal transduction, protein folding, protein degradation and they are necessary for viability. Hsp90 binds, stabilizes and regulates steroid hormone receptor function and protein kinases and is therefore essential in cellular signal transduction networks (Young et al., 2001). In addition to these roles Hsp90 is thought to play an important role in evolutionary capacitance (Bergman and Siegal, 2003). Stressful events leading to developmental remodelling by Hsp90 could allow variations in several processes to occur, leading to productive changes in multiple systems (Rutherford et al., 2007).

Hsp70 (BiP, DnaK in *E. coli*). 13 members of the Hsp70 chaperone family are encoded by the human genome (Kampinga et al., 2009). Key members of this family include inducible Hsp70, constitutively expressed cognate Hsc70, the ER-localised Grp78 (Bip) and mitochondrial MtHsp75. Hsp70 proteins interact with Hsp40 proteins (DnaJ in *E. coli*) to increase their chaperone activity by increasing the ATP consumption rate. The Hsp70 family recognizes short hydrophobic sequences which become exposed in misfolded proteins and proteins emerging from the ribosome. They are also involved in membrane translocation and regulation of the heat shock response (Saibil, 2000).

Hsp60 (GroEL/GroES complex in *E. coli*) can be found in a large (~ 1 MDa) chaperone complex that forms a barrel-shaped structure. GroES which acts as a protein cap binds to GroEL in the presence of ATP confining the enclosed substrate protein in the barrel, thus

allowing the protein to fold in a favourable environment. Members of the Hsp60 family are located in both the cytoplasm and the mitochondria where they are involved in protein folding and assembly after synthesis (Horwich et al., 2007).

Hsp40 (DNAJ). The Hsp40 family are co-chaperone proteins that regulate complex formation between Hsp70 and substrate proteins by driving the conversion of ATP to ADP (Fewell et al., 2004). The Hsp40 family is probably the largest Hsp family in humans and is identified by the conserved J-domain which regulates Hsp70 ATPase activity (Kampinga et al., 2009). The Hsp40 family can be divided into 3 different subtypes. Type I and type II proteins function as ATP-dependent chaperones that bind non-native polypeptides and protect cells from stress by preventing protein aggregation. Type III proteins do not appear to be general chaperones and have evolved to contain polypeptide-binding domains that recognize specific substrates (Fan et al., 2004).

Small heat shock proteins (sHsps) are low molecular weight chaperone proteins (Taylor and Benjamin, 2005). They form large dynamic oligomeric structures and are able to bind several non-native proteins per oligomeric complex (Haslbeck et al., 2008). They have been suggested to be involved in the inhibition of apoptosis, organization of the cytoskeleton and also in preventing protein aggregation (Haslbeck, 2002, Sun and MacRae, 2005b). In contrast to other Hsp families, the sHsps do not require ATP for their chaperone function (Jakob et al., 1993, Ganea, 2001). The tissue specific expression, general characteristics and properties of the sHsps will be discussed in section 1.3 and in detail in Chapter 3.

1.2. Protein degradation

In addition to protein folding processes, protein degradation is important in regulating protein quality control and turnover. This highly regulated process involves two major pathways; the ubiquitin-proteasome pathway (UPP) and the autophagic-lysosomal pathway.

1.2.1. The ubiquitin-proteasome pathway

The eukaryotic proteasome consists of the 20S catalytic core proteasome. This can be bound by different regulators such as the 11S and 19S subunits. These can modify the activity and selectivity of the degradation process (Volker and Lupas, 2002). The 20S core proteasomal particle is an enzymatic hollow barrel made up of 4 stacked rings. Each ring consists of 7 subunits with the outer rings being composed of homologous alpha subunits and the inner rings of beta subunits. Catalytic activity resides in 3 of the beta subunits in each ring, giving 6 catalytically active sites in the core of the proteasomal structure (Zwickl et al., 2001). Binding of the 11S and 19S subunits to the 20S core proteasome leads to differing proteasomal protease activity, substrate specificity and degradation. For example the 26S proteasome, consisting of the core with a 19S regulatory subunit on each side, is mainly responsible for the recognition and degradation of poly-ubiquitinated proteins (Glickman and Maytal, 2002). However, addition of two 11S regulatory subunits on each side leads to increased peptidase activity and generation of small peptide products for antigen presentation by the MHC-I complex (Hill et al., 2002).

Proteins targeted for degradation by the proteasome via the addition of ubiquitin (ub) typically involves three enzymes: E1 (ub activating enzyme) which hydrolyses ATP and forms a thioester bond with ub; E2 (ub- conjugating enzyme) removes ub from E1 and forms a similar thioester bond with it; and E3 (ub ligase) binds both the substrate protein and E2/ub complex and transfers the ub molecule to the substrate protein (Figure 1.1). Chains of four or more ub molecules form the recognition signal for targeting/shuttling to the proteasome (Korhonen and Lindholm, 2004).

Figure 1.1. The ubiquitin-proteasome system. Proteins targeted for proteasomal degradation are covalently modified with ub. Typically, three enzymes are involved in this process; E1 (ub-activating), E2 (ub-conjugating) and E3 (ub-ligase) enzymes. Proteins tagged with four or more ub molecules are shuttled to the proteasome where they are reduced to peptides. Peptides are further broken down by peptidases in the cytosol (Burger and Seth, 2004).

1.2.2.   The autophagic-lysosomal pathway

Proteins and protein aggregates that are not targeted to the proteasome or are poor substrates for proteasomal processing can be processed by autophagy (Rubinsztein, 2006). Three pathways exist that can target proteins for lysosomal degradation (Figure 1.2). In microautophagy, small areas of the cytosol are engulfed via lysosomal invaginations, and proteins are degraded in the lumen of this organelle. During macroautophagy the cytoplasm is sequestered into double membrane vesicles or autophagosomes. Autophagosomes fuse with lysosomes and the vacuolar contents are enzymatically degraded by acidic lysosomal hydrolases (Yorimitsu and Klionsky, 2005). The third pathway for cytosolic protein clearance is chaperone mediated autophagy (CMA). This pathway does not require any vesicular trafficking (Majeski and Dice, 2004), but involves the recognition of a pentapeptide motif (KFERQ) by the cognate molecular chaperone Hsc70, which then translocates the protein across the lysosomal membrane through

binding with the receptor lysosome-associated membrane protein 2A (LAMP-2A) (Zhou et al., 2005). The translocated protein can then be degraded in the lumen of the lysosome.
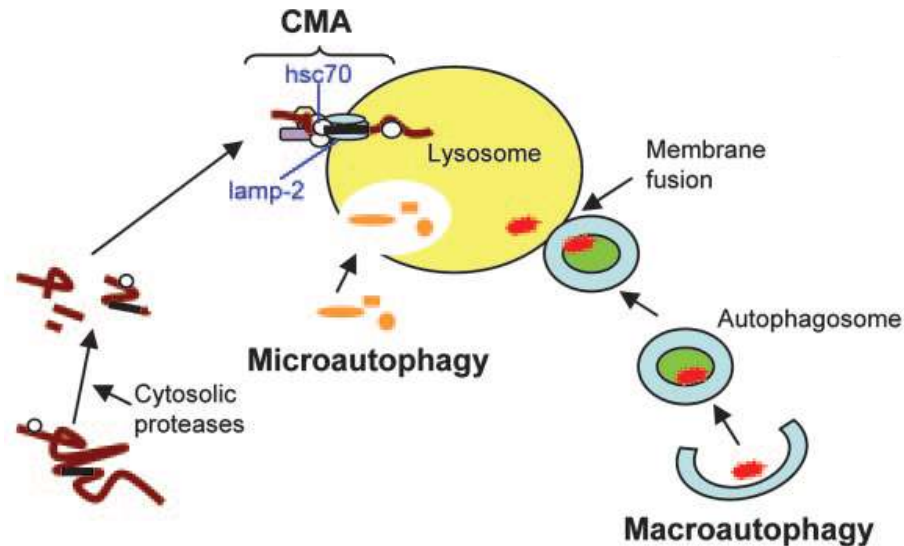
Figure 1.2. Multiple pathways of protein degradation in lysosomes. In microautophagy, portions of the cytosol are continuously internalized via lysosomal invaginations. In macroautophagy, the cytoplasm is sequestered into double-membrane structures, known as autophagosomes, which fuse with lysosomes. In CMA, specific cytosolic proteins are transported into lysosomes via a molecular chaperone receptor complex composed of Hsp70 and LAMP-2 (Crotzer and Blum, 2005).

Previously it was thought that protein folding by molecular chaperones and protein degradation pathways were distinct and opposing processes, but it has been suggested that molecular chaperones cooperate directly with the UPP and the autophagic pathways (Esser et al., 2004). An example of cooperation with the UPP is given by the co-chaperone CHIP (C-terminus of Hsp70-Interacting protein), which facilitates poly-ubiquitination of target proteins and shuttles misfolded proteins from Hsp70 to the UPP. CHIP inhibits Hsp70 refolding activity through tetratricopeptide repeat (TPR) domains at its N-terminal, and facilitates ubiquitination of the substrate protein through its ubiquitin-ligase (U-box) domain (Kabashi and Durham, 2006). An example of the involvement of molecular chaperones in autophagy can be illustrated by HspB8. It has recently been shown to associate with Bag3, a stimulator of autophagy. The ability of HspB8 to prevent the

accumulation of aggregation prone proteins (huntingtin containing 43 glutamines) was found to be dependent on its interaction with Bag3 (Carra et al., 2008).

1.3.   The small Heat Shock Protein (sHsp) family

1.3.1. Structures of the sHsps

  sHsps represent a diverse family of proteins that are grouped together based on their structural homology and low molecular weight. The homology and number of sHsps in different species varies considerably, with up to 19 in Arabidopsis thaliana and 10 in mammals (Kappe et al., 2003, Waters and Rioflorido, 2007). They share significant sequence similarity within the approximately 90 residue C-terminal α-crystallin domain, which is the characteristic region of these sHsps (Figure 1.3). They have a more variable N-terminal region and a short and variable C-terminal tail.

  The sHsps form high oligomeric, globular structures. However the number of subunits and flexibility of the complex varies in different species. For three members the structure of the oligomeric complexes have been solved (Figure 1.4). HspB5 oligomers are structurally variable due to the continuous exchange of subunits (Haley et al., 1998). However, the quaternary structure of Hsp16.5 from *Methanococcus jannaschii*, a hyperthermophilic organism, is well defined. The building block is a dimer interacting via β-sheets in each monomer. The oligomer forms a hollow barrel of 24 monomers (Kim et al., 1998). The wheat Hsp16.9 assembles into a dodecameric double disk.   The structures that have been solved so far support the idea that the dimer is the smallest exchangeable unit and the building block of large oligomeric complexes (Haslbeck and Buchner, 2002).
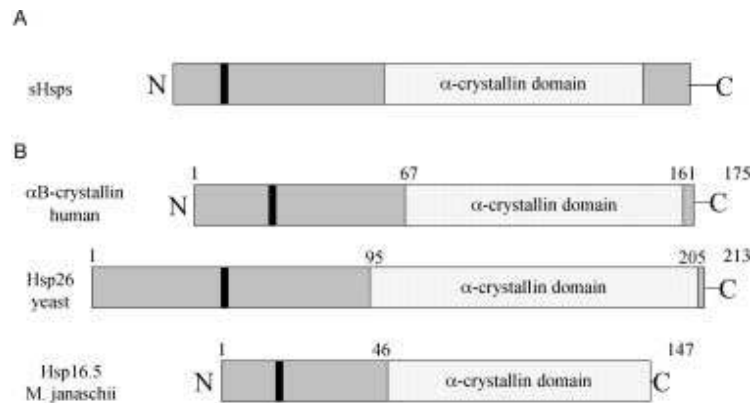
Figure 1.3. Schematic showing the domain structure of different sHsps.
The N-terminal is of variable length and is not conserved throughout the sHsp family. The α-crystallin domain folds into an anti-parallel β-sheet sandwich (conserved region in sHsps). The C-terminal is variable in length and is moderately conserved.
(A) General domain structure. (B) Comparison of different sHsps. Black regions indicate Phe-Pro rich regions (Haslbeck, 2002).
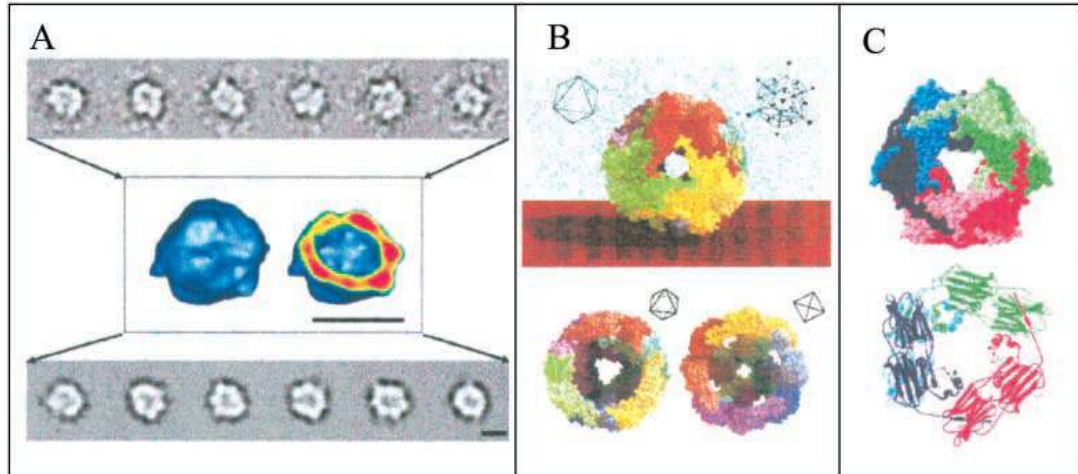
Figure 1.4. Three dimensional structures of the sHsps. (A) Cryoelectron microscopy structure of α-crystallin shows a 32mer with an outer diameter of 18nm (Haley et al., 1998). (B) Crystal structure of Hsp16.5 from *Methanococcus jannaschii* shows a 24mer with an outer diameter of 12nm (Kim et al., 1998). (C) Crystal structure of wheat Hsp16.9 shows a dodecamer, arranged as 2 disks (Van Montfort et al., 2001)(Van Montford et al., 2001).

Mammalian sHsps are found as homo- or heteromeric complexes, consisting of 2-40 subunits (Bova et al., 2000, Sugiyama et al., 2000). The α-crystallin domain consists of two layers of three and five anti-parallel strands, respectively, connected by a short inter-domain loop, forming the β-sheet (Haslbeck et al., 2005). The α-crystallin domains of 2 monomers interact tightly to form the dimeric building block of the sHsp oligomers. The N-terminal region contains α-helical components and is variable in structure (Kappe et al., 2003). The N-terminal of many of the sHsps contains a small prolinephenylalanine-rich region with one or two WD/EPF motifs. This region seems to be important in oligomeric complex formation and also for chaperone activity (Kim et al., 1998, Theriault et al., 2004, Stamler et al., 2005). The C-terminal tail is highly motile and flexible, and is also involved in stabilizing the oligomeric structure through contacts between a conserved motif in the C-terminal region and a hydrophobic patch in the α-crystallin domain of a neighbouring subunit (Haslbeck et al., 2005). The structure of the sHsps is important for its functional role as will be described below.

1.3.2. Functions of the sHsps

The sHsps prevent stress induced irreversible aggregation of unfolded and damaged proteins (Van Montfort et al., 2001). Expression of most sHsps is developmentally regulated, and increases in response to heat stress (Basha et al., 2004), oxidative stress (Volkov et al., 2006), ischemia (Golenhofen et al., 2004) and environmental stresses (Siddique et al., 2008). Cytoskeletal rearrangement, redox homeostasis, inflammation and apoptosis are amongst the cellular processes in which the sHsps are involved, as will be described below (Kappe et al., 2003, Verschuure et al., 2003, van Noort, 2008). These processes are also modulated in disease conditions therefore the potential modulation of these processes by the sHsps during disease will be discussed in section 1.6.3.

sHsps associate with non-native substrate proteins to form stable sHsp-substrate complexes (Basha et al., 2006). This allows efficient prevention of irreversible substrate aggregation. Release of active substrate proteins from these complexes occurs spontaneously or requires cooperation with proteins from ATP-dependent chaperone families such as Hsp70-Hsp40 and Hsp100. Although Hsp70-Hsp40 can act directly on

protein aggregates, the presence of sHsps increases the efficiency of the process (Cashikar et al., 2005).

As described above the sHsps normally exist as large oligomers, which change dynamic properties (shape and size) on exposure to stress and/or a substrate (Haslbeck et al., 2005). The exact mechanism involved in binding of misfolded proteins is unclear, however three modes of action have been proposed for the sHsps: (1) substrates are directly bound by the large chaperone oligomer (Kim et al., 2003), (2) the oligomer dissociates into smaller subunits exposing hydrophobic surfaces which can bind unfolded substrates. Then large soluble complexes are formed which are processed by the ATP-dependent refolding machinery (Haslbeck et al., 1999, Van Montfort et al., 2001), or (3) sHsp molecules combine with insoluble protein aggregates, which allows disaggregation and refolding by the ATP-dependent refolding machinery (Stamler et al., 2005, Cashikar et al., 2005).

The function of the sHsps is intricately linked to their phosphorylation states. They can be reversibly phosphorylated at several serine residues by a multitude of kinases. Phosphorylation results in a change in the oligomerisation status of several sHsps (Bukach et al., 2009). For example, phosphorylation of HspB1 reduces the large HspB1 oligomeric complexes to much smaller oligomers and additionally shifts chaperone function to actin stabilization (Figure 1.5) (Arrigo et al., 2007).
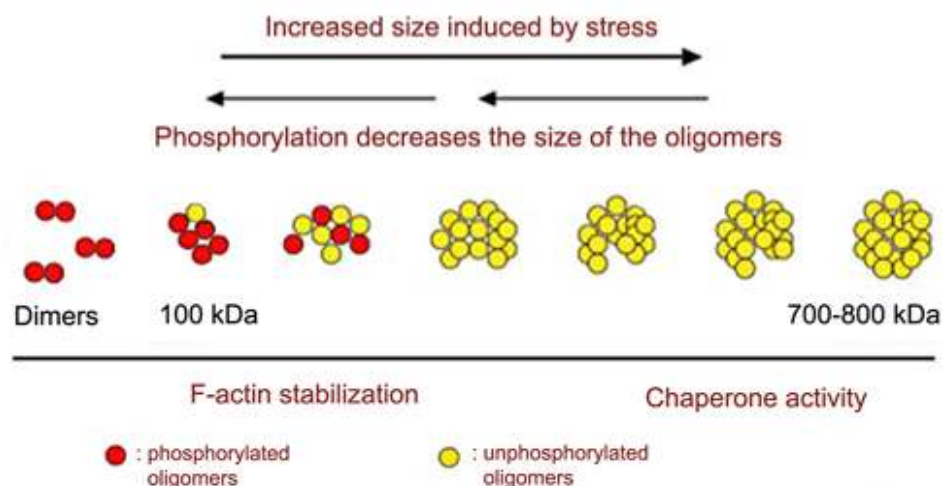
Figure 1.5. Biochemical properties of the sHsps. Large sHsp oligomeric structures are favoured under conditions of stress and associate with unfolded proteins. Phosphorylation decreases the size of the oligomers. Large non-phosphorylated oligomers of sHsp (>300 kDa) can protect cells through their chaperone activity (Rogalla et al., 1999) and small oligomers may act at the level of F-actin polymerization/depolymerization (Benndorf et al., 1994).

HspB1 is able to cap the barbed end of the actin filament in its monomeric and/or non-phosphorylated form, preventing the addition of monomers and subsequent filament growth (Williams et al., 2005). The degree of phosphorylation and the structural organization of the sHsps dictate the modulatory activity on actin polymerization/ stabilisation.

1.3.3. The mammalian sHsp family.

The mammalian sHsp family comprises of 10 members, HspB1-HspB10 (Table 1.2) which have varying expression patterns with some being ubiquitously expressed and others specific to certain tissues such as the lens and testis (Verschuure et al., 2003, de Wit et al., 2004). Heart and muscle are the two tissues in which up to seven sHsps are expressed at the same time and at relatively high levels (Verschuure et al., 2003). The general and selective expression may reflect the particular needs of certain tissues and the potential, selective use of their activities in protection against physiological stress particularly associated with a cell type. Each member of the mammalian sHsp family will be described below. For clarity, physiological stress encompasses the normal homeostatic mechanisms which are able to buffer changes for example in levels of misfolded proteins and oxidative stress as a result of normal cellular functions. However pathological stress refers to an abnormal acute and/or chronic stress conditions such as the presence of misfolded protein above and beyond the normal cellular buffering capacity eventually leading to cellular dysfunction.

Formal name	Alternative name	Distribution
HspB1	Hsp27/Hsp25	Ubiquitous (a)
HspB2	MKBP	Cardiac and Skeletal muscle (b)
HspB3	-	Cardiac and Skeletal muscle (c)
HspB4	αA-crystallin	Lens (d)
HspB5	αB-crystallin	Ubiquitous (a)
HspB6	Hsp20	Ubiquitous (b)
HspB7	cvHsp	Cardiac and Skeletal muscle (e)
HspB8	Hsp22/H11	Ubiquitous (b)
HspB9	-	Testis (b)
HspB10	ODF1	Testis (f)

Table 1.2. sHsps nomenclature and distribution. Currently accepted nomenclature, alternative names and tissue distribution are described. Highlighted names are the preferred use in this thesis. HspB1, HspB5, HspB6 and HspB8 are ubiquitously expressed whereas HspB4, HspB9 and HspB10 show selective expression. (a) (Tallot et al., 2003); (b) (Verschuure et al., 2003); (c) (Sugiyama et al., 2000); (d) (Brady et al., 1997); e). (Krief et al., 1999); (f) (Fontaine et al., 2003).

HspB1/*Hsp25/27* is a ubiquitously expressed protein with high levels in cardiac and skeletal muscle. HspB1 is one of the most efficient thermo-protective Hsps when over-expressed alone. It is found in large oligomers with a molecular mass of about 700kDa (Theriault et al., 2004). It is involved in cytoskeleton rearrangement and stabilization by its interaction with actin and the intermediate filaments in a phosphorylation dependent manner as described above (Perng et al., 1999). Mitogen activated protein kinases associated protein kinases (MAPKAP kinase-2, 3) are involved in the phosphorylation of HspB1 on three serine residues (Figure 1.6). Phosphorylation of Ser^{82} allows HspB1 oligomers to dissociate and phosphorylation on Ser^{15} allows HspB1 to perform its thermo-protective role (Theriault et al., 2004).

Figure 1.6. Domain structure of HspB1. Light box: conserved region in N-terminus; black box: α-crystallin domain; grey box: WDPF domain; ^^^^: flexible domain; P: phosphorylated serine residues of human protein. Position 137 corresponds to the only cysteine residue in the protein sequence. If deleted, dimer formation and the protective capacity of HspB1 are eliminated. Positions of point mutations that are responsible for pathologies are indicated by arrows (Arrigo et al., 2007).

HspB1 is involved in intracellular redox homeostasis proposed to occur via its interactions with enzymes (e.g. glutathione reductase) involved in keeping glutathione (GSH), an antioxidant, in its reduced form. Additionally HspB1 expression correlates with a decrease in iron levels, a catalyser of hydroxyl radical production (Arrigo et al., 2005a).

HspB1 is also involved in the signalling pathways that modulate the inflammatory response; however there is conflicting evidence on the role of HspB1 in inflammation. For example HspB1 is a component of the p38 MAPK signalling pathway, which has important functions in the inflammatory response. It has been shown to regulate a pro-inflammatory response in HeLa cells and fibroblasts (Alford et al., 2007), however in keratinocytes, HspB1 was found to have a protective effect against pro- inflammatory mediator release. Interestingly this was associated with the NF-kB signalling pathway and not MAPK (Sur et al., 2008).

HspB1 plays a further significant role in apoptosis via its interactions with and inhibition of caspase-3 and -9 (Theriault et al., 2004). It has also been shown to inhibit Bax activation, oligomerisation, and translocation to mitochondria, reducing cytochrome *c* release by promoting Akt activation, an anti-apoptotic serine/threonine kinase (Havasi et al., 2008). The protective activity of HspB1 may be cell-type specific as it was shown to protects against apoptotic stimuli in neuronal and other cell types (Wyttenbach et al., 2002), but not in cardiomyocytes (Kamradt et al., 2002).

HspB2*/MKBP (myotonic dystrophy protein kinase binding protein)* expression is restricted to the heart and muscle (Verschuure et al., 2003). HspB2 binds and activates myotonic dystrophy protein kinase (DMPK), an enzyme that when absent results in myotonic dystrophy. DMPK plays an essential role in maintaining muscle structure and function and HspB2 protects DMPK from heat/stress induced inactivation. HspB2 is localized to the neuromuscular junction in skeletal muscle cells where DMPK is concentrated, but also at the Z-bands of myofibrils (Suzuki et al., 1998). There is limited information regarding the role of this sHsp in regulation of the cytoskeleton, oxidative stress and inflammation. However, HspB2 has been shown to interact with the actin cytoskeleton in cell lines subjected to proteasomal inhibition (Verschuure et al., 2002). A functional relationship between HspB2 and the mitochondria has also been suggested by its association with the outer mitochondrial membrane. HspB2 may play a protective role here under stress conditions or it may mediate the transfer of proteins from the cytosol to the mitochondria (Nakagawa et al., 2001). Although not previously implicated in the regulation of apoptosis, HspB2 has recently been described as a novel inhibitor of caspase activation by TRAIL (TNF-related apoptosis-inducing ligand) and TNF-α (tumour necrosis factor) in the extrinsic apoptotic pathway by suppressing caspase-8 and -10 activation (Oshita et al., 2010).

  The restricted expression of this sHsp has been ascribed to its gene location. HspB2 and HspB5 genes are located in a head-to head manner in the human, mouse and rat genomes (Doerwald et al., 2004) and are transcribed in opposite directions. An intergenic enhancer region preferentially activates the HspB5 promoter, additionally 2 cis-elements that interact with glucocorticoid receptor (GR) and SP1, differentially regulate the promoters of both genes (Swamynathan and Piatigorsky, 2007).

HspB3 is expressed in muscle cells along with HspB2. It is induced during muscle differentiation under the control of MyoD. HspB3 and HspB2 form oligomeric complexes of approximately 150 kDa (Suzuki et al., 1998). This complex is independent of the complexes formed by HspB1, HspB5 and HspB6. It has been proposed that HspB3/HspB2 complexes represent an additional stress response system to that observed by HspB1 and HspB5 in muscle (Sugiyama et al., 2000). HspB3 was also shown to interact with the actin

cytoskeleton in the same study showing HspB2 association in cell lines subjected to proteasomal inhibition (Verschuure et al., 2002). There is currently no information regarding the involvement of HspB3 in oxidative stress, inflammation and apoptosis.

HspB4/αA-crystallin was thought to be specifically expressed in the lens, but non-lenticular expression has been reported in the rat in significant amounts in the spleen and thymus whereas low levels were found in retina, intestines, liver, kidney, adrenal, cerebellum and brainstem (Kato et al., 1991). HspB4 (and HspB5) play structural roles and are important in maintaining the transparent properties of the lens (Peterson et al., 2005). They display chaperone activity, thereby preventing proteins from forming light-scattering aggregates. The two isoforms make up one-third of the proteins in the eye lens (Yan and Hui, 2000).

HspB4 is thought to be important in microtubule integrity and assembly in lens epithelial cells by maintaining a pool of unassembled tubulin (Xi et al., 2006). The contribution of HspB4 to redox homeostasis has been demonstrated in knockout studies showing increased susceptibility of retinal pigment epithelium to apoptosis induced by hydrogen peroxide treatment (Yaung et al., 2007). HspB4 inhibits apoptosis by inhibiting the caspase3/6 pathway (Morozov and Wawrousek, 2006).

HspB5/αB-crystallin is a ubiquitously expressed protein (Verschuure et al., 2003) and is a major constituent of the eye lens. It is associated with cytoskeleton proteins, for example HspB5 modulates the assembly of the intermediate filament protein vimentin and stabilizes actin filaments in a phosphorylation-dependent manner (Singh et al., 2007). HspB5 also associates with tubulin, and microtubule-associated protein (MAP) (Sakurai et al., 2005). This is mediated through the alpha-crystallin domain (Ohto-Fujita et al., 2007).

HspB5 has been found to interact with FBX4, an F-box-containing protein that is a component of the ubiquitin-protein isopeptide ligase SCF (SKP1/CUL1/F-box). This interaction is dependent on phosphorylation of HspB5 (den Engelsman et al., 2003). It is phosphorylated at three serine sites by protein kinases (Figure 1.7). At least two pathways are implicated in HspB5 phosphorylation; the MAPKAPK2 kinases phosphorylate serine

59 whereas serine 45 is thought to be regulated by p42/p44 MAPK. The kinase involved in the phosphorylation of serine 19 is still unknown (Rouse et al., 1994).
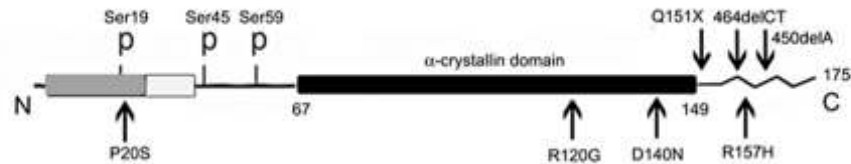
Figure 1.7. Domain structure of HspB5. Light box: conserved region in N-terminus; black box: α-crystallin domain; grey box: WDPF domain; ^^^^: flexible domain; P: phosphorylated serine residues. Positions of point mutations that are responsible for pathologies are indicated by arrows (Arrigo et al., 2007).

HspB5 is reported to bind Cu^{2+} with close to picomolar affinity, and has been shown to inhibit Cu^{2+}-induced oxidation of ascorbate and hence the production of reactive oxygen species (ROS) (Ahmad et al., 2008). HspB5 is directly involved in inflammatory processes in multiple sclerosis (MS); however this will be discussed in section 1.6.3 in the context of modulation of disease processes by sHsps.

HspB5 has anti-apoptotic functions through its potential interactions with the p53 and caspase-3 pathway (Kamradt et al., 2002, Liu et al., 2007). HspB5 was able to reduce the levels of hydrogen peroxide induced apoptosis in C6 astroglioma cell lines (Shin et al., 2009). Its expression is also correlated with TRAIL resistance in a number of human cancer cell lines (Kamradt et al., 2005, Liu et al., 2007).

HspB6/*Hsp20* is a ubiquitously expressed protein, with varying expression levels during development (Verschuure et al., 2003). It plays a role in the relaxation of vascular muscle and in the inhibition of platelet aggregation (Bukach et al., 2004). HspB6 interacts with itself, HspB1, HspB5 and HspB8 (Fontaine et al., 2005), however it is not heat inducible and has been shown to have a much lower chaperone activity than HspB5 (van de Klundert et al., 1998). It is regulated by several cellular pathways for example the cyclic nucleotide (cAMP)-dependent protein kinase (PK) pathways involving PKA and PKG eliciting functions such as smooth muscle relaxation (Komalavilas et al., 2008). HspB6 is

phosphorylated at Ser16 by PKA (Brophy et al., 1997). Although limited, there is evidence for HspB6 binding to actin in a phosphorylation dependent manner and a potential role in cytoskeletal stabilization (Dreiza et al., 2005).

HspB6 over-expression in cells exposed to doxorubicin (DOX) a widely used anti-tumour drug was found to enhance cardiac function by improving cell contraction, attenuating DOX-induced oxidative stress and was cardioprotective by interacting with Bax, a pro-apoptotic protein, thereby exerting anti-apoptotic actions. These effects were mediated by the Akt kinase pathway (Fan et al., 2005, Fan et al., 2008).

HspB7*/cvHsp* is abundantly expressed in the heart and muscle (Verschuure et al., 2003). HspB7 mRNA is over-expressed in insulin-sensitive tissue in obese rats, suggesting that HspB7 may be associated with obesity and related metabolic disorders. It binds to the cytoskeletal protein α-filamin (an actin binding protein) in the heart (Krief et al., 1999).

HspB8*/Hsp22* is a ubiquitously expressed protein (Verschuure et al., 2003)**.** HspB8 interacts with itself, HspB2, HspB5, HspB6 and HspB7 (Sun et al., 2004, Fontaine et al., 2005) as well as with other chaperones, such as the Hsp70 family. It is thought to have kinase activity *in vitro* (Kim et al., 2004) and potentially has a direct link to the Akt/PKB kinase pathway (Sui et al., 2009). HspB8 forms a stable complex with the co-chaperone Bag3 *in vitro* and is thought to facilitate the removal of abnormal proteins by the stimulation of autophagy (Carra et al., 2008). Although HspB8 has not been shown to interact directly with intermediate filaments, it is possible it does via interactions with HspB1 (Der Perng and Quinlan, 2004, Sun et al., 2004).

HspB8 has recently been suggested to play a role during the inflammatory process in autoimmune diseases such as rheumatoid arthritis, by the activation of dendritic cells via Toll-like receptor-4 (TLR-4) (Roelofs et al., 2006).

HspB8 is an anti-apoptotic protein, regulating its pro-survival effects via activation of the phosphatidylinositol 3-kinase (PI3K)/Akt pathway thus promoting cell growth and survival (Sui et al., 2009).

HspB9 is expressed in the testis, and in various types of cancer. HspB9 interacts with TCTELI, a light chain component of dynein (tubulin motor protein), which may transport it to the nucleus. It is found in the seminiferous tubuli, specifically in the nuclei of spermatogonia and early spermatids (de Wit et al., 2004; Kappe et al., 2001).

HspB10*/ODF1* is also expressed in testis. It has a C-terminal tail that is similar to some keratins and possibly serves a cytoskeletal-structural role in the sperm tail (Fontaine et al., 2003).

As described above and in addition to their chaperone functions, the sHsps are important in regulating a variety of cellular functions such as cytoskeleton homeostasis, oxidative stress and pro/anti-survival pathways. Interestingly these cellular functions are perturbed in many diseases, particularly protein misfolding diseases (also called "proteinopathies") which will be discussed below.

1.4.   Protein misfolding, proteinopathies and sHsps

Protein aggregates and deposits do not accumulate at steady state suggesting that the cellular machinery regulating protein folding and degradation, including the sHsps is sufficient to prevent accumulation of misfolded proteins. In contrast protein homeostasis becomes disrupted in disease and misfolding and aggregation are recognized as common molecular events for a large number of human diseases (proteinopathies) (Chiti et al., 2001; Chiti and Dobson, 2006; Perutz, 1999).

The characteristic abnormal protein deposits in proteinopathies can be found extracellularly and are referred to as 'amyloids' or 'plaques', or they can be present intracellularly and are referred to as Lewy bodies (LBs) or inclusion bodies, (IBs). Among these diseases are severe neurodegenerative disorders, such as AD, Huntington's disease (HD), Parkinson's disease (PD) and spongiform encephalopathies or Prion disease (Table 1.3) (Stefani and Dobson, 2003). HD and prion disease will be discussed in detail in section 1.7 and 1.8 respectively to represent an intracellular misfolding (HD) and an extracellular misfolding (prion) disease. Neurodegeneration is a general term used to describe the progressive loss of structure and function of neurons and their demise.

Disease	Protein	Intracellular/extracellular (misfolded protein)	Brain region mostly affected
Alzheimer's	APP and Tau	Both Plaques ($A\beta_{1-40/42}$), and NFT (hyper phosphorylated-tau)	Cortex
Prion	Prion (PrP^c)	Extracellular (PrP^{sc} aggregates)	Various
Huntington's	Huntingtin (htt)	Intracellular (mtHtt inclusions)	Cortex, Striatum
Parkinson's	α-synuclein	Intracellular (Lewy bodies)	Substantia nigra, Putamen

Table 1.3. Examples of proteinopathies characterized by intracellular/ extracellular aggregates. The proteins associated with each disease are given along with the location of aggregates. The most vulnerable brain regions are noted.

The accumulation of protein aggregates of normal cellular proteins (tau , huntingtin (htt), prion (PrP^c)) that have become misfolded or modified in these diseases suggests the involvement of common molecular pathways and pathogenic mechanisms leading to neurodegeneration (Bucciantini et al., 2002). These include abnormal protein dynamics and degradation, ROS generation, impaired bioenergetics, disruption of cellular transport and a neuro-inflammatory response. These mechanisms are extensively discussed in the context of commonalities in neurodegenerative diseases in the recent review by (Jellinger, 2009). All of these diseases (proteinopathies) have differing region and cell specific vulnerabilities/ pathologies in the CNS. This may be indicative of molecular differences between cell types and brain regions as well as the misfolded protein and location of aggregates, providing a context for disease (Chung et al., 2005).

Although it is still unclear whether the presence of microscopically visible protein aggregates is a cause or a consequence of pathology, it is clear that the process of protein misfolding and aggregation can affect cellular function and cause cytotoxicity (Esser et al., 2004).

Misfolded proteins aggregate into fibrillar structures or amyloids. However amyloid fibrils appear to be less toxic than pre-fibrillar structures/precursors (Figure 1.8). Soluble levels of Aβ more closely correlate with pathology than insoluble, fibrillar amyloid plaques (Walsh et al., 2002). These intermediate species that form different structures (annular and spherical) as determined by atomic force microscopy (Wacker et al., 2004) are thought to

confer toxicity by their intrinsic ability to impair fundamental cellular processes (Stefani and Dobson, 2003). It may be speculated that chaperones act at the level of protofibrils promoting the generation of amorphous, non toxic aggregates, thus protecting against neurodegeneration (Muchowski, 2002).
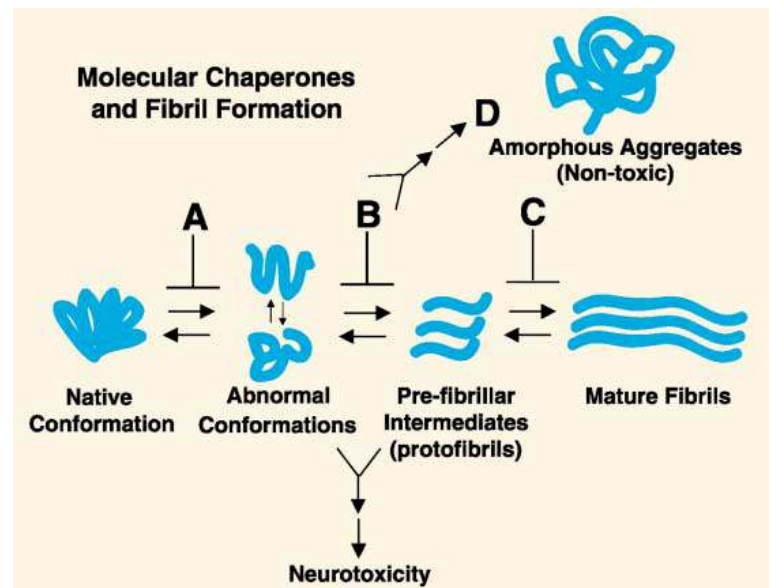
Figure 1.8. A model for molecular chaperone suppression of neurotoxicity. Fibril formation is a multi step process involving a number of intermediate structures that are thought to mediate neurotoxicity. Chaperone proteins may prevent neurotoxicity by preventing the conversion of native proteins to abnormal toxic conformations, (A) by preventing the formation of pre-fibrillar intermediates, (B) by preventing the conversion to mature fibrils, (C) and/or by facilitating the conversion of toxic intermediates to non-toxic amorphous aggregates (D). (Muchowski, 2002; Wacker et al., 2004).

The current body of evidence suggests expression of the sHsps in neurodegenerative conditions is predominantly associated with non-neuronal cells (Wyttenbach et al, 2010 in press). Whether abnormal protein aggregates are localized to neurons or glial cells, up-regulation of the sHsps during disease occurs predominantly in glial cells (section 1.6.2) and implies distinct pathological mechanisms for both cell types. Cultured neurons and astrocytes show different expression levels and compositions of individual sHsps. HspB1 and HspB5 are predominantly expressed in unstressed cells, and even after stress, sHsp levels are increased in glial cells but remain low in neurons (Schwarz et al., 2010).

Oligodendrocytes similarly respond to oxidative and proteasomal stress by inducing the endogenously expressed HspB5 (Goldbaum and Richter-Landsberg, 2001). As all brain cell types (neurons and glia) are potentially involved in neurodegenerative processes, these cell types will be described below.

1.5. The central nervous system (CNS) and vulnerability to proteinopathies

The mammalian CNS is subdivided into many regions and interconnected circuits. This requires highly specialized cell types such as neurons involved in information processing and storage, immuno-reactive microglial cells, astrocytes that interact with synapses and blood vessels regulating key aspects of brain bioenergetics and oligodendrocytes the myelin producing cells of the CNS.

1.5.1. Neuronal cells

Neuronal cells are highly compartmentalized structures, with distinct functional roles (Somogyi et al., 1998). For example, neuronal dendrites are involved in plastic adaptation including long term potentiation and depression and homeostatic plasticity which allows neuronal cells to stabilize synaptic strength and intrinsic excitability (Yu and Goda, 2009). The spatial organization of neurons with presynaptic terminals often a great distance from the cell body makes it crucial for this sub-compartment to be partially independent of the cell body for certain processes, such as regulating the manufacture of proteins needed for specialized function at the synapse (Chicurel et al., 1993). Indeed protein synthesis has been shown to occur in axons and nerve terminals (Macara et al., 2009). This local synthesis and availability of crucial proteins would allow neurons to respond promptly to environmental stimuli (Giuditta et al., 2008). Increasingly, synaptic changes, dysfunction and death are reported in neurodegenerative diseases, preceding loss of cell bodies (Gray et al., 2009, Nimmrich and Ebert, 2009). The cell autonomous properties of the synapse may underlie the vulnerability of this region to neurodegeneration and misfolded protein insult.

The initial loss of neurons in CNS neurodegenerative diseases is selective to specific brain regions and neuronal sub-types in each individual proteinopathy. For example in AD there is selective loss of large pyramidal neurons in layer III and V of the cortex (Hampel et al., 2002). In HD, an early loss of medium-spiny neurons and a relative sparing of interneurons (Cowan and Raymond, 2006) occurs in the severely affected basal ganglia

(caudate and putamen). In PD, dopaminergic neuronal cell loss is most prominent in the substantia nigra pars compacta (Gasser, 2009). In prion disease neuronal loss in the CNS is more extensive. In variant Creutzfeldt-Jacob disease (vCJD) neuronal death occurs in the cerebral cortex with the primary visual cortex most severely affected, the thalamus and midbrain structures are also affected (Liberski and Ironside, 2004).

Although neurons seem to be particularly vulnerable to stress (e.g. protein misfolding, oxidative stress), they are known to respond to such insult by up-regulating protective proteins such as the sHsps under conditions of acute stress (e.g. ischemia) and chronic stress. Such up-regulation is more widely known for the non-neuronal astrocytes and microglia cells with limited information about the response in oligodendrocytes. These cell types will be discussed below, particularly as the broad cellular responses during disease highlight the potential for cell-autonomous neuroprotective mechanisms in specific cell types and/or indeed a concerted, multifaceted response involving cell-cell interaction.

Glial cells are classified into three main groups: microglia, astrocytes and oligodendrocytes (Garcia-Marin et al., 2007).

1.5.2. Microglia

Microglial cells are the resident mononuclear phagocytes and immune cells of the nervous system. They possess highly ramified processes under normal "physiological" conditions (Napoli and Neumann, 2009). Microglia are activated in response to insult or injury to the brain, resulting in retraction of their processes and a transformation into an amoeboid morphology (Lynch, 2009). The response that is taken by the activated microglia depends on the pathological stimulus and is termed microgliosis. Microglia may up-regulate distinct profiles of cell surface markers, become motile and mediate an inflammatory response (Chan et al., 2007, Pocock and Kettenmann, 2007). The activation of microglia is graded and when fully activated may contribute to and increase damage to neurons by the release of cytokines and ROS (Streit et al., 1999). The microglial response has been attributed to the interaction of neurotransmitters and cytokines with cognate receptors that are expressed on the microglia (Pocock and Kettenmann, 2007).

1.5.3. Astrocytes

Astrocytes provide structural and metabolic support in the CNS. They are involved in neurotransmitter re-uptake and release, supplying nutrients to neurons, removing toxic waste products of neuronal metabolism, regulating cerebral blood flow and synaptic activity (Maragakis and Rothstein, 2006, Garcia-Marin et al., 2007). The astrocytic response to any form of injury to the CNS is referred to as astrocytosis or astrogliosis. Changes in glial fibrillary acidic protein (GFAP) an intermediate filament protein localised to astrocytes is generally used as an indicator of astrogliosis (Correa-Cerro and Mandell, 2007).

Astrogliosis can be both beneficial and deleterious. Astrocytes can mediate repair at the site of injury by the secretion of neurotrophic factors (Jean et al., 2008). They can also minimize damage and neuronal death by maintaining neurotransmitter homeostasis. Detrimental effects are seen when the presence of glial scars inhibit neurite outgrowth as well as remyelination of axons in white mater lesions (Carmen et al., 2007). Despite this prohibitive nature of glial scars, non-reactive astrocytes have been shown to be important for oligodendrocyte maturation and myelin formation (Carmen et al., 2007).

Perisynaptic astrocytes are intimately associated with the synaptic compartment. The processes of these astrocytes enwrap synapses, forming a 'tripartite' synapse (Todd et al., 2006, Bains and Oliet, 2007). This proximity allows astrocytes to sense neuronal activity and modulate synaptic transmission thereby contributing to neural plasticity (Reichenbach et al., 2010).

1.5.4. Oligodendrocytes

Oligodendrocytes form one of the most highly specialised cellular structures in the body, the myelin sheath. The myelin sheath is formed by the spiral wrapping of plasma membrane extensions around the axon, followed by the extrusion of cytoplasm and compaction of the stacked membrane bilayers. These membrane stacks provide electrical insulation around nerve fibres to minimize metabolic expense and maximize conductance velocity (Simons and Trajkovic, 2006). The myelin membrane has biochemically distinct domains. Proteins such as myelin basic protein (MBP) and proteolipid protein (PLP) are localised to 'compact' myelin, which as the name suggests, consists of tightly packed

membranous structures from which the cytoplasmic content has been extruded. 2', 3'-cyclic nucleotide 3'-phosphodiesterase (CNP) and myelin associated protein (MAG) are localised to non-compact myelin, this sub-compartment is involved in cell signalling events and forms contacts with the ensheathed axon. MBP is responsible for adhesion of the cytosolic surfaces of these membrane stacks. It may also interact with the cytoskeleton and participate in signalling events (Ahmed et al., 2009). There are many size isoforms of MBP due to differential splicing of a single mRNA transcript (Boggs, 2006). Neurons control the development of oligodendrocytes by regulating their proliferation, differentiation and survival. The timing of signals between neurons and oligodendrocytes is crucial in coordinating myelin biogenesis (Simons and Trajkovic, 2006).

1.6. sHsps in Diseases

1.6.1. Mutation in the sHsps and disease

Mutations in the sHsps have been reported in a number of human diseases. In particular four members of the sHsp family (HspB1, HspB4, HspB5 and HspB8) have been found as genes responsible for human degenerative myopathy, neuropathy and congenital cataract (Table 1.4). The majority of mutations in the sHsps are contained in the conserved α-crystallin domain, suggesting that oligomerisation and chaperone function of the sHsps is impaired (Dierick et al., 2005).

Mutations in HspB1 and HspB8 overlap in their disease outcomes (Der Perng and Quinlan, 2004). Mutations in both of these sHsps result in either Charcot-Marie-Tooth (CMT2) disease, a sensory and motor neuropathy, characterised by premature axonal degeneration; or distal hereditary motor neuropathy (DHMN), resulting in premature axonal loss, neuronal degeneration and death. These diseases result in progressive weakness and wasting of the limbs, hands and feet (Irobi et al., 2004, Tang et al., 2005a, Tang et al., 2005b). CMT can be divided into two major classes; the demyelinating forms (CMT1) and axonal forms (CMT2). Mutations in the sHsps give rise to axonal forms of this disease which is selective to a population of large motor neurons in the spinal cord (Evgrafov et al., 2004, Tang et al., 2005a).

The cellular effect of the HspB1 mutant P182L was demonstrated in primary neuronal cultures. Mutant HspB1 protein resulted in the formation of insoluble intracellular

aggregates (Ackerley et al., 2006). Cellular components including intermediate neurofilament middle chain subunit (NF-M) and p150 subunit of dynactin were sequestered into these aggregates, thus disruption of axonal transport and structure were suggested as possible pathogenic mechanisms of mutant HspB1 (Ackerley et al., 2006).

Missense mutations in both HspB4 (R116C) and HspB5 were found in familial congenital cataracts (Litt et al., 1998). The normal function of these proteins as chaperones and their involvement in maintaining the refractive properties of the lens suggests mutation and aggregation has a two fold effect, firstly in loss of the normal function, indeed the R116C mutation has been shown to have a lower actin binding affinity compared to wild type HspB4 (Brown et al., 2007), and secondly an increase in light diffraction by aggregates.

HspB5 has been linked to inclusion-based diseases involving the cytoskeleton, in particular desmin related myopathy. The R120G mutation in HspB5 induces intermediate filament aggregation in skeletal muscle (Sun and MacRae, 2005a). The same mutation induces desmin related cardiomyopathy in the hearts of transgenic mice (Sanbe et al., 2005). HspB5 may play a nuclear role during cardiomyopathy as the R120G mutant inhibits the formation of inter-chromatin granule clusters by the wild type HspB5 protein. These granules are thought to be involved in RNA transcription and splicing (van den et al., 2003).

The K141N mutation in HspB8 occurs in families with distal hereditary motor neuropathy. This mutation is in the α-crystallin domain and is equivalent to the HspB4-R116C and HspB5- R120G mutations (Irobi et al., 2004).

Interestingly, it is increasingly apparent that these mutations perturb the normal function of the cytoskeleton, as described in the above examples. The formation of protein aggregates by proteins inherently involved in preventing such misfolding processes suggests this may be attributed to either a loss of function of the sHsps in their normal cellular and protein homeostatic processes, or indeed a gain of function by formation of aggregates and sequestration of cellular components (Sanbe et al., 2007).

sHsp	Mutation	Disease	Reference
HspB1	R127W	CMT2, DHMN	(Evgrafov et al., 2004; Liu et al., 2005)
	S135F	CMT2, DHMN	(Evgrafov et al., 2004)
	R136W	CMT2	(Evgrafov et al., 2004)
	T151I	DHMN	(Evgrafov et al., 2004)
	P182S	DHMN	(Kijima et al., 2005)
	P182L	DHMN	(Evgrafov et al., 2004)
HspB4	W9X	CC	(Pras et al., 2000)
	R49C	CC	(Mackay et al., 2002)
	R116C	CC	(Litt et al., 1998)
	R116H	CC	(Gu et al., 2008)
	G98R	CC	(Santhiya et al., 2004)
HspB5	R120G	DRM, CC, MM	(Vicart et al., 1998)
	Q151X	MM	(Selcen and Engel, 2003)
	R157H	CM	(Inagaki et al., 2006)
	P20S	CC	(Liu et al., 2006)
	D140N	CC	(Berry et al., 2001)
HspB8	K141N	CMT2, DHMN	(Irobi et al., 2004, Tang et al., 2005b)
	K141E	DHMN	(Irobi et al., 2004)

Table 1.4. Human mutations in sHsps associated with degenerative disease.
Abbreviations: CC, congenital cataract; CM, cardiomyopathy; CMT2, Charcot-Marie-Tooth disease type 2; DHMN, distal hereditary motor neuropathy; DRM, desmin-related myopathy; MM, myofibrillar myopathy.

1.6.2. Induction of the sHsps associated with disease

Increased expression of the sHsps has also been associated with a number of acute and chronic conditions such as stroke (ischemia), and neurodegenerative diseases.

1.6.2.1. Acute stress (ischemia)

Ischemic/reperfusion injury to cells during stroke involves a complex sequence of neurochemical events such as cellular bioenergetic failure and excitotoxicity by glutamate release, oxidative stress by the generation of free radicals, post-ischemic inflammation resulting in death of neurons, glia and endothelial cells (reviewed in (Brouns and De Deyn,

2009). The sHsps are involved in several of these events under basal conditions and could therefore potentially provide a protective mechanism in such conditions. Indeed, in a rat model of middle cerebral artery occlusion (MCAO), HspB1 was induced in microglia at the site of ischemic insult after 4 hours. This was followed by induction in reactive astrocytes for an extended period of 1 day to 2 weeks (Kato et al., 1995). Lowe et al. (1992) reported increased HspB5 expression in a small proportion of ballooned neurons at the edges of areas with cerebral infarction (CI) in CI patients. Up-regulation of this otherwise non-neuronal sHsp under basal conditions was suggested to represent regenerating neurons (Lowe et al., 1992). In another study of MCAO in the rat brain, HspB5 was also shown to be transiently expressed only 4 hours after MCAO in pyramidal neurons in the vicinity of ischemic insult. Induction was localized to astrocytes, 2 days after MCAO in the penumbra and was sustained for a number of days. This induction was associated with up-regulation and co-localisation with MAPKAP-2 (Piao et al., 2005).

1.6.2.2. Chronic stress (neurodegenerative diseases)

Increased expression of the sHsps has been observed in several chronic neurodegenerative diseases, such as AD and PD.

1.6.2.2.a. sHsp expression in AD

AD is characterized by deposition of Aβ in senile plaques (SPs) and tau in neurofibrillary tangles (NFTs). HspB1 and HspB5 are up-regulated in AD brains and are localized to astrocytes and degenerating neurons (Bjorkdahl et al., 2008). HspB6 reactivity was also found in astrocytes surrounding these sites, whereas HspB8 expression was localized to oligodendrocytes and microglia based on morphological criteria (Wilhelmus et al., 2006b, Wilhelmus et al., 2006c). HspB1 and HspB5 were associated with extracellular Aβ SPs (Iwaki et al., 1992, Renkawek et al., 1994, Dabir et al., 2004), and elevated levels of HspB2, HspB6 and HspB8 immunoreactivity were also associated with SPs in AD (Wilhelmus et al., 2006b, Wilhelmus et al., 2006c). Interestingly the sHsps were not found to associate with NFTs suggesting a non-neuronal induction and involvement in this protein misfolding disease.

1.6.2.2.b.   sHsp expression in PD

PD is characterized by LBs, comprised of intraneuronal α-synuclein aggregates and ubiquitin (Spillantini et al., 1997). Although induction of some of the sHsps has been reported in PD it is not as pronounced as observed in AD with extracellular aggregates (Renkawek et al., 1999). However, increased expression of HspB1 and HspB5 was associated with reactive glial cells in degenerating regions (Renkawek et al., 1999). Additionally a 2/3-fold up-regulation of HspB1 mRNA and protein were reported in patients with dementia with LBs (DML) (Outeiro et al., 2006).

HspB5 staining has also been described in neurons of the cerebral cortex and amygdala in PD patients. The immuno-positive cells did not develop LBs suggesting a neuroprotective role for HspB5 (Braak et al., 2001).

1.6.2.2.c.   sHsp expression in polyQ diseases

HspB1 expression also increased in post-mortem brains of spinocerebellar ataxia 3 (SCA-3) patients. This disease is one of a repertoire of poly-glutamine (polyQ) disorders characterized by proteins containing pathologically long polyQ repeats within the protein (Chang et al., 2005). However HspB1 expression has also been shown to be decreased in patients with SCA-7 and in SCA-17 transgenic (tg) mice (Tsai et al., 2005, Friedman et al., 2007), suggesting modulation of the sHsps depending on the disease context (discussed below).

Induction of the sHsps in disease conditions in neuronal and non-neuronal cells as described above and their involvement in cellular processes in addition to protein folding as described for each sHsp in section 1.3.3 suggest the sHsps could play an important modulatory role during disease as many of these cellular processes are also perturbed or abnormally activated in disease. This aspect of sHsp function will be discussed below.

1.6.3.   Modulation of disease mechanisms and pathways

1.6.3.a.   Modulation of aggregation

The capacity of the sHsps to modulate disease processes has been demonstrated in a number of studies. As described above the sHsp co-localise with Aβ deposits in SPs, therefore an *in vitro* investigation using cerebrovascular cells was conducted to investigate

the binding capacity of the sHsps (HspB1, HspB5 and HspB6) to $A\beta_{1-40}$ and $A\beta_{1-42}$. The sHsps were able to bind to both species, however they were able to modulate and inhibit the aggregation of the more toxic $A\beta_{1-40}$ species into fibrils without affecting $A\beta_{1-42}$ aggregation. Additionally they were also able to reduce toxicity of $A\beta_{1-40}$ and $A\beta_{1-42}$. However the degree of protection was correlated with binding affinity for each peptide (Wilhelmus et al., 2006a). In an earlier study, inhibition of $A\beta_{1-40}$ fibril formation by HspB5 was associated with increased toxicity in cultured neurons (Stege et al., 1999). HspB5/ $A\beta$ complexes were suggested to maintain $A\beta$ as a toxic non-fibrillar protein. In this case the sHsps intrinsic chaperone activity could potentially increase rather than alleviate Alzheimer's symptoms (Stege et al., 1999).

HspB5 modulation of protein aggregation was also demonstrated in a study where mice expressing a mutation in the intermediate filament protein desmin were crossed with HspB5-R120G tg mice. These mice had significantly higher levels of desmin aggregates than mice expressing the desmin mutant protein alone. Additionally in the same study *in vitro* expression of a desmin mutant protein and over-expression of wild-type (wt) HspB5 protein resulted in reduction of desmin aggregation (Wang et al., 2003).

HspB8 has also been shown to block the formation of IBs formed by the polyQ protein, and has been shown to inhibit accumulation of SDS insoluble htt with 43 glutamines (htt43Q) as efficiently as Hsp40 (Carra et al., 2005, Carra et al., 2008).

1.6.3.b.   Modulation of the cytoskeleton

As described in section 1.6.1 mutations in the sHsps result in perturbations of the cytoskeleton. Disruption and dysregulation of the cytoskeleton is one of the key features observed in disease processes. For example, Alexander's disease (AxD) is a primary disorder of astrocytes occurring as a consequence of mutations in GFAP. The resultant aggregates that form are termed Rosenthal fibers or astrocytic inclusions containing cytoskeletal proteins in addition to molecular chaperones (HspB1 and HspB5) (Der Perng and Quinlan, 2004). HspB5 regulates GFAP assembly (Nicholl and Quinlan, 1994, Ghosh et al., 2007) and modulation of the levels of HspB5 were found to either increase mortality (loss of HspB5) in an AxD mouse model or reduce disease symptoms such as seizures (increased HspB5) (Hagemann et al., 2009).

1.6.3.c. Modulation of inflammation

Inflammation is often associated with disease processes and induction of the sHsps may regulate this pathway. HspB5 is a major target of T-cells immunity to the myelin sheath in MS and is thus directly linked with inflammatory disease. HspB5 was shown to be protective in a model of demyelination, experimental autoimmune encephalomyelitis (EAE). HspB5 knockout mice showed worse EAE with a heightened T-cell and immune response compared to controls. Administration of recombinant HspB5 was able to alleviate the symptoms of EAE, demonstrating its protective role as a negative regulator of the inflammatory response (Ousman et al., 2007).

1.6.3.d. Modulation of oxidative stress and apoptosis

HspB1 has been reported to modulate oxidative stress and toxicity in a cell model of HD. It was able to suppress polyQ induced toxicity and cell death by reducing the levels of ROS. This process was independent of changes in aggregation, as polyQ aggregation was not affected (Wyttenbach et al., 2002).

Mice expressing mutant superoxide dismutase (SOD1^{G93A}) as a model of amyotrophic lateral sclerosis (ALS) have severe motor phenotype and motor neuron cell loss. When SOD1^{G93A} mice were crossed with mice over-expressing mice HspB1, the resultant double tg mice showed an improved phenotype with increased survival of motor neurons at early stage of disease (Sharp et al., 2008), suggesting modulation of apoptotic pathway and stabilization of the cytoskeleton (Perng et al., 1999). However this protection was not sustained as HspB1 protein was down-regulated in double tg animals although the mRNA levels remained unchanged (Sharp et al., 2008).

Both HspB1 and HspB5 are also able to reduce α-synuclein induced toxicity (by ~80% and 20% respectively) in a cell culture model (Outeiro et al., 2006). The sHsps have also been shown to prevent cataract formation and protect against ischemia and reperfusion injury during heart attack and stroke (Sun and MacRae, 2005a).

The sHsps likely play a critical role in tempering disease pathology particularly in protein misfolding diseases or proteinopathies. Thus it would be useful to study the roles of the sHsps in the context of intra- and extracellular misfolding diseases. An example of a chronic neurodegenerative disease characterised by either intracellular misfolded

aggregates (HD, section 1.7) or extracellular misfolded aggregates (prion, section 1.8) will be described in detail below.

1.7. Huntington's disease (intracellular proteinopathy)

HD is an inherited autosomal dominant neurodegenerative disorder that was first described by Charles Oscar Walters in 1841 and then classically defined by George Huntington in 1872 (Imarisio et al., 2008). In Western countries it is estimated that about five to seven people per 100,000 are affected by HD (Walker, 2007). Symptoms of HD include chorea (involuntary movements), weight loss as well as psychiatric and cognitive dysfunction. HD is a progressive disorder resulting in death within 15-20 years after disease onset, and even more rapidly in young patients (7-9 years after disease onset) (Estrada Sanchez et al., 2008). HD occurs due to an expansion of a polyQ tract (CAG) in the first exon of the gene IT15, which is located on the short arm of chromosome 4 (Walling et al., 1998, Imarisio et al., 2008). Generally, fewer than 36 CAG repeats results in the production of the cytoplasmic htt. However, a sequence of 36 or more polyQ repeats results in the manifestation of the disease during adulthood (Walker, 2007). 36–40 repeats result in a reduced-penetrance form of the disease, with a much later onset and slower progression of symptoms. When the number of repeats exceeds ca. 60, HD has full penetrance and disease symptoms are seen in young adolescents (15-20 years old) and this juvenile form of HD shows a different more aggressive pathology (Nance and Myers, 2001). Thus there is a strong inverse relationship between the age of onset of HD and the number of CAG repeats (Farrer et al., 1992).

1.7.1. HD pathogenesis

Expanded polyQ repeats have been suggested to confer toxic gain of function properties on the mutant protein, but also result in a loss of function (reviewed in(Cattaneo et al., 2001). Over-expression of polyQ expansions (full length htt or exon 1 of htt (httEx1)) in monkeys, sheep, mice, *Drosophila, C.elegans* and zebrafish have been shown to be associated with neurodegenerative phenotypes (Rubinsztein, 2002, Yang et al., 2008, Jacobsen et al., 2010). In human subjects, this expansion in the htt protein leads to a severe loss of medium spiny neurons (MSN) in the striatum. The MSN constitute 95% of the total neuronal population of the striatum and receive cortical inputs releasing

glutamate, the main excitatory neurotransmitter in the brain. Glutamate can cause cell death by excitotoxicity and this has been suggested to be one of the mechanisms involved in the pathogenesis of HD (Estrada Sanchez et al., 2008).

Although HD pathology is predominantly associated with degeneration of the striatum, it also involves cortical areas. Atrophy of the brain is initially observed in the basal ganglia (up to 60% loss of mass), with the caudate nucleus affected progressively and more severely than the putamen or global pallidus (Walling et al., 1998). Atrophy is less severe (20% loss of mass) and non-progressive in other areas of the brain such as the cortex (Walling et al., 1998). In late stage HD other brain regions such as the hippocampus, hypothalamus and the cerebellum are also affected (Li and Li, 2004).

Although early research on HD focused on changes in the gray matter, changes in the white matter do occur (Fennema-Notestine et al., 2004, Kassubek et al., 2004). MRI imaging of HD subjects with pre-symptomatic to advanced HD revealed decreased brain white matter volume many years before the onset of clinical HD and even before evidence of gray matter atrophy over time. Additionally a correlation between white matter atrophy and time to onset in pre-symptomatic subjects was observed (Ciarmiello et al., 2006). Such white matter changes are suggested to contribute to the compromised function of cortical circuits potentially contributing to the early clinical symptoms, such as early cognitive and subtle motor impairment that occur in HD (Rosas et al., 2006).

The (efferent) MSNs of the striatum send projections to the globus pallidus and are associated with the inhibitory neurotransmitter gamma-aminobutyric acid (GABA). Decrease in inhibition of the globus pallidus externa as a consequence of MSN cell death, results in excessive inhibition of the subthalamic nucleus, leading to increased thalamic excitation and choreic movements (Albin et al., 1990, Aron et al., 2003). Large cholinergic aspiny neurons in the striatum are generally spared in disease. The basal ganglia often show depletion of GABA, substance P and enkephalins (Storey and Beal, 1993). Dendritic abnormalities are observed in transgenic mouse models of HD, with a significant decrease in the number of dendritic spines and a thickening of proximal dendrites before cell death (Li et al., 2003).

1.7.2. Functions of htt and its associated cellular mechanisms implicated in HD

A number of roles and functions have been proposed for the htt protein such as protein trafficking, vesicle transport, anchoring to the cytoskeleton, clathrin mediated endocytosis, postsynaptic signalling, transcriptional regulation and anti-apoptotic functions (Gil and Rego, 2008, Imarisio et al., 2008). Only a few potential functions that relate to pathology and a potential modulatory role of the sHsps as described in section 1.6.3 will be discussed below. These will include protein aggregation and degradation, axonal transport and the cytoskeleton, oxidative stress, and transcriptional dysregulation.

1.7.2.a.   Intracellular aggregation and alterations in the protein degradation systems

MtHtt IBs are found in the nucleus and the cytoplasmic compartments of neurons and are often immunoreactive for ubiquitin and chaperone proteins (Waelter et al., 2001). Although mtHtt is expressed in glial cells, it is the neuronal population that contains the majority of htt aggregates (DiFiglia et al., 1997). Neurons are post-mitotic cells and their ability to cope with misfolded proteins is likely to be different to glial cells, which can proliferate and regenerate (Barres and Barde, 2000). MtHtt IBs sequester transcription factors, cytoskeletal proteins, protein kinases, ubiquitin and proteasomal subunits (Kopito, 2000, Taylor et al., 2002). Sequestration of these proteins into IBs could be detrimental to normal cellular functions and induce cellular toxicity (Perutz et al., 1994). Indeed, cellular studies support the findings that there is a correlation between aggregate formation and cellular toxicity (Wyttenbach et al., 2000, Wyttenbach et al., 2002). Furthermore, in HD mice expressing mutant httEx1, intra-nuclear IBs were detected close or well before the appearance of behavioural changes (Bates et al., 1997, Morton et al., 2009), implicating polyQ aggregation as a contributor to toxicity.

Over-expression of molecular chaperones, including Hsp40 and 70 reduced both aggregation and cell death induced by httEx1 *in vitro* (Kobayashi et al., 2000, Wyttenbach et al., 2000). These chaperones may be reducing large inclusion formation by preventing oligomer formation, and it may be the oligomeric precursors that are the most toxic species (Wacker et al., 2004, Takahashi and Mihara, 2008). Indeed neurons containing IBs are less likely to die *in vitro* (Arrasate et al., 2004).

Toxicity of mtHtt aggregates has also been linked to the UPP. Under basal conditions, UPP activity decreases in an age-dependent manner and is lower in neurons versus glia (Tydlacka et al., 2008). It is suggested that the intrinsically lower UPP activity in neurons contributes to the accumulation of misfolded proteins in neurons and hence this could be a potential mechanism driving neuronal toxicity. PolyQ aggregation could impair the UPP in polyQ diseases hinted to by studies that positively labelled polyQ aggregates with antibodies against ubiquitin and proteasome subunits (Diaz-Hernandez et al., 2006). This suggested that sequestration of UPP components in aggregates might affect UPP activity. It is thought that proteins containing expanded polyQ tracts cannot be easily degraded by the eukaryotic proteasome and therefore become trapped in the proteasome and block entry of other substrates into the barrel of the 20S catalytic core (Bennett et al., 2005). It has also been suggested that the proteasome is able to remove flanking sequences around the polyQ tract, resulting in production of polyQ stretches that may in fact be more toxic than the pre-proteasomal species (Rubinsztein, 2006). Although most *in vivo* studies do not directly show impaired UPP activity due to expanded polyQ, the accumulation of ubiquitinated aggregates in HD implies nevertheless a disruption and inability of chaperones and the UPP in preventing the build up of misfolded proteins (Jana and Nukina, 2003). Htt aggregates in cell and mouse models have also been suggested to inhibit mTOR (mammalian target for rapamycin) function thereby inducing autophagy (Ravikumar et al., 2004). Aggregation prone proteins may indeed be degraded via autophagic mechanisms (review by (Rubinsztein, 2006). Inhibition of mTOR by rapamycin reduces the levels and toxicity of soluble mtHtt and aggregated mtHtt (Ravikumar et al., 2004). However, mTOR also regulates protein synthesis and rapamycin has been suggested to reduce polyQ toxicity via both activation of autophagy and inhibition of translation (King et al., 2008).

1.7.2.b.   Axonal transport and the cytoskeleton in HD

Htt has been implicated in vesicular transport due to its localization to endocytic/ endosomal vesicles in axons and synaptic terminals, as well as its interaction with endocytic/trafficking proteins, including clathrin and dynamin. MtHtt binds to synaptic vesicles with higher affinity than htt (Li et al., 2003). It has recently been proposed that

mtHtt inhibits Rab11 activity, a GTPase involved in endosomal recycling, resulting in impairment of vesicle formation and recycling endosomes (Li et al., 2009).

Htt is known to facilitate transport along microtubules (Gunawardena et al., 2003), however mtHtt aggregates are able to physically inhibit the movement of vesicles and mitochondria along neural projections (Lee et al., 2004). Htt interacts directly with the dynein/dynactin microtubule-based motor complexes (retrograde transport), as well as via its binding partner huntingtin-associated protein-1 (HAP1) (Gauthier et al., 2004). HAP1 binds kinesin, another motor protein involved in anterograde axonal transport (Walling et al., 1998, Imarisio et al., 2008). It also functions as an adaptor protein between htt and InsP3R1 (inositol (1, 4, 5)-tri-phosphate receptor) in lipid bilayers and sensitises calcium release by InsP3R1 in the presence of htt. This leads to an increase in the intracellular calcium load, which may contribute to the increased susceptibility to death of MSNs in the striatum (Tang et al., 2004).

1.7.2.c. Oxidative stress

Oxidative stress and mitochondrial dysfunction have been implicated in many neurodegenerative diseases. Oxidative stress is brought about by the abnormal production of ROS. ROS are highly reactive oxygen molecules that have gained unpaired electrons in the outer shell to form superoxide anions, hydrogen peroxide or hydroxyl radicals (Cash et al., 2007). These species can be generated by the mitochondria, in the cytoplasm via several enzymes or by lipid peroxidation. ROS is produced by the cell as a normal by-product of oxygen metabolism and is buffered by enzymes such as superoxide dismutase and peroxiredoxins (Calabrese et al., 2007). However, increases in ROS levels can result in damage to cellular structures, DNA and proteins.

Mitochondria are a major source of ROS production (Kowaltowski et al., 2009), but are also the major target of ROS damage (Guidot et al., 1993). To protect the cell against ROS, mitochondria contain an antioxidant system including non-enzymatic proteins, such as coenzyme Q10 or glutathione, as well as enzymatic proteins such as MnSOD, catalase and glutathione peroxidase (Valko et al., 2007). However excessive production of ROS or perturbations of the antioxidant mechanisms can lead to oxidative damage of mitochondrial proteins, lipid and DNA (Sohal, 2002). ROS may also result in the

formation of protein carbonyls. These modified proteins are dysfunctional and may lead to decreased activity of key metabolic enzymes and disturbed cellular signalling systems. Indeed, evidence from post-mortem brains of HD patients and tg mouse models suggests the presence of mitochondrial metabolic dysfunction (Mangiarini et al., 1996, Browne and Beal, 2004). Mitochondrial impairment and oxidative stress have also been detected in asymptomatic HD carriers (Saft et al., 2005).

Interestingly *in vitro* studies have demonstrated that up-regulation of molecular chaperones (HspB1) is protective against ROS induced by httEx1 (Wyttenbach et al., 2002). It is thought that mitochondrial metabolic dysfunction could play a key role in HD pathogenesis, but it is not clear if this a primary cause or a secondary consequence of neuronal death (Orth and Schapira, 2001).

1.7.2.d.   Transcriptional and, post-translational dysregulation and cleavage of htt

Altered gene expression has been reported in the human HD caudate (Hodges et al., 2006) and is one of the earliest molecular changes to occur in the brains of HD mice (Chan et al., 2002). Htt interacts with many transcription factors and other proteins involved in mRNA production, and is involved in their nucleo-cytoplasmic shuttling thereby regulating transcription (Truant et al., 2007). An example of the adverse effects of mtHtt can be illustrated by CREB binding protein (CBP) regulation. MtHtt inhibits CBP, a small regulatory protein that is important for cell survival (Nucifora et al., 2001) and interferes with CRE-mediated transcription (Wyttenbach et al., 2001). CBP has 18 glutamines which directly interact with mtHtt. It normally binds DNA and has histone acetyltransferase activity, allowing transcription factors to access DNA. The interaction of CBP with mtHtt causes CBP relocalisation from the nucleus into htt aggregates, removing this protein from its normal cellular localisation (Steffan et al., 2000).

Phosphorylation is an important post-translational modification of htt. Phosphorylation at serine 421 in the mtHtt protein has been shown to restore its functions in axonal transport (Zala et al., 2008) and abolishes mtHtt-induced toxicity in cell models of HD (Rangone et al., 2004, Zala et al., 2008). Phosphorylation at serine 434 by cdk5 reduces its cleavage by caspases (Luo et al., 2005). These post-translational modifications may regulate the half-

life, localization and nuclear export of htt, as well as altering the toxicity of mtHtt (Steffan et al., 2004).

Both htt and mtHtt are also post-translationally modified by caspases and calpains which cleave at the N-terminal end (Gafni and Ellerby, 2002, Hermel et al., 2004). These N-terminal fragments are thought to form β-pleated sheet structures. The significance of proteolysis for the physiological function of htt is not clear, but mtHtt cleavage is known to result in the production of toxic mtHtt fragments (Imarisio et al., 2008).

1.8. Prion disease (extracellular proteinopathy)

Prion diseases or transmissible spongiform encephalopathies (TSE's) are fatal neurodegenerative disorders which occur in both humans and animals. TSE's are clinically characterized by dementia and motor dysfunction, and neuropathologically by amyloid deposition, vacuolation of the neurophil which gives a 'sponge' like appearance to the brain, neuronal cell death and activation of astrocytes and microglia (Liberski and Ironside, 2004). Disease may occur sporadically, be acquired by infection or may be hereditary. Many strains of prion disease exist, these are defined by different incubation periods and neuropathologies (Prusiner, 1996).

CJD is the most common human prion disease with an incident rate of between 0.5 and 1.5 per million worldwide (Johnson, 2005). Cases of atypical CJD raised the possibility of transmission of bovine spongiform encephalopathies (BSE) to humans (Prusiner, 1996, Johnson, 2005). The spread of human prion diseases through consumption of infected material as was suggested after the BSE outbreak had been implicated historically in kuru, a disease of the Fore people practicing ritualistic cannibalism. The neuropathology seen in kuru was compared to that seen in scrapie by William Hadlow, and later kuru was likened to CJD by Igor Klatzo (Prusiner, 1998).

Initially the causative agent in TSE's remained unidentified. It was found to be resistant to inactivation by formaldehyde, ethanol, proteases, nucleases and even ultraviolet and ionizing radiation. It was subsequently suggested that the infectious agent was in fact a single protein devoid of nucleic acid which was named 'prion' (PrP) to describe this small proteinaceous infectious particle (Prusiner et al., 1982). A single gene was found to encode PrP in the host and not a nucleic acid carried within infectious particles (Oesch et

al., 1985, Prusiner, 1996). A 27-30kDa isoform of the normal membrane glycoprotein (prion protein) was found to co-purify with infectivity, leading to the identification of the 33-35kDa prion protein (PrP^c), a protease sensitive protein, and the smaller 27-30kDa protease-resistant core of a 33-35kDa disease specific protein (PrP^{sc}) (Prusiner, 1991, 1996).

1.8.1. Prion pathogenesis

Prion propagation in the nervous system is thought to occur as a result of axonal transport, passive translocation in perineural lymphatics, and conversion of PrP^c to PrP^{sc} along neural cell membranes (Figure 1.9). The conversion of the soluble, protease-sensitive PrP^c into PrP^{sc} occurs through a process whereby a portion of its α-helical structure is refolded into a β-sheet, making PrP^{sc} prone to aggregation and protease resistant (Figure 1.10). PrP^{sc} acts as a template for PrP^c to refold and adopt the PrP^{sc} conformation (Hu et al., 2007). This misfolding insult produces a selective neuronal degeneration in the CNS despite the proteins wide cellular expression. Irrespective of whether the disease is triggered by infection or genetic mutations, it leads to extracellular deposition of misfolded PrP^{sc}. Neuronal loss in prion diseases as observed in post mortem tissue from CJD sufferers was found in the cerebellum, thalamus and also the cerebral cortex (Liberski and Ironside, 2004). However animal models of prion disease display more selective neuronal death in specific regions of the brain preceded by synaptic loss (Cunningham et al., 2003; Siskova et al., 2009).

It has been suggested that either a gain of function of the PrP^{sc} conformer or a loss of function by conversion of the native PrP^c to PrP^{sc} is key to pathogenesis (Unterberger et al., 2005). Host PrP^c expression is necessary for disease transmission, as ablation of the PrP^c gene prevents disease (Prusiner et al., 1993) and overexpression of PrP^c followed by PrP^{sc} challenge accelerates disease (DeArmond et al., 1994).
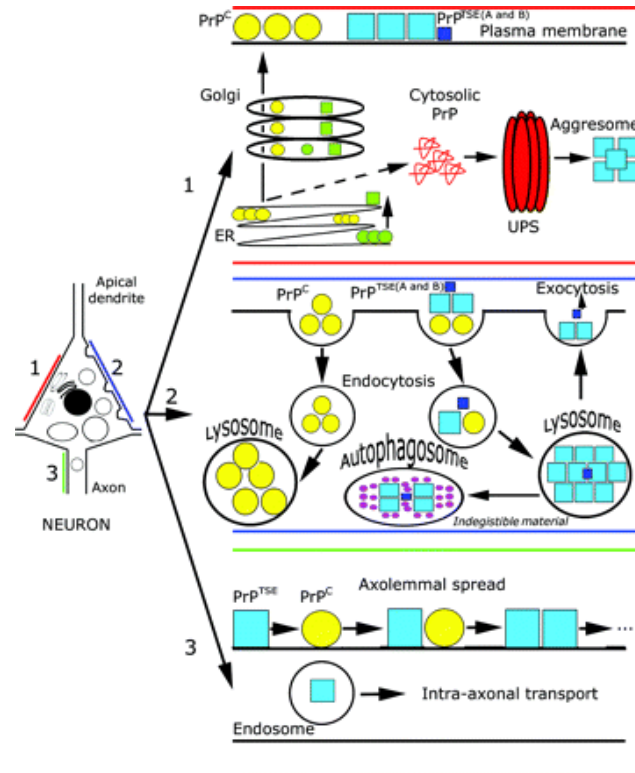
Figure 1.9. Summary of PrP processing pathways. Pathway 1 (intracellular PrP processing, red): The PrP^c polypeptide (yellow circles), including genetic mutants (green circles), is synthesized in the ER, processed in the Golgi apparatus, and then carried in its mature form to the cell surface where most of it is found in lipid rafts. Generation of PrP^{TSE} (PrP^{sc}) (blue and dark blue boxes), from PrP^c occurs after the arrival of PrP^c at the cell surface. Misfolded cytosolic PrP may result in the formation of aggresomes via the ubiquitin-proteasome system. Pathway 2 (processing of external PrP^c and PrP^{TSE} (PrP^{sc}) blue): PrP^c from the plasma membrane is internalized and processed in lysosomes. PrP^{TSE} (PrP^{sc}), (blue and dark blue boxes), leads to a conformational change of PrP^c before or during internalization via endosomes. Overloading of the endosomal-lysosomal system may lead to accumulation of indigestible material or exocytosis of PrP^{TSE} (PrP^{sc}) that forms extracellular aggregated deposits. This process may be accompanied by release of lysosomal enzymes leading to tissue damage. Pathway 3 (spread of PrP^{TSE} (PrP^{sc}), green): Endosomes may transport PrP^{TSE} (PrP^{sc}) in the axons, in addition to the domino-like spread of PrP^{TSE} axolemmally (Kovacs and Budka, 2008).
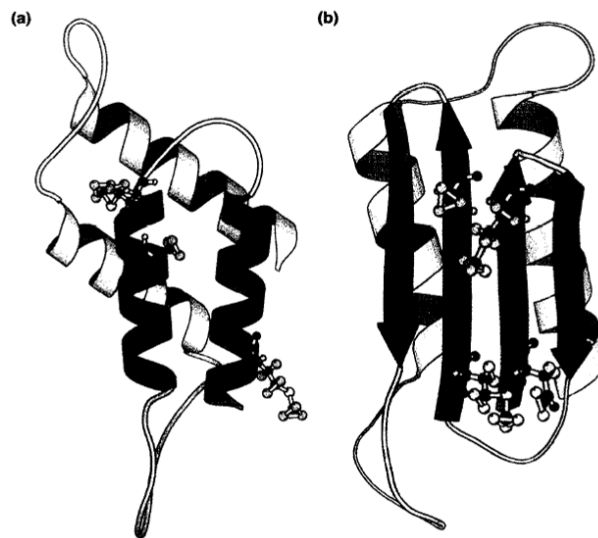
Figure 1.10. Model of the tertiary structure of PrPc and PrPsc. (a) Proposed structure of PrP^c with a high alpha helical content. (b) Proposed structure of PrP^{sc}, with an high beta sheet content (Prusiner, 1996).

The phenotype of PrP null mice is controversial as genetic ablation of PrP expression in mice has been shown to produce little phenotypic effect apart from the inability to propagate prions (Bueler et al., 1992). However subtle abnormalities have been described in these mice (reviewed in (Steele et al., 2007). For example PrP-null mice have been shown to display deficits in spatial learning (Criado et al., 2005), altered long term potentiation (Maglio et al., 2004) and increased excitability of hippocampal neurons (Mallucci et al., 2002). *In vivo* models of seizure activity have shown increased mortality in PrP-null mice (Walz et al., 1999, Khosravani et al., 2008).

Excitability and excitotoxicity are associated with N-methyl-D-asparatate receptor (NMDAR) activity. It has recently been shown that PrP^c is able to modulate synaptic NMDA currents, and is neuroprotective by its ability to suppress NMDAR activity, thereby preventing excitotoxicity and cell death (Khosravani et al., 2008). So, loss of function may promote excitotoxicity due to enhanced NMDA activity.

1.8.2. Functions of PrP and its associated cellular mechanisms implicated in prion disease

As for HD (see above), only a few functions that relate to prion pathology and a potential modulatory role of the sHsps as described in section 1.6.3 will be considered below. These

will include protein aggregation and degradation, oxidative stress, and gliosis and inflammation.

1.8.2.a.   Extracellular aggregation and alterations in the protein degradation systems

The presence and pattern of histopathological changes in prion disease are variable between individuals and disease subtypes (Budka, 2003). Originally it was thought that disease associated histopathological changes in the brain were correlated with PrP^{sc} deposition (Jendroska et al., 1991). However it was later noted that the consistency between the amount and distribution of PrP^{sc} and the severity of local tissue damage did not always correlate. For example in a time course study in mice with experimental CJD, spongiform changes preceded PrP^{sc} deposition in various brain regions (Kordek et al., 1999). Accumulation of PrP^{sc} in the nervous system is a gradual process occurring during disease progression and ultrastructural studies have shown that the process begins at the cell membrane of neurons and in the extracellular space (Jeffrey et al., 1994).

Impairment/alteration of protein degradation processes are observed in prion disease. For example, autophagy is involved in processing both PrP^{c} and PrP^{sc} and changes in levels of lysosomal enzymes have been reported in CJD brain regions with prominent pathology (Kovacs et al., 2007). Pathological PrP^{sc} oligomers may be released from cells to the extracellular environment by direct recycling and/or via exosome secretion (Fevrier et al., 2004). Neurons in the vicinity of tissue damage were found to contain PrP^{sc} in lysosomes, indicating that overloading endosomal/lysosomal function may correlate with regional pathology (Kovacs et al., 2007).

PrP^{sc} has been shown to inhibit and impair the UPP in a number of cell lines. This has been attributed to oligomeric species of PrP^{sc} directly inhibiting the catalytic subunits of the 26S proteasome (Kristiansen et al., 2007). In humans cytosolic PrP^{sc} aggregates supporting the above process have not yet been observed. However, in sCJD nuclear redistribution and accumulation of UPP components have been observed in areas of tissue damage, suggesting involvement in DNA repair mechanisms and/or cell death machinery (Adori et al., 2005).

1.8.2.b.   Oxidative stress

An antioxidative function of PrP^c has been suggested by *in vitro* studies. PrP^c deficient mice have lower levels of Zn/Cu SOD activity compared to controls (Prusiner, 1998). Additionally neurons lacking PrP^c were more vulnerable to hydrogen peroxide toxicity than wt cells (White et al., 1999), whereas increased activity of SOD and glutathione peroxide is seen in neurons expressing higher levels of PrP^c. This suggests a role of PrP^c in the cellular defence mechanisms. PrP^c may protect against oxidative damage by simply chelating redox-active copper or by acting as a quencher of ROS (Brown et al., 1999). The N-terminal octarepeat region is thought to be important in this function (Mitteregger et al., 2007). PrP^c null mice have also been shown to exhibit higher levels of oxidative damage to proteins and lipids in the brain compared to wt animals (Klamt et al., 2001). Correlation of PrP^c expression and the copper content of the brain, cellular copper uptake, and copper incorporation into Zn/Cu SOD have been described (Brown et al., 1997, Brown et al., 1998) suggesting PrP^c is involved in cellular oxidative defence mechanisms (Rachidi et al., 2003).

Mitochondrial function is shown to be compromised in prion disease before symptoms are apparent (Ferreiro et al., 2008). A significant reduction of mitochondrial manganese (Mn) SOD activity was described in animal models of prion disease (Choi et al., 1998, Lee et al., 1999). Oxidative damage to DNA, proteins and lipids was also shown in late stage prion disease (Choi et al., 1998, Choi et al., 2000, Guentchev et al., 2000).

Additionally *in vitro* studies have reported that accumulation of PrP^{sc} correlated with reduced proteasomal activity and increased levels of ROS (Lee et al., 1999). Increased ROS production has been associated with increased MAPK activation in hamster brains infected with scrapie (Lee et al., 2005a, Pamplona et al., 2008).

1.8.2.c.   Gliosis and inflammation

GFAP up-regulation and astrocytosis is a prominent feature of prion diseases. Up-regulation of astrocytic enzymes precedes development of lesions but follows the increase in PrP^{sc}, suggesting that the astrocytic response is induced by PrP^{sc} (Kordek et al., 1997). Microglial activation is seen in human and mouse prion disease (Sasaki et al., 1993, Giese et al., 1998) and is confined to areas with spongiform changes and PrP^{sc} deposition

(Williams et al., 1994). *In vitro* studies show that microglia produce inflammatory cytokines IL-1β (interleukin-1 beta) and IL-6 (interleukin-6) in response to the neurotoxic PrP106-126 peptide (Brown et al., 1996). Microglia have also been shown to contain PrP^{sc} suggesting that it may be degraded or processed in some way in these cells consistent with a macrophage-like role (Rezaie and Lantos, 2001). Indeed, the immunological anti-inflammatory phenotype of microglia *in vivo* has been suggested to closely resemble that of macrophages having ingested apoptotic cells (Perry et al., 2002). TNF-α, as well as IL-6 deficient mice are fully susceptible to prion disease when challenged with ME7 scrapie (Mabbott et al., 2000) supporting a redundant role of pro-inflammatory cytokines in prion pathogenesis. However, it has been proposed that although microglia do not express significant amounts of pro-inflammatory cytokines, they could be in a "primed" state, and if further stimulated by peripheral infections are able to alter their response and secrete inflammatory mediators which promote the neurodegenerative process (Perry et al., 2002).

1.9. Models of neurodegenerative disease

The importance of the numerous neurodegenerative diseases has given rise to many *in vitro and in vivo* models of chronic neurodegeneration. The neurodegenerative process can be triggered in many ways and is most tractable in the face of an acute insult whereby the sequence of events resulting from neuronal insult, dysfunction and death can be followed in a short period. *In vitro* models are useful in studying the toxic effects of mutant proteins and also allow cellular changes to be investigated in a very short time period. However the nature of these models makes it difficult to resolve the full sequelae which are much better studied in *in vivo* systems. Additionally, although the sHsps react to acute stress as described in the previous section and also reviewed in Wyttenbach et al. (2010 in press) their role during chronic conditions of stress are the main focus of this thesis, therefore only examples of chronic models of neurodegeneration will be described below followed by more detailed descriptions of a HD and prion mouse models.

1.9.1. Chronic models of neurodegeneration

In vivo models of chronic neurodegeneration are routinely used to provide a disease setting that much better reflect the human conditions. These models develop neurodegeneration over a time course of a number of weeks and months thus taking into

account the slow and progressive distinctive nature of these diseases, but still in an experimentally tractable timescale (Turmaine et al., 2000).

Tg models of PD and AD have been described, for example mice overexpressing mutant α-synuclein A53T from the mouse prion promoter develop adult-onset neurodegeneration and motor dysfunction leading to death (Lee et al., 2002). These mice also show neuronal abnormalities including pathological accumulations of detergent insoluble α-synuclein, ubiquitin and thioflavin-S-positive structures. The α-synuclein inclusions are reported to be similar to LBs and contain fibrils similar to those observed in PD patients (Giasson et al., 2002).

Drosophila models of tauopathies such as fronto-temporal dementia with parkinsonism linked to chromosome 17 (FTDP-17) have also been established. Tg flies expressing FTDP-17 mutant (R406W or V337M) tau show late-onset disease, accumulation of mutant tau, progressive degeneration, shortened lifespan and selective neuronal vulnerability (Wittmann et al., 2001).

Non-human primate models have also been used to study chronic neurodegeneration. Due to the high degree of physiological, neurological and genetic similarities with humans, non-human primates such as rhesus macaques are considered one of the best models for understanding human physiology and disease (Yang et al., 2008). Lentiviral gene transfer has been used to genetically modify animal genomes and was the basis of the generation of tg HD monkeys. These monkeys reveal unique cellular changes and pathogenesis, including clinical features such as dystonia, chorea and seizure that could be compared to HD patients (Wang et al., 2008, Yang et al., 2008).

In vivo models have been particularly useful in contributing a greater understanding of pathogenesis and offer the possibility of using genetic screens to unravel the mechanisms of pathogenesis. All of these disease models have differing pathologies, with region and cell type specific vulnerabilities and abnormal deposits of protein aggregates as described above. The locations of these aggregates differ with some being extracellular and others intracellular. Two well established models of extra/intracellular aggregation are the R6/2 HD mouse model and the ME7 prion disease mouse models that show different disease pathologies that will be described below. The analysis of these particular models in relation to chaperone expression would allow a comparison of the consequences of

extracellular and intracellular protein deposition respectively. Indeed, there is good evidence that both HD and prion diseases are modulated by chaperone pathways (Sakahira et al., 2002, Summers et al., 2009). Given than many of the cellular functions that can be modulated by the sHsps are also altered during either disease as described above, suggests a potential involvement for the sHsps in both intracellular and extracellular proteinopathies.

1.9.2. Models of polyQ diseases

Examples of models include a variety of fly and mouse models of polyQ diseases such as SCA1 (Fernandez-Funez et al., 2000) and SCA3 (Warrick et al., 1998). These models vary in the length of the mutant protein and number of polyQ repeats. For example SCA1 tg mice have been established bearing full-length ataxin-1 with 82 polyQ residues and are characterized by Purkinje cell dysfunction as determined by loss of motor coordination (Clark et al., 1997). Knock-in mice expressing full length ataxin-1 SCA1 79Q produce only a mild, late-onset phenotype (Lorenzetti et al., 2000).

Many transgenic model of HD are currently utilized to investigate the pathological mechanisms associated with the expression of mtHtt. These models consist of either full length htt or exon 1 fragments of the mtHtt protein in which there is an expanded poly Q repeat. For example, the yeast artificial chromosome (YAC) mouse model expresses a full-length human mtHtt gene with 46 or 72 polyQ repeats (Hodgson et al., 1999). These mice show selective degeneration of the MSNs and present with intranuclear inclusions. The R6/1 and R6/2 transgenic lines on the contrary only express the first exon of the human mtHtt gene with an expanded polyQ tract and were the first mouse models developed to study HD (Mangiarini et al., 1996). R6/2 transgenic mice also show phenotypic features of HD such as motor alterations, cognitive impairment and loss of body weight (Carter et al., 1999, Lione et al., 1999, Stack et al., 2005). Several knock-in mice have also been generated by the insertion of CAG repeats into the endogenous htt gene (Menalled, 2005). The R6/1 (approximately 115 polyQ repeats) and R6/2 (approximately 150 polyQ repeats) transgenic lines differ in CAG repeat length and disease onset. R6/1 animals develop a progressive neurological phenotype at

approximately 4-5 months of age, whereas for the R6/2 line this occurs at around 2 months (Mangiarini et al., 1996).

1.9.2.a.   The R6/2 HD mouse model

  The R6/2 mouse model of HD is routinely used to investigate the progression of HD, as it serves as a valuable model of chronic neurodegeneration with region and cell specific vulnerabilities. R6/2 mice show initial signs of motor symptoms at 5-6 weeks and difficulties in a number of tasks such as swimming and rotarod performance are observed (Carter et al., 1999). MtHtt intranuclear and extranuclear ubiquitinated inclusions appear intracellularly in the striatum and the cortex at 3-4 weeks of age (Morton et al., 2009). Neurological abnormalities are seen by 8 weeks, particularly stereotypical hind limb grooming movements. Between 8-12 weeks, balance and coordination become increasingly impaired (Carter et al., 1999). Impairments in learning and memory are seen in the Morris water maze test, which worsen up to the age of 7 weeks after which this cognitive task cannot be used due to severe motor deficits. Typically R6/2 mice are severely impaired by 7-12 weeks of age and show progressive loss of body weight after 12 weeks (Mangiarini et al., 1996, Carter et al., 1999). The R6/2 mice in most colonies die at around 13-16 weeks of age, but this may vary by a few weeks.

  Although no gross or microscopic abnormalities in the brain structures of R6/2 mice are observed (Mangiarini et al., 1996), motor dysfunction involving resting tremor in all limbs in R6/2 animals strongly suggests a basal ganglia lesion. Additionally, epileptic seizures have a cerebral focus and are observed in these animals. These mice do not develop a pronounced ataxia, wide-based gait or fall when moving; neither do they lose their righting reflex. This suggests that there is no major cerebellar lesion in the R6/2 mice (Mangiarini et al., 1996). Thus the striatum and the cortex could be considered to be regions particularly vulnerable in this disease model and the cerebellum as a relatively spared area of the brain. In the R6/2 striatum, the cell bodies of the MSNs shrink by about 20% and the size of their dendritic fields are also reduced (Klapstein et al., 2001). However, there are also a number of peripheral pathologies and inclusion bodies have been detected in several other non-CNS tissues (Sathasivam et al., 1999). The pathological events associated with the R6/2 model are summarized in Figure 1.11.
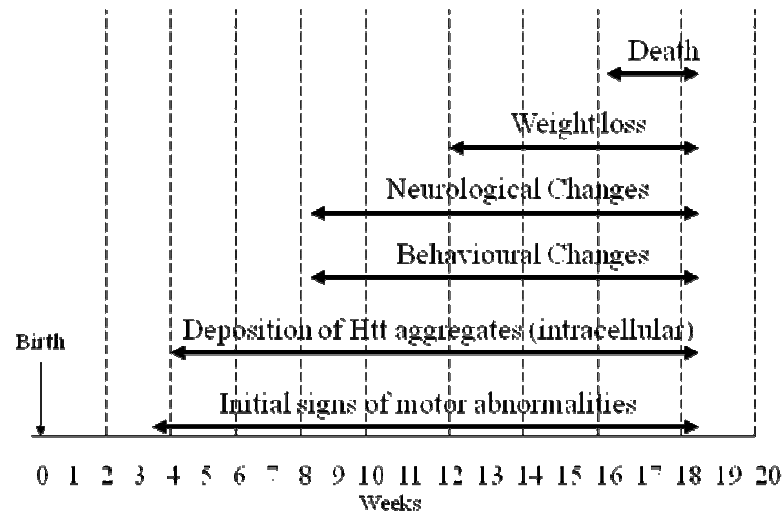
Figure 1.11. Summary of pathological events in the R6/2 mouse model of HD. Arrows indicate the time at which pathological events have been described (Carter et al., 1999, Morton et al., 2009).

1.9.3. Models of prion disease

Infection of mice with sheep scrapie and subsequent mouse to mouse passages has led to the identification of different scrapie strains which differ in the neuropathological changes they induce. These strains are used as models of prion disease and are distinguished by their incubation times and patterns of vacuolation (Bruce, 2003). Additionally the same strains are able to produce different disease outcomes, such as severity, location, and duration of disease, as a consequence of interactions with the host genotype (Gonzalez et al., 2002). Examples of some scrapie strains used in many studies are shown in Table 1.5. The ME7 strain displays distinct hippocampal pathology with selective neuronal loss (Cunningham et al., 2003).

Strain	Pathology
ME7	Deposition of PrP mainly in the hippocampus. Synaptic and cell loss in CA1 (Gray et al., 2009)
22L	PrP^{sc} deposition and vacuolation in the cerebellar cortex (Skinner et al., 2006)
RML	PrP^{sc} deposition and vacuolation mainly in the pons, midbrain and thalamus (Siso et al., 2002)
87V	PrP^{sc} deposition and selective CA2 cell loss (Jamieson et al., 2001)

Table 1.5. Examples of scrapie stains with specific neuropathology.

1.9.3.a. ME7 mouse model of prion disease

The ME7 mouse model of prion disease in C57BL/6J mice is routinely used to investigate the progression of prion disease in mammals and serves as a model of chronic neurodegeneration with cell specific vulnerabilities (Gray et al., 2009). Disease is transmitted by injecting prion infected brain homogenate (ME7) into the dorsal hippocampus of C57/BL mice. Control animals are injected with non-infected brain homogenate (NBH). Prion infected mice develop progressive neurodegeneration with hippocampal pathology over a number of weeks post injection (pi). The selective hippocampal deficits observed in this model has been shown to be independent of the site of injection in the brain (Bruce et al., 1991). The distinct pattern of degeneration in the hippocampus and the defined anatomical pathways and neuronal circuitry allows the investigator to specifically study hippocampal pathology in a tractable way. It is also important to note that ME7 infected mice show pathological changes in other brain regions at end stage of disease, for example neuronal loss, vacuolation and astrocytosis are observed in the thalamus (Bruce et al., 1991, Cunningham et al., 2005).

One of the early events to occur in ME7 animals is the extracellular deposition of abnormal misfolded PrP^{sc} (Jeffrey et al., 2000). This is first observed in the hilus of the dentate gyrus (DG) at 8 weeks post inoculation followed by the CA3 and CA1 regions. Increasing burden and deposition of misfolded PrP^{sc} occurs in a time dependent, anterograde fashion (Cunningham et al., 2003). At late stage of disease deposits are present throughout the hippocampus in the extracellular space surrounding neurons and

their processes. This is similar to the deposition seen in human brains (Armstrong et al., 2001b). PrP^{sc} accumulation does not correlate with neuronal/synaptic loss, as neurodegeneration is first seen in the stratum radiatum of the CA1 at which point PrP^{sc} is sparsely distributed in this region (Siso et al., 2002, Cunningham et al., 2003).

Prior to the onset of clinical symptoms and neuronal death, degeneration within the CA1 region of the hippocampus is seen.   Synaptophysin staining was found to be significantly reduced at 12 weeks with increasing disorganization of the CA1 region (Cunningham et al., 2003, Gray et al., 2009). This was associated with a loss of synapses in the stratum radiatum of the hippocampus. By 19 weeks 40% neuronal loss was observed in the CA1 region (Jeffrey et al., 2000, Cunningham et al., 2003, Siskova et al., 2009).

ME7 infected animals produce an inflammatory response with activation of microglia and astrocytes as early as 8 weeks, coinciding with PrP^{sc} deposition (Betmouni et al., 1996). The inflammatory response seen during ME7-induced prion disease is atypical in nature (Perry et al., 2002). Pro-inflammatory cytokines interleukin-1β (IL-1β), tumor necrosis factor-α (TNF-α) and interleukin-6 (IL-6) are modestly induced, however the anti-inflammatory molecule TGFβ1 is induced and an ensuing anti-inflammatory response is observed (Betmouni et al., 1996, Walsh et al., 2001, Cunningham et al., 2002). Activated microglial morphology along with an anti-inflammatory profile is rather indicative of a macrophage like response associated with phagocytosis and digestion of apoptotic cells (Fadok et al., 2001). This activation correlates with synapse loss leading to the speculation that activated microglia are involved in removal of these synapses. However, recent data suggests that this may not be the case and microglia may not be involved in 'synaptic stripping', but that this could be a neuron autonomous event (Siskova et al., 2009).

Synaptic loss and dysfunction are thought to underlie the early behavioural deficits seen in this mouse model of neurodegeneration. Mice display impairment of burrowing behaviour, nesting, glucose consumption, and increased open field activity at 13 weeks. Impairments in other behavioural readouts such as rotarod and horizontal bar tasks become apparent later in disease (Deacon et al., 2001). By 21 weeks clinical signs are visible. The pathological events that occur in the ME7 model are summarized in Figure 1.12.
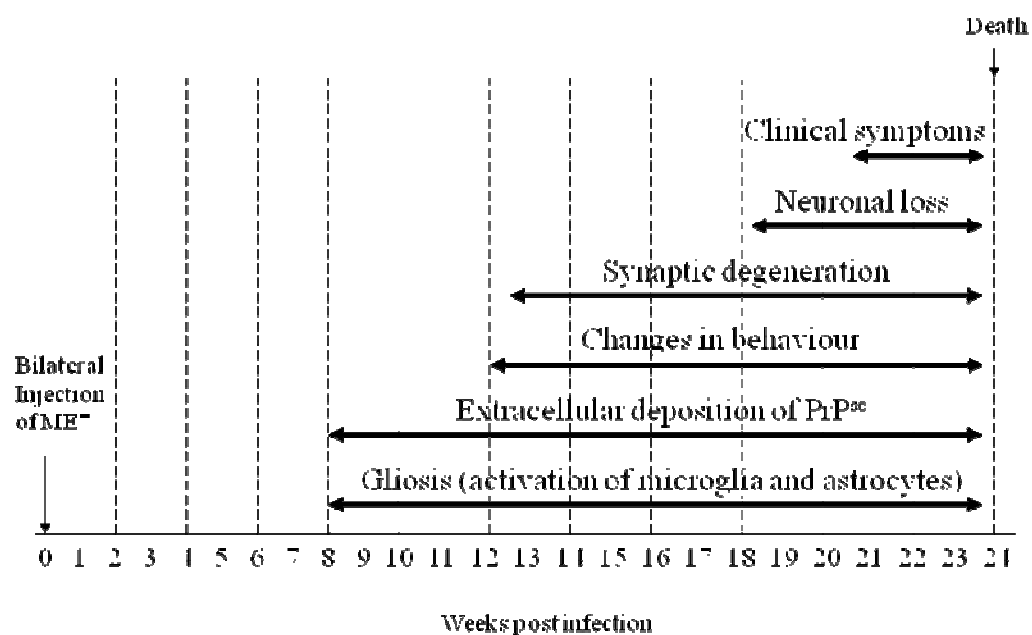
Figure 1.12. Summary of pathological events in the ME7 mouse model of prion disease. Arrows indicate the time post infections (pi) at which pathological events have been described (Betmouni et al., 1996, Cunningham et al., 2003, Gray et al., 2009).

The hallmarks and tractability of the ME7 model is useful to study chronic neurodegenerative changes in a relatively short time window. While this model allows investigation into the neurodegenerative processes associated with extracellular protein aggregation, the R6/2 model of HD (described in section 1.9.2 a) allows examination of chronic neurodegeneration in the context of intracellular aggregation. Due to the tractable neuropathology and the similarly short lifespan of these two animal models, they offer an excellent opportunity to investigate the involvement of molecular chaperones at specific time points during disease progression.

1.10. Aims

The importance of the sHsps is evident by the key cellular processes in which they participate and hence dysregulation of sHsp function could participate in proteinopathies of the CNS. Little is known about the physiological role of the sHsps under normal conditions in the CNS or their contribution to CNS disease progression. Therefore, the aims of this project are (i) to investigate and establish a baseline of mRNA and protein expression for the sHsp family in the mouse CNS under physiological conditions, (ii) with a focus on the sHsps found to be constitutively expressed as established in (i), investigate their expression under pathological conditions by using two mouse models of protein misfolding disease (ME7 and R6/2). The use of these two models would allow analysis in the context of chronic neurodegeneration associated with intra- and extracellular misfolding.

Chapter 2 – Materials and Methods

2.1. Animal husbandry

C57BL/6J inbred mouse strain resulting from the crossing of consecutive generations of brother/sister matings, allowing offspring to posses genetic and phenotypic uniformity were housed in groups of 5 or 10 and maintained at a room temperature of 21-23°C and the relative humidity was controlled (55 ± 10%) on a standard 12 hour light: 12 hour dark cycle. Mice had *ad libitum* access to food (standard laboratory chow [RM-1, Special Diet Services, UK]) and water. Mice were purchased from Harlan Laboratories (UK) or Charles River Laboratories (UK) and were permitted to acclimatise for at least seven days prior to undergoing any surgical procedures. C57BL/6J mice from either Harlan or Charles River do not differ in pathology (Asuni et al., 2010).

R6/2 tg mice were genotyped and maintained in the Department of Pharmacology, University of Cambridge through a collaboration (courtesy of Dr. A. Jennifer Morton). Husbandry was performed as above; in addition, mice were given a supplementary feed each morning of a mash prepared by soaking 100g dry food in 230ml of tap water until the pellets were soft and fully expanded. Genotyping was carried out as previously described (Mangiarini et al., 1996, Morton and Leavens, 2000). Briefly genotyping was performed by PCR from tail snips taken at 3 weeks of age and CAG repeat lengths measured by sequencing (Laragen, USA). Mice with CAG repeat lengths of 227-236 and age-matched wt littermates were used for all experiments. All procedures were carried out in accordance with the Animals (Scientific Procedures) Act, 1986.

2.2. Animal Surgery

2.2.1. Surgery (NBH and ME7 models of prion disease)

Surgery was performed on C57BL/6J mice between 8 and 10 weeks old. Mice were anaesthetised with a cocktail of Ketamine/Xylazine given at a dose of 0.1ml/10g intra-peritoneally (1ml Ketaset, 0.5ml Rompun and 8.5ml sterile saline were mixed via inversion and stored at 4°C). The anaesthetic was kept on ice on the day of use, and was administered at 0.1ml per 10g of mouse. Lacrilube was used to prevent the eyes of the mice drying out during surgery, and Lidocaine ointment (BioRex Laboratories) was applied in both ears for local anaesthesia. Once fully anaesthetised, mice were mounted in

a stereotaxic frame (David Kopf instruments, CA). The scalp was cut and the skull exposed. The stereotaxic coordinates relative to Bregma were -0.2mm (anterior to posterior) and ± 0.17mm (medial - lateral), for the dorsal hippocampus. Holes were made at these coordinates and 1μl of normal (NBH) or ME7-infected (ME7) brain homogenate was injected bilaterally over a period of 1 minute, at a depth of -0.16mm. The incision was sutured using Mersilk (0.2mm). Animals were placed in a heated chamber (37°C) and allowed to recover as Ketamine/Xylazine may result in hypothermia. Once full righting reflex was restored, animals were re-housed in groups of 5 or 10. Experiments were conducted under project licence no: 30/2543 with personal licence: 30/8604. All procedures were carried out in accordance with the Animals (Scientific Procedures) Act, 1986.

2.2.2. Perfusion and tissue fixation

Animals were terminally anaesthetised with Pentobarbital and the thoracic cavity opened to expose the heart. A butterfly needle (27-gauge, Venisystems, Eire) was inserted into the left ventricle, and the right atrium was cut. Animals were perfused with heparin saline (0.9% saline containing 5000U/L heparin) until the perfusate ran clear. Where tissue was required for immunohistochemical analysis, animals were perfusion fixed with 10% neutral buffered formalin. R6/2 animals were perfusion fixed with 4% paraformaldehyde (PFA) at the University of Cambridge (courtesy of Dr. A. Jennifer Morton). ME7 and NBH animals were sacrificed at 8, 13 and 20 weeks post surgery. R6/2 tg and wt littermates were sacrificed at 4, 9 and 17 weeks of age.

2.3. Tissue extraction

2.3.1. Immunohistochemistry

Animals were terminally anaesthetised and perfusion fixed (section 2.2.2) before decapitation. The skull was removed and the exposed brain was carefully isolated, post fixed in formalin or 4% PFA (R6/2) and stored at 4°C. The brain tissue was dehydrated through an increasing alcohol series and immersed in Histoclear in a Leica-TP 1020 tissue processor:

70% ethanol	2 hours
70% ethanol	2 hours
80% ethanol	1 hour
90% ethanol	1 hour
Absolute ethanol I	1 hour
Absolute ethanol II	1 hour
Absolute ethanol III	overnight
Histoclear 2 I	4 hours
Histoclear 2 II	2 hours
Histoclear 2 III	overnight

The brains were submerged in paraffin wax (Polywax, UK) at 40°C, embedded in fresh wax and allowed to cool. The wax blocks were stored at room temperature. 10µm sections were cut on a Leica RM2255 rotary microtome and floated on dH$_2$O at 40°C (tissue floatation bath, LAMB). Sections were mounted on SuperFrost Plus (Fischer) microscope slides and dried overnight at 37°C. Slides were stored at room temperature.

2.3.2. NBH and ME7 tissue extraction

Animals were terminally anaesthetised and perfused with heparin saline (section 2.2.2). Animals were decapitated and the skull removed before the brain was lifted out. The forebrain and the cerebellum were removed. The brain was opened out from the midline, and the midbrain removed to reveal the hippocampi. The hippocampi were rolled away from the cortex, detached and the white matter removed from the two lobes of the hippocampus. The hippocampus was further microdissected into CA1, CA3 and DG regions. Tissue was weighed and kept on ice before homogenisation (10% w/v) in buffer (20mM Hepes/100mM KCl, pH 7.4, with Complete^{TM} protease inhibitors). 100µl equivalent to 20mgs (weight) of tissue was used immediately for RNA extraction using the RNeasy kit (section 2.5.1) and the remaining homogenates were stored at -20°C. Aliquots of all samples were taken to determine protein concentrations (section 2.8.2). 40µg of protein from each region was resolved by SDS-PAGE unless otherwise stated (section 2.8).

2.3.3. R6/2 transgenic and wild-type (and human) mouse tissue extraction

R6/2 tg and wt littermates were sacrificed by cervical dislocation and decapitated. The brains were carefully removed, snap frozen in liquid nitrogen and stored at -80°C until

required. This allowed the subsequent extraction of both protein and mRNA from the same tissue. Specific brain regions such as frontal cortex, striatum and cerebellum from 9 and 17 week R6/2 tg and wt animal were dissected on ice from frozen mice brains under a dissection microscope. Samples were processed for protein and mRNA extraction as described in section 2.5.1 and 2.8.1.

Frontal cortex, striatum and cerebellum from 4 and 9 week old R6/2 tg and wt animals and human samples were extracted at the University of Cardiff by Dr. Andreas Wyttenbach as follows. Pre-cut or microdissected brain tissue was added to pre-cooled 0.5ml tubes (-20C) containing half of the amount of beads from "Lysing D tubes" (obtained from Q-biogene). 400µl of ice-cold lysis buffer was then added on ice, containing:

> 40mM beta-glycerolphosphate
> 1mM EDTA
> 1mM Na-orthovanadate
> 25mM NaF
> 50mM Tris-HCl, pH 7.5
> 1% NP-40
> 120mM NaCl
> 1mM Benzamidine
> Roche Protease inhibitor Coctail
> Antifoam (1:1000, Sigma)

This lysis buffer was chosen as it inhibits proteases and phosphatases for analysis of phospho-proteins. Groups of 12 tubes were then processed in a fast preparation machine (using a bead-extraction approach) for 30 seconds (speed rotation: 4), left to cool down and extracted for 5 minutes on ice after which the tubes were spun for 3 minutes at 6000rpm in a microfuge. This ensured that tissue chunks and beads were not used for analysis. Then 3-4 x 100 µl aliquots of supernatant from each extraction tube was aliquoted into eppendorf tubes and frozen on dry ice with subsequent storage at minus 80°C.

Subsequently, human brain tissue was re-extracted by adding the supernatants back to the tubes containing the beads and remaining tissue chunks with addition of 2% SDS after which the tubes were transferred to a heating block and left for 4 minutes at 95C, after which the tubes were spun for 3 minutes at 6000rpm to remove any remaining SDS-insoluble materials and the beads.

Human tissue was provided by Drs. Richard Faull (University of Auckland, NZ) and Lesley Jones (University of Cardiff, UK) and all human samples were processed and analysed by A. Wyttenbach and M. U. Sajjad. Protein concentrations were estimated by BioRad protein assay (section 2.8.2). 40μg of protein from each brain region were resolved by SDS-PAGE for all experiments unless otherwise indicated (section 2.8).

2.3.4. C57BL/6J tissue extraction

For characterization of the sHsps under physiological conditions, (Chapter 3) adult (p60, C57BL/6J) mice were sacrificed by cervical dislocation and decapitated. Each was pinned dorsal side up and a laminectomy performed to extract the spinal cord. The mice were then pinned ventral side up, the skin was cut and pulled back to expose internal organs and skeletal muscle. Skeletal muscle from upper fore and hind limbs were removed. Testis, heart and eyes were also removed. Brains were carefully removed with olfactory bulbs intact. Brain and spinal cord tissue to be used for *in situ* hybridization was immediately placed in Tissue Tek OCT (Bayer Diagnostics) on dry ice (section 2.7). All samples were wrapped in foil and placed immediately in liquid nitrogen. The frozen tissues were stored at -80°C until required.

2.3.5. C57BL/6J whole brain tissue extraction

Whole brain from p60 adult mice (C57BL/6J) were removed and dissected in half. Each half was either homogenised in 10 volumes Hepes/KCl buffer (20mM Hepes/100mM KCl, pH 7.4, with Complete™ protease inhibitors) or lysis buffer as described in section 2.3.3 using a PowerGen 125 homogenizer (Fisher Scientific). Brain tissue homogenised in detergent (NP-40) was subsequently extracted on ice for 10min before spinning at 4°C for 10min at 3,000rpm. The resultant pellet (P1) was re-suspended in 5% SDS. An aliquot of the supernatant (S1) was kept for analysis and the remaining S1 sample was extracted on ice for 15min prior to spinning at 4°C for 6min at 6,000rpm. The pellet (P2) and supernatant (S2) were retained for analysis. This protocol was designed to investigate the differential distribution of the sHsps.

2.4. Reverse transcription-Polymerase Chain Reaction (RT-PCR)

2.4.1. RNA extraction

Brain, muscle, testis, heart and eye tissues (section 2.3.4) were weighed and homogenized in 1ml of TRIzol Reagent (Invitrogen) per 50-100mg of tissue using a PowerGen-125 homogenizer (Fisher Scientific). Muscle homogenates were first centrifuged at 4˚C for 10mins at 12,000 x g. This additional isolation step was performed to remove polysaccharides and high molecular weight DNA into the pellet, and retain RNA in the supernatant. The supernatant was transferred to a clean eppendorf tube and treated in the same way as other samples. Homogenized samples were incubated at 15-30˚C for 5min to allow the complete dissociation of nucleoprotein complexes. 0.2ml of chloroform was added per 1ml of TRIzol Reagent in a fume hood. Samples were shaken vigorously by hand for 15sec and incubated at 15-30˚C for 3min. Samples were then centrifuged at 4˚C for 15mins at 12,000 x g. Following centrifugation, the colourless mRNA containing upper aqueous phase was removed carefully to prevent disruption of the lower phenol phase and mRNA was precipitated by adding propan-2-ol. The samples were incubated at 15-30˚C for 10min, and centrifuged at 4˚C for 10mins at 12,000 x g. The supernatant was removed and the RNA pellet washed once with 75% ethanol (at least 1ml) by vortexing prior to centrifuging at 4˚C for 5min at 7,500 x g. The supernatant was removed and the mRNA pellets air dried for 10min. Pellets were dissolved in diethylpyrocarbonate (DEPC) -H_2O by passing the solution a few times through a pipette tip, giving an approximate concentration of 2mg/ml; samples were then incubated at 55˚C for 10min to promote dissolution of the mRNA pellet.

2.4.2. cDNA synthesis

The concentration and quality of mRNA was determined using a spectrophotometer and the Agilent 2100 Bioanalyser. First strand cDNA synthesis was set up as follows using SuperScript^{TM} II RT (Invitrogen):

Oligo (dT)$_{12-18}$(500μg/ml)   1μl
Total RNA   (1ng-5μg)   4μl
dNTP Mix   (10mM each) 1μl
DEPC-H_2O 6μl

The above reaction was heated to 65°C for 5min and quick chilled on ice. Tubes were briefly centrifuged and the following reagents added:

5X First-Strand Buffer	4μl
0.1M DTT	2μl
ddH$_2$O	1μl

Tubes were mixed gently and incubated at 42°C for 2min. 1μl of SuperScript^{TM} II RT was added, and mixed by pipetting. Reaction tubes were incubated at 42°C for 50min and the reaction was inactivated by heating at 70°C for 15min. cDNA was stored at -20°C.

2.4.3. Polymerase Chain reaction (PCR)

Oligonucleotide primers designed against mRNA were supplied by Invitrogen (Table 2.1) and were used to amplify cDNA specific targets. A master mix (x7) was set up as follows for each primer pair:

10x PCR Buffer	5μl	
dNTP mix (10mM each)	1μl	
Forward Primer (10μM)	1μl	
Rev Primer (10μM)	1μl	50μl
Taq DNA polymerase	0.5μl	
ddH$_2$O	39.5μl	
TEMPLATE	1μl	

A thermal cycler (Gene AMP PCR System 9700 – Applied Biosystems) with a heated lid was used to set up cycling conditions for PCR. The cycling parameters highlighted in boxes were adjusted in order to optimize conditions for each primer pair, details are listed in Table 2.1:

Initial denaturation:	2min	94°C	
Denaturation:	40sec	94°C	
Annealing:	30sec	57°C	35 cycles
Extension:	2min	72°C	
Final Extension:	10min	72°C	

Re-amplified cDNA products were stored at -20°C.

2.4.3.1. Oligonucleotide primer design

All sequences were subjected to an NCBI nucleotide-to-nucleotide blast search to check for specificity. Self-annealing and hairpin formation was checked using the Oligonucleotide Properties Calculator. All oligonucleotides are listed in pairs.

Probe	Primer	5'-3' Primer sequence	Predicted PCR product size (bp)	annealing temp (°C)	extension time (min)
HspB1 A	Forward	CGC CTC TTC GAT CAA GCT TTC	549	58	1
HspB1 B	Reverse	CTA CTT GGC TCC AGA CTG TTC			
HspB2 A	Forward	CTG CCG AGT ACG AAT TTG CC	501	57	1
HspB2 B	Reverse	CTC TGG CTA TCT CTT CCT CTT			
HspB3 A	Forward	TGC GTT ATC AGG AGG AGT TTG	392	57	1
HspB3 B	Reverse	CCA CCA AGA TTC CAT CAT GAC			
HspB4 A	Forward	TCA GCA TCC TTG GTT CAA GCG	427	58	1
HspB4 B	Reverse	CAC ATT GGA AGG CAG ACG GTA			
HspB5 A	Forward	TTC TTC GGA GAG CAC CTG TTG	417	58	1
HspB5 B	Reverse	CTC TTC ACG GGT GAT GGG AAT			
HspB6 A	Forward	TGC TTC AGS TCC TTT ACC AG	305	57	1
HspB6 B	Reverse	CTC GAG CAA TGA ATC CGT GT			
HspB7 A	Forward	TTC AGA GCG GAG AGA AGC TTC	466	59	1
HspB7 B	Reverse	GGA AGG TCT GCT GGA CAT GTT			
HspB8 A	Forward	CTT TTC CAG ACG ACT TGA CAG	466	57	1
HspB8 B	Reverse	GTG ACT TCC TGG TTG TCT TGA			
HspB9 A	Forward	AAC GGA ATC AAG TGG CCA CTC	360	58	1
HspB9 B	Reverse	TTT CTG GGA CTG GCC TGT TTG			
HspB10 A	Forward	TTG GAC AGT GTT AGG AGG GAC	699	58	1
HspB10 B	Reverse	GAA TCG GCT TCC ACA GGG ATA			
Hsc70 A	Forward	CCT GCA GTT GGC ATT GAT CTC	1903	57	2
Hsc70 B	Reverse	CTG AAG AAG CAC CAC CAG ATG			
18S A	Forward	CTC CTC TCC TAC TTG GAT AAC	1663	57	2
18S B	Reverse	CTC ACT AAA CCA TCC AAT CGG			
HspB1 A	**Forward**	**ATG AGT GGT CGC AGT GGT T**	**275**	**56**	**1**
HspB1 B	**Reverse**	**CCG AGA GAT GTA GCC ATG TT**			
HspB8 A	**Forward**	**AGG TTT GGA GTG CCC GCT**	**349**	**56**	**1**
HspB8 B	**Reverse**	**GTG ACT TCC TGG TTG TCT TGA**			
ATP5b A	Forward	CAC GGT CAG AAC TAT TGC TAT G	1152	58	1.5
ATP5b B	Reverse	TCC TTT AAT GGT CTC CTT CAA			

Table 2.1. Oligonucleotide list used for PCR amplification

2.5. Quantitative-PCR (QT-PCR)

2.5.1. RNA extraction

Tissue was extracted as detailed sections 2.3.2 and 2.3.3. 20mg of tissue was used to extract total RNA using a Qiagen RNeasy Mini kit, according to the manufacturer's instructions (QIAGEN). Briefly, tissues were homogenised using a hand held Pellet Pestle

Motor (Kontes) in RLT buffer containing 1% β-mercaptoethanol. Samples were centrifuged for 5min at 14,000 rpm; the supernatant was removed and mixed with 1 volume 70% ethanol. Samples were loaded onto RNeasy mini columns. Columns were washed with RW1 buffer, followed by RPE buffer. RNA collected onto RNeasy mini columns was eluted in 50μl of RNase-free water.

2.5.2. Reverse transcription (RT)

The concentration of RNA was measured on a NanoDrop spectrophotometer; all samples had an absorbance A_{260}/A_{280} ratio close to 2 or above, denoting an acceptably pure nucleic acid sample. Using OligodT primers, 800ng of RNA from each sample was converted to cDNA using iScript cDNA synthesis Kit BIO-RAD. Briefly, first strand cDNA synthesis was set up as follows:

Oligo (dT)$_{12-18}$ (500μg/ml)	2μl
Total RNA (800ng)	-μl
5x iScript reaction mix	8μl
iScript Reverse transcriptase	2μl
Nuclease-free H$_2$O	up to 40μl

Samples were incubated for 5min at 25˚C, 30min at 42˚C, 5mins at 85˚C and the reaction was terminated at 4˚C. cDNA was stored at -20˚C.

2.5.3. Polymerase Chain reaction (QT-PCR)

HspB1, B5, B6 and B8 primers used for non-quantitative PCR (section 2.4.3) were tested for use by QT-PCR. HspB5 and HspB6 primers showed good amplification efficiency and melting curves showed a single peak. However HspB1 and HspB8 primers produced additional peaks in the melting curves, suggesting non-specific amplification and potential primer-dimer formation. For optimal PCR efficiency amplicon length should ideally be between 50-250bp, therefore additional primers were designed for HspB1 and HspB8 with the shortest possible amplicon size (Table 2.1 in bold). Additionally primers were designed against the housekeeping genes GAPDH (Applied Biosystems -TaqMan Rodent GAPDH Control Reagents) and ATP5b (Table 2.1). For HspB8, the reverse primer used

for non-quantitative PCR and the forward primer specifically designed for QT-PCR (in bold Table 2.1) provided the most optimal combination for QT-PCR analysis.

Reactions for QT-PCR were conducted in 96-well Microseal PCR plates (BIORAD) in a total volume of 25μl per well, using 1μl of cDNA, 10μM each of forward and reverse primers and 12.5μl of iQ SYBR Green supermix (BIO-RAD). Each sample was processed in duplicates. Cycling conditions were as described in section 2.4.3; additionally HspB1, HspB6 and HspB8 were run for 40 cycles. Cycle threshold levels (Ct) were automatically set at x1 standard deviation over the cycle range using Opticon Monitor 3 software. Melting curves of primer/template were checked to confirm the presence of a single peak indicating selective amplification of target cDNA (see Appendix 1).

QT-PCR and data collection were conducted using a Chromo4 real-time PCR machine. A "no template control" in which cDNA was omitted was included for each gene. cDNA (starting material = 800ng of RNA) from physiological tissue was used to generate a standard curve. This was constructed from 5-fold serial dilutions, starting with undiluted cDNA up to a 1:625 dilution. These samples were processed by QT-PCR with each of the mRNA specific primers so that a standard curve could be constructed from the resulting Ct values for each gene. The standard curve for each target gene was then used to calculate the relative concentrations of the target gene in all samples (as relative expression (arbitary units)). The relative expression of the target genes (sHsps) were normalised to the relative expression of the reference genes (GAPDH or ATP5b). Student's paired t-test was used to compare normalised data between ME7 and NBH; and R6/2 wt and tg animals. All brain regions were analysed separately. All statistical analyses were made using Graph Pad Prism 4.0 (section 2.15).

2.6. Agarose gel electrophoresis

Agarose gels containing ethidium bromide were used to separate DNA (PCR products) according to size. 1% gels were made by dissolving 0.5g of agarose in 50ml Tris acetate (TAE-1X) (mini-gel), or 1.5g agarose in 150ml TAE (maxi-gel). The TAE was prepared from a 50X stock (100ml/L 0.5M EDTA pH 8.0, 2M TrisBase, 57.1ml/L Glacial Acetic Acid, made up to 1L with ddH$_2$0). The agarose was dissolved by heating the mixture in a microwave. The molten agarose was allowed to cool slightly before pouring into a casting

mould. 10mg/ml of ethidium bromide was added; the gel was allowed to set and then placed into an electrophoresis chamber containing 1X TAE. Samples were mixed with gel loading buffer (6X, Invitrogen; 30% (v/v) glycerol, 60mM Tris-HCl (pH 7.5), 60mM EDTA, 0.36% (w/v) XCFF, and 3.6% (w/v) Tartrazine) to achieve a 1X final concentration. A molecular weight marker (1Kb Plus DNA Ladder, Invitrogen) was included in an adjacent lane to asses the size of the separated DNA. Mini-gels were run at 75mV and large-gels at 120mV.

2.7.   *In situ* Hybridization

2.7.1. Sectioning of Mouse Brains and Spinal Cords

Adult p60 mice (C57BL/6J) were sacrificed by cervical dislocation. Brains and spinal cords were carefully removed to keep all structures intact and immediately immersed in Tissue Tek OCT (Bayer Diagnostics), on 2-methylbutane over dry ice. The Frozen tissues were stored at -80˚C until required.

Brain and spinal cord tissue were placed in a cryostat (Leica, CM3050S) set at a chamber temperature of -16˚C to -18˚C for a minimum of 1 hour prior to cutting sections. 12μM sections were cut and thaw mounted onto slides (SuperFrost Plus, Fischer), air dried for 10mins, and desiccated at -80˚C until required.

Mouse brains were cut in three orientations: longitudinal, sagittal, and coronal. Coronal sections were cut approximately 1.10mm to -2.70mm (dorsal-ventral), sagittal sections were cut ± 2.76mm (medial-lateral), and horizontal sections were cut 0mm to 4mm (anterior-posterior) relative to Bregma. Spinal cords were cut longitudinally and coronally. Cell bodies were visualized with Nissl stain to determine the position of the sections relative to Bregma, every 10th slide was stained.

2.7.2. Nissl staining

Cresyl Violet was used to stain every 10th slide using the following protocol:

4% PFA (Chilled, on ice)	5min
dH$_2$O (X2)	3min
dH$_2$O/acetic acid	3min
0.25% Cresyl Violet	10min
dH$_2$O/acetic acid	5-10sec
70% ethanol	5-10sec
80% ethanol	5-10sec
95% ethanol	5-10sec
100% ethanol I	5-10sec
100% ethanol II	1min
Xylene	3min

Coverslips were then placed over the sections using DPX (Dibutyl phthalate - Xylene)-Mounting medium.

2.7.3. Probe selection for *In situ* Hybridization

Oligonucleotide probes were designed against sense and anti-sense mRNA sequences for each target gene. The probes were 45 bases long and supplied by Eurogentec (Table 2.2). Self-annealing and hairpin formation was checked to determine specificity of primers. Primers with potential self-annealing and hairpin formation were excluded and alternative primers designed (Oligonucleotide Properties Calculator). Sequence specificity for the desired target mRNA was determined using NCBI nucleotide-to-nucleotide BLAST searches (no homology to other transcripts >60%).

Position in gene	Name	5'-3' sequence
669-713	HspB1 antisense	GAG ATA GGC AGC AGG CTG ATG GCT TCT ACT TGG CTC CAG ACT GTT
	HspB1 sense	AAC AGT CTG GAG CCA AGT AGA AGC CAT CAG CCT GCT GCC TAT CTC
491-535	HspB3 antisense	TTG TAC TGT CTG GTG AAA CTC CGC GAT ATA AAC CCG TGT TCG TCC
	HspB3 sense	GGA CGA ACA CGG CTT TAT ATC GCG GAG TTT CAC CAG ACA GTA CAA
1025-1069	HspB5 antisense	AAA CTC AAT GAG GAA AGG GGA TCT ACT TCT TAG GGG CTG CGG CGA
	HspB5 sense	TCG CCG CAG CCC CTA AGA AGT AGA TCC CCT TTC CTC ATT GAG TTT
361-495	HspB6 antisense	GGC AGG CGG TAT CGG CGG TGG AAC TCT CGA GCA ATG AAT CCG TGT
	HspB6 sense	ACA CGG ATT CAT TGC TCG AGA GTT CCA CCG CCG ATA CCG CCT GCC
1271-1315	*HspB6 antisense*	*TGC ATT TAT TGG GGA CTG ATG GTA GGA AGG CCT GCG GAG ATG GGA*
	HspB6 sense	*TCC CAT CTC CGC AGG CCT TCC TAC CAT CAG TCC CCA ATA AAT GCA*
1519-1563	HspB7 antisense	GCC AGT GGG GGA GGA GAT AAG GGG GAG GCC AGG GGT GGA GAG ACC
	HspB7 sense	GGT CTC TCC ACC CCT GGC CTC CCC CTT ATC TCC TCC CCC ACT GGC
1083-1127	*HspB7 antisense*	*CAT GGG TGG GTC CTG GGC TGG AAG GGC ACG GGA GGC CGA AGA AGA*
	HspB7 sense	*TCT TCT TCG GCC TCC CGT GCC CTT CCA GCC CAG GAC CCA CCC ATG*
976-1020	HspB8 antisense	CCT GGG GCT GGG GAT GGG AGC GAA GGA CCA AGG CTG ACG TCT
	HspB8 sense	AGA CGT CAG CCT TGG TCC TTC TTC GCT CCC ATC CCC AGC CCC AGG
303-347	HspB9 antisense	GGA TCT AAG GTC GGC GGG AGC TGC ATT TGT CGG TGA ACA CTC TGC
	HspB9 sense	GCA GAG TGT TCA CCG ACA AAT GCA GCT CCC GCC GAC CTT AGA TCC
916-960	HspB10 antisense	CCT ACA GGA GAA TCG GCT TCC ACA GGG ATA GCA GGG GTT GCA AGG
	HspB10 sense	CCT TGC AAC CCC TGC TAT CCC TGT GGA AGC CGA TTC TCC TGT AGG

Table 2.2. Oligonucleotide primer sequences used for *In situ* hybridization

2.7.4. Radioactive labeling of probes for *In situ* Hybridization

A typical labelling reaction consisted of:

Oligonucleotide probe (20ng)	4µl
5X TdT Reaction buffer (Roche)	2µl
[alpha-^{35}S] dATP (Amersham, 9.25MBq, 250Ci (25µl))	1.3µl
CoCl$_2$	0.4µl
Terminal Transferase (Roche @ 10U/ µl)	1µl
ddH$_2$O	1.3 µl

The reaction was placed in a 33˚C water bath for 2hrs and the reaction volume was adjusted to 50µl by adding 40µl of ddH$_2$O. Labelled oligonucleotides were purified using ProbQuant G-50 Micro Columns (Amersham) according to manufacturer's instructions. To assess the quality of the labelling reaction the counts/min (cpm) were measured before (total count) and after (column count) purification of the oligonucleotide. These values were used to calculate specific activity of the probe as described below.

% incorporation = (Column count / Total count) × 100

Total cpm incorporated = (Column count × reaction volume) / volume counted

Average number of bases = (% incorporation / 100) × molar ratio of nucleotide to
    added to each oligo oligo in reaction

Amount of DNA synthesized = Average base added × 330 (average MW of base)
  × pmol of oligo present in the reaction

Specific activity = Total cpm incorporate

  µg DNA template + µg of DNA synthesized

HspB1 is used as example below:

The Total count for the HspB1 anti-sense probe was 766,139 cpm and the Column count was 373,338 cpm. A 50µl reaction was set up containing 1.3pmol of ^{35}S-dATP and 20ng (13pmol) of oligonucleotide:

% incorporation = (373338cpm / 766139cpm) × 100 = 48%

Total cpm incorporated = (373338cpm × 50µl) / 2µl = $9.3 × 10^6$

Average number of bases $\quad$ = (48% / 100) × (13/1.3) $\qquad$ = 4.8/oligo

Amount of DNA synthesized = 4.8 × 330 × 1.3pmol $\qquad$ = 2ng

Specific activity $\qquad\qquad$ = $\qquad\qquad\dfrac{9.3 \times 10^6}{0.02\mu g + 0.0019\mu g}$ $\qquad$ = 4.2 ×10^{8}cpm/μg

Typically the specific activity should be in the range of $1\times10^8 - 1\times10^9$ cpm/μg.

2.7.5. Prehybridization

To preserve the tissue, and prepare it for the hybridisation protocol, the section were fixed, delipidated, acetylated, and dehydrated. All solutions were made using DEPC treated ddH$_2$O and all reagents used were 'molecular biology grade' (i.e. RNAase free)

Sections were removed from the -80˚C freezer, and allowed to thaw for 10min. Sections were fixed in chilled 4% PFA made in phosphate buffered saline (PBS) pH 7.0 for 5min and rinsed twice with PBS. The slides were then rinsed twice with PBS. For each coplin jar, 50ml of TEA/AA solution was made immediately prior to use:

> 0.7ml Triethanolamine, TEA
> 0.125ml Acetic anhydride, AA
> 49.75ml DEPC-treated ddH$_2$0

The slides were immersed in the TEA/AA solution for 10min to allow positively charged amine acid groups within the section to become acetylated, which will subsequently reduce non-specific binding. The TEA/AA solution was removed and the sections dehydrated with graded ethanol solutions, delipidated in chloroform, and dehydrated again:

> 70% ethanol $\quad$ 1min
> 80% ethanol $\quad$ 1min
> 95% ethanol $\quad$ 2min
> 100% ethanol $\quad$ 1min
> Chloroform $\quad$ 5min
> 100% ethanol $\quad$ 1min
> 95% ethanol $\quad$ 1min

The sections were then placed upright in a slide holder and allowed to air dry.

2.7.6. Hybridization

Hybridization buffer containing the following reagents was made a day prior to use and stored at 4˚C:

> 50% Formamide (molecular biology grade)
> 4X SSC (20X stock: 175.3g NaCl, 88.2g Sodium Citrate, up to 1L with DEPC-ddH$_2$0)
> 200μg/ml sheared salmon sperm DNA
> 100μg/ml long-chain polyadenylic acid
> 25mM Sodium phosphate (pH7)
> 1mM Sodium pyrophosphate
> 10% Dextran Sulphate
> 5X Denhardt's solution (100X Stock: 20g Ficoll, 20g Polyvinylpyrolidone, and 20ng)
> Bovine Serum Albumin, up to 1L with DEPC-ddH$_2$0
> 20μl/ml of 1M DTT (added just before use)

The labelled probes were added at 200,000cpm/100μl of hybridization buffer, and mixed by vortexing. A 500-fold xs of unlabelled anti-sense probe was added to the remainder of hybridization buffer containing labelled anti-sense probe as an addition control. 100μl of hybridization buffer containing the specific probe was pipetted onto each slide (~50μl per section). Parafilm coverslips were carefully placed over the sections using forceps, whilst ensuring that there were no air bubble and the buffer was evenly spread. The slides were placed into chambers containing tissue paper saturated in 50% formamide and 4X SSC. The containers were sealed with parafilm and placed in an incubator at 42˚C overnight.

2.7.7. Post-hybridization

1X SSC was preheated in a water bath at 55˚C. The slides were placed in a rack after overnight hybridization and transferred to a wash chamber containing 1X SSC at room temperature for 10 minutes. The parafilm coverslips were gently removed from the slides. The slides were then transferred to wash chambers containing 55˚C 1X SSC for 30min. The slides were subsequently washed with 1X SSC (room temp) for 1 min, followed by a 5min wash in 0.1X SSC. The sections were dehydrated with 70% ethanol for 1 min and 95% for 5min. Finally, the slides were left to dry for 30min.

2.7.8. Signal detection – Film autoradiography

Dried slides were placed into an x-ray cassette and secured using 'magic tape'. BioMax 'Maximum Resolution' (Amersham) film which contains a single dull emulsion side was placed (emulsion face down) onto the slides. The cassette was closed, wrapped in plastic bags, and left at room temperature. Exposure times were set at 2 and 6 weeks for all probes.

2.7.9. *In situ* hybridization – Emulsion radiography

Slides used for film autoradiography were subsequently subjected to emulsion radiography. A light box fitted with a Kodak Safelight No.1 filter was used throughout the procedure. The light box was kept as far from the work bench as possible to minimize light exposure.

25ml of distilled water, plus one drop of glycerol was pre-warmed to 42ºC in a Coplin jar. Shreds of emulsion (Ilford K5 emulsion) were added to bring the solution up to 45ml and the solution was warmed to 42ºC to melt the emulsion. The solution was stirred carefully to avoid production of bubbles. Each slide was dipped in the emulsion and the back wiped clean before placing onto a metal sheet, which had been covered with ice. The slides were left to dry for 10min before being placed into slide holders and air dried for 2 hours in the dark. Slides were placed into racks and stored in a light proof box at 4ºC until ready for developing (3-5 fold exposure time for film autoradiography).

2.7.10. Signal detection – Emulsion radiography

Slides were removed from the fridge and allowed to equilibrate at room temperature. Kodak D19 developer was diluted 1:1 with distilled water and Ilford Hypam fixer was diluted 1:5 with distilled water. Under the same safelight conditions, the slides were placed into developer for 6min. The slides were then rinsed in distilled water and placed into fixer for 4min. The slides were then rinsed twice in distilled water and left to air dry. Sections were counterstained with cresyl violet by the following protocol:

ddH$_2$O + acetic acid	3min
Cresyl violet (0.25%)	2min
ddH$_2$O + acetic acid	10 seconds
70% ethanol	10 seconds

80% ethanol	10 seconds
95% ethanol	10 seconds
100% ethanol 1	30 seconds
100% ethanol 2	1min

Coverslips were then placed over the sections using DPX-Mounting medium. Slides were left to dry at room temperature overnight.

2.8. Western Blotting

2.8.1. Protein extraction

Tissues were extracted as described in section 2.3. Where tissue was not immediately homogenized after extraction, it was thawed on ice and homogenized in 10%w/v buffer (20mM Hepes/100mM KCl, pH 7.4, with Complete^{TM} protease inhibitors). Samples were stored at -20ºC until required.

2.8.2. BioRad protein assay

Serial dilutions of the tissue homogenates were used to assay protein concentration using the BioRad D_c protein assay method. Quantification was determined against a bovine serum albumin (BSA) standard curve (2mg/ml - 0.062mg/ml). All samples were tested in triplicates on a 96 well microtitre plate. Samples were incubated for 15min at room temperature before taking absorbance readings at 630nm.

2.8.3. SDS-Polyacrylamide Gel electrophoresis (SDS-PAGE)

The BioRad mini Protean II gel system was used for casting and running SDS-PAGE gels. The amounts of each reagent used to make the resolving and stacking gels is described in Table 2.3.

% Resolving gel	Stacker	30% Acrylamide	3M Tris (pH8.8)	10% APS	10% SDS	H$_2$O	TEMED
15	-	5ml	1.25ml	50μl	100μl	Up	10μl
12.5	-	4.2ml	1.25ml	50μl	100μl	To	10μl
10	-	3.3ml	1.25ml	50μl	100μl	10	10μl
7.5	-	2.5ml	1.25ml	50μl	100μl	Mls	10μl
Stacking Gel	5ml	-	-	50μl	-	-	10μl

Table 2.3. Amounts of reagents used to make SDS-PAGE gels. APS = ammonium persulphate, TEMED = N, N, N', N'-tetramethyl-ethylenediamine. Stacker solution (15ml acrylamide, 37.5ml 0.25M TRIS HCL (pH6.8), 1ml 10% SDS, (made up in 100mls ddH$_2$O))

TEMED was added to the resolving and stacking gels immediately prior to pouring. The resolving gel (pH 8.8) was poured and carefully overlaid with water until the gel polymerized. The water was removed and the stacking gel (pH 6.8) was poured onto the resolving gel. A 10-well comb was carefully inserted into the stacking gel avoiding formation of bubbles, until the gel was set.

Gels were placed in a gel tank containing 1X Laemlli buffer (5mM Tris pH8.3, 192mM Glycine, 0.1% SDS) and gel combs removed. 5X Sample buffer (10% SDS, 50% Glycerin, 25% β-mercaptoethanol, 312.5mM TRIS (pH 6.8), 0.005% Bromophenol Blue dye) was added to samples to get a 1X concentration. The samples were boiled at 95˚C for 4mins and centrifuged for 1min at 14,000rpm. Samples and 5μl of molecular weight markers (BioRad, Precision Plus Protein Standards) were loaded into the wells. The gels were run at 30mA through the stacking gel, and 50mA through the resolving gel.

2.8.4. Colloidal coomassie staining

To quantify the relative protein load of individual samples in each lane, fluorescence intensity derived from Colloidal Coomassie stained gels was used. After electrophoresis, protein gels were fixed for 1hr in 7% glacial acetic acid/40% methanol. Gels were soaked in colloidal stain (4 parts 1X working solution to 1 part methanol (Sigma)) overnight. Gels were placed in destain (45% ddH20, 45%Methanol, 10% Glacial acetic acid) for 60secs with shaking before rinsing in 25% methanol. Gels were further destained in 25% methanol for 4-6 hours before scanning at 700nm to visualize and quantify total protein content in each lane using an Odyssey Infrared Imaging Scanner and software (Licor).

Intensity values from boxed areas around single lanes were calculated by measuring the pixel intensity of the lane and subtracting the background pixel intensity value. Lanes were normalized to one another based on intensity values. The ratios were then used to normalize the calculated intensity for each antibody labelled protein band (Gray et al., 2009). Student's paired t-test was used to compare data. All statistical analyses were made using Graph Pad Prism 4.0 (section 2.15).

2.8.5. Semi-dry/overnight protein transfer

After electrophoresis gels were processed by semi-dry or overnight wet transfer. Blotting paper (Whatmans) and nitrocellulose membrane were immersed in transfer buffer (1X Laemmli buffer containing 20% (v/v) methanol). Gels were layered between sponge, blotting paper, and a nitrocellulose membrane. The nitrocellulose membrane was placed facing the positive electrode. For semi dry transfer, the blotting paper, nitrocellulose, gel sandwich was placed in a semi dry blotter, moistened with transfer buffer and run at 90mA for 90min. Overnight transfer involved placing the sandwich in an electrophoresis transfer chamber overnight at 4°C at a voltage of 30V. Protein transfer was checked by washing the nitrocellulose membrane in dH$_2$O, staining for 10min in Ponceau Red (BDH, UK), and rinsing in dH$_2$O to visualize the protein bands.

2.8.6. Antibody labeling

The nitrocellulose membranes were blocked with TBS (Trizma buffered saline (TBS, 25mM Tris, 0.15M NaCl, pH7.2) + 4% (w/v) milk powder + 0.5% (v/v) Tween-20)) for 1hr at room temperature and then incubated with primary antibody as indicated (Table 2.4) for 90min or overnight with shaking. Following overnight incubation membranes were washed in TBS-Tween (TBS + 0.5% (v/v) Tween-20) and incubated in 2.5% milk powder with the appropriate Alexa-fluorophore coupled secondary antibody (Alexa Fluor-680; Alexa Fluor-800, Molecular Probes), or one conjugated with horse radish peroxidase (HRP) (1:10,000 dilution), for 45min in the dark. The membranes were washed in TBS-Tween. Fluorescence was visualized and quantified with an Odyssey Infrared Imaging Scanner (Licor) at 700nm and 800nm to give intensity values in pixels/mm^2. The enhanced chemiluminescence (ECL) detection method was used according to

manufacturer's instructions, when detecting a signal with HRP conjugated secondary antibody. BioMax chemiluminescence film was used to develop the signal.

Antibody	Supplier	Dilution	Species
αA-crystallin	Stressgen (SPA-221)	1:1000	Rabbit
αB-crystallin	Stressgen (SPA-222)	1:500	Mouse
β-catenin	Sigma, UK (C2206)	1:1000	Rabbit
Hsc70	Stressgen (SPA-816)	1:2000	Rabbit
Hsp22	Abcam (ab15896)	1:500	Mouse
HspB8	Dr. Ch. Mohan Rao	1:500	Rabbit
Hsp22	Abcam (ab66063)	1:2000	Mouse
Hsp25	Stressgen (SPA-801)	1:1000	Rabbit
HspB2	Dr. W. Boelens	1:1000	Rabbit
HspB6	Dr. W. Boelens	1:1000	Rabbit
Hsp20	Stressgen (SPA-796)	1:2000	Rabbit
HspB7	Dr. W. Boelens	1:1000	Rabbit
HspB8	Dr. W. Boelens	1:1000	Rabbit
HspB9	Dr. W. Boelens	1:1000	Rabbit
Synaptophysin	Chemicon (Sy38)	1:1000	Mouse
PSD-95	Upstate signalling	1:1000	Mouse
GFAP	DAKO (Z 0334)	1:5000	Rabbit
MBP	Upstate signalling	1:5000	Mouse
Htt exon1	Dr. Gill Bates (S830)	1:3000	Sheep
Ubiquitin	Sigma (U 5379)	1:500	Mouse
Huntingtin (full length)	Chemicon (MAB2166)	1:500	Mouse

Table 2.4. **List of primary antibodies used for western blotting.**
Dr W. Boelens (Radboud University, The Netherlands); Dr. M. Rao (Centre for cellular and molecular biology, India); Prof G. Bates (University of London, UK).

2.9. Dot Blot analysis

Brain homogenate samples were extracted from R6/2 and wild type mice and subjected to dot blot analysis. Samples were treated with 100μl of DNase I (0.5mg/ml) for 1hr at 37ºC, triturated and left for 30min at 37ºC. Samples were quenched by adjusting the mixture to 20mM EDTA, 2% (w/v) SDS and 50mM DTT before boiling for 5min. 200μl (40μg) of the samples and a 2 fold dilution were loaded onto BioRad 96 well dot blot apparatus containing nitrocellulose acetate membrane (Whatman -200nm pore size). The nitrocellulose membrane was soaked in 2% SDS prior to use. Samples were extracted through the membrane by suction, and each well washed through twice with 0.1% SDS.

The membrane was then subjected to antibody labelling as described in section 2.8.6. Dot blots were developed by ECL.

2.10. Brain fractionation and synaptosome sub-fractionation

This method was adapted from (Cohen et al., 1977, Phillips et al., 2001). Whole brains (~0.5g) or hippocampi were homogenised in buffer A (0.32M sucrose, 1mM MgCl2, 0.1mM $CaCl_2$, 0.1mM PMSF) using a glass Teflon homogeniser (12 strokes), at 4°C. The homogenate was split into ultracentrifuge tubes and brought to a final sucrose concentration of 1.25M, by the addition of 2M sucrose and 0.1M $CaCl_2$. An aliquot of the homogenate was taken to assay protein content and to be used in western blotting. The homogenate was overlaid with 10mls of 1M sucrose, containing 0.1mM $CaCl_2$ and 5mls buffer A. This was centrifuged at 24,000rpm for 3hrs at 4ºC (Beckman L7 ultracentrifuge – SW28 Rotor). A band representing the synaptosome layer was collected at the 1.25M/1M sucrose interface; the myelin band was collected at the 1M sucrose/0.1M $CaCl_2$ buffer interface. The pellet (P1) was also collected and resuspended in buffer A. The synaptosome fraction was diluted in 1:10 ice cold $CaCl_2$, and brought to a final concentration of 1% Triton-X100 and 20mM Tris (buffered to pH6 or pH8). The samples were incubated on ice for 30 minutes and the insoluble material was pelleted by centrifugation at 20,000rpm for 30mins at 4ºC (Beckman L7 ultracentrifuge – Ti 70 Rotor. The insoluble pellets were resuspended in 5% SDS. Proteins in the soluble fractions were precipitated in 4 volumes acetone at -20ºC overnight, and recovered by centrifugation at 11,200rpm for 30min at 4ºC (Beckman – JA-20 Rotor). Resultant pellets were resuspended in 5% SDS. 12-18µg of protein from each fraction were separated by SDS-PAGE, electroblotted onto nitrocellulose membranes and probed with antibodies.

2.11. Immunohistochemistry

Coronal sections (10µm) were slide-mounted as described in section 2.3.1. Sections were heated for 30min at 60°C before being de-waxed in xylene I and II for 10min and re-hydrated through a series of decreasing ethanol concentrations (100% - 70%) at room temperature.

Slides were washed in PBS for 5min and incubated in 1% hydrogen peroxide/PBS for 15mins before washing in PBS-Tween (0.05%). Slides were microwaved for 3min in

citrate buffer (pH6), cooled and washed again in PBS-Tween (0.05%). Non-specific immunolabelling was blocked by incubation with 5% BSA for 1hr in a covered chamber. Sections were incubated with primary antibodies overnight in a covered chamber at 4°C using appropriate dilutions (Table 2.5), while the negative control sections were covered in 0.25%BSA/PBS. Slides were washed in PBS-Tween (0.05%) and incubating in appropriate biotinylated secondary antibody, diluted 1:200 (Vector Laboratories, UK). Sections were incubated in ABC complex (Vector Laboratories) for 45min and washed further in PBS-Tween (0.05%). Location of antibody binding was determined by immersing the sections in a diaminibenzidine (DAB) solution. The reaction was halted by transferring the slides to PBS. Sections were routinely developed for 1-3mins for optimal immunoreactivity. After washing further in PBS, sections were counterstained with Harris haematoxylin (BDH) for approximately 10 seconds. Once developed, sections were rehydrated through an increasing alcohol series (70% - 100%) and placed in xylene (Fisher Scientific) before coverslips were applied with DPX (VWR). Treatment with 1% hydrogen peroxide/PBS was omitted in sections used for fluorescent labelling.

Alexa-fluorophore coupled secondary antibodies (Alexa Fluor-488; Alexa Fluor-546, Molecular Probes) were diluted to 1:250 and used in place of biotinylated secondary antibodies. Slides were washed in PBS-Tween (0.05%); sections were counterstained with DAPI (Vector Shield) and coverslips were placed on top of sections and stored at 4°C prior to imaging.

Some minor changes to the protocol above were necessary for certain primary antibodies. For ubiquitin staining, the antigen retrieval step (citrate buffer treatment) was omitted and the sections were incubated in primary antibody for 1 week at 4°C with the addition of 0.1% sodium azide (personal communication, Dr J Morton). Lectin staining required the use of a manganese buffer (Na-Tris 25mM, 0.1mM $MgCl_2$, 0.1mM $CaCl_2$, 0.1 mM $MnCl_2$, 1% Triton X-100) which was used to incubate both primary and secondary antibodies. All control and disease tissue were treated in parallel. All images were taken using a Leica CM5000 microscope with settings as shown in Table 2.6. LAS-AF software was used for fluorescence microscopy and Q-Win image analysis for brightfield images.

2.12. Luxol fast blue staining

Slide mounted coronal (10μm) sections from R6/2 tg and wt littermates (section 2.3.1) were warmed for 30min at 37ºC. Sections were de-waxed in xylene I and II for 5min and hydrated up to 95% alcohol (100% I, 100% II and 95%) for 3mins. Sections were stained with Luxol fast blue (0.1% luxol fast blue powder, 95% alcohol, 0.5% acetic acid) for 2 hours at 60ºC. Slides were washed in distilled water and differentiated in 0.01% lithium carbonate till grey/ white matter was clearly distinguishable. Slides were further washed in distilled water and dehydrated in 95%, 100% II and 100% I alcohol, before clearing in xylene. Coverslips were placed on sections using DPX.

2.13. Tissue culture

HeLa cells were seeded on coverslips at a cell density of 20,000 cells per/well in a 24 well plate. Cells were supplemented with high glucose DMEM containing L-Glutamine (2mM), 10% fetal bovine serum (FBS) and penicillin/streptomycin (all from Sigma, UK). After 24 hours a 50-80% cells confluency was achieved and cells were transfected with constructs for EGFP-Q25 as a transfection efficiency control, HspB1 (Hsp25), HspB5 (αB-crystallin), HspB6 (Hsp20) and HspB8 (Hsp22). 0.6μg of DNA (constructs) and 1.2μl of lipofectamine (Invitrogen, UK) were diluted in 50μl of OPTI-MEM and incubated for 15min. DMEM was removed and replaced with pre-warmed OPTI-MEM (37ºC). 50μl of lipofectamine/DNA was added to wells and mixed gently. Cells were incubated at 37ºC with 95% humidity and 10% CO_2 for 5 hours. 1ml of DMEM with 20% FBS, L-glutamine, penicillin and streptomycin was then added per well to obtain a final FBS concentration of 10%. 24 hours after transfection, media was replaced with fresh supplemented DMEM.

Cells were either extracted (section 2.13.1) or processed for immunocytochemistry (section 2.13.2). Tissue culture and cell lyses were conducted by Dr. Andreas Wyttenbach and Ben Samson.

2.13.1. Collection of sHsp transfected cell lysates

Transfected cells were trypsinised and spun for 5min at 1,500rpm. Supernatant was removed and the pellet was overlaid with PBS. Pellets were spun for 1min at 3,000rpm. Supernatant was removed and pellets were resuspended in 30μl cell lyses buffer containing protease inhibitor (Roche) (1mM Tris HCL (pH 7.5), NP-40, 0.2M NaCl, 0.2M EDTA,

0.5M NaF, 1M β-glycerol phosphate, 1M benzamidine). Samples were incubated on ice for 30min and the cell lysates stored at -20°C. Lysates were subjected to western blot analysis (section 2.8).

2.13.2. Immunocytochemistry of cell culture

Transfected cells were fixed onto the coverslips with 4% PFA for 15min. Coverslips were washed 3 times for 5min in PBS and placed in fresh PBS before storing in 24 well plates at 4ºC. Coverslips containing cells were incubated in PBS containing 0.2% Triton-X100/1%BSA for 30mins before washing in PBS and incubating with monoclonal Hsp22 (a kind gift from Dr Mohan Roa) for 1hour. Coverslips were washed in PBS, and incubated in secondary antibody, diluted 1:500 (mouse Alexa-488) for 1 hour at antibody dilution of 1:50. Coverslips were washed in PBS, counterstained with Hoechst for 5min (1:1000) and washed further in PBS before being mounted with flouromount G. Coverslips were allowed to dry and stored in the dark at 4ºC. Images were taken using a Leica CM5000 microscope. LAS-AF software was used for fluorescence microscopy.

Antibody	Supplier	Dilution	Species
6H4 (PrP^{sc})	Prionics	1:4000	Mouse
GFAP	Dako (Z0334)	1:1000	Rabbit
GFAP	Sigma (G3893)	1:1000	Mouse
Tomato Lectin	Sigma (L0651)	1:100	Biotinylated glycoprotein
Synaptophysin	Chemicon (sy38)	1:1000	Mouse
HspB1	Stressgen (SPA801)	1:1000	Rabbit
HspB5	Stressgen (SPA223)	1:400	Rabbit
HspB5	Stressgen (SPA222)	1:200	Mouse
MBP	Upstate signalling	1:1000	Mouse
CNPASE	Abcam (AB6319)	1:400	Mouse
HspB8	Dr. Ch. Mohan. Roa	1:50	Mouse
Hsp22	DAKO (Z0458)	1:50	Mouse
Ubiquitin	Sigma (U5379)	1:1000	Rabbit

Table 2.5. Antibodies and conditions for use in immunohistochemistry and immunocytochemistry

2.14. Microscopy

2.14.1. Fluorescence

Tissue sections were imaged with a Leica DCF 300 FX microscope. Leica Application Suite Advanced Fluorescence imaging software was used to process images. Tissue sections were processed simultaneously from age matched NBH and ME7 animals (13 and 20 weeks) or R6/2 wt and tg (17 weeks) animals. Microscope settings were kept constant within age matched tissue; however it was necessary to adjust microscope settings for different objectives and between antibodies (Table 2.6).

Objective	10X			20X			40X			63X		
13wks (ME7/NBH)	E	G	I	E	G	I	E	G	I	E	G	I
HspB1	1	2	5	1	2	5	1	1	5	0.5	1	4
GFAP	1	2	5	2	3	5	1	3	5	1	3	4
DAPI	1	2	5	1	1	5	0.7	1	5	0.3	1	4
20wks (ME7/NBH)												
HspB1	4	1	5	0.7	3	5	1	1.5	5	0.7	1	5
GFAP	6	1	5	3	3	5	1.5	5	5	2	2	5
DAPI	4	1	5	1.5	2	5	1	2	5	0.2	1	5
20wks (ME7/NBH)												
HspB5	4	2	5	2	2	5	1	2	5	-	-	-
GFAP	3	2	5	2	4	5	2	4	5	-	-	-
DAPI	2	1.5	5	1.5	1	5	1	2	5	-	-	-
20wks (ME7/NBH)												
HspB8	2	4	5	1	4	5	1	4	5	-	-	-
GFAP	3	5	5	3	4	5	1	5	5	-	-	-
DAPI	1	3.1	5	1.6	4	4	1	3.5	4	-	-	-
17wks (R6/2 tg/wt)												
HspB5	2.4	4.1	5	1	7	5	1	5	5	-	-	-
CNP	5	3	3	5	3	4	2	4	5	-	-	-
DAPI	2	4	4	2	4	4	1	2	5	-	-	-
17wks (R6/2 tg/wt)												
MBP	4	5	5	2	2	5	2	4	5	-	-	-
DAPI	2	2	5	3	5	5	1	2	5	-	-	-

Table 2.6. Microscope fluorescence imaging settings. E = exposure; G = Gain; I = intensity. Unless otherwise stated in the results chapters, all settings were as shown in Table 2.6.

2.14.2. Visualising DAB staining

Tissue sections were imaged with a Leica DCF 300 FX microscope. Leica QWin V3 software was used to process images. Microscope settings were kept constant for all tissue analysed (Brightness = 77%; Gain = 1.0; Intensity = 1.5). It was not necessary to adjust these settings for different objectives. Shading corrections were set to none and where necessary white balance was automatically adjusted.

2.14.3. HspB5 cell count (R6/2 animals)

Images taken from the CA1, CA3 and DG (20X objective) of R6/2 wt and tg animals that had been processed for HspB5 and CNP (2'-3'-cyclic nucleotide 3'phosphodiesterase) double immunofluorescence were used to analyze the number of HspB5 and CNP positive oligodendrocyte cell bodies. Leica Application Suite Advanced Fluorescence software was used to identify positive cells. 20X magnification allowed analysis of the entire CA1, CA3 and DG field. Identifiable CNP positive cells (i.e. cell bodies that were immunopositive) were highlighted with a circle using software tools; this was automatically transferred to the equivalent image showing HspB5 immunofluorescence. The number of cell bodies stained for both proteins were manually counted. All cells that were CNP positive were also HspB5 positive therefore the total numbers of CNP/HspB5 positive cells from each hippocampal region in NBH animals were directly compared to the number of positive cells in ME7 animals. Student's paired t-test was used to compare data (section 2.15).

2.14.4. Confocal microscopy

13 week ME7 brain sections were imaged with a Zeiss LSM 510 Meta microscope and confocal images for excitations at 385-470 and 505 were scanned sequentially. DAPI (4',6-diamidino-2-phenylindole) was visualised using excitation at 558-719. Images were taken with a 63X objective. The gain, offset and pin hole were setup for each wavelength as shown in Table 2.7.

Wavelength (nm)	385-470	505	558-719
Gain	854	682	719
Offset	0.1%	0.1%	0.1%
Pin hole μM	88	86	80

Table **2.7. Confocal imaging settings.** GFAP fluorescence was analysed at 385-470nm and HspB1 fluorescence was analysed at 505nm.

2.15. Statistics

Western blot and QT-PCR data was analysed in Graph Pad prism (version 4.0). Student's paired t-test (two-tailed) was used to compare ME7 microdissected hippocampal tissue to age matched NBH tissue at all time points analysed, at a significance level of $P<0.05$. Unless otherwise stated, one-way analysis of variance (ANOVA) was used to compare expression of R6/2 tg tissue from each region to age matched wt littermates from the same region and between brain regions at each time point. This was followed by Newman-Keuls post-hoc test to determine significance ($P<0.05$).

Chapter 3 – Expression of the small heat shock protein family in the mouse CNS under physiological conditions

3.1. Introduction

The importance of molecular chaperones is evident by the physiological and pathological processes in which they participate (see general introduction). "Physiological" will be used to refer to a non-pathological state from this point forward. Some members of the sHsp family have been characterized and studied extensively; in particular HspB1 and HspB5. Many of these studies have focused on the role of the sHsps under stress and disease conditions (for review see (Sun and MacRae, 2005a, Ackerley et al., 2006) with few studies addressing their roles under physiological conditions (Plumier et al., 1997, Armstrong et al., 2001a). The sHsps are believed to have a unique expression profile in different tissues and some, like HspB9, are reported to be exclusively expressed in the testis (de Wit et al., 2004). Others, such as HspB1 have been shown to be ubiquitously expressed (Sugiyama et al., 2000, Kappe et al., 2001).

Little is known about the physiological roles of the sHsps in the CNS. However they are known to be involved in the regulation of cytoskeleton dynamics, redox-homeostasis and apoptosis, (see general introduction). Table 3.1 summarises what is known from the literature about the expression of the sHsps under physiological conditions prior to this study. The data consists of studies using rat, rabbit, pig and human tissue and reflects mRNA expression and/or protein expression. Currently the tissue expression profile of all 10 members of the sHsp family has not been systematically and comparatively characterized within a distinct tissue (e.g. the brain) from the same organism under physiological conditions in a single study.

3.2. Aims

The aims of this chapter are 1) to characterize the mRNA expression profile of the sHsps by RT-PCR in the mouse CNS and in control tissue (were they have been well documented); 2) to investigate the anatomical/spatial distribution of the sHsps in the CNS by *in situ* hybridization; 3) to investigate the protein expression of the sHsps in the CNS relative to control tissue; 4) to investigate the potential compartmentalization of the sHsps using brain and synaptosome fractions. This will allow a baseline for sHsp expression in the mouse brain to be established under physiological conditions.

3.3. Experimental design

We have used a number of techniques to measure transcript and protein in different tissues from adult mice. The choice of tissue used to characterise expression was determined by tissues previously reported to show expression. Brain and spinal cord tissue were used to represent the CNS. Non-CNS tissue such as muscle was used as control tissue, as up to 7 of the sHsps are known to be expressed in this tissue (Table 3.1). Eye was used as a control for HspB4 as this sHsp is abundantly expressed in this tissue. The testes were used as a control tissue for HspB9 and HspB10 expression, due to their selective expression in this tissue.

mRNA expression was investigated by two complementary techniques; RT-PCR and *in situ* hybridization (section 2.4 and 2.7). Protein expression of the sHsps was investigated by western blotting. In order to expand the characterization of the sHsp family, brain fractions and synaptosome sub-fractions (section 2.10) were used to investigate potential compartmentalization of the sHsps in the CNS.

	Brain	Lens	Heart	Liver	Kidney	Lung	Muscle	Testis
HspB1	√ (a)	√ (a)	√ (a)	√ (a)	√ (a)	√ (a)	√ (a)	√ (d)
HspB2			√ (b)				√ (e)	
HspB3			√ (h)				√ (h)	
HspB4		√ (i)						
HspB5	√ (a), (c)	√ (a)	√ (a)	√ (a)	√ (a)	√ (a)	√ (a)	
HspB6	√ (b), (c)	√ (b)	√ (b)	√ (b)	√ (b)	√ (b)	√ (b)	
HspB7			√ (g)	√ (b)			√ (g)	
HspB8	√ (b), (c)		√ (b)	√ (b)	√ (d)	√ (b)	√ (b)	√ (d)
HspB9								√ (d)
HspB10								√ (f)

Table 3.1. Literature based expression profile of the sHsps in various tissues. Combining data from a number of studies shows the different expression profiles of the sHsps. HspB1, HspB5, HspB6 and HspB8 show expression in most of the tissue analyzed. The heart and muscle are two tissues in which up to 7 of the sHsps are expressed. HspB4, HspB8 and HspB10 show selective expression in one tissue only. This table represents data from a number of species and techniques, so the expression profile of the sHsps are not directly comparable to one another. (a) (Tallot et al., 2003), (b) (Verschuure et al., 2003), (c) (Lein et al., 2007), (d) (Kappe et al., 2001), (e) (Golenhofen et al., 2004), (f) (Petersen et al., 1999), (g) (Krief et al., 1999), (h) (Sugiyama et al., 2000), (i) (Yang and Cvekl, 2005).

3.3.1. 10 members of the sHsp family in the mouse genome (sequence alignment)

The α-crystallin domain defines the sHsps, and is characteristic of this family of molecular chaperones. The 10 members were originally identified using databases provided by the public International human Genome Sequencing Consortium (IHGSC) and the private Celera human genome project. The human Hsp27 (HspB1) protein sequence was initially used as the query protein sequence to search the databases; this resulted in the identification of the 10 sHsps in humans (Kappe et al., 2003).

To determine whether the 10 sHsps present in the human genome, were also present in the mouse genome and to confirm they all contained the homologous and characteristic α-crystallin domain the NCBI (National Centre for Biotechnology Information) database (www.ncbi.nlm.nih.gov) was used to search for the sHsp.

BlastN and BlastP were used to search the NCBI database. The NCBI nucleotide search was used to search for proteins by name. In order to confirm that each sHsp contained the α-crystallin domain, the blast program rpsblast was used to search the conserved domain database (data not shown). The sequences obtained were used to perform a protein sequence alignment of all 10 members of the sHsp mouse family using ClustaW (www.ebi.ac.uk), a multiple sequence alignment program (Figure 3.1).

Figure 3.1. Alignment of the 10 mouse sHsps made in ClustalW. The alpha-crystallin domain is located approximately between positions 103 and 190. Colours are assigned according to the physiochemical characteristics of the amino acids. Residues in block colours are conserved, for example at position 130 there is a block of residues coloured blue. These valine residues are conserved in 9 of the sHsps. The histogram below represents the degree of sequence similarity, with highly conserved regions depicted by larger peaks and those that are different by small peaks. The greatest degree of homology occurs in the alpha-crystallin domain while the N- and C-terminal regions are more variable. Accessions Nos. are: NM_013560 (HspB1/Hsp25), NM_024441 (HspB2/MKBP), NM_019960 (HspB3), NM_013501 (HspB4/αA-crystallin), NM_009964 (HspB5/ αB-crystallin), NM_001012401 (HspB6/Hsp20), NM_013868 (HspB7/cvHsp), NM_030704 (HspB8/H11), AJ302069 (HspB9) and X79446 (HspB10/ODF1).

3.3.2. mRNA expression of the sHsps family

3.3.2.1.   RT-PCR

  mRNA was extracted from brain, spinal cord, eye, testis and muscle tissue (see section 2.4). The quality of the mRNA was monitored by the use of a spectrophotometer, agarose gel (data not shown) and Agilent bioanalyser. The spectrophotometer was used to determine the concentration and quality of the mRNA samples. 10μl of each RNA sample were run on agarose gels containing ethidium bromide, so that the two bands corresponding to 18S and 28S ribosomal subunits could be visualized (data not shown). In addition to this, the Agilent bioanalyser was used to determine mRNA concentration, quality and DNA contamination if present with the use of just 1μl of sample (Figure 3.2).

  The mRNA samples were reverse transcribed with equal amounts of template to produce cDNA. The cDNA was used to amplify target mRNA transcripts by PCR using gene specific primers designed to amplify across introns with the exception of the intronless genes HspB3 and HspB9 (Table 2.1). 5μl of PCR product were run on agarose gels (Figure 3.3), amplicons were of the predicted size for cDNA amplification (Table 2.1). Control reactions lacking reverse transcriptase were set up to exclude genomic amplification of the sHsps. All family members showed mRNA specific amplification in control tissue; HspB1, B2, B3, B5, B6, B7 and B8 displayed amplification in muscle homogenate, HspB4 expression was restricted to the eyes, and HspB9 and HspB10 showed expression in the testis (Figure 3.3). Five of the sHsps (HspB1, HspB5, HspB6, HspB7 and HspB8) showed mRNA amplification in the brain.
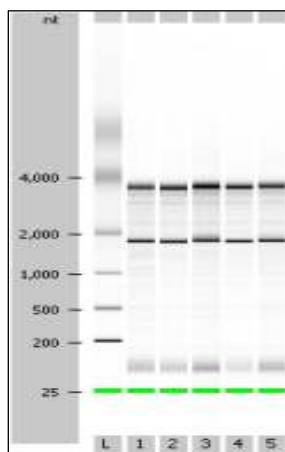
Figure 3.2 a. Computer generated gel of mouse tissue RNA.
Virtual gel image produced by Agilent 2100 bioanalyser, showing 28S and 18S ribosomal bands. Intactness of these bands and lack of smearing is indicative of good quality mRNA. 1μl of each sample was loaded onto a microchip and analyzed by the Agilent bioanalyser. (L: ladder; 1: eye; 2: brain; 3: spinal cord; 4: testis; 5: muscle).

1: EYE   rRNA ratio: 1.3

2: BRAIN   rRNA ratio: 1.4

3: SPINAL CORD   rRNA ratio: 1.3

4: TESTIS   rRNA ratio: 1.6

5. MUSCLE   rRNA ratio: 1.3
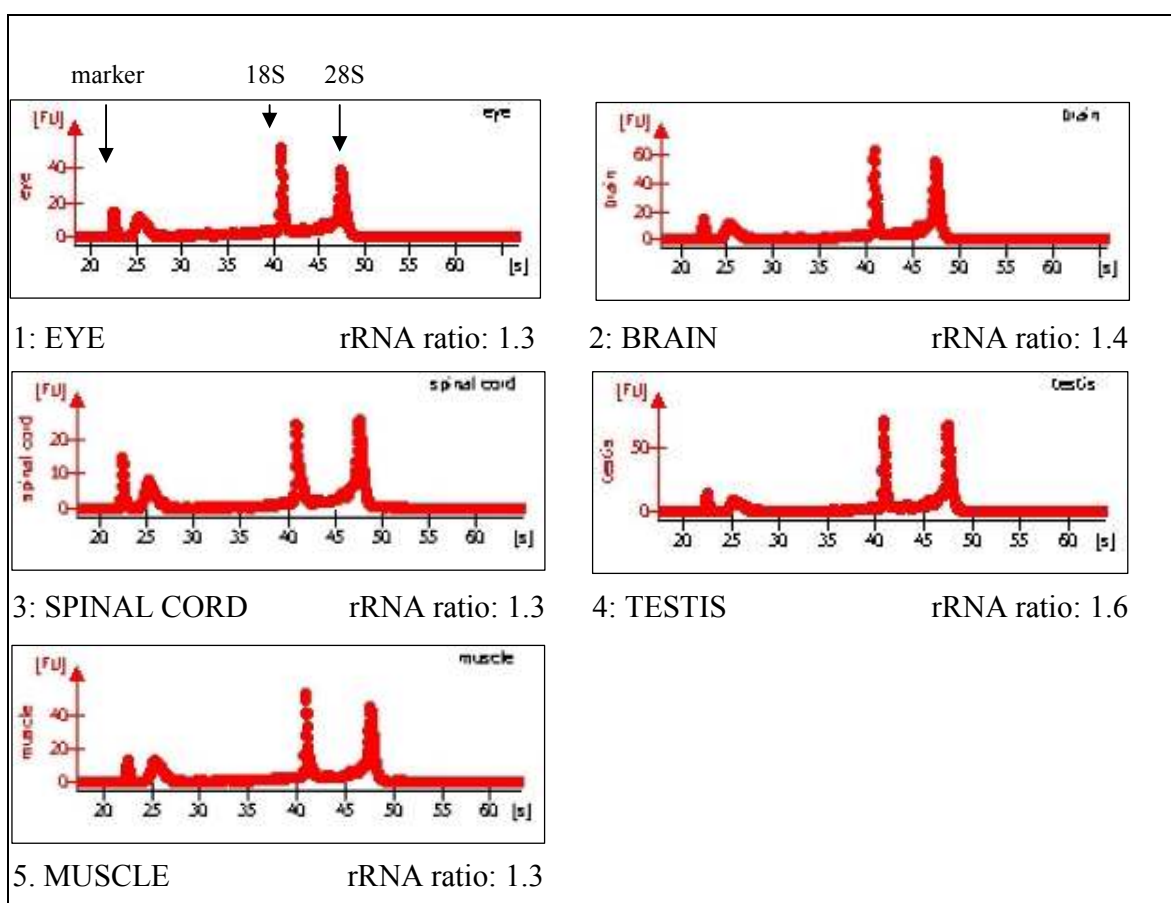
Figure 3.2 b. Electropherograms of RNA samples from mouse tissue.
Electropherograms produced by the Agilent bioanalyser for each mRNA sample are shown. Peaks correspond to 18S and 28S ribosomal RNA that are also visualized as bands in Figure.3.1a. Ribosomal RNA (rRNA) ratios (28S/18S) for each tissue are shown, these ratios provides information regarding quality of the mRNA sample (ratios greater that 1 represent good quality RNA). This mRNA was used to make cDNA for subsequent PCR reactions.
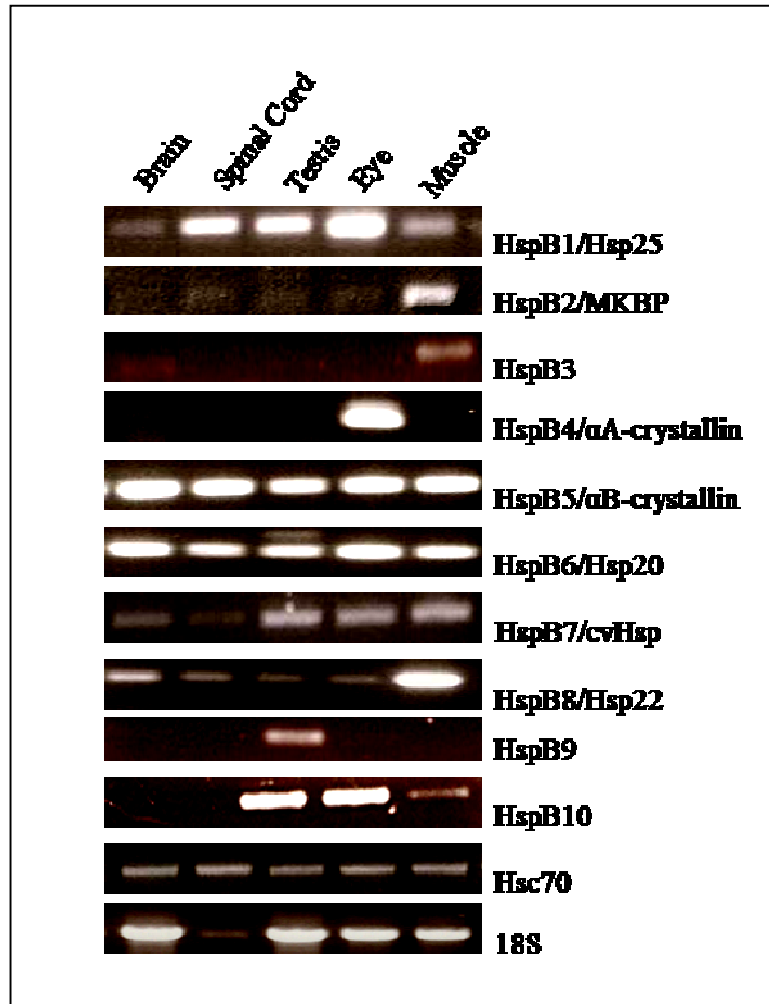
Figure 3.3. mRNA expression profile of the sHsp family in various mouse tissues by RT-PCR. All 10 family members of the sHsp family are expressed in control tissues. For HspB1, B2, B3, B5, B6, B7 and B8 this is the muscle; for HspB4 this is the eye; and for HspB9 and HspB10 it is the testis. 5 of the sHsps (HspB1, HspB5, HspB6, HspB7 and HspB8) show mRNA expression in the CNS. 35 PCR cycles were performed for all the sHsps and 25 cycles for Hsc70 and 18S. All cDNA amplifications were of the expected size (see Table 2.1) (n=4).

3.3.2.2.   *In situ* hybridization

The anatomical/spatial expression of the sHsp family in brain and spinal cord tissue was investigated by *in situ* hybridization. Mice brains were cut in three orientations: coronal, sagittal and horizontal. Spinal cords were cut in both longitudinal and coronal orientations (see section 2.7.1). A high throughput *in situ* hybridisation study of a vast number of genes has been established (Lein et al., 2007). The data has been compiled into a database called the Allen Brain Atlas (http://brain-map.org). This database is useful in that it provides a point of comparison for the characterisation of the sHsps by *in situ* hybridisation, which previously was not possible.

3.3.2.2.a.   Film autoradiography

In situ hybridization was performed as described in section 2.7. Films were developed after 2 and 6 week exposure times. In all cases signals not detected at 2 weeks, did not become detectable if left for another 6 weeks. Figure 3.4 - 3.8 show *in situ* hybridization images of the sHsps for which a signal was detectable at 2 and 6 weeks. Images are shown after a 2 week exposure as there was no difference at 6 weeks.

HspB1, HspB5 and HspB8 showed specific patterns of expression. HspB1 is expressed in the lateral (lv) and dorsal (d3v) ventricles of the brain (Figure 3.4 a). HspB5 shows a pattern suggestive of white matter specific expression (Figure 3.5 a). White matter structures such as the corpus callosum (cc), external capsule (ec) and fimbria (f) are labelled. Other white matter containing structures labelled by the HspB5 probe are listed in Table 3.2.
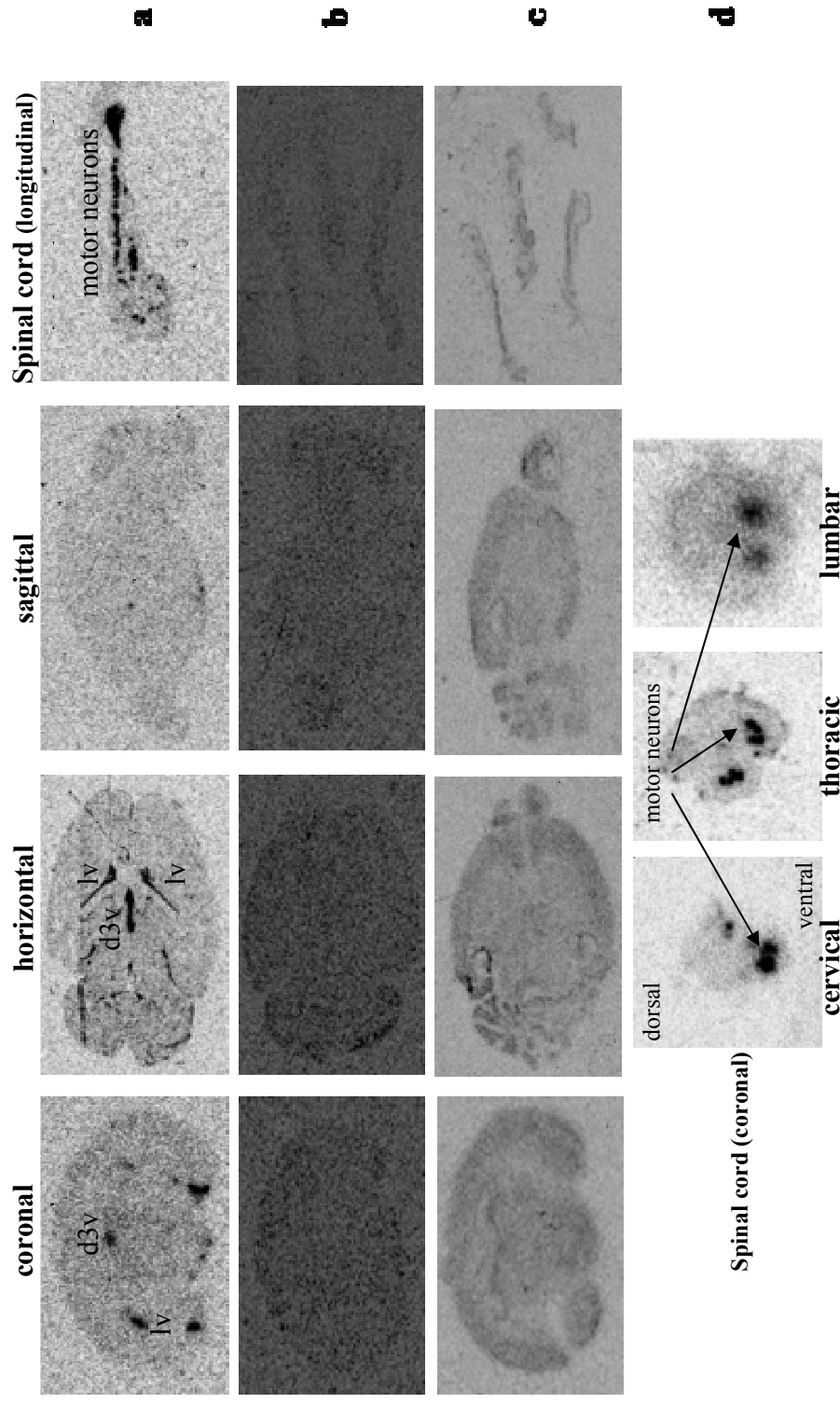
Figure 3.4. Anatomical expression of HspB1 by *in situ* hybridization.
Mouse brain sections were cut in coronal, horizontal and sagittal orientations. Spinal cords were cut in transverse and coronal orientations. Coronal sections were taken from lumbar, thoracic and cervical spinal cord segments. Labelling by the antisense probe for HspB1 is shown in row a; 500 fold excess of unlabelled antisense probe is shown in row b; complementary sense probe is shown in row c. Coronal spinal cord sections labelled by the antisense probe are shown in row d (n=3).
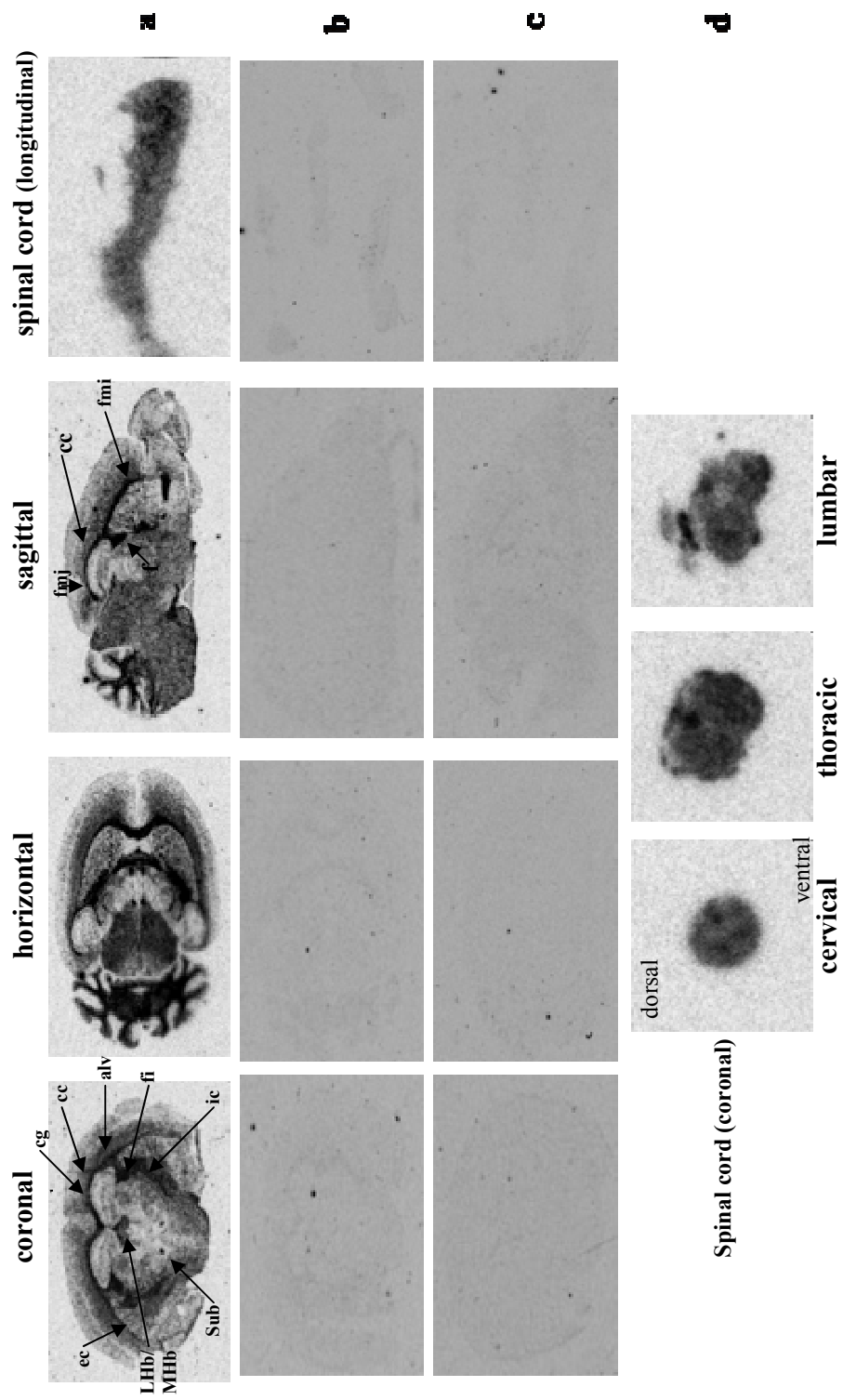
Figure 3.5. Anatomical expression of HspB5 by *in situ* hybridization.
Mouse brain sections were cut in coronal, horizontal and sagittal orientations. Spinal cords were cut in transverse and coronal orientations. Coronal sections were taken from lumber, thoraci c and cervical spinal cord segments. Labelling by antisense probe for HspB5 is shown in row a; 500 fold excess of unlabelled antisense probe is shown in row b; complementary sense probe is shown in row c. Coronal spinal cord sections labelled by antisense probe are shown in row d (n=3).
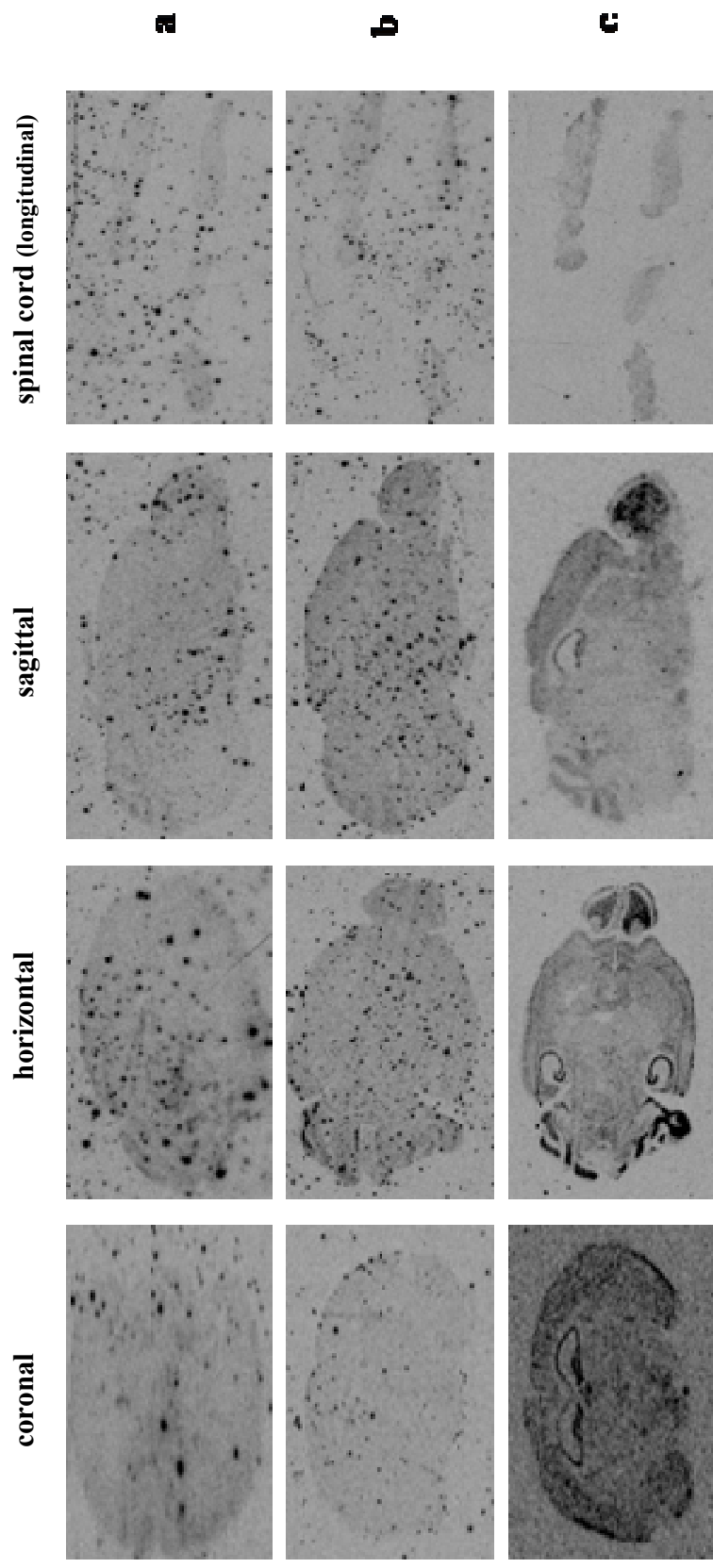
Figure 3.6. Anatomical expression of HspB7 by *in situ* hybridization.
Mouse brain sections were cut in coronal, horizontal and sagittal orientations. Spinal cords were cut in transverse and coronal orientations. Labelling by antisense probe for HspB7 is shown in row a; 500 fold excess of unlabelled antisense probe is shown in row b; complementary sense probe is shown in row c (n=3).

115
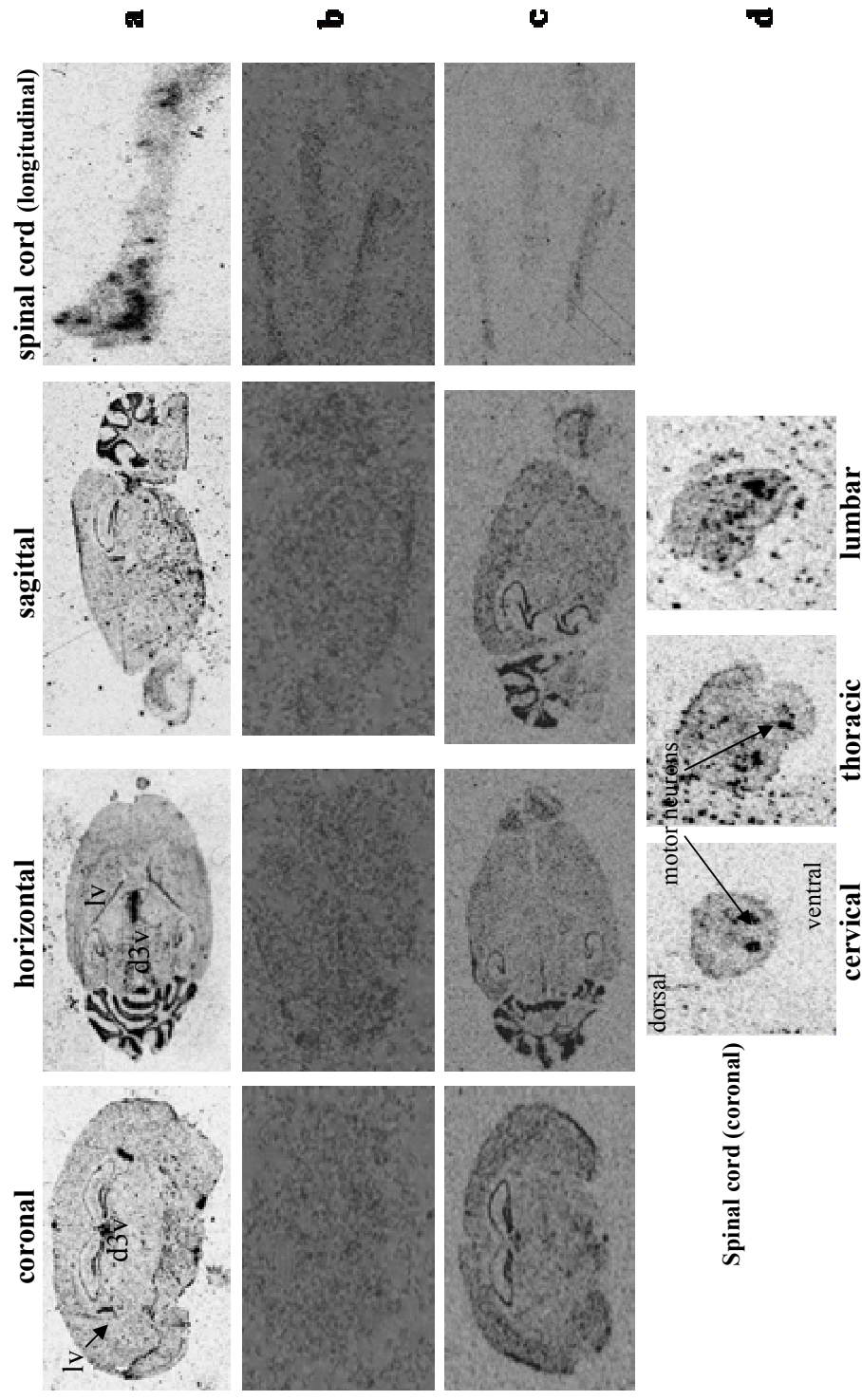
Figure 3.7. Anatomical expression of HspB8 by *in situ* hybridization.
Mouse brain sections were cut in coronal, horizontal and sagittal orientations. Spinal cords were cut in transverse and coronal orientations. Coronal sections were taken from lumbar, thoracic and cervical spinal cord segments. Labelling by antisense probe for HspB8 is shown in row a; 500 fold excess of unlabelled antisense probe is shown in row b; complementary sense probe is shown in row c. Coronal spinal cord sections labelled by antisense probe are shown in row d (n=3).

Structure	Function
Alveus of the hippocampus (alv)	Thin layer of myelinated fibers that cover the lateral ventricles
Corpus Callosum (cc)	Connects left and right cerebral hemispheres
Cingulate cortex (cg)	Connects cingulate gyrus to the entorhinal cortex
Internal capsule (ic)	White matter that connects the thalamus and the cortex
Lateral/Medial habenular nucleus (LHb/MHb)	Input pathway of stria medullaris thalami
Fimbria (fi)	Major output pathway of the hippocampus (myelinated axons –mostly efferent)
Stria terminalis (st)	Subcortical fiber system of the amygdala
Paraventricular thalamic nucleus (PV)	Sends projections to the nucleus accumbens
Submedius thalamic nucleus (Sub)	Receives spinal and medullary input
Forceps minor of the corpus callosum (fmi)	Links both hemispheres
Forceps major of the corpus callosum (fmj)	Links both hemispheres

Table 3.2. White matter containing brain structures labelled by HspB5 probe.
This table lists some of the white matter structures that are shown to express HspB5 by *In situ* hybridization. A brief description of the function of these structures is given.

The expression pattern of HspB8 (Figure 3.7) overlaps with that seen for HspB1. The signal detected in the cerebellum and hippocampi are non-specific as they are also seen with the sense probe (Figure 3.7 c), but expression in the lateral and dorsal ventricles is specific to the antisense probe. HspB1, B5 and B8 also show expression in the spinal cord by *in situ* hybridization (Figure 3.4 d, 3.5 d and 3.7 d). Coronal section reveal distinct puncta for HspB1 and HspB8 (Figure 3.4 d and 3.7 d) in the ventral horn of the spinal cord. HspB5 shows diffuse expression throughout the coronal and transverse spinal cord sections (Figure 3.5 d). The strength of the signal masks the specificity of the expression at this level of analysis, but emulsion radiography was able to resolve this (see below and Figure 3.8)

Neither HspB6 (data not shown) nor HspB7 produced a signal with the antisense probe, but a specific signal with a pattern similar to that seen in Nissl stained sections was observed with the HspB7 sense probe (Figure 3.6). A second set of oligonucleotides for both these sHsps were used for *in situ* hybridization (Table 2.2 - italics), but again a similar pattern was seen for both HspB6 and HspB7 (data not

shown). The remaining 5 sHsps did not produce a signal by *in situ* hybridization (data not shown).

3.3.2.2.b.   Emulsion autoradiography

Emulsion autoradioagraphy allows visualization of the cellular basis of the *in situ* hybridization signals. The slides require an exposure of 3-5 times of that needed to see a strong signal by film autoradiography. Radiolabelled sections for HspB1, B5 and B8 were coated with emulsion and left for 12 weeks at 4ºC, in the dark. Sections were developed and counterstained with cresyl violet to visualize cell bodies (section 2.7.9 and 2.7.10).

Expression of HspB1 and HspB8 in spinal cord sections was confirmed to be specific to the large motor neurons in the ventral horn (Figure 3.8). The distinct white matter specific expression of HspB5 in brain sections as seen by *in situ* hybridization (Figure 3.5) was confirmed to be specific to oligodendrocytes. The diffuse staining in the spinal cord sections revealed a specific and selective expression in cells typical of oligodendrocytes (Figure 3.8 c, d). Oligodendrocytes characteristically form tandem array structures in white matter regions and labelling of HspB5 can be seen to follow this typical pattern. HspB5 expression will be discussed in detail in Chapter 4.
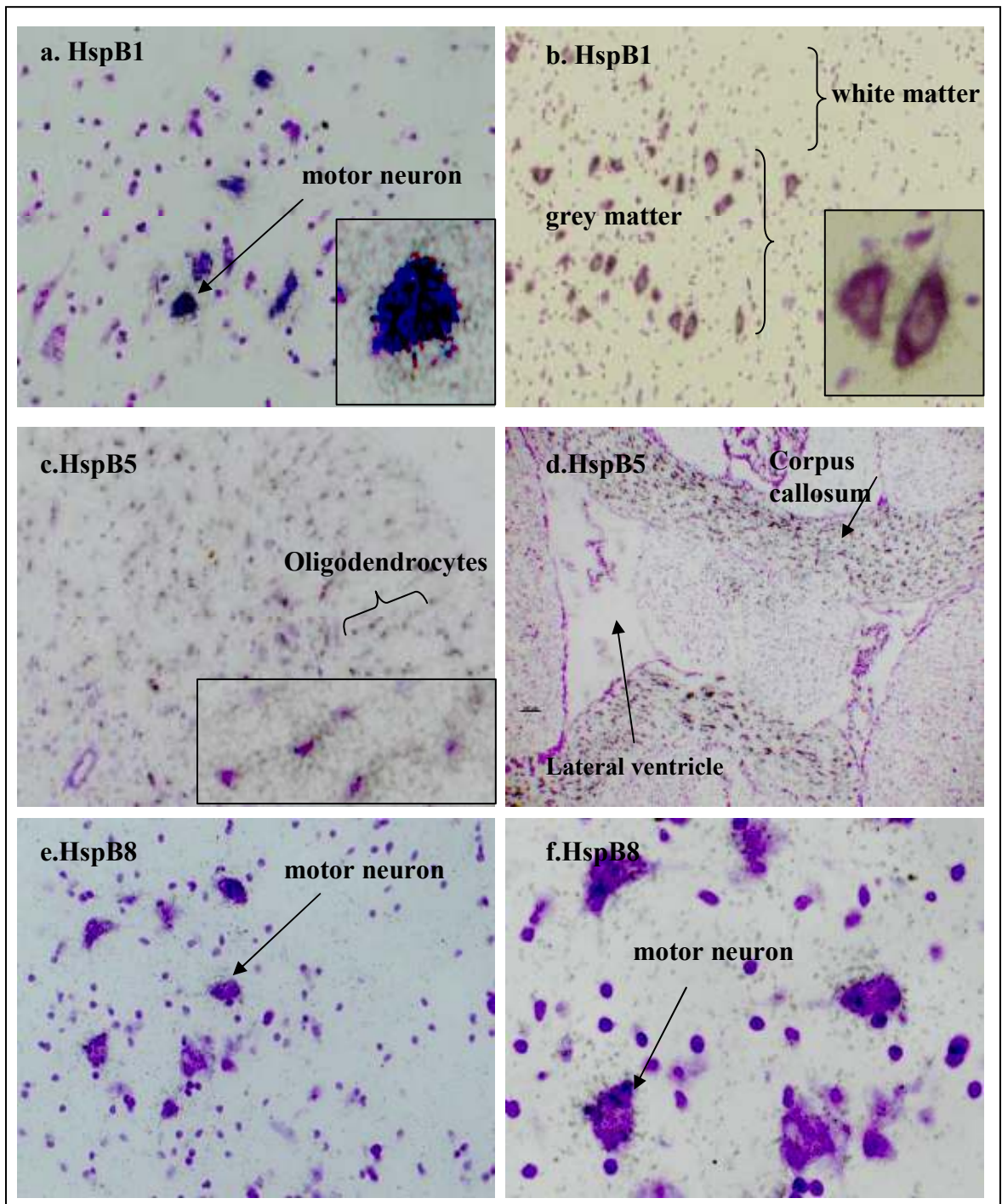
Figure 3.8. Cellular mRNA expression of the sHsps by emulsion *in situ* hybridization.
Spinal cords were cut in transverse and coronal orientations and mouse brain sections were cut
coronally. Emulsion audioradiography was used to visualise the expression of the sHsps at a
cellular level. (a) HspB1 labelling of coronal spinal cord section shows expression in the large
motor neurons in the ventral horn, (b) HspB1 labelling of transverse spinal cord sections, also
showing labelling of large motor neurons. (c) HspB5 labelling of coronal spinal cord section
shows labelling over populations of cells characteristic of oligodendrocytes (see inset), (d)
horizontal brain sections also show labelling of oligodendrocytes in the white matter tracts. (e)
HspB8 labelling of coronal spinal cord section shows expression in the large motor neurons in
the ventral horn, (f) HspB8 labelling of transverse spinal cord sections, also showing labelling
of large motor neurons. Magnifications: a, x20; b, x10; c, x10; d, x10; e, x20; f, x40). Sections
were counterstained with cresyl violet.

3.3.3. Protein expression of the sHsp family

3.3.3.1.   Characterization of sHsp expression in various mouse tissue

Total tissue homogenates from heart, testis, eye, muscle and brain were extracted and homogenised in Hepes/KCl buffer (section 2.8.1). Samples were used to analyse the protein expression of the sHsp family by western blotting (section 2.8). Expression of HspB3 and HspB10 could not be determined due to lack of antibodies. As these two sHsps did not show mRNA expression in the CNS by RT-PCR and *in situ* hybridization, antibody production was not pursued. Three antibodies for HspB8 were tested on homogenate samples (data not shown). The non-commercial antibody provided by Dr. Boelens (Radboud University, The Netherlands) showed the strongest immunoreactivity and was therefore the preferred antibody. The other two antibodies (ab66063 and HspB8 gifted by Dr. Mohan Rao (Centre for cellular and molecular biology, India)) showed very faint or no immunoreactivity using 50μg of homogenate (data not shown).

Many of the polyclonal non-commercial antibodies produced background immunoreactivity, mainly high molecular weight bands, but specific bands of the correct size where clearly distinguishable. Due to the sequence similarity and conserved α-crystallin domain of the sHsps, the potential for cross-reactivity was addressed. Firstly there were clear differences in the size of some of the sHsps (Figure 3.9). Where there was not a size difference, for example HspB2 and HspB5 both showed immunoreactivity at ~20kDa, specificity was determined by expression in control tissue versus non-control. So, HspB2 only showed immunoreactivity in the heart and muscle, whereas HspB5 showed ubiquitous expression. Where more than one band was present close to the predicted molecular weight of the target protein, as was the case for HspB6, specificity was determined by pre-absorption of the antibody (Figure 3.9 B).

Secondly, the antigen used to produce the antibodies was considered. The antigen sequences were subjected to BlastP analysis to determine any homology or sequence similarity to other mouse protein. Proteins showing highest homology with the antigen apart from that specific sHsp are shown in Table 3.3. Although antigens used to raise commercial antibodies show some sequence homology with other sHsps, these antibodies do not cross react with other sHsps as stated on the data sheet (stressgen.com) in addition to the observed differences in molecular weight and tissue

specificity (Figure 3.9 and Figure 3.10). Moreover, the specificity of the non-commercial antibodies had previously been described (Verschuure et al., 2003, de Wit et al., 2004).
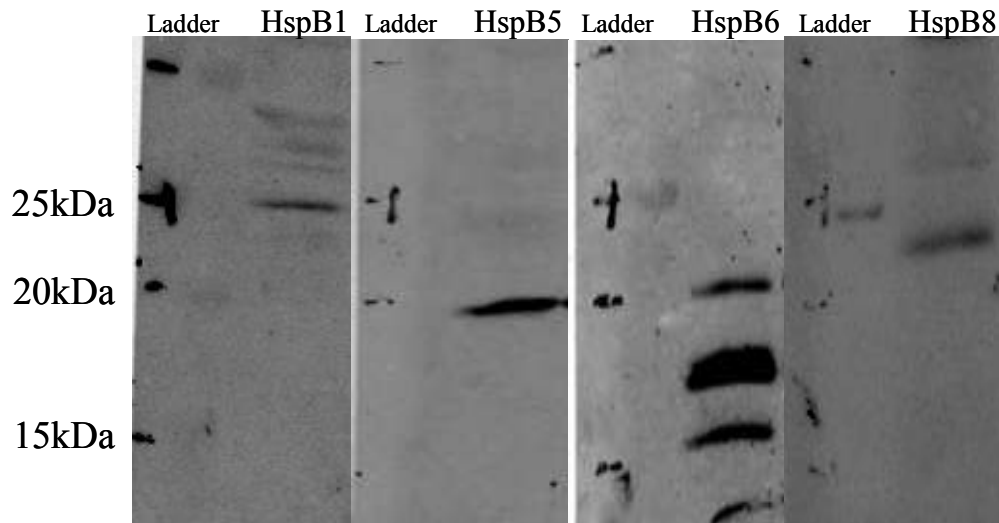
Figure 3.9. Specificity of antibodies against sHsps expressed in the mouse CNS. 50µg of brain homogenate were loaded onto polyacrylamide gels and transferred to nitrocellulose membrane. Antibodies against the sHsps were tested and the 4 sHsps that showed immunoreactivity in the CNS are shown. All show bands of differing sizes. HspB1 (SPA-801) antibody recognises a band at ~25kDa, HspB5 (SPA-222) antibody recognises a band at ~20kDa, HspB6 (non-commercial) antibody recognises 3 isoforms of the protein, bands are at ~21, 18 and 16kDa and the HspB8 (non-commercial) antibody recognises a band at ~22kDa.

sHsp	Antigen	Homology (H)	Predicted kDa	Actual kDa
HspB1 (SPA-801)	Recombinant mouse Hsp25	44% H to HspB4	25	25
HspB2 (Boelens)	Rat full length recombinant protein	43% H to HspB4	20	20
HspB4 (SPA-221)	Human synthetic peptide (164-173)	52% H to HspB5	20	20
HspB5 (SPA-222)	Purified HspB5 from bovine lens	49% H to HspB4	20	20
HspB6 (Boelens)	Rat Full length recombinant protein	50% H to HspB5	16.8	21/18/16
HspB7 (Boelens)	Human Synthetic peptide (156-170)	80% H to SWI/SNF	18.5	18
HspB8 (Boelens)	Human Synthetic peptide (179-193)	80% H to ankyrin-2	21.5	22
HspB9 (Boelens)	Human Synthetic peptide (137-151)	58% H to guanylate cyclase	~16	18

Table 3.3. Sequence homology of antigens recognised by antibodies against the sHsps. This table shows the antigens used to produce antibodies against the sHsps. BlastP was used to determine if the antigen sequences had any sequence similarity with other proteins in the mouse genome. The protein with the highest homology is listed. (SWI/SNF, related, matrix associated, actin dependent regulator of chromatin, subfamily e, member 1).

Antibodies against four of the sHsps (HspB1, B5, B6 and B8) showed immunoreactivity in control tissue and showed ubiquitous expression in other mouse tissues including the brain (Figure 3.9). HspB2 and HspB7 showed expression in heart and muscle tissue and HspB4 expression was restricted to the eye. The HspB6 antibody detected 3 distinct bands (Figure 3.10 a). To confirm specificity a competition experiment was set up where the HspB6 antibody was pre-absorbed with the antigen (recombinant Hsp20, provided by Dr. Boelens (Radboud University, The Netherlands)). All bands seen in the brain, heart, testis and muscle disappeared supporting the specificity of the antibody for the target protein. The large band/s seen in the eye in the original blot also decreased to some extent but two bands still remained visible (Figure 3.10 b). This is probably due to cross-reactivity of the antibody with the αA-/αB-crystallins which constitute about one third of the total protein in the lens and present 50% homology to HspB6.
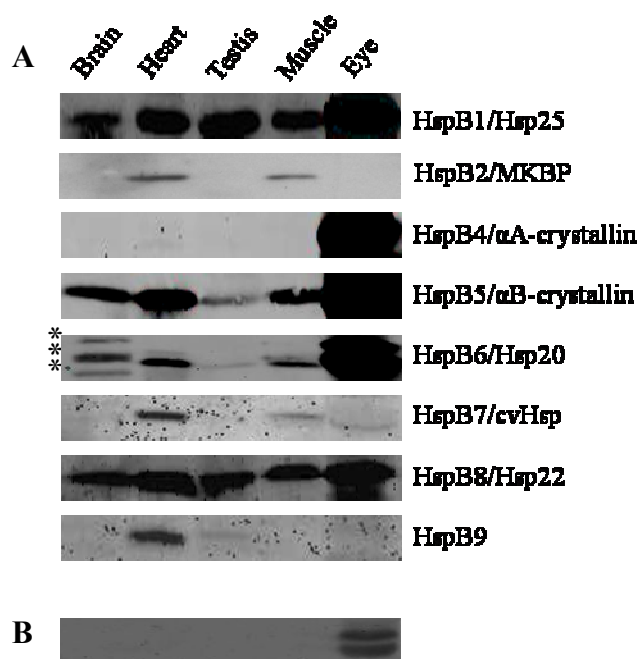
Figure 3.10. Protein expression of the sHsp family in various mouse tissues and brain. (A) All of the sHsps show immunoreactivity in control tissues. A total of 50μg of total protein was loaded for each tissue. However the protein concentration was increased to 100μg to detect immunoreactivity in control tissue for HspB2, HspB7 and HspB9. HspB1, HspB5, HspB6, HspB8 show expression in the brain (n=3). **(B)** The HspB6 antibody was pre-absorbed with antigen confirming the specificity of the signal. All three bands seen in the brain tissue (asterisks) disappeared. Immunoreactivity decreased in the eye tissue, leaving two fainter bands, suggesting cross-reactivity of the antibody with the crystallin proteins in the eye. Molecular weights (HspB1 = 25kDa, HspB2 = 20kDa, HspB4 = 20kDa, HspB5 = 20kDa, HspB6 = 18 (middle band), HspB7 = 18kDa, HspB8 = 22kDa, HspB9 = 18kDa)

3.3.3.2. Protein expression of the sHsps in brain and synaptosomal fractions

To extend the protein analysis of the sHsps and to address the cellular and sub-cellular expression and possible enrichment in specific compartments we analysed expression of the sHsps in brain and synaptosome sub-fractions (section 2.10).

Fractions consisted of total brain homogenate, cell body/nuclear (P1), myelin and synaptosomes. The synaptosome fraction was treated with Triton-X100 at pH6 and pH8. The soluble fraction at pH6 consists of plasma membrane proteins and the insoluble fraction contains paired pre- and post-synaptic structures. At pH8 the presynaptic specialization disintegrates leaving the postsynaptic density (PSD) as the insoluble fraction and the presynaptic components in the soluble fraction (Phillips et al., 2001).

The fractions were tested with the use of four control antibodies with known distinct patterns of compartmentalization (Figure 3.11 a). Beta-catenin was found in all fractions with a slight enrichment in the P1 (cell body) fraction, synaptosome, and pH6 insoluble compartment. Beta-catenin is part of the synaptic adhesion junction where it actively regulates cadherin function. The vesicular protein synaptophysin is enriched in the synaptosome fraction and is completely solubilised at pH6 and pH8 (Figure 3.10 a). PSD-95 is a post-synaptic protein and as expected is enriched in the insoluble fractions particularly at pH8. Myelin basic protein (MBP) was found to be highly enriched in the myelin light membrane fraction, and de-enriched in the non-myelin fractions apart from the insoluble pH8 synaptosome fraction (Figure 3.12 a). This is indicative of some myelin contamination of the synaptosome insoluble fractions.

HspB2, HspB7 and HspB9 did not show immunoreactivity in homogenate fractions, or appear enriched in other brain fraction (data not shown). The four sHsps for which robust protein expression was found in the brain (Figure 3.10) showed differential distributions and solubilities in the brain and synaptosome sub-fractions. HspB1 and HspB8 were both present in the synaptosomal fraction, but with differential detergent extractability (Figure 3.11 b). HspB1 was present mainly in the soluble fractions at both pH6 and pH8, whereas HspB8 displayed most reactivity in the insoluble fraction at pH6, but solubility increased at pH8. HspB5 and HspB6 were both enriched in the myelin fraction (10-fold and 5-fold respectively as measured in two independent experiments). This was derived by measuring fluorescence intensities and normalizing to protein loading. Enrichment of HspB5 in the white matter was consistent with the

white matter specific expression profile seen by *in situ* hybridization (Figure 3.5) and confirmed both presence of the transcript and proteins in this compartment. HspB5 and HspB6 are also found in the synaptosomal fraction, but their biochemical properties are quite distinct upon treatment with detergent. HspB6 was completely insoluble at pH6 and pH8, whereas the solubility of HspB5 increased as the pH increased (Figure 3.11 b).
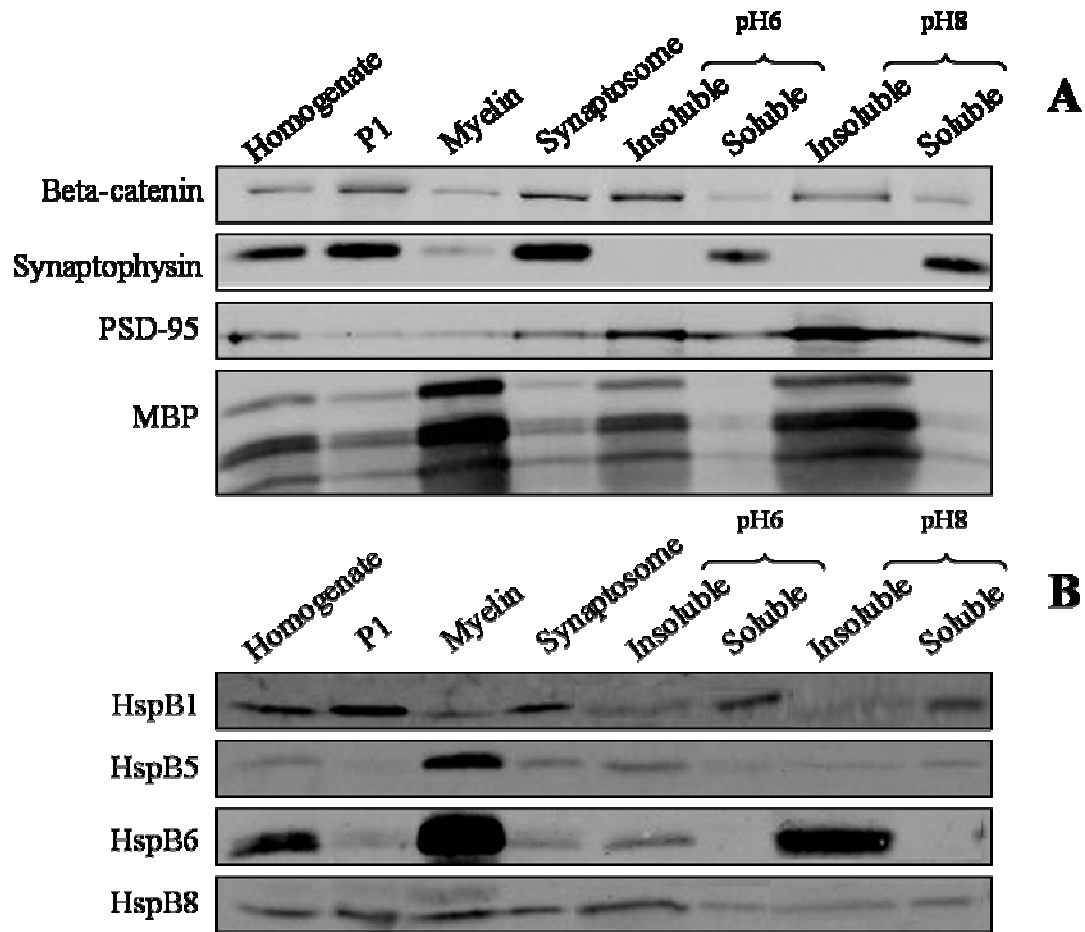
Figure 3.11. sHsp expression in brain fractions and synaptosomal subfractions.
(A) Fractions extracted from whole brain homogenate were tested with β-catenin, synaptophysin, PSD-95 and MBP antibodies. Beta-catenin showed expression in all fractions, with enrichment in the P1 and synaptosome insoluble fractions; synaptophysin showed enrichment in the synaptosomes and localization to the soluble fractions (pre-synaptic compartment); PSD-95 showed enrichment in the insoluble fractions of the synaptosome, particularly at pH8 which consists of the PSD specialization. MBP shows enrichment in the myelin fraction, de-enrichment in the synaptosome fraction, but enrichment in the pH8 insoluble fraction (this is indicative of a minor myelin contamination). **(B)** HspB1 and HspB8 are found in all fractions with HspB1 being moderately enriched in the cell body/nucleus (P1) compartment and present mainly in the soluble synaptosomal fractions. HspB5 and B6 show enrichment in the myelin fraction to varying degrees. HspB6 is also enriched in the PSD synaptosome fraction. 18μg of protein were loaded for each fraction, n=2 (also see Appendix 2).

3.4.   Discussion

The aim of this chapter was to systematically characterize the expression profile of all 10 members of the sHsp family in naïve mouse tissue in order to establish a baseline for sHsp expression in the CNS under physiological conditions.

3.4.1. Summary of sHsp expression in the mouse CNS

The mRNA and protein data obtained for sHsp expression in the mouse CNS is summarized in Table 3.4. All of the sHsps were expressed in reference/control tissue; additionally 4 were expressed in the brain. RT-PCR highlighted expression of 5 of the sHsp in the brain; however, *in situ* hybridization was only able to confirm mRNA expression of 3 sHsps. *In situ* hybridization allowed the identification of cell types expressing the mRNA, with HspB1 and HspB8 expressed in motor neurons and HspB5 in oligodendrocytes. This data highlights the constitutive expression of four sHsps, HspB1, HspB5, HspB6 and HspB8 in the naïve mouse CNS.

The sHsps were given a new classification scheme by Taylor and Benjamin, (2005). They proposed a simple scheme to reflect their specialized roles (apoptosis, protein trafficking, redox control and cytoskeletal interactions). In this classification HspB1, HspB5, HspB6 and HspB8 were grouped as Class I proteins, that are ubiquitously expressed, have similar properties and form multimeric complexes with one another (Taylor and Benjamin, 2005). Identification of this subset of sHsps that show specific and selective expression in the CNS is consistent with this classification and may reflect a common/overlapping function in different cells. These sHsps share between 28 and 45 percent sequence homology (Taylor and Benjamin, 2005) and are able to form hetero-oligomeric complexes with one another (Sun et al., 2004, Fontaine et al., 2005).

sHsp	Reference tissue (protein)	Expressed in reference tissue (protein)?	Expressed in brain?				
			Protein	RT-PCR	*In situ*	Cell type	Cell type (literature)
HspB1	Muscle	Yes	Yes	Yes	Yes	Motor neurons/ endothelial	Neurons/ endothelial/ astrocytes (a,b)
HspB2	Muscle	Yes	No	No	No	-	-
HspB3	Muscle	Yes	-	No	No	-	-
HspB4	Eye	Yes	No	No	No	-	-
HspB5	Muscle/ Eye	Yes	Yes	Yes	Yes	Oligodendrocytes	Oligodendrocytes/ astrocytes (c,d)
HspB6	Muscle	Yes	Yes	Yes	No	-	-
HspB7	Muscle	Yes	No	Yes	No	-	-
HspB8	Muscle	Yes	Yes	Yes	Yes	Motor neurons/ endothelial	Motor neurons (e)
HspB9	Testis	Yes	No	No	No	-	-
HspB10	Testis	Yes	-	No	No	-	-

Table 3.4. Summary of sHsp expression data in the mouse CNS. This table summarises expression of the sHsp in the CNS, as shown by the three techniques employed in this study. mRNA expression data has confirmed tissue specific expression of the sHsps in the various tissues of the mouse by RT-PCR, highlighting 5 of the sHsps to be expressed in the brain. Expression of only 3 of these sHsp was confirmed by *in situ* hybridization. HspB6 and HspB7 did not show expression using 2 distinct oligonucleotides. HspB1 and HspB8 showed expression in motor neurons and HspB5 was expressed in oligodendrocytes. 4 of the sHsps were detected in the CNS using antibody staining by western blotting. Although HspB7 showed immunoreactivity in control tissue, protein expression was not confirmed in the brain. It may be likely that this protein is below the limit of detection or that better reagents are required. Combining this information has highlighted HspB1, HspB5, HspB6 and HspB8 as members of the sHsp family that are constitutively expressed at detectable levels, in the CNS under physiological conditions. (a)(Armstrong et al., 2001a), (b) (Plumier et al., 1997), (c) (Klemenz et al., 1993), (d) (Iwaki et al., 1992), (e) (Irobi et al., 2004).

3.4.2. mRNA expression

RT-PCR data identified expression of five of the sHsps (HspB1, B5, B6, B7 and B8) in the brain (Figure 3.3). HspB7 expression was thought to be confined to heart and muscle tissue, but RT-PCR revealed expression in the brain and all other tissues tested. The mRNA expression of HspB1, HspB5 and HspB8 was confirmed by *in situ* hybridization, but expression of HspB6 and HspB7 could not be detected in the brain and spinal cord sections despite using two sets of oligonucleotide probes. In the case of HspB6 the Allen Atlas also fails to detect a signal hence a lack of sensitivity may explain this finding (Figure 3.12 C). However we detect protein expression of this sHsp by western blotting in

the brain. Although *in situ* hybridization of HspB7 did not show expression using two different antisense probes, a signal was seen using the sense probes (Figure 3.6 c). The signal detected was very similar to that seen on Nissl stained sections. This suggests that the signal may reflect the biochemical properties of the probe, allowing it to hybridize to mRNA rich regions (Nissl bodies) contained within cell bodies. The lack of specific signal using antisense probe and the specific signal seen by the sense probe additionally suggests the possibility that the sense oligonucleotide probe is reacting with genomic DNA. The Allen brain Atlas shows an abundant expression of the HspB7 transcript in the adult mouse brain (Figure 3.12 D) (Lein et al., 2007). This signal is also very similar to that seen with the sense probe. However the Allen Atlas used gene-specific ribo-nucleotide probes labelled with non-isotopic digoxigenin (DIG) (Lein et al., 2007), thus the inconsistencies could arise from the differences in probes used. Protein expression of HspB7 in the brain was undetectable with the available antibody, and a good signal in control tissues (heart and muscle) required loading of 100μg of total protein in a lane (Figure 3.10). Thus the expression and specificity of HspB7 remains to be defined. HspB7 does not appear to share the same phylogenetic class as the other 4 sHsps expressed in the CNS (Figure 3.13) (Taylor and Benjamin, 2005). The divergence suggests HspB7 does not fall into the same functional group as HspB1, B5, B6 and B8, and may reflect the lack of protein expression in the CNS.

 In situ hybridization has shown HspB1 and HspB8 expression to be localized to the lateral and dorsal ventricles of the brain. These ventricles are lined with ependymal cells that make the cerebrospinal fluid (csf) (Brown et al., 2004) and these could be the cells that show high levels of HspB1 and HspB8. Expression was also observed in discrete populations of cells in the spinal cord as is evident by the distinct puncta seen in the ventral horn (Figure 3.4 d and Figure 3.7 d). Emulsion radiography can be used to reveal the cellular localization of the signal seen and showed HspB1 and HspB8 expression to localise to the large motor neurons in the spinal cord, as previously described (Armstrong et al., 2001a). Expression of HspB1 has previously been studied in rat, mouse and human brain and spinal cord tissue, showing association with blood vessels (Armstrong et al., 2001a, Wilhelmus et al., 2006c), cells of the choroid plexus (Plumier et al., 1997) and motor neurons in the spinal cord (Armstrong et al., 2001a, Irobi et al., 2004). The

anatomical expression seen by *in situ* hybridization is therefore in keeping with previous studies. HspB1 mRNA expression in the brain as documented in the Allen Brain Atlas shows a very weak signal in regions localized to the lateral and dorsal ventricles (Figure 3.12 A) (Lein et al., 2007). HspB8 also shows expression in the ventricles (Figure 3.7 a) that is very similar to the staining observed for HspB1 (Figure 3.4 a). Staining of the ventricles was not seen with the HspB8 sense probe suggesting specificity of this signal. Indeed similar staining of the lateral and dorsal ventricles was also documented in the Allen Brain Atlas (Figure 3.12 E). Expression of these two sHsps in the ventricles and choroid plexus in the normal mouse brain may reflect the very high metabolic activity of these tissues. The choroid plexus contains a high number of mitochondria to support its function potentially leading to higher levels of oxidative stress (Cornford et al., 1997). It is known that HspB1 can protect against oxidative stress (Wyttenbach et al., 2002), indeed HspB8 may serve a similar function, and hence this tissue may be able to use the sHsps to counteract possible oxidative stress due to leakage of free radicals from the mitochondria (Preville et al., 1999, Wyttenbach et al., 2002). The similarity in expression of HspB1 and HspB8 is also suggested by their potential structural similarity as shown in Figure 3.13. Both HspB1 and HspB8 originate from the same main branch point.

HspB5 is known to be expressed in the CNS, particularly in glial cells (Iwaki et al., 1992, Klemenz et al., 1993). Analysis by RT-PCR and *in situ* hybridization shows HspB5 expression in the brain and spinal cord (Figure 3.5 and 3.8). A clear and distinct white matter expression pattern is seen by *in situ* hybridization and emulsion radiography (Figure 3.8), which is also confirmed in the Allen Brain Atlas (Figure 3.12 B) (Lein et al., 2007). The expression profile is consistent with localization to oligodendrocytes.

The mRNA expression pattern of HspB5 in the brain and the spinal cord is distinct from that of HspB1 and HspB8, implying cell specific transcriptional regulation of these sHsps. The selective expression of HspB5 in the white matter may reflect the intrinsic vulnerabilities of oligodendrocytes (Husain and Juurlink, 1995), thus supporting the need of a molecular chaperone that can regulate/modulate many cellular processes such as redox homeostasis, apoptosis and cytoskeleton regulation (Kappe et al., 2003, Verschuure et al., 2003, van Noort, 2008). The expression and potential contribution to the white matter compartment and oligodendrocytes will be discussed in greater detail in Chapter 4.
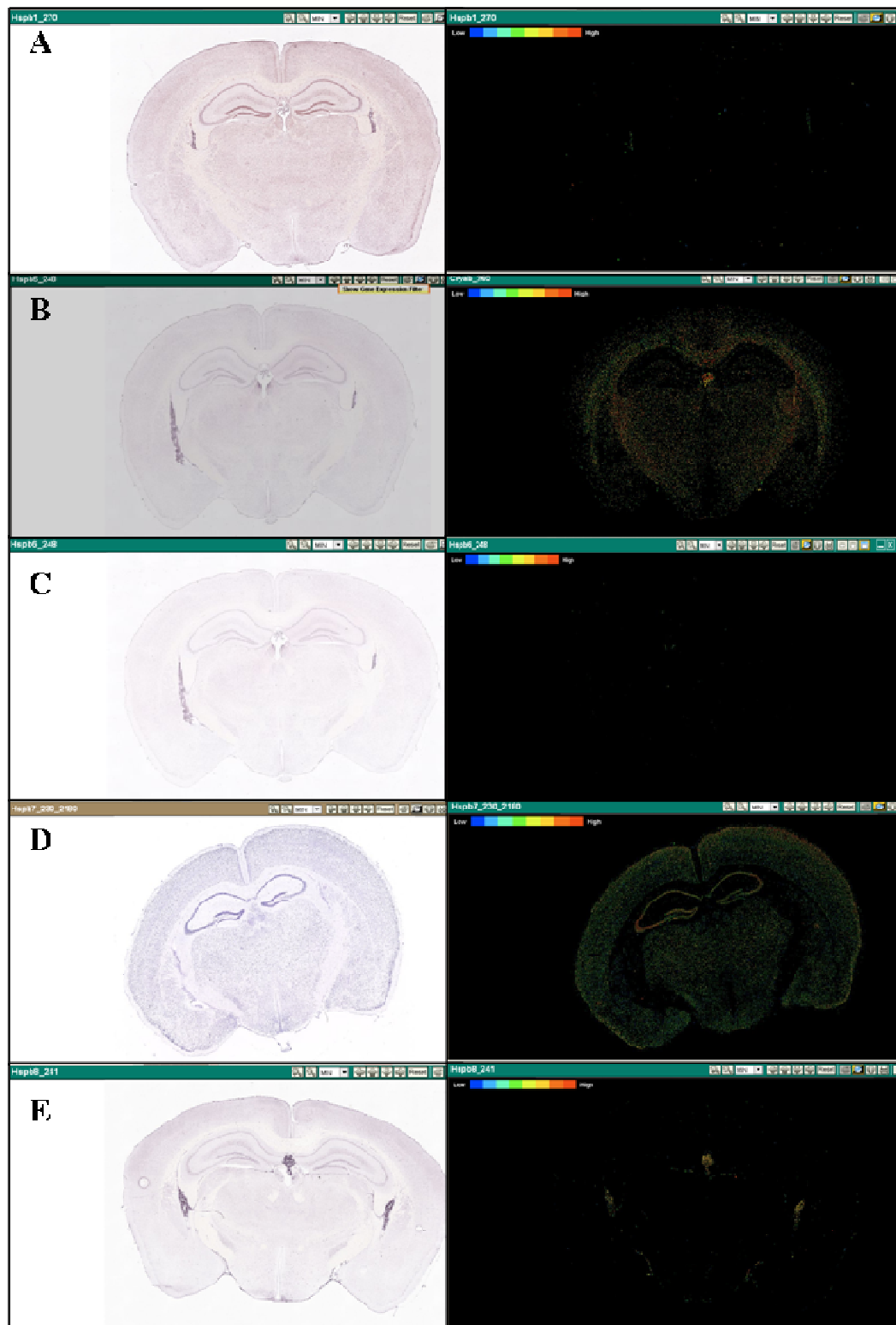
Figure 3.12. *In situ* **hybridization images of the sHsps as determined by the Allen Brain Atlas.** Nissl stained images are shown in the left panel and corresponding *in situ* hybridization images are shown in the right panel. Levels of gene expression are depicted by colour, ranging from blue (low expression) to red (high expression). (A) HspB1, (B) HspB5, (C) HspB6, (D) HspB7, (E) HspB8 (Images taken from Lein et al., 2007; http://mouse.brain-map.org).
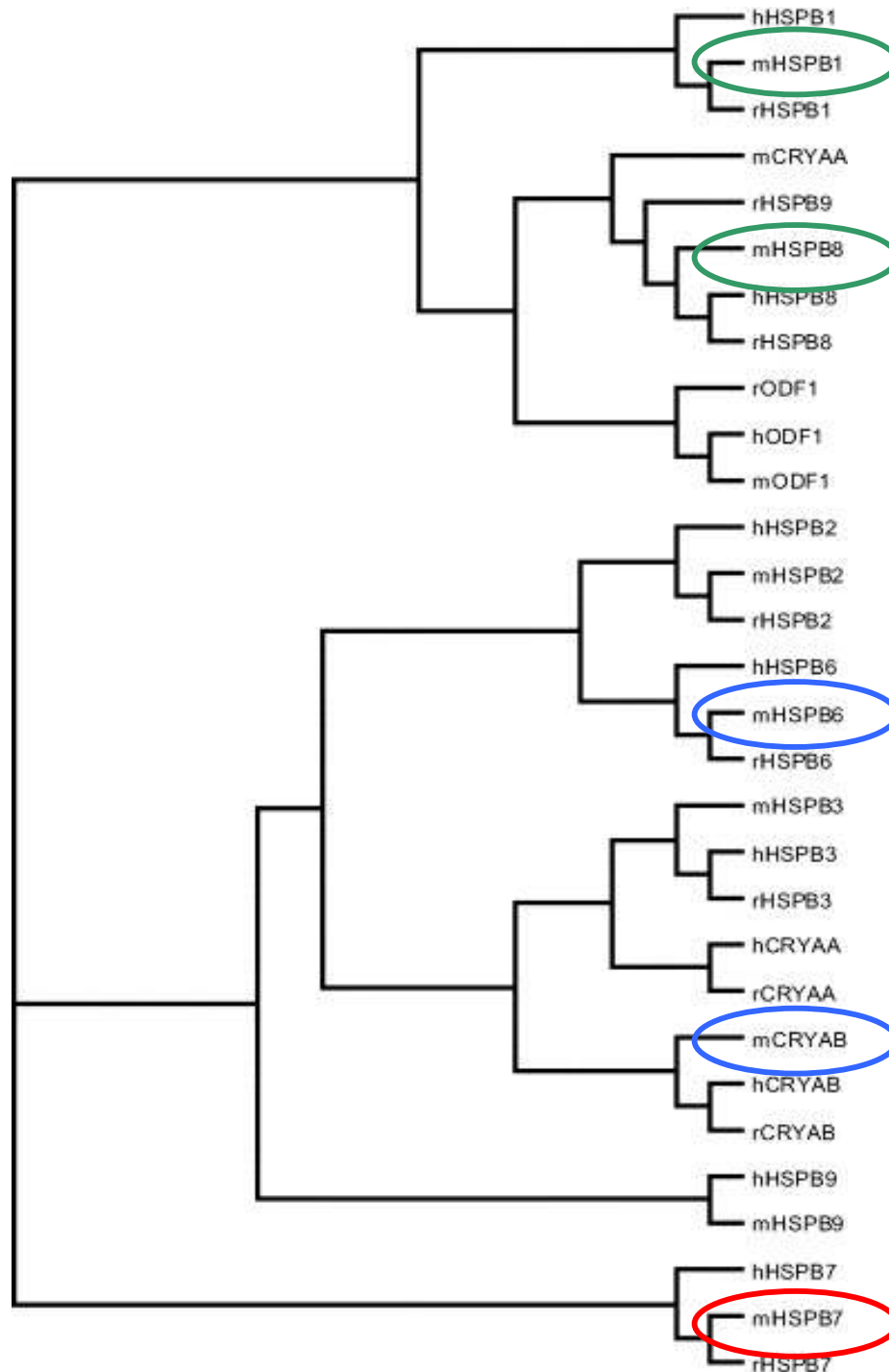
Figure 3.13. sHsp phylogenetic tree (Cladogram). Representative Cladogram of translated sHsps proteins. Cladogram was created using TreeView and diagrams the evolutionary divergence of the sHsps within and between species. sHsps expressed in the CNS are highlighted by ovals. HspB1 and HspB8 (green) appear to be more closely related to one another compared to HspB5, B6 and B7. HspB5 and HspB6 also extend from a common branch point (blue); HspB7 extends from the main root node suggesting greater divergence in sequence compared to other sHsps. m (mouse), r (rat), and h (human) (Adapted from Taylor and Benjamin, 2005).

3.4.3. Protein expression

Western blot analysis of the sHsps has highlighted protein expression of HspB1, HspB5, HspB6 and HspB8 in the brain (Figure 3.10). These four sHsps are constitutively expressed but to varying degrees in the tissues analyzed. HspB6 is known to be present as four phospho-isoforms in bovine heart, consisting of 3 phosphorylated species and one un-phosphorylated (Beall et al., 1999). The three distinct bands seen in Figure 3.11 are likely three of these phospho-isoforms. The human protein atlas (http://www.proteinatlas.org/) provides limited information on the protein expression of HspB1, B5 and B6 by immunohistochemistry. HspB1 was shown to have moderate expression in neuronal cells of the cerebral cortex, cerebellum and lateral ventricle, while HspB5 showed moderate to strong staining in non-neuronal cells in these regions. To some extent this is consistent with the *in situ* hybridization data, where HspB1 expression is seen in the lateral ventricles and HspB5 shows non-neuronal expression (oligodendrocytes). The human protein atlas detects weak expression of HspB6 in the cerebral cortex and moderate expression in the lateral ventricles.

3.4.3.1. Protein expression in brain and synaptosome subfractions

Protein expression and potential compartmentalisation of the sHsps in brain and synaptosome fractions was also investigated. HspB1 showed presence in all the fractions which is consistent with its ubiquitous expression and broad role in various cellular processes such as regulation of the cytoskeleton and redox homeostasis (Figure 3.12 b). Its presence in the synaptosomal fractions and its differential distribution across detergent (Triton X-100) soluble and insoluble fractions follows the trends shown by a number of synaptic proteins including those associated with the cytomatrix (Figure 3.11) (Phillips et al., 2001). It is well established that HspB1 is able to regulate cytoskeletal homeostasis (Richter-Landsberg and Goldbaum, 2003), suggesting this role could be extended to the synaptic compartment. Indeed, other molecular chaperones are known to play significant roles in this compartment such as Hsc70, cystein string protein and small glutamine-rich tetratricopeptide repeat containing proteins (Tobaben et al., 2001).

HspB8 also showed immunoreactivity in all fractions but with a different distribution across detergent treated fractions. HspB8 was preferentially present in the pH6 insoluble

fraction suggesting localization to the paired pre- and post-synaptic structure. The lack of enrichment in pH8 soluble and insoluble fractions suggests that this protein is not preferentially associated with either the pre- or post-synaptic structures and may potentially be associated with synaptic scaffolding proteins.

HspB5 and HspB6 show a similar expression pattern in brain fractions, however with differential Triton X-100 solubility in the synaptosomal fractions. This may support a role for these sHsps in a sub-cellular organization that is involved in synaptic regulation. The presence of MBP in synaptosomal fractions suggests expression of these otherwise white matter enriched sHsps may occur as a result of myelin contamination in these fractions, therefore suggesting alternative functions in non-neuronal cells. Accordingly, the apparent PSD association of HspB6 may arise through genuine synaptic compartmentalization or be indicative of biochemical specializations within the myelin membrane. For HspB5, enrichment in the white matter is expected as it is expressed specifically in oligodendrocytes (also see Chapter 4). But evidence would support that HspB6 is similarly highly expressed in the white matter. Indeed phylogenetic data (Figure 3.12) also suggest structural similarity of these two sHsps and lends weight to similar expression profiles. One concern would be cross-reactivity of the HspB6 antibody with the conserved alpha-crystallin domain of HspB5, but size and preabsorption suggest bono fide distinct reactivity in the brain (Figure.3.10). The data indicates that both HspB5 and HspB6 can be organized around the biochemical assemblies defined by differential Triton X-100 extraction (Phillips et al., 2001).

The overlapping but distinct compartmentalization of these four sHsps reflects their known cooperativity and interactions (Sun et al., 2004, Fontaine et al., 2005) and illustrates the potential for distinct functional outcomes in different cellular compartments.

3.5.   Summary

This chapter has described the expression profile of the sHsp family in the naïve mouse CNS by a number of techniques providing a baseline for sHsp expression and distribution. The results suggest the presence of different cellular pools of sHsps distributed in a cellular and sub-cellular specific fashion. Some of this work has been published (Quraishe et al., 2008) and has complemented other published work and public databases. This

characterisation of the sHsps can now be extended to investigate changes under disease conditions during which a region and cell specific pathology occurs in the brain. The schematic shown in Figure 3.14 summarizes what is presently known about the sHsps in the CNS under "physiological" conditions. The major sites of expression with known functions/identified roles as described in the general introduction are illustrated.
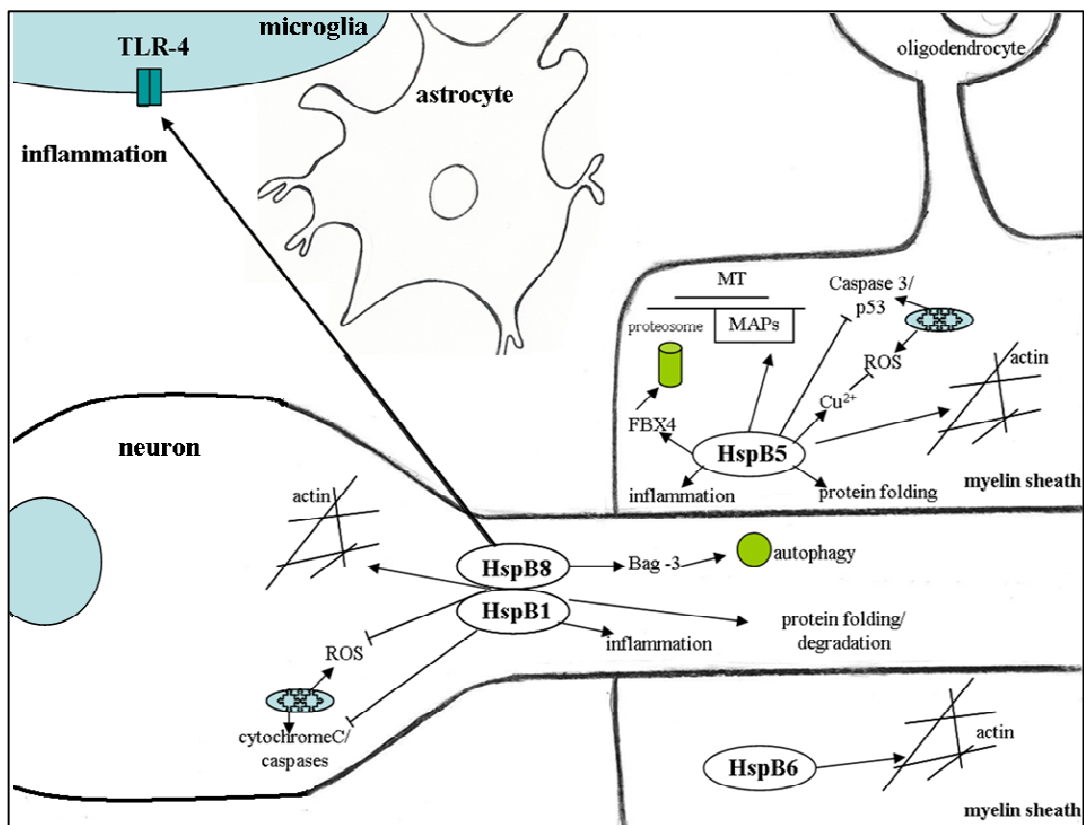
Figure 3.14. Schematic illustrating the major sites and functions of the 4 sHsps constitutively expressed in the CNS. HspB5 and HspB6 are expressed in the white matter as depicted by the myelin sheath. HspB5 is enriched (5 fold) in this compartment). HspB1 and HspB8 are localized to neuronal cells. The sHsps are involved in modulating many cellular processes as shown. These include: regulation of protein folding and degradation by their chaperone capacity and interaction with other proteins such as Bag-3, a stimulator of autophagy; modulation of the inflammatory pathway, by interacting with receptors on antigen presenting cells; preventing oxidative stress by sequestering ions such as Cu2+ or Zn2+ as well as maintaining antioxidants in a reduced state; and modulation of the cytoskeleton. ⟶ indicate potential stimulation of pathways, and ——| indicate potential block of pathways.

Chapter 4: White matter expression of HspB5

4.1. Introduction

As shown in the previous chapter, four out of the 10 sHsps were found to be unequivocally expressed in the mouse CNS under physiological conditions by a number of techniques. Expression of a fifth Hsp (HspB7) remained unclear. Of these, HspB5 was shown to have a selective expression in non-neuronal cells, displaying the characteristic profile associated with the oligodendroglial cell populations which typically align in tandem arrays in tissue. The expression pattern for HspB5 is also consistent with the literature, where HspB5 has been shown to be expressed in oligodendrocytes and Schwann cells under physiological conditions (Iwaki et al., 1992, Klemenz et al., 1993). HspB5 expression is highly induced in Schwann cells during peripheral nerve development and myelination. Sciatic nerve axotomy was shown to downregulate HspB5 levels suggesting that HspB5 expression depends on axonal signals (D'Antonio et al., 2006).

Oligodendrocytes perform an essential function by providing insulation to axons which contributes to rapid conduction of nerve impulses. The counterparts of oligodendrocytes in the peripheral nervous system (PNS) are Schwann cells. Both oligodendrocytes and Schwann cells encapsulate nerve fibres with a specialised plasma membrane structure, the myelin sheath. Schwann cells encapsulate a single axon, however, oligodendrocytes are able to send out many projections (up to 40) each of which is able to wrap extensively around a single axon (Fanarraga et al., 1998). The CNS myelin may lie a significant distance from the cell body, being connected to it by a slender cellular process (Figure 4.1 A) (Ludwin and Bakker, 1988). The myelin sheath is tightly packed by extrusion of the cytoplasm that provides insulation to the ensheathed axon and minimises loss of electrical signal caused by transverse diffusion (Waxman and Ritchie, 1993).

The myelin membrane is divided into sub-domains (compact and non-compact myelin) with distinct protein and lipid compositions (Simons et al., 2000). Compact myelin contains virtually no cytoplasm whereas the non-compact regions (abaxonal, periaxonal and adaxonal) contain cytoplasm (Figure 4.1 B) (Scherer and Arroyo, 2002). At the lateral ends of the myelin sheath, where opposing internodes form the nodes of Ranvier, the membrane splits to form cytoplasmic paranodal loops that attach to the axons. The innermost membrane in contact with the axon also contains cytoplasmic channels such as

the potassium channels that may be involved in signal transduction between axon and oligodendrocyte (Scherer and Arroyo, 2002) (Figure 4.1 C). The molecular organization of the paranode contains heterodimers of the adhesion proteins contactin and Caspr (contactin associated protein) that are localized to the paranodal axolemma in myelinated fibers of the PNS and CNS (Einheber et al., 1997, Rios et al., 2000).
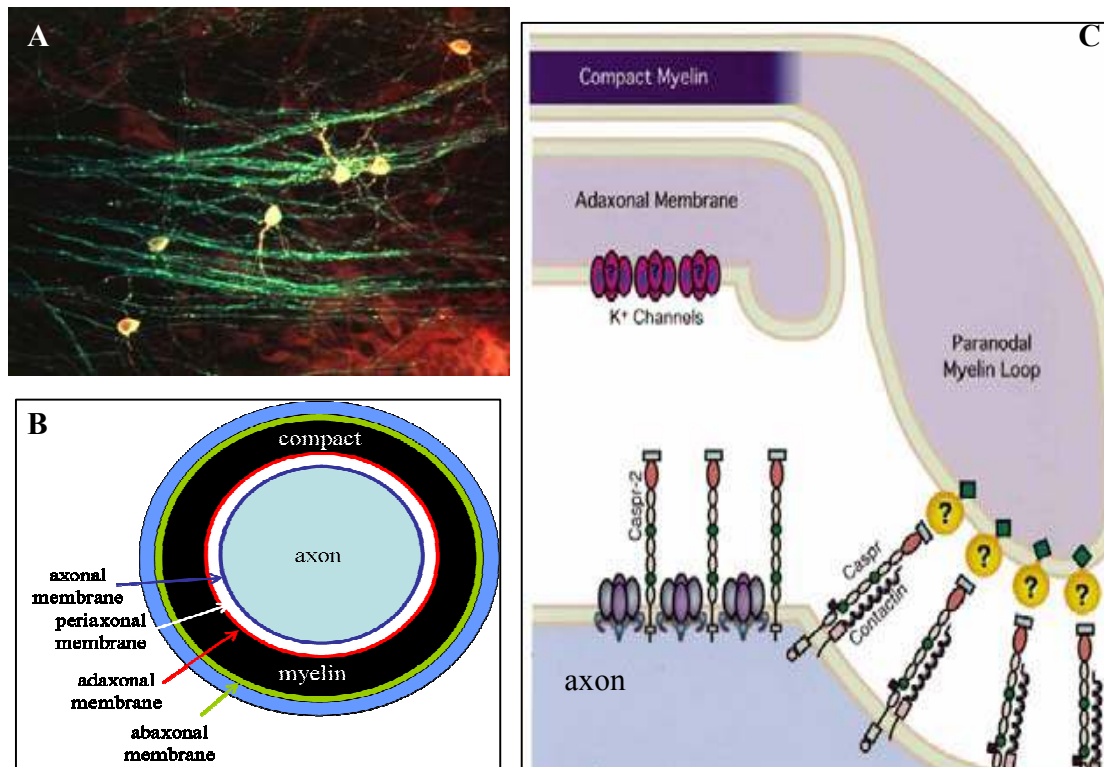
Figure 4.1. Myelinating schwann cells and oligodendrocytes. The myelin sheath is segregated in different sub-domains with unequal protein and lipid distribution. (A) Oligodendrocytes cell bodies and processes are labelled yellow, extending to myelinating axons labelled green. A single oligodendrocyte can send out many projections to myelinate many axons. (B) The circumferential organization of a myelinated axon is shown. (C) A complex set of adhesion molecules, cytoskeleton elements and membrane receptors are important for nodal integrity and correct localization of ion channels (modified from (Scherer and Arroyo, 2002).

4.1.1. Molecular composition of myelin

The myelin membrane consists of distinct sub-sets of proteins associated with either compact or non-compact compartments. In compact myelin, the myelin membrane forms

tightly packed structures implying that the specific set of proteins in this compartment have intimate interaction with the myelin membrane. In non-compact myelin the intracellular space hold significant amounts of cytoplasm and cytoskeleton assemblies. In addition to specific proteins associated with this compartment, ubiquitous cytoplasmic proteins are present in high concentration (Kursula, 2008).

Table 4.1 shows the localization and function of major myelin proteins in the compact and non-compact myelin compartments.

Protein	Localization	Proposed function
PLP/DM20[a]	Compact myelin (intraperiod line)	Compaction: adhesion of extracellular membrane leaflets
MBP[b]	Exon2[neg]: compact myelin (major dense line) Exon2^{pos}: cell body & noncompact myelin	Compaction: adhesion of intracellular membrane leaflets
MOBP[c]	Compact myelin	Maintenance of the paranodal structure stabilization of compact myelin structure?
MAL[d]	Compact and noncompact myelin	Stabilization of the radial compartment Transport of myelin proteins?
CNP[e]	Throughout noncompact myelin	Process outgrowth Stabilization of the paranodal structure
MAG[f]	Noncompact myelin: periaxonal membrane	Interaction with axonal membrane
MOG[g]	Noncompact myelin: abaxonal membrane	Interaction with extracellular matrix?
NF155[h]	Noncompact myelin: paranodal septate junction	Interaction with axonal complex of Caspr and contactin in the paranodal junction
CD9[i]	Noncompact myelin: abaxonal membrane and paranodes	Stabilization of the paranodal junction
OSP/claudin11[j]	Noncompact myelin: paranodes and radial compartment	Segregation of compact and noncompact myelin areas

Table 4.1. Localisation and function of major myelin proteins in compact and non-compact myelin. (a) (Griffiths et al., 1998), (b) (Fitzner et al., 2006), (c) (Yamamoto et al., 1994, Yamamoto et al., 1999), (d) (Schaeren-Wiemers et al., 1995, Frank et al., 1998), (e) (Brunner et al., 1989, Rasband et al., 2005), (f) (Bartsch et al., 1989, Schachner and Bartsch, 2000), (g) (Brunner et al., 1989), (h) (Tait et al., 2000), (i) (Ishibashi et al., 2004), (j) (Gow et al., 1999). (Taken from (Maier et al., 2008).

  Compact myelin proteins include; proteolipid protein (PLP) and myelin basic protein (MBP) which are required for compaction of the myelin sheath, myelin associated oligodendrocytic basic protein (MOBP) and myelin and lymphocyte protein (MAL). Proteins specific to the non-compact myelin compartment include 2'-3'-cyclic nucleotide 3'phosphodiesterase (CNP), myelin associated glycoprotein (MAG), myelin/oligodendrocyte glycoprotein (MOG), neurofascin155 (NF155), the tetraspanin protein CD9, and the oligodendrocyte specific protein (OSP)/claudin11 (Maier et al., 2008).

The relative abundance of myelin proteins in the CNS has previously been hugely over-estimated with PLP accounting for 30-45% of total myelin protein, two of the four MBP splice isoforms account for 22-53%, CNP account for 4-15 % and the remaining proteins account for 5-25% (Morell et al., 1972, Norton and Poduslo, 1973, Banik and Smith, 1977, Deber and Reynolds, 1991). However, a recent systematic proteomics study has revealed 342 proteins associated with CNS myelin and consequently lower levels of the proteins that have previously been described as abundant (Table 4.2).

Relative abundance of myelin proteins (%)		
Protein	Literature	LC-MS^E
PLP	30-45	17
MBP	22-35	8
CNP	4-15	4
MOG	ND	1
MAG	1-4	1
SIRT2	ND	1
OSP	ND	1
Others	5-25	67

Table 4.2. Comparison of myelin protein abundance. Myelin protein abundance was quantified by liquid chromatography-mass spectrophotometry (LC-MSE) with previous estimates based on band intensity after 1D-PAGE and various protein staining techniques. The abundance of PLP and MBP was previously overestimated because low abundant proteins did not constitute significant bands due to limitations in the resolving power of the 1D gels and in the dynamic range of protein staining (Taken from (Jahn et al., 2009).

Interestingly, and in keeping with the white matter specific expression, this study also highlighted the presence of Cryab (an alternative nomenclature for HspB5), as part of the CNS myelin proteome (Jahn et al., 2009).

  CNP is one of the myelin proteins found throughout the non-compact myelin compartment and is absent from the compact myelin, it is an enzymatic protein that catalyses the hydrolysis of 2',3'-cyclic nucleotides into their corresponding 2' nucleotides (Sprinkle, 1989). CNP associates with the cytoskeleton and is involved in the biogenesis and differentiation of myelin (De Angelis and Braun, 1996). It is among the first proteins detected in developing oligodendrocytes and it is enriched in the periaxonal membrane during axonal ensheathment prior to the formation of compact myelin membranes (Trapp

et al., 1988). The importance of CNP in myelination arises from studies involving transgenic (tg) mice overexpressing CNP or CNP null mice. Mice overexpressing CNP via a potential gain of function, produce abberant myelin membranes, lacking the distinct major dense lines (MDL) in compact myelin (Yin et al., 1997). The characteristic structure of the myelin sheath as determined by electron microscopy shows the presence of MDL that alternate with thinner intraperiod lines to form repeating units. The MDL results from the fusion of the thicker, inner leaflet of the oligodendrocytic plasma membrane, whereas the intraperiod line is formed by the apposition of the thinner, outer leaflet of this membrane (Figure 4.2) (Baumann and Pham-Dinh, 2001).
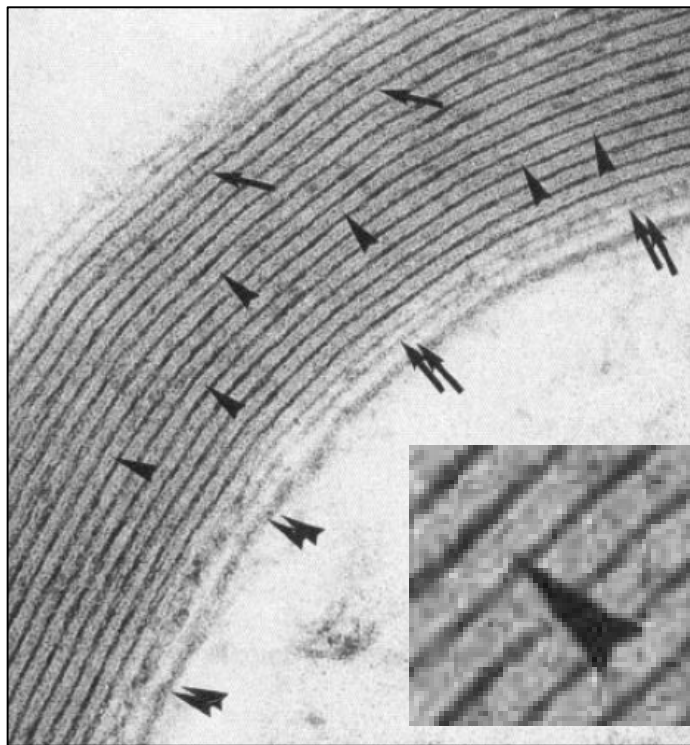
Figure 4.2. Electron microscope image showing structure of the myelin sheath. The myelin sheath is appears in a regular organization of major dense lines (arrows) and the double-stranded intraperiod lines (arrowheads) (see inset). Double arrows indicate the cytoplasmic Schwann cell collar around the myelinated axon, double arrowheads the axolemma (Adapted form (Martini et al., 1995).

Myelin membranes without MDLs were found to be deficient in MBP and enriched in CNP. CNP is thought to inhibit the accumulation of MBP by preventing its binding to membranes and targetting to the correct compartment (Yin et al., 1997). mRNA levels of

MBP were unaltered in CNP overexpressing mice, however protein levels were reduced by 30% suggesting reduced MBP translation and/or increased turover. CNP is likely to modulate these effects by participating in the dynamic regulation of submembranous actin microfilaments (Gravel et al., 1996). The mechanism by which this occurs could resemble those involving the the Rho family of GTP binding proteins (Zigmond, 1996) as CNP share several structural features with these molecules (Gravel et al., 1996). Additionally, CNP knockout mice have disrupted axoglial interactions. These mice contain mislocalised proteins such as the paranodal adhesion proteins (Caspr) and ion channels. These mice develop axonal degeneration, suggesting the importance of CNP in maintaining the integrity of paranodes and axoglial signalling (Rasband et al., 2005).

4.1.2. Transport and cytoskeletal elements

Both oligodendrocytes and Schwann cells synthesize a vast amount of myelin membrane with the appropriate proteins and lipids that are all targeted, transported and integrated into the emerging myelin sheath by an orchestrated interplay of cytoskeletal elements including vesicular transport. The myelin sheath; the sub-domains and compartments initially laid out have to be maintained throughout life (Poliak and Peles, 2003). Myelin sheath production and maintenance occurs as a result of polarized transport in oligodendrocytes involving: (1) the sorting of proteins and lipids destined for the different plasma membrane domains, (2) the directed transport towards the different plasma membrane domains along the cytoskeleton and finally (3) the specific targeting to and incorporation in the correct membrane domains. Most of the major myelin proteins are transmembrane proteins and are synthesized at the endoplasmic reticulum (ER). They are transported by vesicular transport to the golgi apparatus and further to the plasma membrane (Maier et al., 2008). However compact myelin proteins MBP and MOBP are transported towards the myelin in the form of their mRNA and subjected to local synthesis. As both proteins are extremely adhesive this may be the reason why their synthesis is restricted to their final location (Barbarese et al., 1995). In contrast, several other myelin proteins such as PLP (compact) and MAG (non-compact) are localized in endosomal compartments (Trapp et al., 1989, Kramer et al., 2001, Trajkovic et al., 2006), suggesting that transport through the endosomal system is also important for myelin proteins. PLP has been localized in late

endosomes/lysosomes however does not co-localise with other myelin proteins such as MOG and MAG, indicating that PLP is transported separately of other myelin proteins and implies that myelin proteins are sorted into distinct trafficking pathways (Kramer et al., 2001).

The cytoskeleton is essential for the coordinated process outgrowth during oligodendrocyte differentiation (Richter-Landsberg, 2000). In addition, the polarized trafficking of mRNA granules and transport vesicles towards the myelin membrane depends on an intact cytoskeleton. Microtubules are thought to provide the tracks for directed vesicular and organelle transport in oligodendrocyte processes allowing production and maintenance of the myelin sheath (Lunn et al., 1997). The MT network is abundant in the cell body and all processes, but does not extend into the most distal ends whereas actin filaments are localised to the fine processes and myelin-like membranes of oligodendrocytes (Kachar et al., 1986, Larocca and Rodriguez-Gabin, 2002).

The motor protein kinesin is important in directing transport towards the plus-end of microtubules and thus towards the myelin sheath (Carson et al., 1997). Actin has been predominantly implicated in the formation of the lamellipodium, which initiates the myelination of the axon. In addition, a number of studies have directly linked the modulation of the actin cytoskeleton to myelin-directed transport (Siskova et al., 2006, Kippert et al., 2007).

Disruption of genes, e.g., CNP and MAL that are likely to affect the transport of myelin components does not impair the initial formation of the myelin sheath, whereas later in life a defect in myelination, in particular in the paranodes becomes apparent (Maier et al., 2008). MAL may be required for the targeting of myelin proteins through the myelin sheath, whereas CNP may be important for the integration of actin and microtubule cytoskeleton thus facilitating the transport towards the paranodal loops (Maier et al., 2008).

4.1.2. White matter diseases

4.1.2.1. Multiple Sclerosis

The importance of functional oligodendrocytes and appropriate myelination becomes clear when considering diseases such as multiple sclerosis (MS), an inflammatory demyelinating disease, where abnormalities in development, maintenance and damage to

the myelin sheath results in a devastating and incapacitating disease with severe neurological symptoms (Lassmann and Lucchinetti, 2008). Additionally there are a number of genetically inherited disorders that affect CNS myelin, collectively termed leukodystrophies (Boespflug-Tanguy et al., 2008). This heterogeneous group of diseases is characterized by the loss of motor, sensory, and mental capabilities and the susceptibility to seizures (reviewed in (Kaye, 2001).

MS occurs as a result of damage to the myelin sheath leading to demyelination and glial scarring (Holley et al., 2003). This affects neuronal function, as axons are no longer able to effectively conduct signals (Compston and Coles, 2002). Approximately two thirds of MS patients have phases of relapse and remission. Relapse phases are characterised by inflammatory lesions, particularly in the white matter, consisting of B-cells, T-cells and macrophages. Inflammation in MS generally occurs in specific regions, including the optic nerve, the brainstem, the cerebellum and the long motor and sensory spinal cord fibers (Steinman, 2009). Relapses involve rapid onset of neurological defects over a short period of hours or days, including problems with vision, sensation and motor function. These periods are generally followed by remission, where there is recovery of some or most of the lost neurological functions (Steinman, 2009).

The continuous cycle of relapse and remittance can lead to a chronic and progressive disease. It is postulated that three key players are involved in the relapse- remitting disease; osteopontin, which acts as a ligand for adhesion molecules which are involved in modulating disease in mice with experimental autoimmune encephalomyelitis (EAE) (Ashkar et al., 2000), α4β1 integrin the main adhesion molecule involved (Brocke et al., 1999) and HspB5 that is essential for the recovery from neurological relapse by its anti-inflammatory properties (Ousman et al., 2007).

Relapse during MS is induced by osteopontin binding to α4β1 integrin on T-cells; this in turn increases the phosphorylation of IkB kinase-β (IKKβ). Subsequent phosphorylation of the NF-kB (nuclear factor-kB) alpha-subunit releases the p50 and p65 subunits of NF-kB, which translocates to the nucleus promoting the production of pro-survival genes (Chabas et al., 2001, Jansson et al., 2002) and blocking apoptosis by inhibition of forkhead box O3A (FOXO3A) (Hur et al., 2007). Thus, reactive T-cell survival is promoted and

subsequent release of cytokines, osteopontin and other molecules by T-cells and antigen presenting cells (APC) damage oligodendrocytes and the myelin sheath (Hur et al., 2007).

HspB5 is the most abundant transcript that is unique to MS lesions (Chabas et al., 2001). HspB5 expression is associated with remission of the effects mediated by osteopontin-α4β1. It specifically decreases the activation of NF-kB and p38MAPK in T-cells, macrophages, dendritic cells and glial cells (Ousman et al., 2007). Additionally HspB5 knockout mice with EAE showed increased T-cell responses to myelin (Ousman et al., 2007). Administration of recombinant HspB5 to mice with EAE showed a lower number of apoptotic glial cells, and decreased T-cell cytokine production, indicating a protective effect of HspB5 (Ousman et al., 2007). However, HspB5 is reported to produce one of the strongest T cell responses in MS patients (van Noort et al., 1995), thus potentially exacerbating inflammation and demyelination in MS (Ousman et al., 2007)

4.1.2.2. White matter changes in protein misfolding diseases

Alexander's disease (AxD) is a fatal neurodegenerative disease that also belongs to the leukodystrophies. It occurs as a result of mutations in the GFAP gene resulting in abnormal folding of GFAP and accumulation into protein aggregates called Rosenthal fibers. The association of misfolding events, (accumulation of Rosenthal fibers) and perturbations of astrocytic function with a failure in myelination are poorly understood (Sawaishi, 2009). However, AxD patients have extensive white matter abnormalities (van der Knaap et al., 2001), suggesting a cell autonomous effect.

Many neurodegenerative diseases characterised by misfolded proteins are also reported to have white matter abnormalities. For example, HD patients have been shown to have pre-symptomatic changes in the white matter prior to neuronal dysfunction and cell death (Ciarmiello et al., 2006). Additionally changes in the white matter have been observed in AD. Fibrillar Aβ pathology in the grey matter of the neocortex was associated with focal demyelination and loss of oligodendrocytes in sporadic and preclinical AD cases (Mitew et al., 2010).

Charcot-Marie-Tooth disease type 1A, is a hereditary demyelinating neuropathy, usually caused by overexpression of peripheral myelin protein 22 (PMP22) due to genomic duplication (Patel et al., 1992, Nelis et al., 1996) or point mutations in one copy of the

PMP22 gene (Gabreels-Festen et al., 1995). PMP22 is a minor white matter protein (Suter and Snipes, 1995) and the mechanism for demyelination is unclear. Tg mice in which PMP22 expression is regulated by a tetracycline promoter were shown to develop normally when overexpression was switched off by feeding the mice tetracycline. However, up-regulation of the gene was shown to rapidly induce active demyelination within 1 week (Perea et al., 2001). Radioactive labelling of myelin proteins suggests they are extremely stable (Sabri et al., 1974) thus the rapid demyelination in PMP22 overexpressing mice suggests PMP22 causes active demyelination either by affecting the differentiation state of the Schwann cells or by the production of abnormal myelin which then affects the whole myelin sheath (Perea et al., 2001).

Furthermore, it is increasingly apparent that it is not only the neuronal cell population that are adversely affected during various age-related neurodegenerative diseases, but associated structures (myelin sheaths) and glial cells are also affected. Hence it is possible that abnormalities in the glial cell compartment (e.g. within oligodendrocytes) either directly contribute to disease progression or modulate disease outcomes through secondary responses, for example via altered cross talk between affected glial cells and neighbouring neurons. Proteins such as HspB5 are therefore interesting candidates potentially involved in neurodegeneration (also see chapter 5 and 6).

4.2.   Aims

In view of the rather selective expression of HspB5 based on the *in situ* hybridisation data and enrichment in the myelin fraction, we wanted to better define the expression of HspB5 in oligodendrocytes by immunohistochemistry and to analyse the mRNA expression observed in Chapter 3 in greater detail.

4.3.   Results

4.3.1. HspB5 mRNA localization in the white matter

In the previous chapter (Chapter 3) HspB5 mRNA was shown to localise to oligodendroglial cells, with intense staining over and diffuse staining around the cell bodies (Figure 3.8). To further investigate mRNA distribution of HspB5 by emulsion radiography, higher magnification images of HspB5 in the corpus callosum and spinal cord

were analysed. HspB5 mRNA showed localisation over cell bodies as previously observed; additionally extra somatic staining was seen to extend away from the cell bodies and potentially order over cellular processes (Figure 4.3). This phenomenon was observed in many areas of the corpus callosum as well as the spinal cord, showing the presence of discrete particles along these processes (Figure 4.4). The signal was competed in controls (using sense and xs anti-sense oligonucleotides) (data not shown).

The staining pattern was very similar to that observed for myelin basic protein (MBP) mRNA (Figure 4.5). MBP mRNA is known to be targeted to the oligodendrocyte processes allowing it to be available for local synthesis at it desired location. Small clumps as indicated by arrows in Figure 4.5 are observed along the processes and are termed 'RNA granules'.
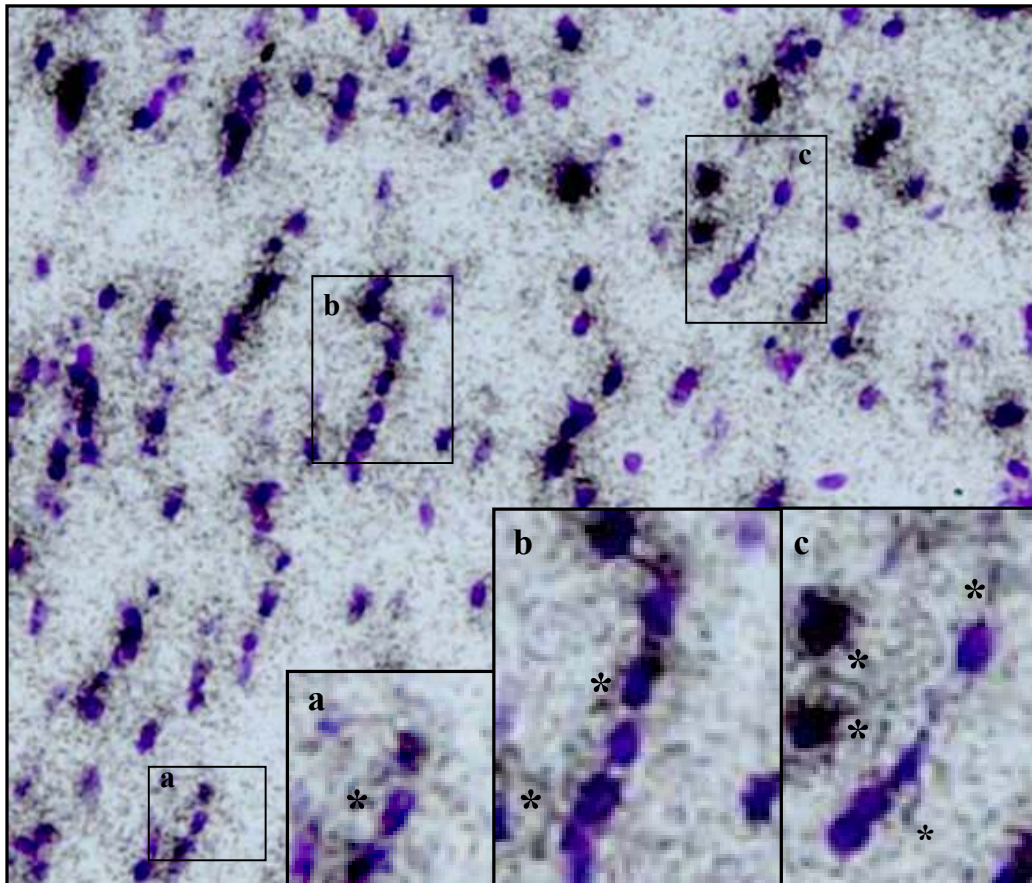
Figure 4.3. mRNA expression of HspB5 by emulsion *in situ* hybridisation in the corpus callosum. Emulsion radiography was used to visualise the expression of HspB5 in coronal mouse brain sections. Along with labelling of oligodendrocytic cell bodies, positive labelling also appeared to occur in processes emanating from the cell bodies (asterisk). Enlarged images of a, b and c are shown in the insets. Magnification: x20. Sections were counterstained with cresyl violet.
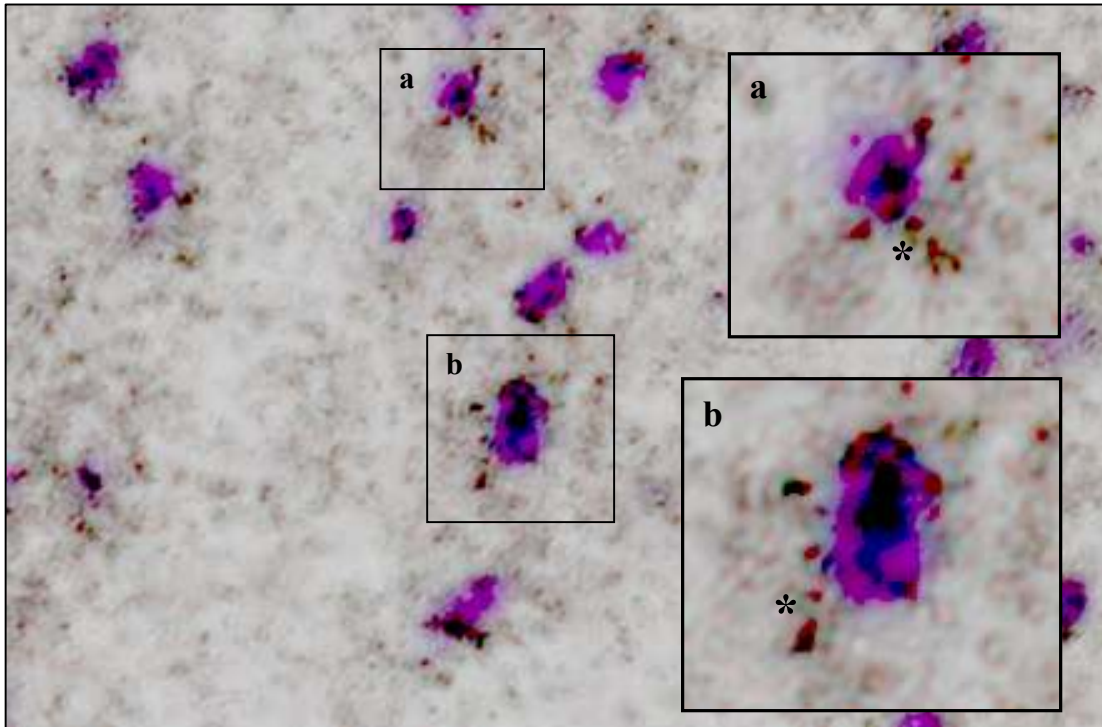
Figure 4.4. mRNA expression of HspB5 by emulsion *in situ* hybridisation in the spinal cord. Emulsion radiography was used to visualise the expression of HspB5 in spinal cord sections. Distinct staining in the form of small clumps (asterisk) that were very similar to MBP RNA granules were observed emanating from the oligodendrocytic cell bodies. Enlarged images of a, and b are shown in the insets. Magnification: x63. Sections were counterstained with cresyl violet.
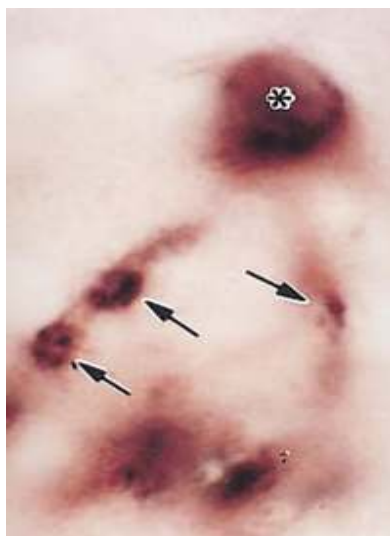
Figure 4.5. High resolution non-radioactive *in situ* hybridisation image of myelin basic protein. The nucleus has no staining (asterisk) but the surrounding cytoplasm is intensely stained. MBP mRNA extends along processes arising from the cell body (arrows). (Taken from (Bessert and Skoff, 1999).

4.3.2. Sequence analysis of transport elements in HspB5 mRNA

Conserved elements have previously been identified for a number of RNA species that are specifically targeted to distinct cellular regions in different cell types (Ainger et al, 1997). These mRNAs contain a 21-nucleotide sequence, termed the RNA transport signal (RTS). The RTS consensus sequence (GCCAAGGAGCCAGAGAGCAUG) contains two partially overlapping, homologous decanucleotide sequences: GCCAAGGAGC (rts1) and GCCAGAGAGC (rts2) (Ainger et al., 1997). A perfect or almost perfect match to either of these sequences is observed in many transported mRNA.

The complete HspB5 mRNA sequence obtained from the NCBI database (accession no: NM_009964) (Figure 4.6) was used to determine homology with either rts1 or rts2 decanucleotide sequences. This was done by processing the sequences in the alignment tool clustaw2 (www.ebi.ac.uk) which revealed an almost perfect match to the first of the decanucleotide sequences (9/10) (Figure 4.7).

5' Capped - CCTAGATCAGCTCAGGGTTCCAGTCAGACACCTAGTTCTGCTCTCCTCTAGGAC
TCCACAAAGAGTTAATGTCCCTGGGGCTAAGCCTAGGAAGATTCCAGTCCCTGCCCAGGCC
CAAGATAGTTGCTGGCTCAATTCCCCTGGCATGCGAGACTGGAGAGGAGGAGGGGCCCAC
CAGCAGCTGCTTGGGATTCCAGGCTCCGTCCTAGCTCCAGAGAACAAGGATGGGGTGGGT
GCCACTGGGTGTGGACAGAGAGCTAGTGAAACAAGACCATGACAAGTCACCGGTCAGCTC
AGCCCTGCCTGTGTTTCTCTTTTCTTAGCTCAGTGAGTACCGGGTATGTGTCACCCTGCCAA
ATCCTGATCACAAGTCTCCATGAACTGGCGGTGAGCTGGGATAATAAAACCCCTGACCTCA
CCATTCCAGAAGCTTCAGAAGACTGCATATATAAGGGGCCGGCTGGAGCTGCTGCTGAAG
GAGTTGACCAGCCAACCGACTCTGCATTCATCTAGCCACAATGGACATCGCCATCCACCAC
CCCTGGATCCGGCGCCCCTTCTTCCCCTTCCACTCCCCAAGCCGCCTCTTCGACCAGTTCTT
CGGAGAGCACCTGTTGGAGTCTGACCTCTTCTCAACAGCCACTTCCCTGAGCCCCTTCTACC
TTCGGCCACCTCCTTCCTGCGGGCACCCAGCTGGATTGACACCGGACTCTCAGAGATGCG
TTTGGAGAAGGACAGATTCTCTGTGAATCTGGACGTGAAGCACTTCTCTCCGGAGGAACTC
AAAGTCAAGGTTCTGGGGGACGTGATTGAGGTCCACGGCAAGCACGAAGAACGCCAGGAC
GAACATGGCTTCATCTCCAGGGAGTTCCACAGGAAGTACCGGATCCCAGCCGATGTGGATC
CTCTCACCATCACTTCATCCCTGTCATCTGATGGAGTCCTCACTGTGAATGGACCAAGGAA
ACAGGTGTCTGGCCCTGAGCGCACCATTCCCATCACCCGTGAAGAGAAGCCTGCTGTCGCC
GCAGCCCCTAAGAAGTAGATCCCCTTTCCTCATTGAGTTTTTTTTAAAACAAGGAAGTTTCC
CATCAGTGATTGAAAATCTGTGACTAGTGCTGAAGCTTATTAATGCTAAGGGCTGGCCCAG
ATTATTAAGCTAATAAAAATATCATTCAGCAAC 1185

Figure 4.6. HspB5 mRNA sequence (NM_009964). The complete mRNA sequence for HspB5 was used to determine homology with rts decanucleotide sequences. The region of rts homology within the entire sequence is highlighted in red. 5' untranslated region (5' UTR) is shown in black. Start and stop codons are highlighted in light blue. 3' UTR is highlighted in dark green and the poly-A tail is highlighted in light green.

```
              247
HspB5        TGGACAGAGAGCTAGTGAAACAAGACCATGACA
rts1            ---GCCAGAGAGC---
rts2            ---GCCAAGGAGC---
```

Figure 4.7. RTS homology in HspB5 mRNA. HspB5 mRNA shows an almost perfect match to one of the RTS consensus decanucleotide sequences using clustalw2 software. No other regions in the HspB5 mRNA sequence produced overlapping sequence similarity. Residues 247 – 279 are shown as this was the region were sequence homology was present. The region of homology is located in the 5' untranslated region (UTR).

4.3.3. HspB5 expression in oligodendrocyte processes (immunohistochemistry)

HspB5 expression was visualised by DAB immunohistochemistry and displayed a similar pattern of staining to that observed by *in situ* hybridisation. The hippocampus showed less HspB5 immunoreactivity in comparison to the corpus callosum and fimbria (Figure 4.8 A). The corpus callosum showed intense staining in cell bodies and fibre tracts (Figure 4.8 B/C) and the striatum oriens showed little immunoreactivity for HspB5 in comparison (Figure 4.8 C). The CA3 hippocampal region displayed an intricate pattern of staining (Figure 4.8 D). This pattern was also observed in other hippocampal regions. Cell bodies were intensely staining with delicate processes extending away into the CA3 pyramidal cell layer and surrounding area. Immunoreactivity in the CA1 displayed a similar pattern to that observed in the CA3, with intense staining of the perikaryon and a meshwork of processes extending into the stratum pyramidal. A fewer number of cell and processes were immunopositive in the CA1 in comparison to the CA3 (Figure 4.8 E). Staining of the lacunosum molecular region of the CA1 demonstrates the elaborate nature of HspB5 expression. Strong immunoreactivity in cells bodies was observed, as well as delicate staining of a number of processes extended away from the cell bodies (Figure 4.5 F).
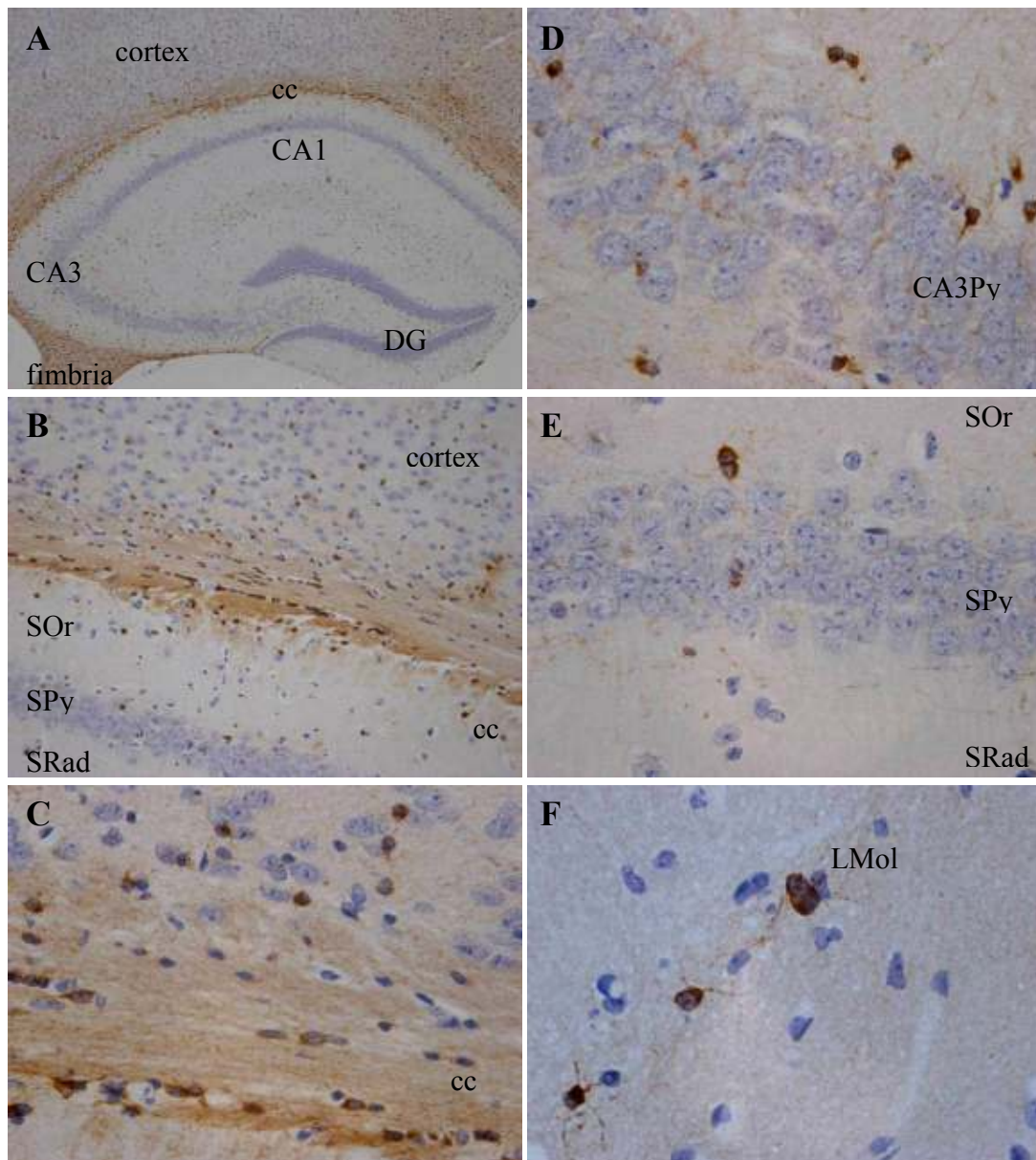
Figure 4.8. Immunohistochemical analysis of HspB5. Coronal brain sections of the dorsal hippocampus including the overlying corpus callosum were subjected to immunohistochemistry for detection of HspB5 immunoreactivity. (A) The hippocampal regions, CA1, CA3 and DG show some immunoreactivity which is sparse in comparison to the myelin rich cc and fimbria. (B) Immunoreactivity is observed in the fibre tracts of the cc as well as staining in cell bodies in and around this region. The SOr is de-enriched for HspB5 in comparison. (C) Higher magnification image of the cc showing distinctive staining of the cell bodies as well as fibre tract. (D) The CA3 hippocampal region shows an intricate pattern of staining also observed in other hippocampal regions. Cell bodies are intensely stained with delicate processes extending away into the CA3 pyramidal cell layer and surrounding area. (E) Immunoreactivity in the CA1 displays a similar pattern to that observed in the CA3, with intense staining of the perikaryon and a meshwork of processes extending into the Spy. (F) Staining of the LMol demonstrates the elaborate nature of HspB5 expression. Cells bodies are clearly and intensely stained. A number of processes extend away from the cell bodies, which line up in register with one another. Images are representative of staining from 4 animals. Corpus Callosum (cc), stratum oriens (SOr), stratum pyramidal (Spy), stratum radiatum (SRad), CA3 pyramidal cell layer (CA3Py) and lacunosum molecular (LMol). (Magnifications: A, x10; B, x20; C, x40; D, x63; E, x63; F, x100).

4.3.4. HspB5 expression in oligodendrocytes (immunofluorescence)

 HspB5 expression in oligodendrocytes was investigated by fluorescence
immunohistochemistry. Tissue was prepared and processed as detailed in section 2.11.
HspB5 staining was consistent with expression in white matter tracts such as the corpus
callosum, cingulate gyrus (Figure 4.9) and the fimbria (data not shown). The anatomical
protein expression was consistent with mRNA expression (Figure 3.5 and 3.8 d) indicating
white matter specific expression. Co-localisation of HspB5 was observed with CNP
double immunofluorescence (Figure 4.9). Immunostaining of HspB5 was more
pronounced in oligodendroglial cell bodies than CNP in comparison to staining of the fiber
tracts in the corpus callosum and fiber bundles in the cingulate gyrus. CNP staining was
more pronounced in the fiber tracts/bundles and although cell body staining was observed
it was predominately masked by the intensity of the staining in the fiber tracts.

 To confirm co-localisation of HspB5 and CNP in oligodendrocyte cell bodies, brain tissue
from the dorsal hippocampus was analysed as the hippocampus is sparsely myelinated in
comparison to the corpus callosum, allowing better visualisation of cell body staining
(Figure 4.10).
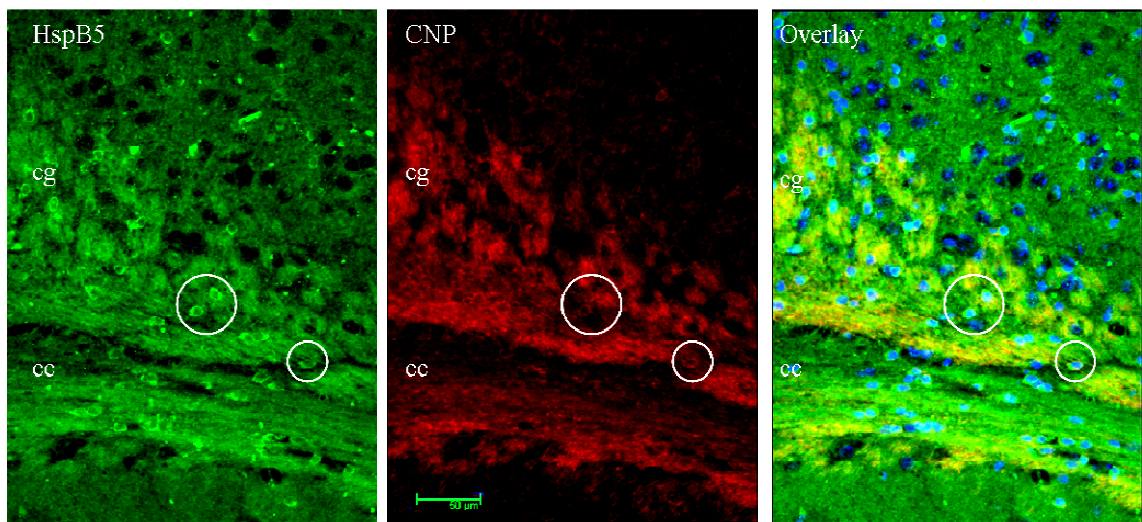
Figure 4.9. Double immunofluorescence staining of HspB5 and CNP. HspB5 shows
co-localisation with CNP staining in the fibre tracts/bundles of the corpus callosum and
cingulate gyrus. Circles show cell body staining of both proteins. Images are
representative of staining from 4 animals. Corpus callosum (cc), cingulate gyrus (cg).
Scale bar, 50µm.
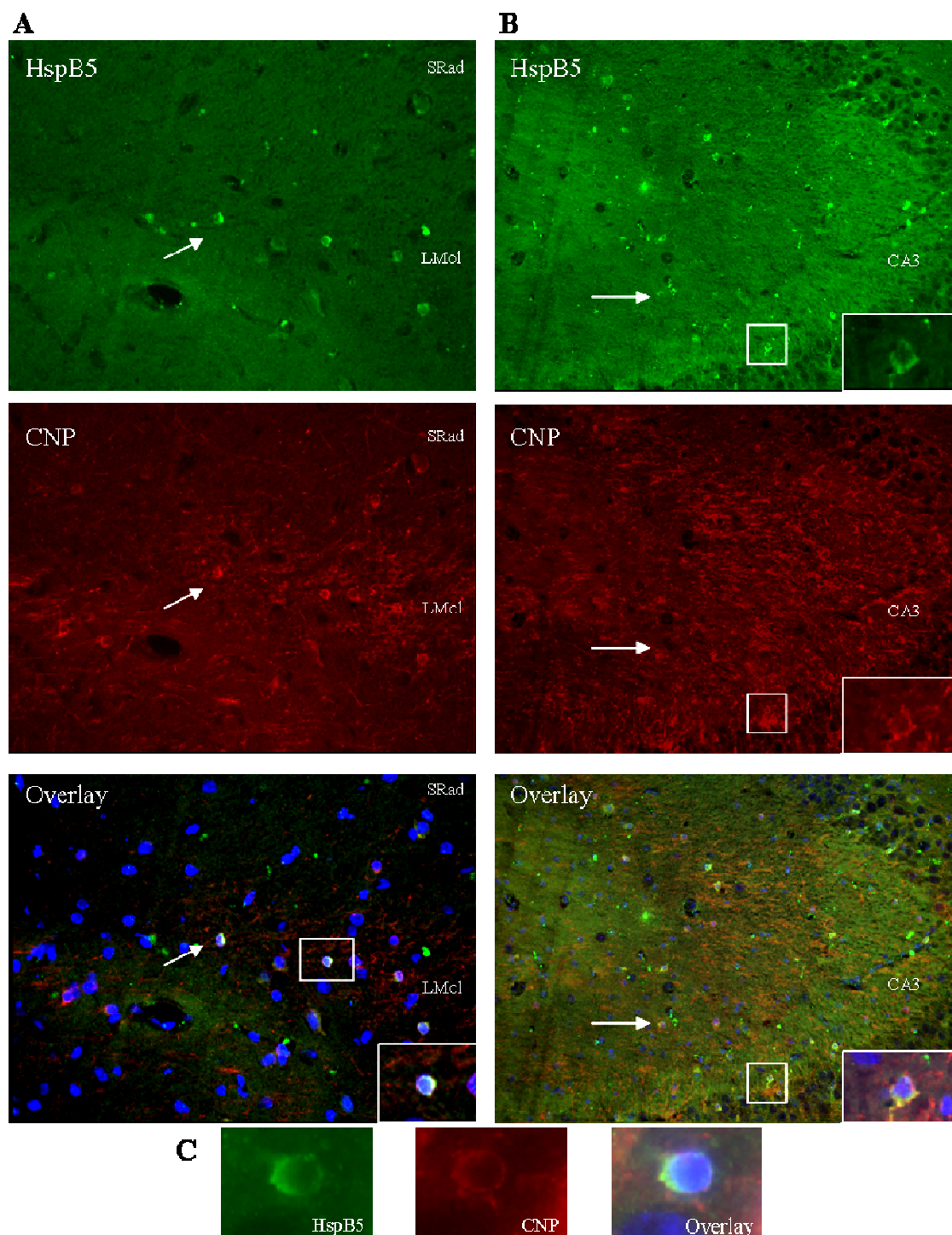
Figure 4.10. Double immunofluorescence staining of HspB5 and CNP in the hippocampus. HspB5 shows co-localisation with CNP staining in cell bodies of oligodendrocytes in all hippocampal regions. The sparse myelination of this brain region in comparison to other highly myelinated regions (cc) allows cell body staining to be observed. (A) The CA1 region LMol shows a number of HspB5 positive cells that are also CNP positive (see arrow and inset). (B) The CA3 region shows many HspB5 positive cells that are also CNP positive (see arrow). Insets show higher magnification images of the boxed cell. (C) Higher magnification images of HspB5 and CNP staining, showing co-localisation in cell body of an oligodendrocyte. Images are representative of staining from 4 animals. Stratum Radiatum (SRad), Stratum Lacunosum Molecular (LMol). (Magnifications: A, x40; B, x20 (inset = x63); C, x63).

4.4. Discussion

4.4.1. Potential targeting of HspB5 mRNA in oligodendrocytes

Emulsion radiography showed intense labelling of HspB5 mRNA over oligodendrocyte cell bodies along with expression in cellular processes extending away from the cell body. This was observed in all myelinated regions analysed (Figure 4.3 and Figure 4.4). The non-somatic expression suggested the possibility that HspB5 mRNA is transported or indeed targeted to specific compartments in the myelin as shown for a number of myelin specific proteins such MBP (Ainger et al., 1997). Selective targeting of mRNA to distinct cellular compartments has also previous been described in neuronal dendrites (Kuhl and Skehel, 1998) suggesting similar mechanisms occur in different systems. HspB5 also displayed a very similar expression pattern by *in situ* hybridization to that observed for MBP. Distinct globular staining was observed for both HspB5 (Figure 4.4) and MBP (Figure 4.5). MBP mRNA is specifically targeted to oligodendrocyte processes in 'RNA granules' that are observed as globular round clumps along the processes as shown Figure 4.5. The transport of MBP protein makes it available for local synthesis on free polysomes primarly in cell processes in close proximity to the myelin forming plasma membrane (Trapp et al., 1987). MBP is synthesised locally to prevent this highly basic protein from interacting non-specifically with membranes. The sequence of events involved in MBP mRNA targetting is depicted in Figure 4.11 illustrating the sub-compartment specific, multistep mechanisms involved. As HspB5 displays a similar pattern of mRNA expression extending into the oligodendrocyte processes, suggests it is specifically targetted, possibly by a similar mechanism as employed for MBP. This would allow localised and rapid synthesis of a chaperone protein, involved in cytoskeletal regulation, redox homeostasis with anti-apoptotic function to counteract any stress or adverse cellular changes.
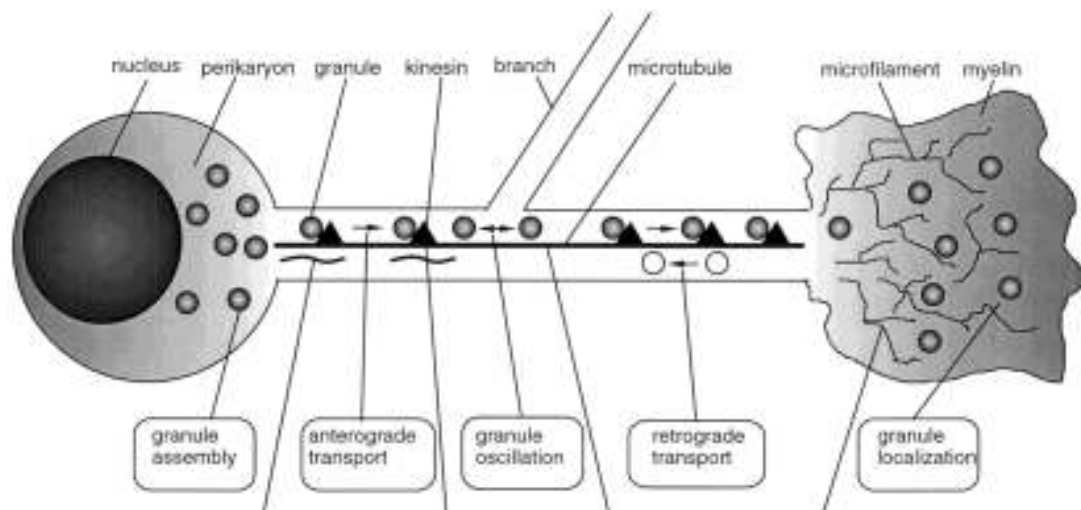
Figure 4.11. Multi-step model for intracellular trafficking of MBP mRNA in oligodendrocytes. A schematic diagram of an oligodendrocyte is shown (not drawn to scale). The following cellular components are labelled above the diagram: nucleus, perikaryon, RNA granules, microtubules, kinesin motors, microfilaments, and myelin membrane. The major steps in translocation of MBP mRNA are indicated in boxes below the diagram (Carson et al., 1997).

Local synthesis of HspB5 has previously been reported in injury conditioned dorsal root ganglion (DRG) neuronal cultures (Willis et al., 2005). The dual localisation of HspB5 in both the perinuclear cytoplasm and also cellular processes, suggest an overlapping function with proteins such as MBP and CNP. CNP mRNA is concentrated around oligodendrocyte perinuclear regions and is sythesised by free ribosomes and MBP is transported and synthesised locally (Trapp et al., 1988). It is possible that a cytoplasmic pool of HspB5 is synthesised and incorporated into the myelin sheath and a targetted pool is retained until it is required. Indeed, a cytoskeletal component neurofilament-M (NF-M) mRNA translation has been shown to be induced by loss of contact of Schwann cells that have been placed in culture and deprived of axonal contact (Kelly et al., 1992). Additionally in spite of the prescence of NF-M mRNA in Schwann cells during development, NF-M protein is not a significant Schwann cell constituent (Fabrizi et al., 1997).

4.4.2. Sequence analysis of HspB5 mRNA

Selective transport of mRNA is not restricted to proteins such as MBP that would otherwise adhere non-specifically to other cellular membranes. Transport of mRNAs

encoding other proteins has been reported in various cell types (Ainger et al., 1997). Targetting and localisation generally requires the prescence of specific sequences or secondary structural motifs. A 21-nucleotide transport sequence (RTS) is necessary and sufficient for transport of mRNA in different cells and in oligodendrocytes. The RTS is found in both the untranslated regions (UTR) or in the coding region of the mRNA. Examples of transported mRNAs containing an RTS are shown in Table 4.3.

Species	mRNA	Region	RTS sequence
Transported RNAs			
Rat	MBP	3'UTR	GCCAAGGAGCCAGAGAGCAUG
Mouse	MBP	3'UTR	GCCAAGGAGCCAGAGAGCAUG
Human	MBP RTS1	3'UTR	GCCAUGGAGGCACACAGC UG
Human	MBP RTS2	3'UTR	GCUGCAGAGACAGAGAGGACG
Rat	MOBP81A	3'UTR	ACCCCCGAGACACAGAGCAUG
Rat	GFAP	ORF	GCCAAGGAGCCCACCAAACUG
Human	Ca-N	ORF	GCCAAGGAGCGAGAGAGGGUG
Mouse	MAP2A	ORF	GCCAAGGAGUCAGAAGAGAUG
Bovine	GABAR(A)	3'UTR	GAGAGGGAGCCAGAGAGCAAA
Bovine	NOS	5'UTR	CACGAGGAGCCACAGAGCAGA
Rat	ARC	ORF	GCUGAGGAGGAGGAGAUCAUU
Rat	RC3	5'UTR	GCCAAGGACCCUCAACACCGG
Mouse	protamine 2	3'UTR	GCCAAGGAGCCACGAGAUCUG
Mouse	**HspB5**	**5' UTR**	**TGGGTGTG****GACAGAGAGC****TAG**
Consensus sequence			**GCCAAGGAGCCAGAGAGCAUG**

Table 4.3. RTS homology in mRNAs known to be transported. All sequences are from mature RNAs. The species and location of the RTS homology are indicated. HspB5 mRNA sequence showing homology to RTS is also indicated. *ARC*, activity-related cytoskeleton-associated protein; Ca-N, N-type calcium channel α1; GABAR(A), gaba amino butyric acid receptor α subunit; GFAP, glial fibrillary acidic protein; MOBP, myelin-associated/oligodendrocytic basic protein; NOS, nitric oxide synthase; RC3, neurogranin (Adapted from Ainger et al., 1997).

The full length RTS was not present in the HspB5 mRNA sequence, but almost complete homology was observed in the 5'UTR with a decanucleotide sequence present in the concensus RTS (rts1) (Figure 4.7). This may be sufficient in mediating RNA transport of HspB5, as many of the mRNAs containing the RTS have almost complete homology to one of the decanucleotide sequences.

4.4.3. Protein expression of HspB5 in oligodendrocytes.

HspB5 staining as observed by IHC displayed an intricate nature of HspB5 expression, not only in the perikaryon, but also in oligodendrocyte processes and myelin tracts. The level of myelination in the hippocampus is relatively sparse in comparison to heavily myelinated structures such as the corpus callosum. It is not clear which neurons are myelinated, however oligodendrocyte expression has recently been investigated in the mouse hippocampus (Vinet et al., 2010). Interestingly this study identified three morphologically distinct sub-populations of oligodendrocytes using mice expressing eGFP under an oligodendrocyte-specific promoter. These subtypes were shown to be differentially distributed in the various layers of the hippocampus.

The hippocampal staining of HspB5 (Figure 4.8) shows overlap with the majority of the identified oligodendrocyte subpopulation as described by Vinet et al. (2010). Interestingly this suggests that HspB5 may potentially be a useful general marker for oligodendrocytes in the hippocampus. The HspB5 staining in the hippocampus does not display the typical organisation observed in structures such as the corpus callosum with cell bodies forming tandem arrays in close register, but cell bodies are distributed throughout the hippocampus. The lacunosum molecular layer shows some oligodendrocytes lining up together, but the separation of the cell bodies is greater than that observed in other white matter regions. The staining pattern observed shows resemblance to the chondroitin sulphate proteoglycan NG2-expressing (NG2) progenitor cells. These cells are oligodendrocyte precursor cells (OPC) that are thought to give rise to oligodendrocytes. Transgenic mice expressing CNP-EGFP were shown to co-localise with a population of NG2 cells in addition to mature oligodendrocytes in the hippocampus (Mangin et al., 2008). As HspB5 co-localised with CNP in the hippocampus it can be speculated that some of these distinctive cells are also NG2 cells. NG2 progenitor cells are anatomically placed close to neuronal cells. They have a small cell bodies and thin radiating processes (Lin and Bergles, 2002). Their processes are usually intertwined with neuronal dendrites and they are anatomically associated with interneurons in the hippocampus (Mangin et al., 2008). This observation is consistent with the remarkable similarities of NG2, CNP and HspB5 staining with interneuronal proteins such as CB1 (cannabinoid receptor 1) (Katona et al., 1999). NG2 cells in the gray matter generally remain quiescent, although these cells are OPC's they

also have the potential to differentiate into interneurons in the hippocampus (Belachew et al., 2003, Aguirre et al., 2004). Vinet et al. (2010), showed that NG2 cells co-localised faintly with CNP-EGFP expressing cells, however olig-2 expression in these cells was high (91.4%) indicating the probable immature oligodendrocytic nature of these cells (Vinet et al., 2010).

4.4.4. HspB5 co-localises with CNP a non-compact myelin protein

Co-localisation of HspB5 and CNP was observed in all regions analysed. Both HspB5 and CNP labelled white matter tracts throughout the tissue sections. Additionally HspB5 staining was stronger in the cell bodies, whereas CNP staining, although present in cell bodies, was masked by intense staining of the surrounding myelin fibres (Figure 4.7). Co-localisation was clearly observed in the cell bodies of the dorsal hippocampus, showing perinuclear expression as well as expression in processes of oligodendrocytes (Figure 4.8 B (inset)).

Colocalisation of HspB5 with CNP not only confirms expression of HspB5 in oligodendrocytes, but also allows functional assumptions to be made. CNP, like HspB5 is expressed in oligodrendrocytes in the CNS and also in Schwann cells in the peripheral nervous system. It is found to be localised to the cytoplasmic membrane of oligodendrocytes and Schwann cells consistent with a role in membrane synthesis and maintanence as well as signal transduction within these cells (Trapp et al., 1988, Lee et al., 2005b).

CNP expression shows significant overlap with that of HspB5, it is expressed in all white matter containing structures, such as the corpus callosum, the optic nerve and the spinal cord. It is also present in the outer rod segment of the visual system where major membrane reorganisation occurs in response to visual input (Heath and Hindman, 1986). CNP is not a major component of myelin in comparison to MBP and PLP, however is still relatively abundant (Kurihara and Tsukada, 1967, Olafson et al., 1969). It is found associated with the non-compact myelin compartment, and is observed in paranodal loops, inner and outer loop and tongue structures, incisure like membranes and in periaxonal regions (Trapp et al., 1988).

Up to 40% of CNP is thought to associate with the detergent insoluble membrane fraction containing lipid rafts (Kim and Pfeiffer, 1999). HspB5 has also been shown to bind membrane lipids *in vitro* (Cobb and Petrash, 2000). The binding capacity is dependent on the lipid composition, with a higher binding capacity associated with a higher amount of sphingolipids and lower amounts of phosphotidylethanolamine (PE) related lipids (Grami et al., 2005). As the white matter is enriched in sphingolipids, it is likely the HspB5 associates with membranous structure such as lipid raft.

HspB5 and CNP associate with both the actin (microfilament) and tubulin (micotubule) cytoskeleton (Dyer et al., 1995). CNP acts as a microtubule-associated protein (MAP) linking tubulin with the plasma membrane (Bifulco et al., 2002), whereas HspB5 binds to microtubules via MAP's (Fujita et al., 2004). CNP is able to induce MT polymerisation, and direct the formation of branched process outgrowth (Lee et al., 2005b) and HspB5 stabilises the MT (Fujita et al., 2004). The overlapping functions of both proteins suggests that HspB5 may also be involved in lipid raft mediated signalling, affecting myelin cytoskeletal components, as suggested for CNP (Hinman et al., 2008).

Along with the potential role of HspB5 in maintaining myelin structure by interaction/regulation of the cytoskeleton, HspB5 may be crucial in regulating a cellular stress response and conferring protection. Indeed, proteolytic stress in oligodendroglial cell line induces aggresome formation containing tau, HspB5 and ubiquitin, close to the microtubule organising centre (MTOC) (Bauer and Richter-Landsberg, 2006).

Myelinated axons have been shown to be protected from oxidative stress in comparison to non-myelinated axons. The known function of HspB5 in redox homeostasis and its potential localisation to lipid rafts in oligodendrocytes places it in a key position where cross talk between neuronal and oligodendrocytes can occur, allowing protective responses to be regulated by this protein. Additionally the abundance of HspB5 may reflect the intrinsic vulnerabilities of oligodendrocytes and the need for a molecular chaperone that is able to modulate many cellular responses.

Oligodendrocytes are more susceptible to stress and injury such as ischemic insult in comparison to other glial cells (Husain and Juurlink, 1995) this is likely associated with increase ROS generation   Rat glial cultures preloaded with DCFH (5-(and-6)-carboxyl-2',7'-dichlorodihydrofluorescein) an indicator of oxidative stress showed pronounced

fluorescence signal in oligodendroglial cells with little signal in astrocytes, (Juurlink, 1997). This was attributed to a higher burden of oxidative stress in oligodendrocytes compared to astrocytes as established by measuring ROS activity under normal culture conditions (Thorburne and Juurlink, 1996). Oligodendrocytes are the major store of iron in the CNS (Connor, 1994). The levels of glutathione (GSH), an antioxidant enzyme, were also measured and were significantly lower in oligodendrocytes compared to astrocytes (1mM vs. 5mM). Combined with a high iron content such a combination makes oligodendrocytes potentially more susceptible to ROS generation. ROS have pronounced effects on lipids, for example de-esterification of membrane phospholipids by ROS with the subsequent release of free fatty acids which can be further oxidized by ROS (Deby and Goutier, 1990). With myelin membranes composed of high amounts of lipid, modulation of ROS levels would seem to be important for maintaining myelin function, and could be one of the potential roles for HspB5 in oligodendrocytes.

Additionally a role for zinc has been proposed in the compaction of the mature myelin sheath (Riccio et al., 1995, Tsang et al., 1997). Interestingly the chaperone activity of HspB5 has been shown to be increased in the presence of zinc (Coi et al., 2008). This raises the potential for HspB5 to be involved in modulating myelin proteins during compaction and facilitating correct structure and localisation by way of chaperone activity.

4.5. Summary

Oligodendroglial expression of HspB5 was investigated by immunohistochemistry in mouse brain sections and co-localisation of HspB5 was observed with CNP. Detailed analysis of *in situ* hybridisation (emulsion radiography) showed mRNA localisation over cell bodies as previously shown in Chapter 3 as well as specific expression along processes emanating from the cell body in a similar fashion to that observed for MBP. Sequence analysis revealed the prescence of a putitive RTS domain in the HspB5 mRNA sequence suggesting targeted transport and expression of HspB5, perhaps similar to what is known about MBP. The schematic shown in Figure 4.12 summarizes expression of HspB5 in oligodendrocytes and also includes a description of specific, potential roles of HspB5 in oligodendrocytes.
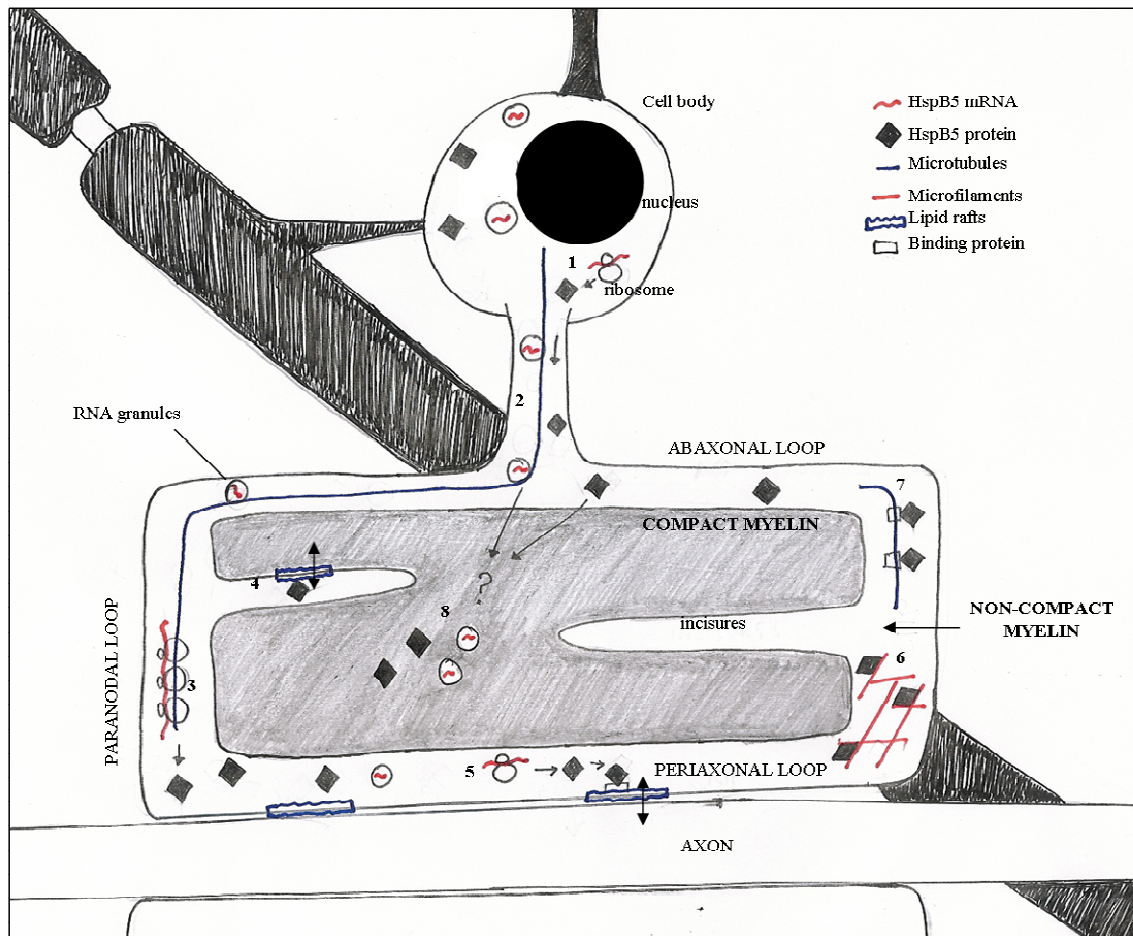
Figure 4.12. Proposed expression/function of HspB5 in oligodendrocytes. A schematic drawing which illustrates the expression of HspB5 in oligodendrocytes and also depicts potential roles. HspB5 mRNA and protein are found within the cell body and in the myelin sheath of oligodendrocytes. (1) mRNA may be translated on free ribosomes, in a similar fashion to CNP before being targetted to non-compact myelin. (2) mRNA may be transported in RNA granules to specific regions. (3) mRNA may be transcribed by free ribosomes or polysomes at the site of function. (4) HspB5 protein may interact with lipid rafts allowing crosstalk between myelin subdomains. (5) Localised synthesis or targetted proteins may interact with lipid rafts in regions where axo-glial crosstalk and signalling events can be initiated/regulated. (6) HspB5 protein binds and stabilises microfilaments, and may be involved in membrane maintanence and synthesis. (7) HspB5 protein interacts with microtubules, likely through accessory proteins (MAPs) to modulate the cytoskeleton. (8) HspB5 protein and mRNA could potentially be targetted to compact myelin, by similar mechanisms as described for MBP. HspB5 may also be involved in counteracting oxidative stress and having a general chaperone role in these specialised oligodendrocyte sub-compartments.

Chapter 5: Selective and progressive downregulation of HspB5 in the R6/2 mouse model of Huntington's disease

5.1. Introduction

Chapter 3 has highlighted the constitutive expression of HspB1, HspB5, HspB6 and HspB8 under physiological conditions in the adult mouse CNS. These four sHsps have varying expression levels in distinct anatomical regions of the CNS, and are also differentially associated within cell types and sub-compartments of the brain (as shown in Chapter 3 and 4). HspB1 and HspB8 displayed selective expression in a subpopulation of motor neurons in the ventral horn of the spinal cord (Figure 3.4 and 3.8) and HspB5 and HspB6 were enriched in the myelin compartment of brain fractions (Figure 3.12). Furthermore, HspB5 mRNA expression was localized to the cell bodies and processes of oligodendrocytes (Chapter 4) suggesting mRNA targeting and a potential for local translation of this sHsp in the myelin compartment. HspB5 also showed co-localisation with CNP, a non-compact white matter protein, suggesting HspB5 expression in the white matter could be selective to the non-compact myelin compartment as discussed in Chapter 4. The constitutive expression of sHsps in neuronal and non-neuronal cells suggests they are important for the normal function of these cells. This is further supported by the fact that mutations in sHsps give rise to myopathies and neuropathies (see Introduction; Table 1.3).

Given that proteinopathies are to some extent associated with brain region- and cell specific pathology, it is conceivable that the 4 sHsps could be involved in modulating disease processes such as protein aggregation, oxidative stress and inflammation, as described in the general introduction. The sHsps are up-regulated in response to insults and stresses in both neuronal and glial cells (Goldbaum and Richter-Landsberg, 2001, Dabir et al., 2004) and have indeed been shown to modulate pathologies in several *in vivo* and *in vitro* studies of chronic neurodegeneration (Wilhelmus et al., 2006a, Ousman et al., 2007, Sharp et al., 2008). To investigate the change in sHsp expression and the potential contribution to chronic neurodegeneration in a model characterized by intracellular aggregates, this chapter will focus on expression of the sHsps in the R6/2 mouse model of HD.

The R6/2 transgenic mice recapitulate and display many of the symptoms and clinical features observed in HD patients. These include impaired motor coordination, tremor, changes in open field activity and progressive weight loss (Menalled and Chesselet, 2002).

For this reason it is considered a useful 'model' for understanding the pathological changes and dysfunction that occurs prior to cell death (Turmaine et al., 2000) and has revealed a number of potentially important and specific details on changes and mechanisms essential to pathology in human disease (Zucker et al., 2005, van der Burg et al., 2008).

Many studies have focused on the events that occur in the late stage of neurodegenerative disease. It is now becoming apparent that the changes that occur early during chronic neurodegeneration, before the manifestation of clinical symptoms are important in disease progression and may provide a pivotal step for therapeutic intervention. Post-mortem studies in HD suggest that the appearance of motor and cognitive symptoms occur in the absence of overt neuronal loss thus impaired cognition is likely caused by cellular dysfunction (Vonsattel et al., 1985). Synaptic dysfunction and reduced/increased excitability that change neuronal plasticity are likely candidates that underlie the cellular dysfunction observed (Murphy et al., 2000, Milnerwood et al., 2006).

Altered levels of neurotransmitter receptors (Cha et al., 1998) and changes in mRNA expression are apparent in the striatum and cortex of the R6/2 mice at 6 weeks. cAMP regulated genes are downregulated, whereas some genes are up-regulated e.g. DNA repair enzymes (Luthi-Carter et al., 2000, Sugars et al., 2004). Dysregulation is not only limited to the transcript level, but changes in protein expression and post-translational regulation are also observed.

Interestingly, the expression of some molecular chaperones and co-chaperones such as Hsp70, Hsp40 and α-SGT (small glutamine-rich tetratricopeptide repeat domain protein) are reduced by about 40 % at 14 weeks of age. This is thought to be a consequence of recruitment into httEx1-positive inclusions as shown by co-localisation studies (Hay et al., 2004).

The brains of R6/2 mice have been reported to weigh approximately 20% less than wild type animals at 12 weeks (Mangiarini et al., 1996). This marked reduction does not correlate with cell death, as limited cell loss is observed in this model. In the cortex and the striatum a small number of neurons were shown to undergo "dark cell degeneration" (Turmaine et al., 2000), but progressive and substantial loss of orexin-neurons was observed in the lateral hypothalamus (Petersen et al., 2005). However, this was not ascribed to the gross reduction in brain volume seen in the R6/2 mice. The reduction could

be a result of atrophy of individual neurons as the cell bodies of MSNs were shown to shrink by ~20% (Klapstein et al., 2001). Interestingly, axonal atrophy was found to be a prominent feature of degenerating myelinated axons, with axoplasms showing a 15% reduction in diameter (Wade et al., 2008). Additionally pre-symptomatic changes in the white matter of HD patients have also been reported suggesting white matter pathology and volume loss may precede neuronal dysfunction and cell death (Ciarmiello et al., 2006). These observations indicate an additional importance of changes in the white matter and hence place two of the sHsps (HspB5 and HspB6) to a perhaps vulnerable glial cell type.

5.2.   Aims

The aim of this chapter is to analyse expression of the 4 sHsps constitutively expressed in the mouse CNS under normal conditions (HspB1, HspB5, HspB6 and HspB8) in the R6/2 mouse model of HD. As early and progressive changes appear to be important in the pathogenesis of disease, three time points will be analysed to encompass the breadth of disease progression (Carter et al., 1999, Morton et al., 2000). Expression will be analysed at an early (pre-symptomatic; 4 weeks), mid (cognitive and behavioural abnormalities; 9 weeks), and late (symptomatic; 17 weeks) stage of disease. As HD is suggested to occur via selective dysfunction in certain brain regions, we investigated expression of sHsps in the striatum and cortex and compared this to the cerebellum. This provides a way to investigate preferentially affected regions (cortex and striatum) to one that is spared from pathology until very late in the disease (cerebellum) in addition to age matched wild type controls. The white matter specific expression of HspB5 in non-compact myelin and the white matter changes that have been documented in HD patients and the R6/2 animals as described above, provoke the need to investigate the expression of this sHsp in a white matter rich region. Indeed, the cerebellum provides an ideal brain region to investigate the potential changes of the white matter specific HspB5.

5.3.   Results

5.3.1. sHsps in soluble brain fractions at early and mid stages of disease

Cortex, striatum and cerebellum samples were microdissected from R6/2 transgenic (tg) and wild type (wt) littermates. Tissue from 4 and 9 week old animals was subjected to

mechanical homogenization in a detergent (NP-40) based lysis buffer and spun at low speed (6000rpm) to pellet nuclei and the resultant supernatant was used for analysis (section 2.3.3). 40µg of protein from each sample was resolved on SDS-PAGE and western blotting was used to analyse expression of the four sHsps expressed in the CNS. The pixel intensity values were normalized to protein loading (section 2.8.4) and the average intensity of the bands was plotted for the three brain regions. Differences in pixel intensity between time points do not correspond to difference in protein levels, but are reflective of differences in individual blots and subsequent normalization to protein loading.

5.3.1.1. HspB1

Protein expression of HspB1 within the frontal cortex, striatum and the cerebellum was quantified by western-blotting. Figure 5.1 shows the protein expression of HspB1 at early (4wks) and mid-stage (9wks) of the disease. Representative western blots are shown below each graph. HspB1 does not show any significant differences in expression between tg and wt animals in the three brain regions, at 4 or 9 weeks of age (Figure 5.1A and B).
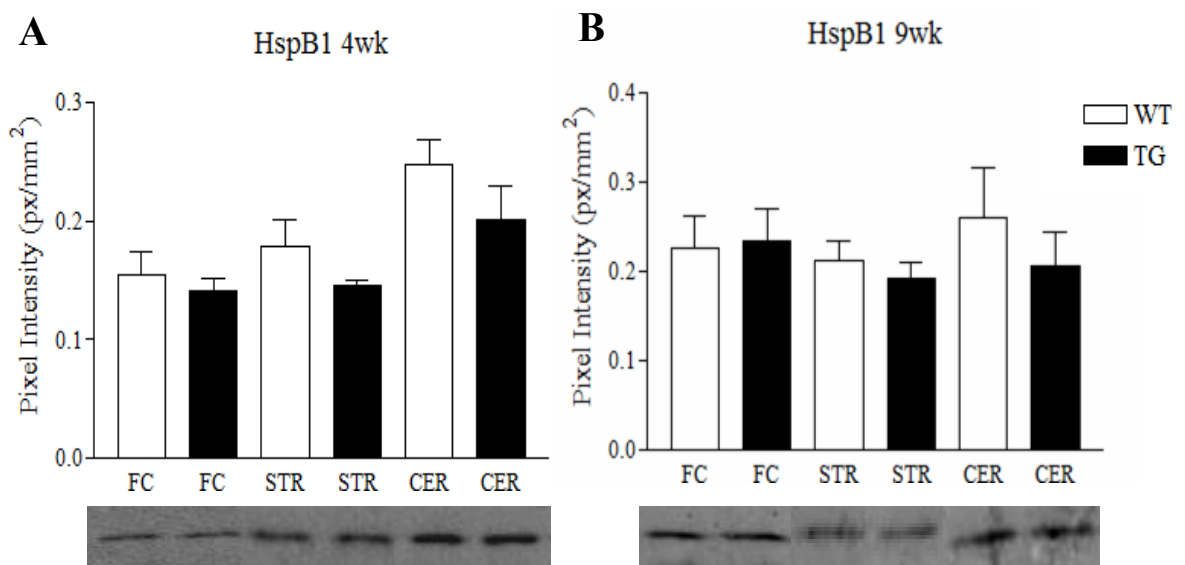
Figure 5.1. HspB1 protein expression in supernatant fractions at early (4wk) and mid (9 wk) stage of disease. 40μg of protein from frontal cortex, striatum and cerebellum homogenates were resolved by SDS-PAGE and expression of HspB1 was measured by incubating membranes with an antibody against HspB1 followed by a fluorescently labelled secondary antibody which was detected by infrared fluorescence. Intensity values were measured using Odyssey Infrared Scanner software and normalized to protein loading and expressed as pixel intensity per mm^2. Expression of HspB1 is shown in distinct brain regions at A, 4 and B, 9 weeks. (A) No changes in HspB1 expression were observed in tg animals in any brain region studied at 4 weeks. (B) There were also no changes in HspB1 expression in tg animals in the three brain regions analyzed at 9 weeks. Representative blots are shown below the corresponding graph (n = 6). One-way analysis of variance (ANOVA), followed by Newman-Keuls post hoc test was used to determine significance between wt and tg samples within regions and between brain regions (p, <0.05), error bars represent SEM. FC (frontal cortex); STR (striatum); CER (cerebellum); WT (wild type); TG (transgenic).

5.3.1.2.   HspB5

Next, protein expression of HspB5 within the frontal cortex, striatum and the cerebellum was quantified by western-blotting. HspB5 showed statistically higher levels of expression in the cerebellum and striatum of wt animals relative to the frontal cortex (Figure 5.4). This may be a reflection of white matter/oligodendrocyte density in this region. Indeed, as shown in Figure 5.17, MBP expression is higher in the cerebellum and striatum compared to the cortex. Figure 5.2 represents the protein expression of HspB5 at early (4wks) and mid-stage (9wks) of the disease. Representative western blots are shown below each graph. HspB5 expression showed a trend towards reduction in tg animals in all three brain regions at 4 weeks. This was more pronounced at 9 weeks, and was statistically significant in the frontal cortex at this time point (Figure 5.2).

Figure 5.2. HspB5 protein expression in supernatant fractions at early (4wk) and mid (9wk) stage of disease. 40μg of protein from frontal cortex, striatum and cerebellum homogenates were resolved by SDS-PAGE and expression of HspB5 was measured by incubating membranes with an antibody against HspB5 followed by a fluorescently labelled secondary antibody which was detected by infrared fluorescence. Intensity values were measured using Odyssey Infrared Scanner software and normalized to protein loading and expressed as pixel intensity per mm^2. Expression of HspB5 is shown in distinct brain regions at A, 4 and B, 9 weeks. (A) HspB5 protein levels were decreased in tg animals in all three brain regions at 4 weeks. (B) Downregulation of HspB5 was more pronounced at 9 weeks in all three brain regions and was statistically significant in the frontal cortex at the later time point. Representative blots are shown below corresponding graph (n = 6). One-way analysis of variance (ANOVA), followed by Newman-Keuls post hoc test was used to determine significance between wt and tg samples within regions and between brain regions (*p, <0.05; **p, <0.01; ***p, <0.001), error bars represent SEM. FC (frontal cortex); STR (striatum); CER (cerebellum); WT (wild type); TG (transgenic).

5.3.1.3.   HspB6

Protein expression of HspB6 within the frontal cortex, striatum and the cerebellum was also quantified by western-blotting. Figure 5.3 represents the protein expression of HspB6 at early (4wks) and mid-stage (9wks) of the disease. HspB6 shows a different profile to that seen for HspB1 and HspB5. There was no detectable expression of HspB6 in the frontal cortex at 4 weeks in both tg and wt animals (Figure 5.3 A). Immunoreactivity was observed in the striatum and cerebellum at this time point, however there were no changes in expression between wt and tg animals. At 9 weeks, the expression profile of HspB6 was very different to that seen at 4 weeks (Figure 5.3 B). Immunoreactivity was now absent in the cerebellum and present in the frontal cortex, albeit low in comparison to the striatum. The differences observed were due the differential detergent extractabilities of this sHsps, as characterized in Chapter 3 (also see appendix 3).
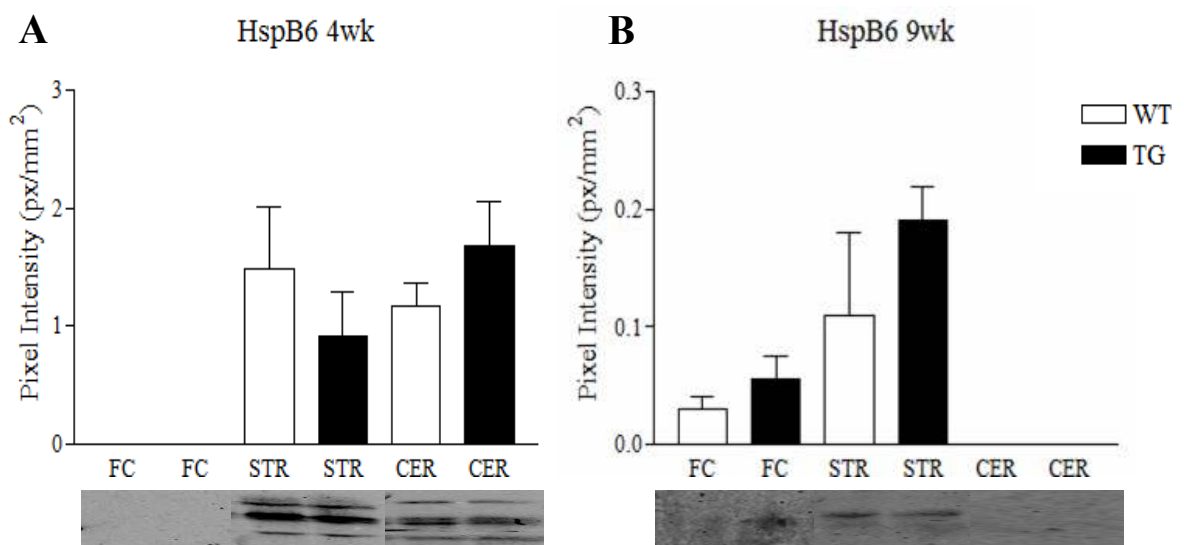
Figure 5.3. HspB6 protein expression in supernatant fractions at early (4wk) and mid (9wk) stage of disease. 40μg of protein from frontal cortex, striatum and cerebellum homogenates were resolved by SDS-PAGE and expression of HspB6 was measured by incubating membranes with an antibody against HspB6 followed by a fluorescently labelled secondary antibody which was detected by infrared fluorescence. Intensity values were measured using Odyssey Infrared Scanner software and normalized to protein loading and expressed as pixel intensity per mm^2. Expression of HspB6 is shown in distinct brain regions at A, 4 and B, 9 weeks. (A) HspB6 immunoreactivity was absent in the frontal cortex at 4 weeks and there were no changes in expression in tg animals in the striatum and cerebellum. (B) At 9 weeks immunoreactivity was absent in the cerebellum and there were no changes in expression in tg animals in the frontal cortex. Representative blots are shown below corresponding graph (n = 6). One-way analysis of variance (ANOVA), followed by Newman-Keuls post hoc test was used to determine significance between wt and tg samples within regions and between brain regions (p, <0.05), error bars represent SEM. FC (frontal cortex); STR (striatum); CER (cerebellum); WT (wild type); TG (transgenic).

5.3.1.4.　HspB8

Finally, protein expression of HspB8 within the frontal cortex, striatum and the cerebellum was quantified using western-blotting at early (4wks) and mid-stage (9wks) of the disease (Figure 5.4). Again, representative western blots are shown below each graph. A decrease in HspB8 protein expression was observed at 4 weeks in the striatum, whereas the frontal cortex and cerebellum did not show any changes (Figure 5.4 A). There were no significant differences between wt and tg animals in any of the brain regions analysed at 9 weeks (Figure 5.4 B). HspB8 also showed statistically higher levels of expression in the cerebellum of wt animals relative to the other brain regions (Figure 5.4).
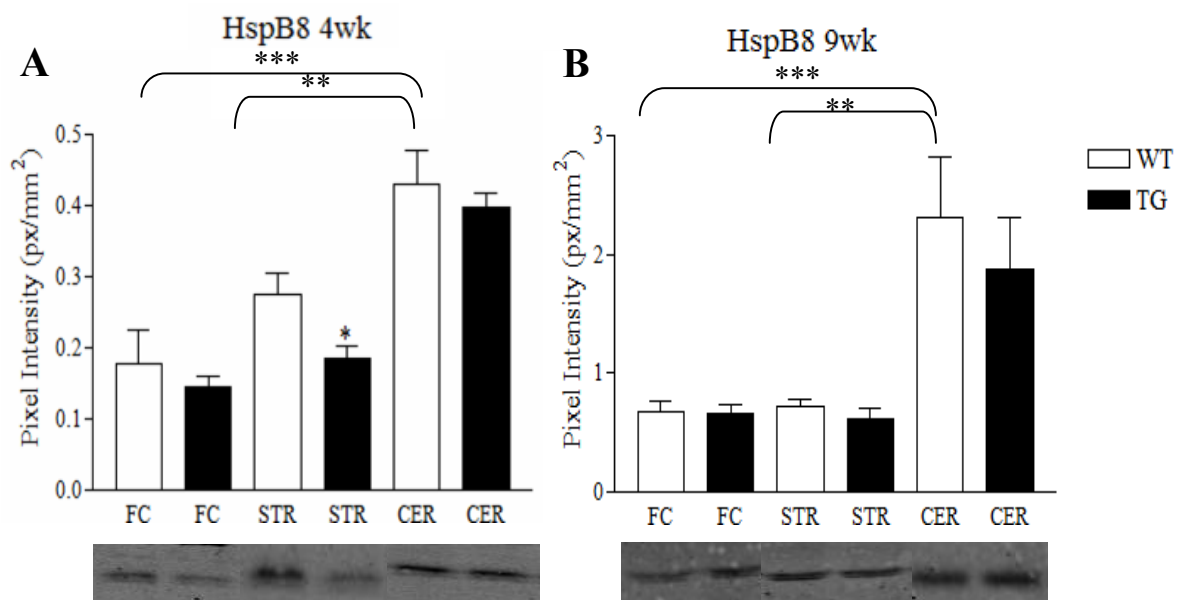
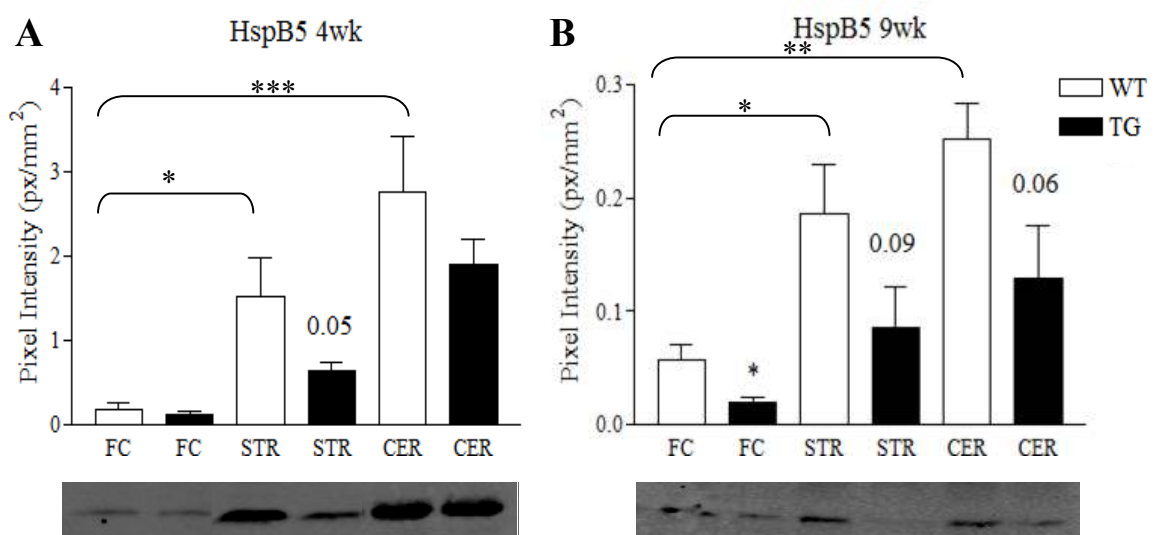**Figure 5.4. HspB8 protein expression in supernatant fractions at early (4wk) and mid (9wk) stage of disease.** 40μg of protein from frontal cortex, striatum and cerebellum homogenates were resolved by SDS-PAGE and expression of HspB8 was measured by incubating membranes with an antibody against HspB8 followed by a fluorescently labelled secondary antibody which was detected by infrared fluorescence. Intensity values were measured using Odyssey Infrared Scanner software and normalized to protein loading and expressed as pixel intensity per mm^2. Expression of HspB8 is shown in distinct brain regions at A, 4 and B, 9 weeks. (A) HspB8 protein levels were decreased in tg animals in the striatum at 4 weeks. (B) There was no change in HspB8 expression at 9 weeks in the three brain regions analysed. Representative blots are shown below corresponding graph (n = 6). One-way analysis of variance (ANOVA), followed by Newman-Keuls post hoc test was used to determine significance between wt and tg samples within regions and between brain regions (*p, <0.05; **p, <0.01; ***p, <0.001), error bars represent SEM. FC (frontal cortex); STR (striatum); CER (cerebellum); WT (wild type); TG (transgenic).

5.3.2. sHsp expression at mid (9wk) and late (17wk) stages of disease

The samples analysed in section 5.3.1 were detergent (NP-40) extracted supernatant fractions and as established in section 3.3.2.2 the sHsps show differential detergent extractabilities in synaptosomal fractions. It was likely that the protein levels of the sHsps in these samples were not representative of the total protein levels, especially as HspB6 did not produce any immunoreactivity in some samples. The sHsps did indeed partition differentially in NP-40 extracted brain homogenates such that the extracted protein was not representative of total protein (see section 2.3.5 for method and Appendix 3). To determine changes in total levels of sHsps, tissue from the cortex, striatum and cerebellum was microdissected from R6/2 tg animals and age matched wt littermates and homogenized to produce a fraction representative of total brain protein (section 2.3.3). Tissue was only available from mid (9 weeks) and late (17 weeks) stages of disease.

40μg of the total homogenate samples from the cortex, striatum and the cerebellum were resolved on SDS-PAGE and western blotting was used to analyze expression of the sHsps. GFAP and MBP expression was also analysed to investigate astrogliosis and expression of a marker protein of the white matter. The average intensity of the bands was plotted for the three brain regions and the intensity values were normalized to protein loading (section 2.8.4). The corresponding western blots are shown below each graph.

5.3.2.1. HspB1

HspB1 did not show any significant difference in expression in the cortex and the striatum at 9 weeks, although the cerebellum shows significantly higher levels of HspB1 in tg animals (Figure 5.5 A). At 17 weeks there were no significant differences in expression between tg and wt animals in all three brain regions (Figure 5.5 B).
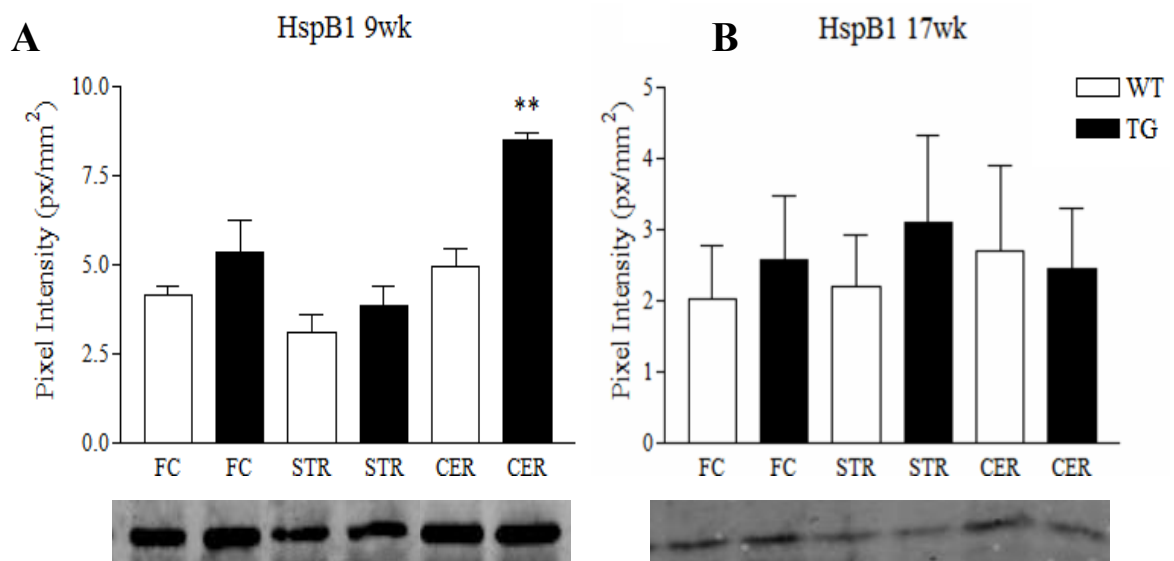
Figure 5.5. HspB1 protein expression at mid (9wk) and late (17wk) stage of disease.
40μg of protein from frontal cortex, striatum and cerebellum homogenates were resolved by SDS-PAGE and expression of HspB1 was measured by incubating membranes with an antibody against HspB1 followed by a fluorescently labelled secondary antibody which was detected by infrared fluorescence. Intensity values were measured using Odyssey Infrared Scanner software and normalized to protein loading and expressed as pixel intensity per mm^2. Expression of HspB1 is shown in distinct brain regions at A, 9 and B, 17 weeks. (A) No changes in HspB1 expression were observed in tg animals in the frontal cortex and striatum at 9 weeks. However HspB1 was up-regulated in the cerebellum of tg animal. (B) There were no changes in HspB1 expression at 17 weeks in tg animals in the three brain regions analysed. Representative blots are shown below corresponding graph (9 wks, n = 3; 17 wks, n = 4). One-way analysis of variance (ANOVA), followed by Newman-Keuls post hoc test was used to determine significance between wt and tg samples within regions and between brain regions (**p, <0.01), error bars represent SEM. FC (frontal cortex); STR (striatum); CER (cerebellum); WT (wild type); TG (transgenic).

5.3.2.2. HspB5

HspB5 showed a very similar expression profile to that seen in Figure 5.2. There was a clear and significant downregulation of HspB5 in tg animals in all three brain regions at 9 weeks. This downregulation was statistically significant in the striatum and the cerebellum (Figure 5.6 A). This observation was more pronounced at 17 weeks and was statistically significant in all three brain regions analysed (Figure 5.6 B). HspB5 showed statistically higher levels of expression in the cerebellum and striatum of wt animals relative to the frontal cortex (Figure 5.6).
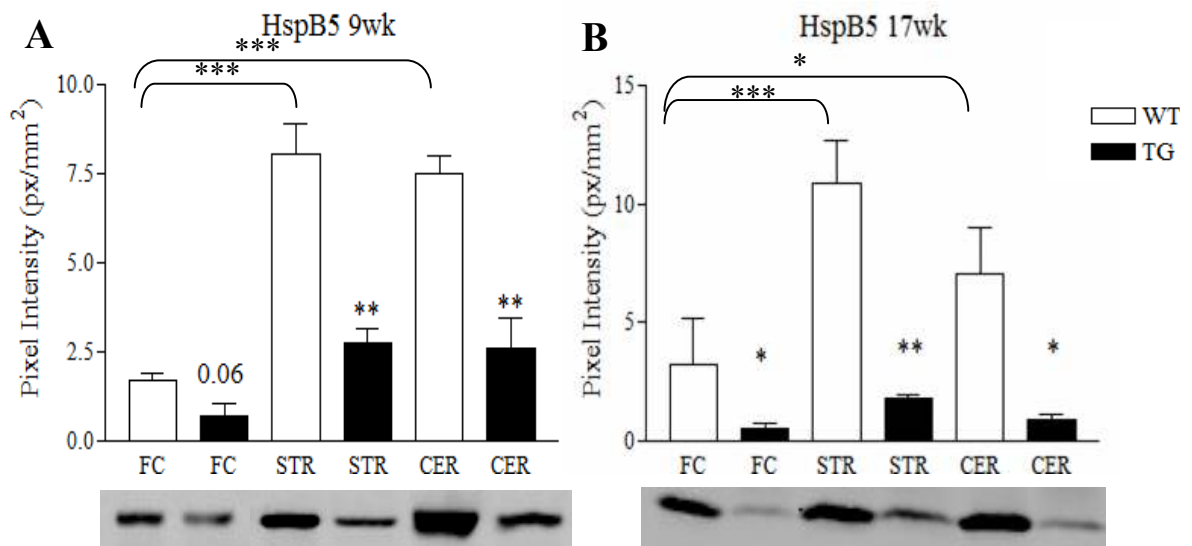
Figure 5.6. HspB5 protein expression at mid (9wk) and late (17wk) stage of disease. 40µg of protein from frontal cortex, striatum and cerebellum homogenates were resolved by SDS-PAGE and expression of HspB5 was measured by incubating membranes with an antibody against HspB5 followed by a fluorescently labelled secondary antibody which was detected by infrared fluorescence. Intensity values were measured using Odyssey Infrared Scanner software and normalized to protein loading and expressed as pixel intensity per mm^2. Expression of HspB5 is shown in distinct brain regions at A, 9 and B, 17 weeks. (A) The amount of HspB5 protein expression decreased in tg animals in all three brain regions at 9 weeks. This was statistically significant in the striatum and cerebellum. (B) HspB5 protein expression was also significantly decreased in tg animals in all three brain regions at 17 weeks. Representative blots are shown below corresponding graph (9 wks, n = 3; 17 wks, n = 4). One-way analysis of variance (ANOVA), followed by Newman-Keuls post hoc test was used to determine significance between wt and tg samples within regions and between brain regions (*p, <0.05; **p, <0.01; ***p, <0.001), error bars represent SEM. FC (frontal cortex); STR (striatum); CER (cerebellum); WT (wild type); TG (transgenic).

5.3.2.3. HspB6

There were no significant differences in HspB6 expression between wt and tg animals in the three brain regions at both 9 and 17 weeks (Figure 5.7). However, HspB6 showed statistically higher levels of expression in the cerebellum and striatum of wt animals relative to the frontal cortex at 9 weeks (Figure 5.7), similar to HspB5 (Figure 5.6) and MBP (Figure 5.17), potentially reflecting the white matter expression of this sHsp as described in chapter 3. Additionally, in these total homogenate samples all brain regions showed HspB6 immunoreactivity in contrast to the detergent extracted supernatant samples as shown in Figure 5.3. The presence of three HspB6 isoforms and their specificity by pre-absorption with antigen was previously established in Chapter 3 (Figure 3.11). However a fourth band was distinguishable as shown by the asterisks (Figure 5.7 B). The relatively similar electrophoretic motilities of the fourth band and the 18kDa isoform makes it very difficult to separate both in samples with high levels of HspB6, however in samples were there is less HspB6 such as the frontal cortex, the fourth band is better visible. The presence of four isoforms is in keeping with the literature as four isoforms (three phosphorylated and one not) have been identified in bovine heart (Beall et al., 1999).
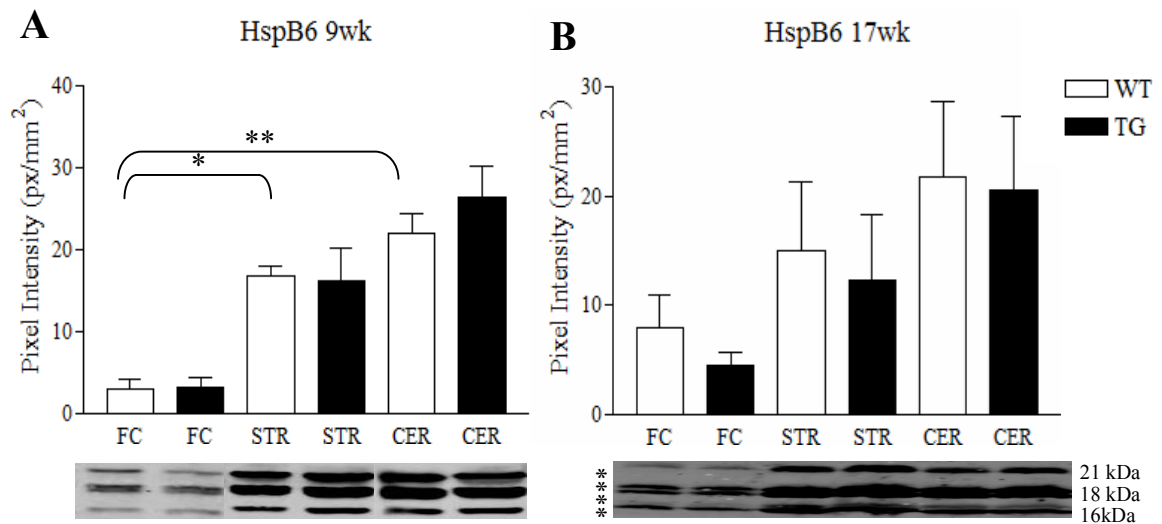
Figure 5.7. HspB6 protein expression at mid (9wk) and late (17wk) stage of disease. 40µg of protein from frontal cortex, striatum and cerebellum homogenates were resolved by SDS-PAGE and expression of HspB6 was measured by incubating membranes with an antibody against HspB6 followed by a fluorescently labelled secondary antibody which was detected by infrared fluorescence. Intensity values were measured using Odyssey Infrared Scanner software and normalized to protein loading and expressed as pixel intensity per mm^2. Expression of HspB6 is shown in distinct brain regions at A, 9 and B, 17 weeks. (A) No changes in HspB6 expression were observed in tg animals in the three brain regions at 9 weeks. (B) There were also no changes in HspB6 expression in tg animals in the three brain regions analyzed at 17 weeks. Representative blots are shown below the corresponding graph (9 wks, n = 3; 17 wks, n = 4). One-way analysis of variance (ANOVA), followed by Newman-Keuls post hoc test was used to determine significance between wt and tg samples within regions and between brain regions (*p, <0.05; **p, <0.01), error bars represent SEM. FC (frontal cortex); STR (striatum); CER (cerebellum); WT (wild type); TG (transgenic).

5.3.2.4. HspB8

HspB8 did not show any significant differences in expression between wt and tg animals in the three brain regions at both time points (Figure 5.8). The profile seen in total homogenate samples is very similar to that seen in supernatant fraction as described earlier in the chapter with higher expression in the cerebellum compared to the frontal cortex and striatum of wt animals (Figure 5.4).
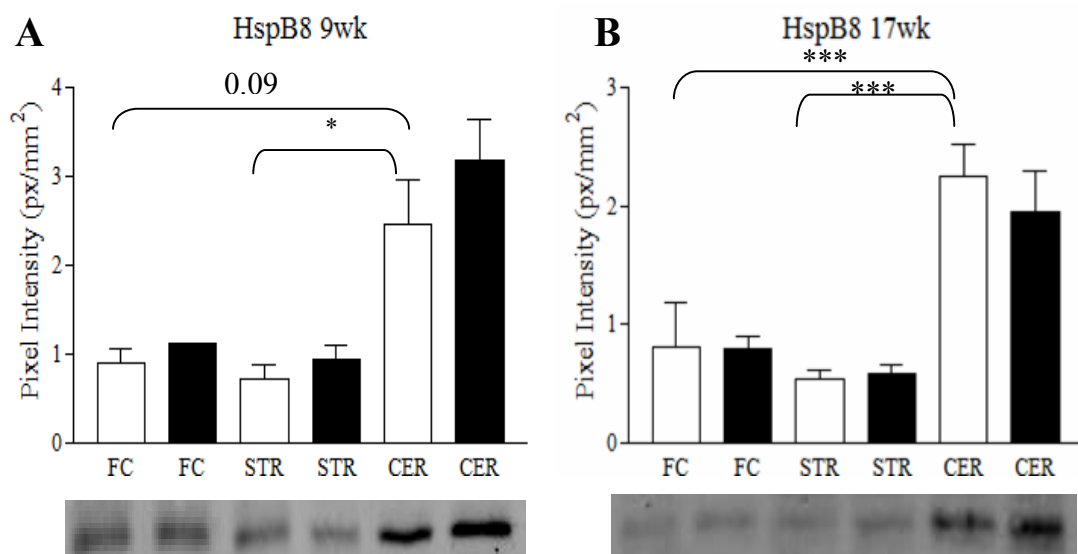
Figure 5.8. HspB8 protein expression at mid (9wk) and late (17wk) stage of disease. 40μg of protein from frontal cortex, striatum and cerebellum homogenates were resolved by SDS-PAGE and expression of HspB8 was measured by incubating membranes with an antibody against HspB8 followed by a fluorescently labelled secondary antibody which was detected by infrared fluorescence. Intensity values were measured using Odyssey Infrared Scanner software and normalized to protein loading and expressed as pixel intensity per mm^2. Expression of HspB8 is shown in distinct brain regions at A, 9 and B, 17 weeks. (A) No changes in HspB8 expression were observed in tg animals in the three brain regions at 9 weeks. (B) There were also no changes in HspB8 expression in tg animals in the three brain regions analyzed at 17 weeks. Representative blots are shown below corresponding graph (9wk, n = 3; 17wks, n = 4). One-way analysis of variance (ANOVA), followed by Newman-Keuls post hoc test was used to determine significance between wt and tg samples within regions and between brain regions (*p, <0.05; **p, <0.01; *p, <0.001), error bars represent SEM. FC (frontal cortex); STR (striatum); CER (cerebellum); WT (wild type); TG (transgenic).

5.3.3. Summary of sHsp protein expression in HD (R6/2 mouse model)

The protein data obtained for the sHsps in detergent (NP-40) extracted supernatant fractions (time points in italics) and non-detergent extracted total homogenate samples (time points in bold) in the frontal cortex, striatum and the cerebellum are summarized in Table 3.1. HspB1 did not show any changes in expression in tg animals in any of the brain regions and time points, apart from an up-regulation in total homogenate samples of the cerebellum at 9 weeks. A similar change in expression was not observed in detergent extracted supernatant samples. HspB5 was significantly downregulated in all three brain regions at all time points analysed apart from the frontal cortex and cerebellum in 4 week supernatant fractions. HspB6 did not show any changes in expression in tg animals in any of the brain regions and time points. HspB8 did not show any changes in expression in tg animals in any of the brain regions and time points, apart from a downregulation in supernatant samples of the striatum at 4 weeks, suggesting compartment shifting.

	Frontal cortex				Striatum				Cerebellum			
	4wk	*9wk*	**9wk**	**17wk**	*4wk*	*9wk*	**9wk**	**17wk**	*4wk*	*9wk*	**9wk**	**17wk**
HspB1	-	-	-	-	-	-	-	-	-	-	↑	-
HspB5	-	↓	↓	↓	↓	↓	↓	↓	-	↓	↓	↓
HspB6	/	-	-	-	-	-	-	-	-	/	-	-
HspB8	-	-	-	-	↓	-	-	-	-	-	-	-

Table 5.1. Summary of sHsp expression at early (4wk) mid (9wk) and late (17wk) stages of disease. HspB1 shows protein up-regulation in homogenate samples of the cerebellum at 9wks. HspB5 displays decrease in protein expression in all regions analysed, at all time points. This downregulation suggests a global change in expression of this sHsp. HspB6 does not show any changes in expression. HspB8 shows protein downregulation in supernatant fractions of the striatum at 4wks. This highlights the selective downregulation of HspB5, a white matter specific sHsp, in R6/2 tg animals. (Time points in: *italics* = detergent extracted supernatant fractions; **bold** = non-detergent extracted total homogenate; ↓ ↓, downregulated; ↑, up-regulated; -, no change; /, no immunoreactivity).

sHsp data from the two extraction protocols summarized in Table 5.1 highlight the selective downregulation of HspB5. The HspB5 data was plotted as a percentage of wild type control samples from each brain region and time point. The collective data displays not only a selective downregulation of this sHsp in all brain regions analysed, but also

shows a progressive downregulation over time, particularly in the cerebellum (Figure 5.9). By 17 weeks, approximately 75-80% reduction of HspB5 levels is observed in all regions analysed.
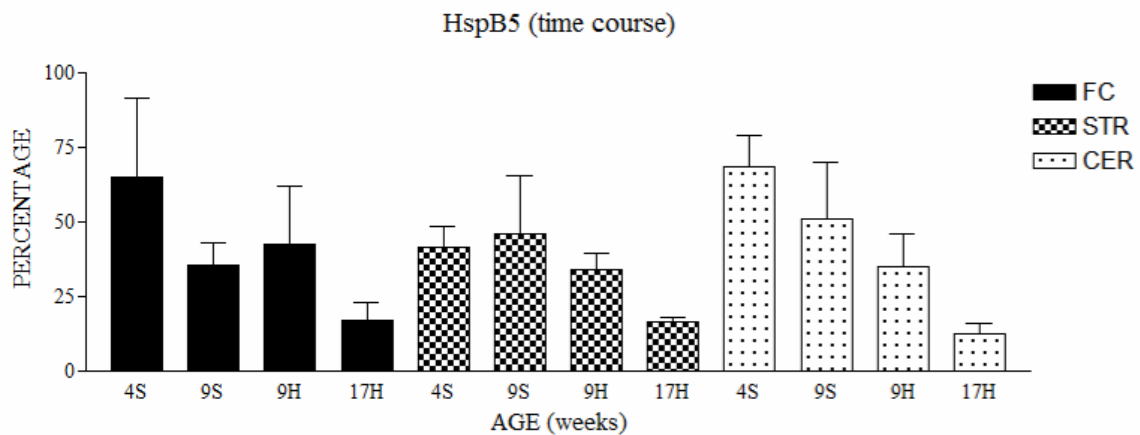
Figure 5.9. HspB5 expression at early (4wk), mid (9wk) and late (17wk) stages of disease. HspB5 immunoreactivity in tg animals was plotted as a percentage of age matched wt samples (100%) from the corresponding brain region. HspB5 shows a decrease in protein expression in all regions analysed, most progressively in the cerebellum. Error bars represent SEM. S (supernatant fraction); H (homogenate sample) FC (frontal cortex); STR (striatum); CER (cerebellum).

5.3.4. Dot blot analysis of HspB5 on late stage striatal samples

To ascertain if the selective and progressive downregulation of HspB5 was due to an association or sequestration of HspB5 with aggregated protein as suggested for other molecular chaperones (Stenoien et al., 1999, Wyttenbach et al., 2000, Hay et al., 2004), a dot blot or filter trap protocol was used (section 2.9). This method allows aggregated proteins or proteins associated with aggregates to be trapped on the surface of a nitrocellulose acetate membrane. As the most significant changes in HspB5 downregulation were observed at late stage in the disease, 17 week striatal homogenate samples were used in the dot blot assay. 40μg and 20μg of 17 week striatal homogenates from tg and wt animals were filtered through the membranes. The potential presence of

HspB5 in htt-exon1 positive aggregates was determined by detecting a signal by enhanced chemiluminescence (ECL). Htt-exon1 showed immunoreactivity as measured by ECL in samples from tg animals as expected (Figure 5.10 A). Additionally, immunoreactivity was absent in wt samples as these did not express htt-exon1. HspB5 did not show any immunoreactivity in material trapped on the nitrocellulose from the tg homogenate samples (Figure 5.10 B). In order to confirm that the dot blot protocol had worked, and that this membrane did contain aggregated proteins, an anti-ubiquitin antibody was used as a positive control to re-probe the same membrane, as the aggregates are normally ubiquitinated (Meade et al., 2002). As expected ubiquitin immunoreactivity was present in tg animals but not in wt animals (Figure 5.10 C).
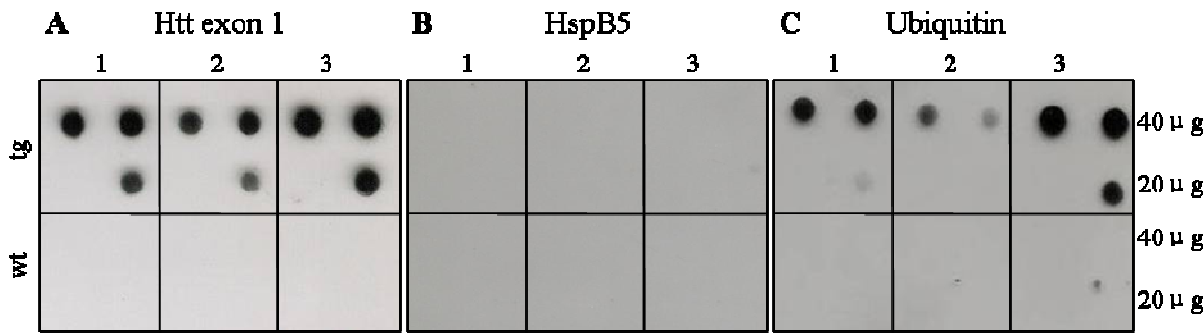
Figure 5.10. Dot blot analysis of HspB5 on late stage striatal samples
40μg and 20μg of 17 week striatal homogenates were passed through nitrocellulose acetate membranes. Immunoreactivity against HspB5, htt-exon1 and ubiquitin was measured by ECL. 1, 2, and 3 represent samples from different animals. Samples were loaded as duplicates (top row) and one subsequent dilution was loaded below. Samples from wt animals were loaded in the same manner as tg animals. (A) Tg samples containing aggregates were immunopositive for Htt exon1 using the S830 antibody. As expected, immunoreactivity was not present in samples from wt animals. (B) HspB5 did not show any immunoreactivity on the nitrocellulose membrane. (C) The HspB5 membrane was re-probed with an ubiquitin antibody. As expected, ubiquitin immunoreactivity was observed in tg animals but not in wt animals, confirming the presence of aggregates captured on this membrane.

5.3.5. R6/2 brain and synaptosomal fractions

The above observation indicates that the loss of HspB5 which we have characterized as being selectively expressed in white matter is not a consequence of incorporation or association with mtHtt aggregates. To determine where the disease related changes in HspB5 expression were occurring, total brain homogenate and synaptosomal fractions (section 2.10) from R6/2 tg and wt littermates were used to investigate expression of HspB5 in different brain compartments (Figure 5.11 A). These fractions as also described in chapter 3, consist of total homogenate, P1 pellet containing cell body/nuclei, myelin and synaptosome fractions. Additionally the synaptosomal fraction is further sub-fractionated allowing the distinct synaptic compartments to be teased apart. The pH6 insoluble fraction represents paired pre- and post-synaptic densities and the soluble fraction represents plasma membrane proteins. The pH8 insoluble fraction enriches for the PSD and the soluble fraction for the presynaptic compartment. The white matter (myelin) enrichment of this sHsp as previously determined (Figure 3.13) suggests the selective downregulation of HspB5 is also occurring in the white matter. Indeed HspB5 expression showed the greatest reduction (5-fold) in the myelin fraction consistent with its association with the white matter (Figure 5.11 A).

The distribution and disease related changes of endogenous full-length htt protein and Exon1 fragments were next analysed to investigate if there was any overlap with HspB5 expression. Htt displayed immunoreactivity in all brain compartments tested, but was predominantly present in the synaptosomal compartment (Figure 5.11 B). It displayed a predominantly pre-synaptic profile in the synaptosome sub-compartments, as it was present in both the insoluble and soluble fractions at pH6 and the majority of the protein appeared solubilised at pH8 (Figure 5.11 B). Although there was a trend towards decreased levels of htt in tg animals compared to wt animals in the synaptosomal compartment and sub-compartments, this was not statistically significant (n = 4).

Wild type animals did not show immunoreactivity against exon1 as expected (data not shown), whereas tg animals showed enrichment of exon 1 in the cell body/nuclei compartment, and immunoreactivity in the synaptosomal and PSD compartment.
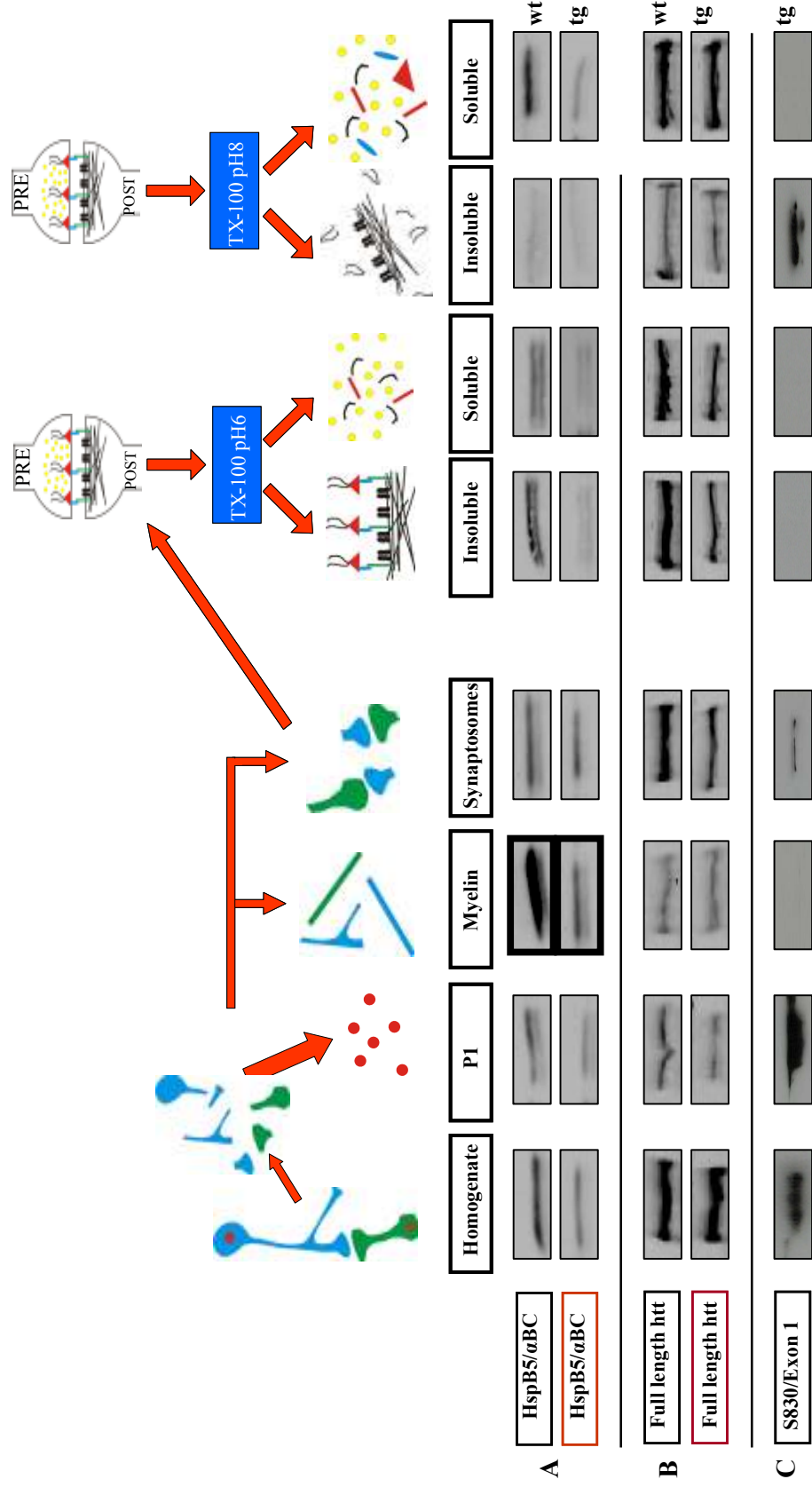
Figure 5.11. sHsp expression in wt and tg brain fractions and synaptosomal subfractions. (A) HspB5 was enriched in the myelin fraction of wt animals and was downregulated in all brain and synaptosomal fractions of tg animals. The myelin fraction showed the highest downregulation (5-fold). (B) Endogenous Huntingtin protein was present in all fractions tested. It was present mainly in the synaptosomal fraction and displayed a presynaptic protein profile with the majority of the protein being solubilised at pH8. Huntingtin did not show a statistically significant decrease in expression in any of the fractions, although a trend towards decreased levels in synaptosome fractions and sub-fractions was apparent. (C) TG animals showed enrichment of mutant huntingtin protein (exon1) in the P1 fraction with immunoreactivity in the synaptosomal and pH8 insoluble fraction (n=1). 18μg of protein were loaded for each fraction, wt and tg samples were loaded in parallel. The intensity values were normalized to protein loading (section.2.8.4.) (A and B, n = 3 (tg) and 5 (wt); C, n =1).

5.3.6. Ubiquitinated inclusions in HD tissue

The previous observations illustrate selective HspB5 downregulation in the white matter which is not associated with incorporation into aggregates. Brain fractions also show a relative lack of Exon1 immunoreactivity in the myelin compartment. However, inclusions have been demonstrated in glial cells in R6/2 animals (Shin et al., 2005). To investigate if inclusions were present in non-neuronal cells with a particular focus in the white matter, the presence of inclusion bodies was analysed immunohistochemically (section 2.11) in wt and tg animals using an anti-ubiquitin antibody, as ubiquitinated proteins are a feature of inclusions as also demonstrated by dot blot analysis (Figure 5.10). Wt animals did not show any inclusion bodies in the sections analysed (Figure 5.12 Ai and ii). Tg animals contained ubiquitinated inclusion bodies in neuronal cell bodies as observed in the CA1 cell body layer (Figure 5.12 Bii). Cytoplasmic inclusions were also present in the surrounding neurophil (Figure 5.12 Bi and ii). Upon close inspection of white matter brain structures in tg animals, cells were identified that contained ubiquitin positive inclusions. Due to the location of these cells in the white matter and being present in tandem arrays, they were likely to be oligodendrocytes. The inclusions were smaller and showed less intense staining in comparison to neuronal inclusions (Figure 5.12 C).
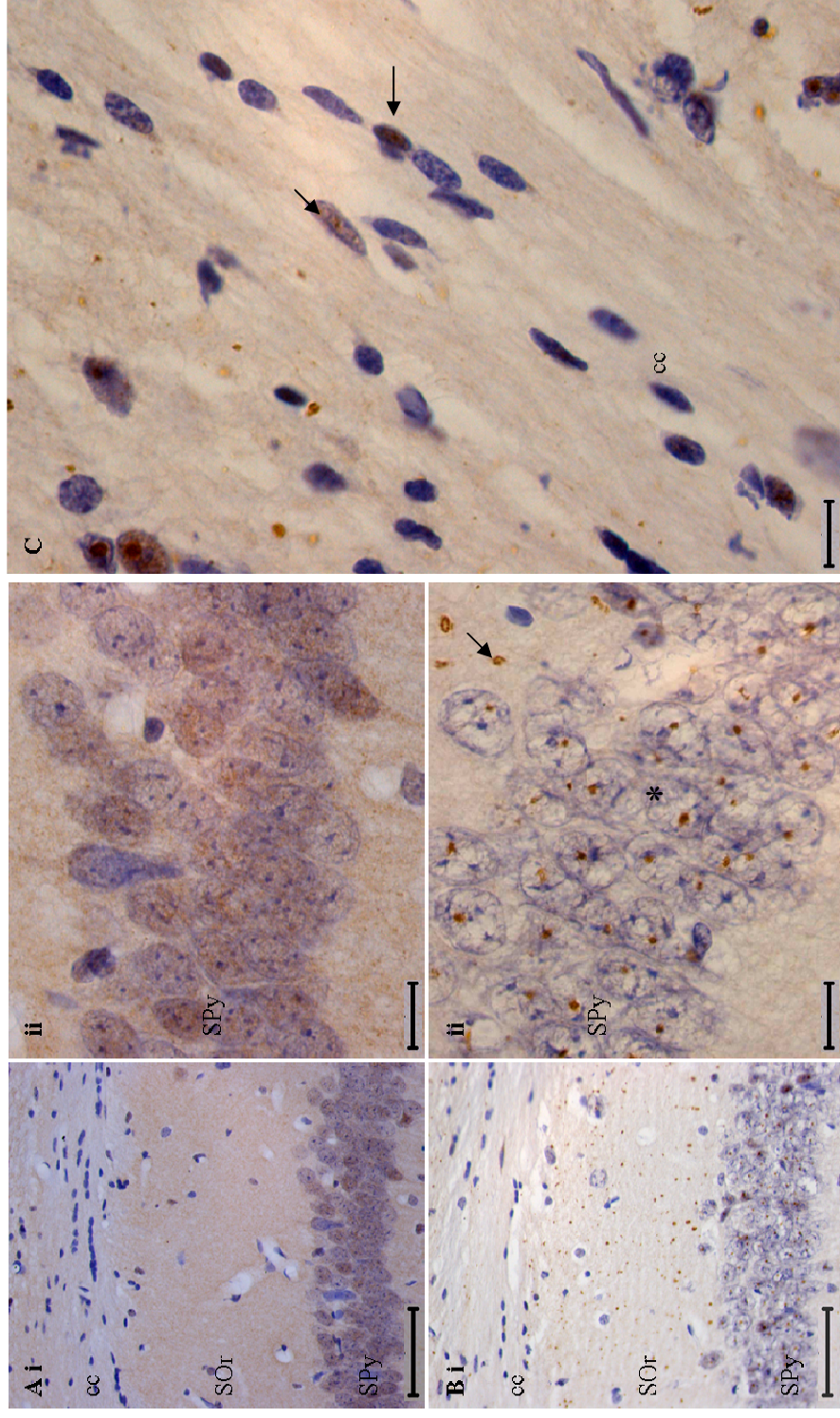
Figure 5.12. Ubiquitinated inclusion bodies in R6/2 tissue. Coronal brain sections from late stage (17 weeks) wt and tg animals were subjected to ubiquitin staining. (A) (i) Ubiquitinated inclusions were absent in wt animals. (ii) Higher magnification image of CA1 pyramidal neurons showed diffuse ubiquitin expression. (B) (i) Ubiquitinated inclusions were present in tg animals. (ii) Ubiquitin positive inclusion bodies were present in the nucleus of neuronal cells (asterisk) and also in the cytoplasm (arrow). (C) Inclusions were present in a few cells (likely oligodendrocytes) of the white matter. Images are representative of staining from 4 animals. Corpus callosum (cc), Stratum Oriens (SOr), Stratum pyramidal (Spy). Scale bar, (Ai and Bi , 50μm; Aii, Bii and C, 100μm).

5.3.7. Immunohistochemical analysis of HspB5 expression

Homogenate samples from R6/2 tg animals showed a selective downregulation of the white matter specific HspB5 protein (Table 5.1). To confirm this finding and provide detailed anatomical information, tissue sections from wt and tg animals were prepared and processed as detailed in section 2.11 for immunohistochemical analysis. Coronal tissue sections between 0.86mm and 0.26mm relative to Bregma were used to analyse expression in the striatum and cortex. Sections between -1.58mm and -2.06mm relative to Bregma were used to analyse expression in the hippocampus and corpus callosum. Sections between -5.80mm and -6.24mm relative to Bregma were used to analyse expression in the cerebellum. All tissue sections from tg and wt animals were processed in parallel and developed in DAB solution for the identical length of time.

Staining in the striatum, cortex, cerebellum and corpus callosum was analysed (Figure 5.13). Wt animals displayed a darker staining pattern in all brain regions (Figure 5.13 A) in comparison to tg animals (Figure 5.13 B). In all sections analysed, staining of the cell bodies was similar in both wt and tg animals.

Sections containing cortex and striatum displayed a reduction in staining of the cortex, external capsule (white matter tract) and fiber bundles in the striatum of tg animals (Figure 5.13 B i) in comparison to wt animals (Figure 5.13 A i). Higher magnification images of the striatum showed the presence of white matter fiber bundles in both wt and tg animals, but staining in tg animals was fainter, indicating a reduction of HspB5 protein (Figure 5.13 B ii) in comparison to wt animals (Figure 5.13 A ii). HspB5 staining in the cerebellum also displayed a similar reduction in immunoreactivity in tg animals (Figure 5.13 B iii). Staining was observed between the cell bodies of the granule cell layer and was more pronounced in the white matter layer of the cerebella lobule (Figure 5.13 A iii). The corpus callosum also showed a reduction of HspB5 protein expression in the fiber tracts of tg animals (Figure 5.13 B iv). Staining of oligodendrocyte cell bodies did not appear reduced in tg animals (Figure 5.13 B v).
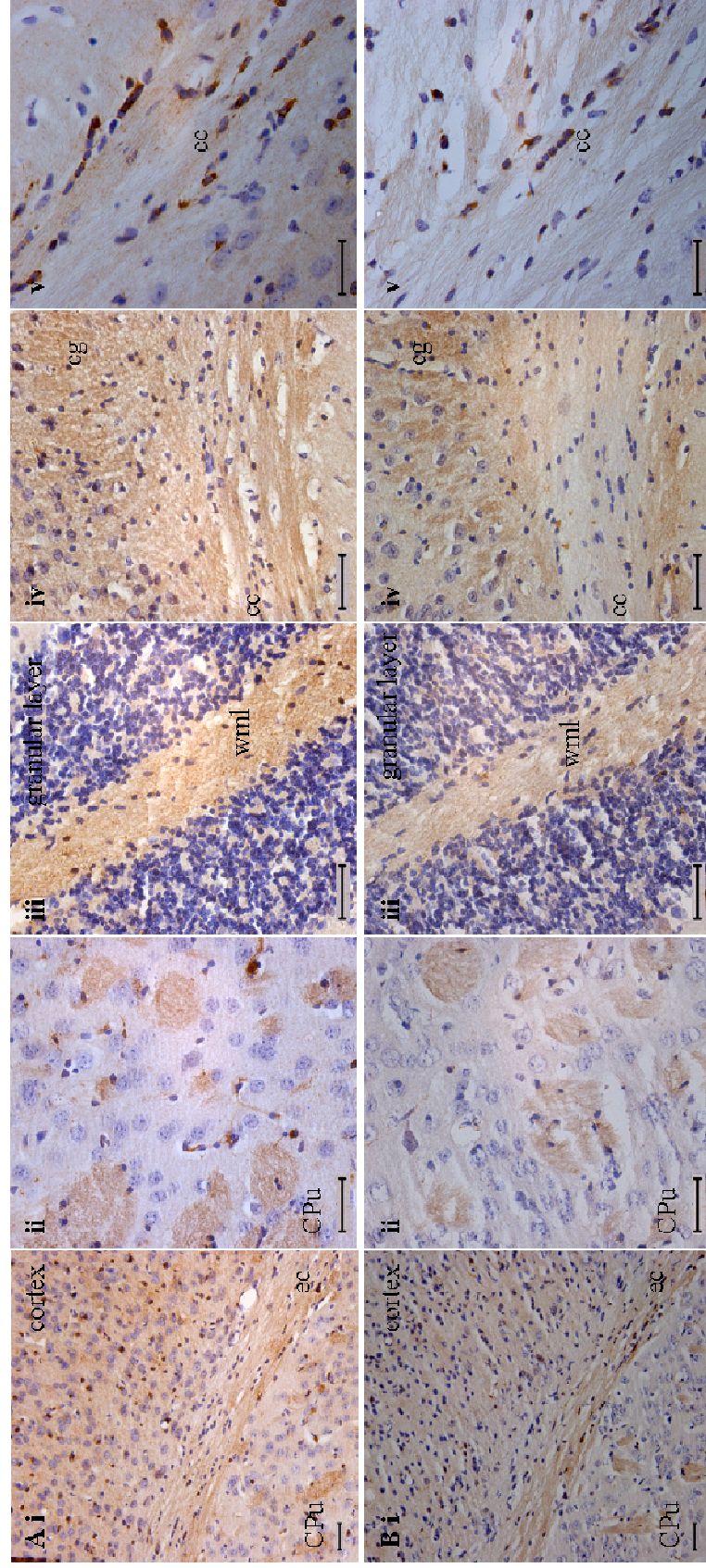
Figure 5.13. Immunohistochemical analysis of HspB5 in HD tissue. Coronal brain sections from late stage (17 weeks) wt and tg animals were subjected to immunohistochemistry for detection of HspB5 immunoreactivity. Tg animals (B) displayed a reduction in HspB5 staining in comparison to wt animals (A). (A) (i) HspB5 immunoreactivity was observed in the cortex, ec and striatum (CPu). (ii) Staining in the CPu was localized to white matter rich fiber bundles and oligodendrocyte cell bodies. (iii) Immunoreactivity in the cerebellum was localized mainly to the wml with extension into the granular cell layer. (iv) Immunoreactivity was observed in the fiber tracts of the cc as well as fiber bundles of the cg. (v) Higher magnification of the cc showed intense staining of the cell bodies as well as the fiber tract. (B) (i) HspB5 immunoreactivity was decreased in the cortex, ec and striatum (CPu). (ii) Staining of the fiber bundles in the CPu was also reduced. (iii) Immunoreactivity in the wml of the cerebellum was reduced. (iv) Fiber tracts of the cc and the cg showed reduced HspB5 staining. (v) Higher magnification of the corpus callosum showed intense staining of the cell bodies but a decrease in staining of the fiber tract. Images are representative of staining obtained from 4 different animals. External capsule (ec), caudate putmen (CPu), white matter layer (wml), corpus callosum (cc), cingulate gyrus (cg). Magnifications: A/B (i, x20; ii-iv, x40; v, x63), scale bar (i-iv, 50µm and v, 30µm).

183

5.3.8. Expression of HspB5 and CNP by immunofluorescence

We previously showed co-localisation of HspB5 with another white matter specific protein CNP which is selectively expressed in the non-compact myelin compartment (Chapter 3). To investigate if the changes in expression were selective to HspB5 or if they were also apparent in another white matter protein expressed in the same myelin compartment (non-compact), double immunofluorescence labelling was used to analyse the expression of HspB5 and CNP in the same tissue sections. Tissue from tg and wt animals were processed and imaged in parallel. All microscopy settings were kept the same between wt and tg animals on equivalent sections and magnifications (section 2.14).

Staining in the cortex, striatum, corpus callosum and cerebellum was analysed. HspB5 staining was reduced in tg animals in all regions analysed (Figure 5.14 Bi/Di and 5.15 Bi/Di) as also described above (Figure 5.13). CNP staining in the same tg sections (Figure 5.14 B/Dii and 5.15 B/Dii) did not show any changes in expression in comparison to wt animals (Figure 5.14 Aii/Cii and 5.15 Aii/Cii).

5.3.9. HspB5 expression in oligodendrocyte cell bodies (cell count)

Oligodendrocyte cell body staining was apparent and appeared not different between wt and tg animals. To determine the number of HspB5/CNP positive cells, hippocampal sections were analysed as this brain region allowed HspB5/CNP positive cell bodies to be clearly distinguished amongst the myelinated processes (Chapter 4). Myelinated tracts such as the corpus callosum were not analysed as CNP cell body staining was masked among intense fiber tract staining. The number of CNP/HspB5 positive cells with DAPI staining were manually counted under x20 magnification in the CA1, CA3 and dentate gyrus of the hippocampus in four animals (Figure 5.16 A) (section 2.14.3). There were no statistically significant differences between HspB5/CNP positive cell bodies in wt and tg animals in any of the hippocampal regions (Figure 5.16 B) suggesting reduction of HspB5 was unlikely due to loss of oligodendrocytes.
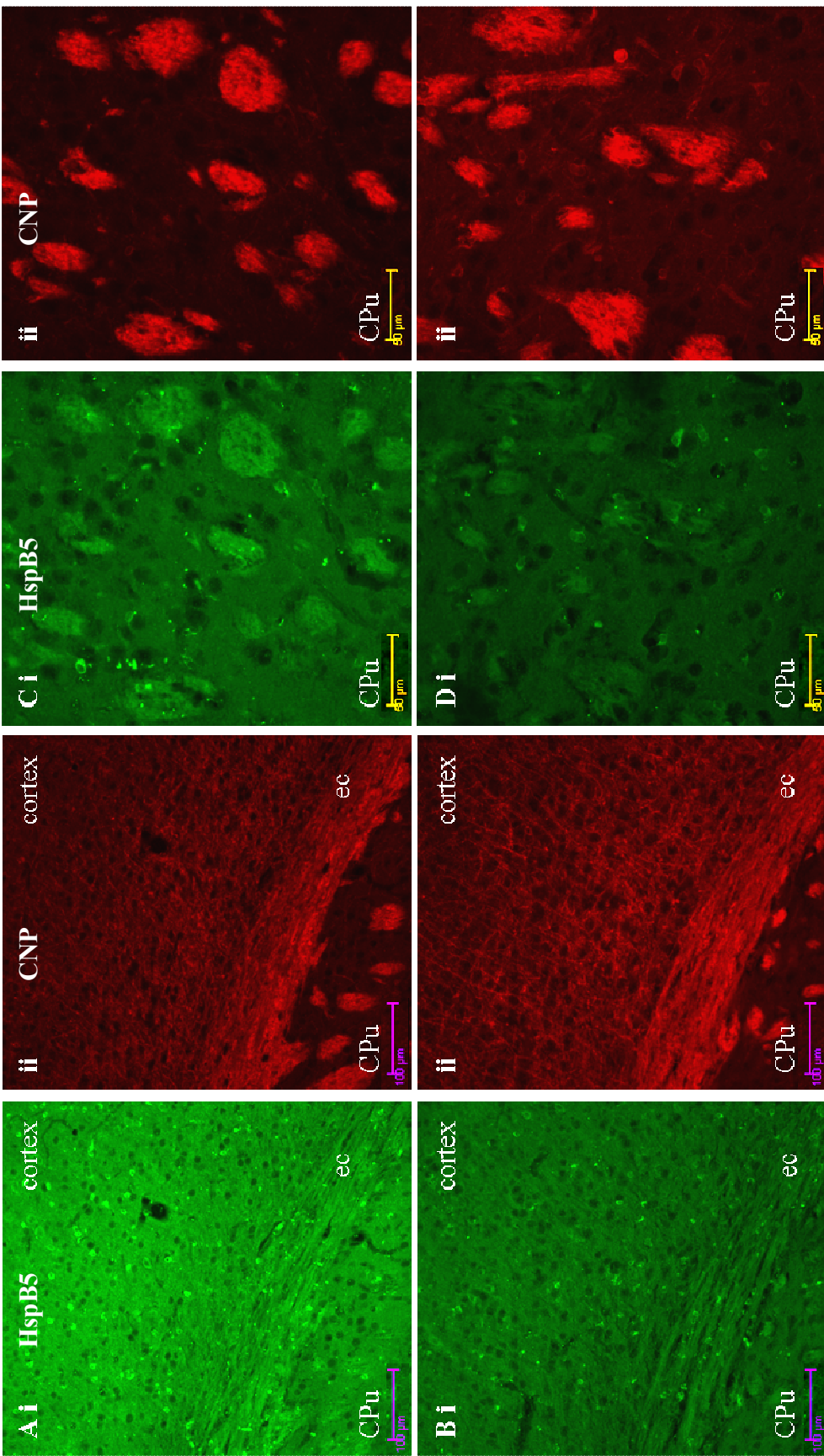
Figure 5.14. Double immunofluorescence staining of HspB5 and CNP in the cortex and striatum. Coronal brain sections from late stage (17 weeks) wt (A) and tg (B) animals were subjected to double immunofluorescence staining with HspB5 (green) and CNP (red) antibodies. Tg animals showed a selective loss of HspB5 staining in the cortex and ec (Bi) and the striatum (Di) in comparison to wt animals (Ai and Ci). CNP staining in the same sections did not show a decrease in immunoreactivity in tg animals (Bii and Dii) but remained similar to staining in wt animals (Aii and Cii). Images are representative of staining from 4 animals. External capsule (ec), caudate putmen (CPu). Magnifications: A/B (x20); C/D (x40). All tissue was processed in parallel; images were taken using same setting for wt and tg animals; scale bar, A/B (100μm) C/D (50μm).
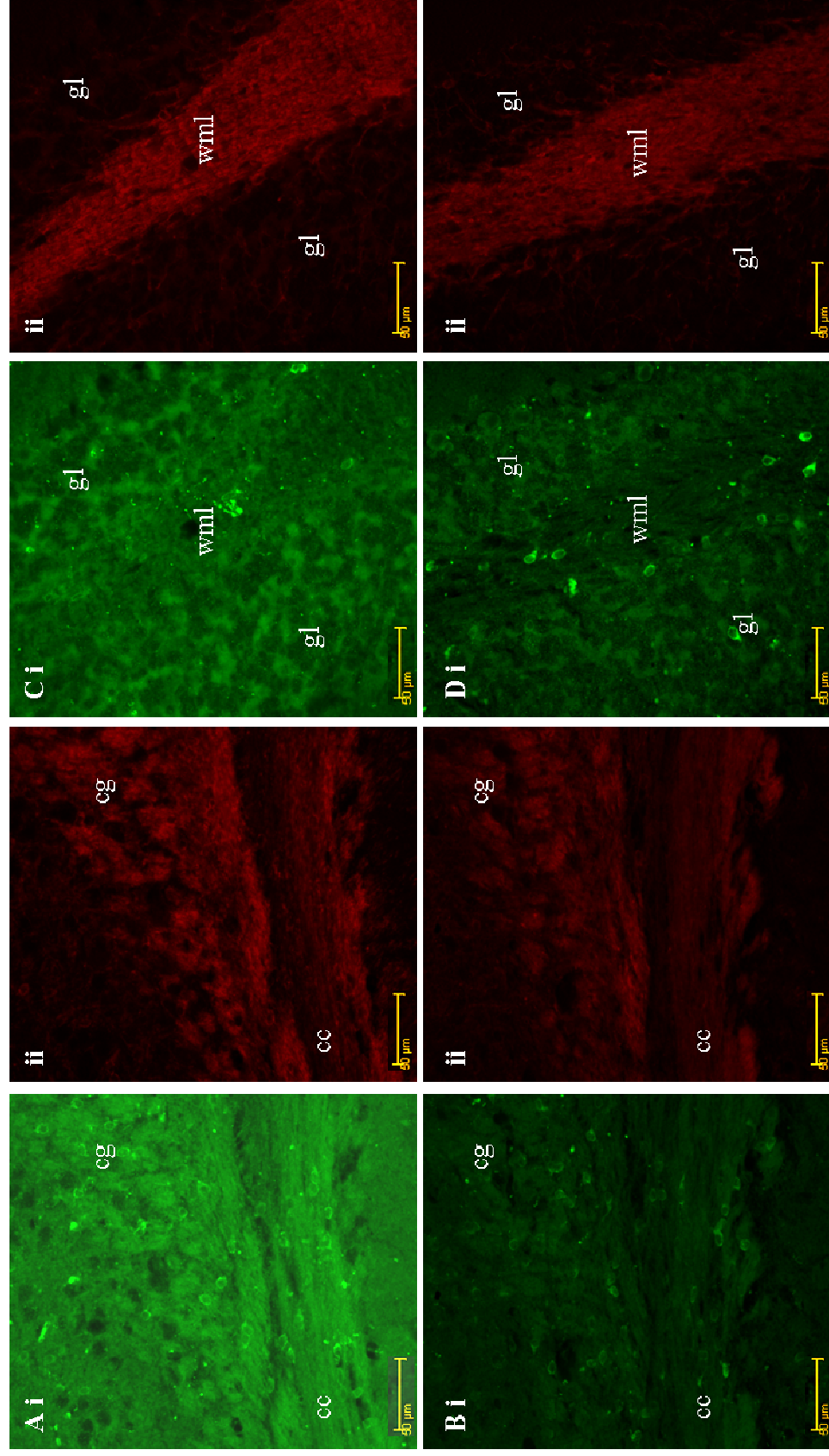
Figure 5.15. Double immunofluorescence staining of HspB5 and CNP in the corpus callosum and cerebellum. Coronal brain sections from late stage (17 weeks) wt (A) and tg (B) animals were subjected to double immunofluorescence staining with HspB5 and CNP antibodies. Tg animals showed a decrease in HspB5 immunoreactivity in the corpus callosum (Bi) and the striatum (Di) in comparison to wt animals (Ai and Ci). CNP staining in the same sections did not show a relative decrease in immunoreactivity in tg animals (Bii and Dii) but remained similar to wt animals (Aii and Cii). Images are representative of staining from 4 animals. Corpus callosum (cc), granular layer (gl), white matter layer (wml). All tissue was processed in parallel. Images were taken using the same setting for wt and tg animals Scale bars, 50μm.

186
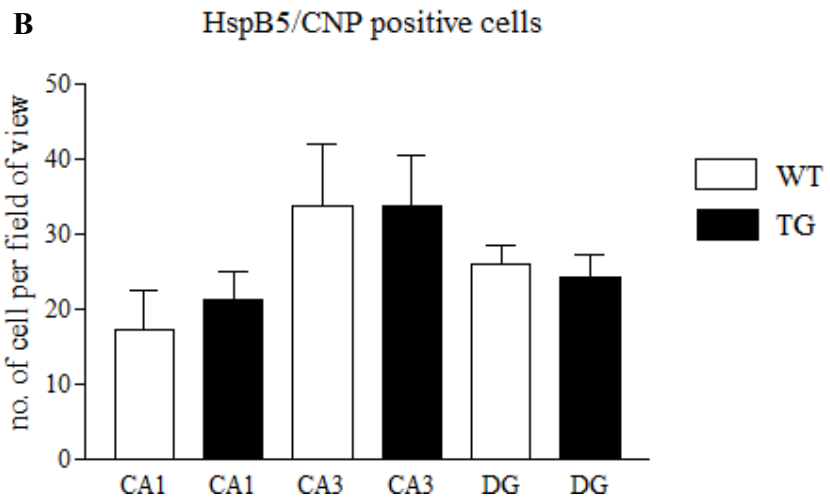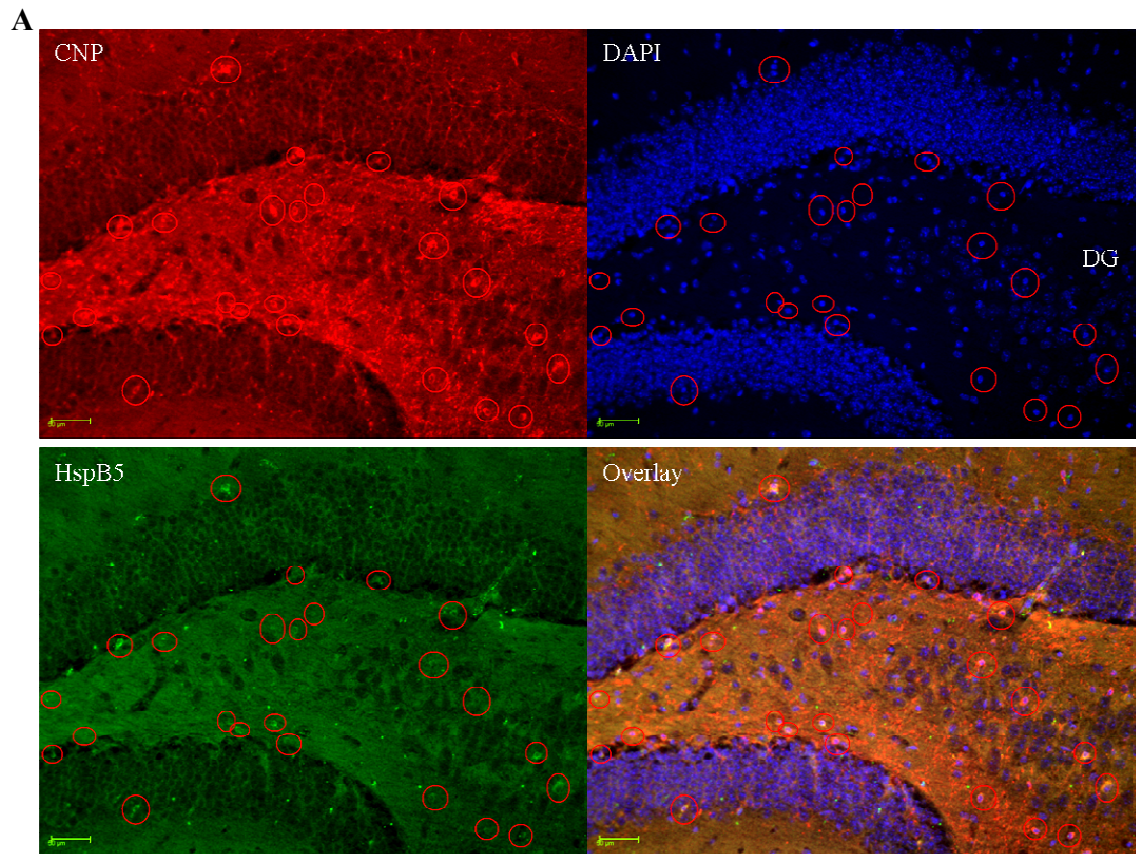
Figure 5.16. HspB5/CNP positive cells count in tg and wt animals. Coronal brain sections from late stage (17 weeks) wt and tg animals from the dorsal hippocampus were analysed for CNP positive cell bodies that were also HspB5 positive. (A) A representative example of how cell counting was conducted is shown from the DG. Cell bodies that were distinguishable as CNP positive were highlighted with a circle using software tools in Leica Application Suite Advanced Fluorescence software. The position of circles was automatically transferred to the equivalent images showing HspB5 immunofluorescence, DAPI stain and an overlay of all the images. (B) Cell bodies were counted in the CA1, CA3 and the DG. There were no statistically significant differences between wt and tg animals in the hippocampus. (n = 4 animals (3 fields per animals: CA1/CA3/DG)).

5.3.10.   White matter changes in R6/2 tissue

5.3.10.1.   MBP expression in brain homogenate samples

Although HspB5 was downregulated in the white matter of tg animals, no changes in the
staining of the non-compact myelin protein CNP were observed in the same tissue. This
suggested that the decrease of HspB5 in non-compact myelin was selective and likely not a
consequence of general changes in the non-compact myelin compartment. To investigate
if the compact myelin compartment was affected during disease, myelin basic protein
(MBP) expression was investigated in wt and tg animals. MBP did not show any
significant changes in protein expression at 9 weeks or 17 weeks in the three brain regions
analysed (Figure 5.17).

5.3.10.2.   MBP expression in R6/2 tissue sections

MBP expression is restricted to the processes by virtue of selective targeting of protein
and/or local translation of targeted RNA (Barbarese et al., 1995), accordingly the
biochemical investigation described above was extended and MBP immunoreactivity
analysed in tissue sections. MBP displayed intense staining of the external capsule with
white matter fibers extending into the cortex. Fiber bundles in the striatum were also
immunopositive for MBP (Figure 5.18 A i). Higher magnification image of the striatum
showed intense MBP expression in fiber bundles as well as fine myelinated processes
forming a meshwork throughout the striatum (Figure 5.18 A ii). Staining in the cerebellum
was observed in the white matter layer of the cerebella lobule as well as some fine staining
emanating into and between the cell bodies of the granule cell layer (Figure 5.18 A iii). A
clear difference in MBP immunoreactivity between wt and tg animals was not apparent in
any of the brain regions analysed (Figure 5.18 B). However quantification of the staining
intensity could allow resolution of any subtle changes.
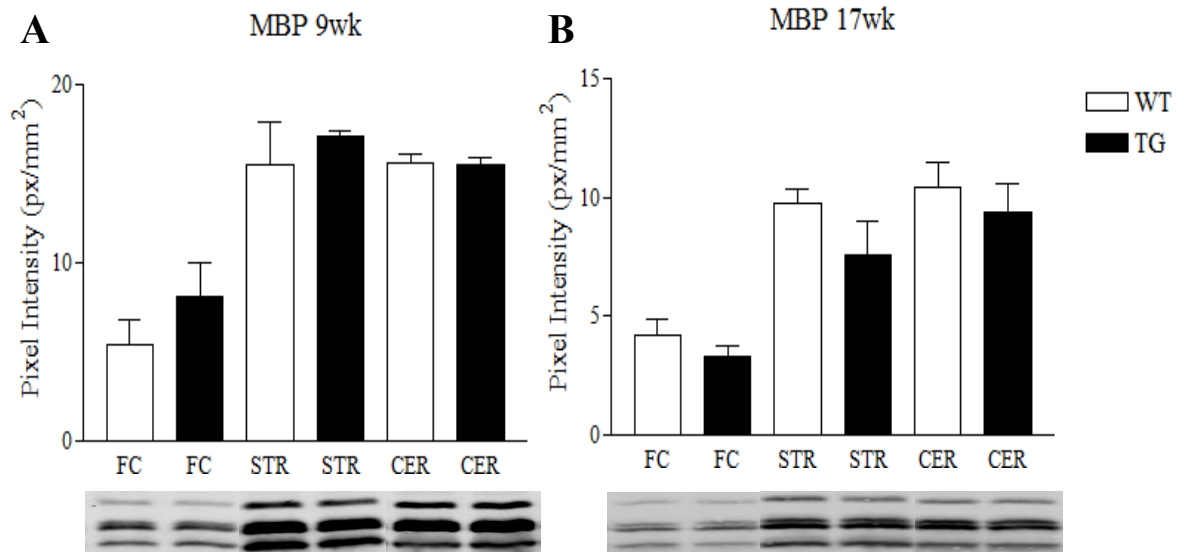
Figure 5.17. MBP expression at mid and late stage of disease.
40µg of protein from the frontal cortex, striatum and the cerebellum were resolved by SDS-PAGE and expression of MBP was detected by infrared fluorescence. Intensity values (pixels/ mm^2) were measured by Odyssey Infrared Scanner software. (A) No changes in MBP expression were observed in tg animals in the three brain regions at 9 weeks. (B) There were also no changes in MBP expression in tg animals in the three brain regions analyzed at 17 weeks. Representative blots are shown below corresponding graph (9wk, n = 3; 17wks, n = 4). Student's *t*-test was used to determine significance (p, <0.05), error bars represent SEM. FC (frontal cortex); STR (striatum); CER (cerebellum); WT (wild type); TG (transgenic).
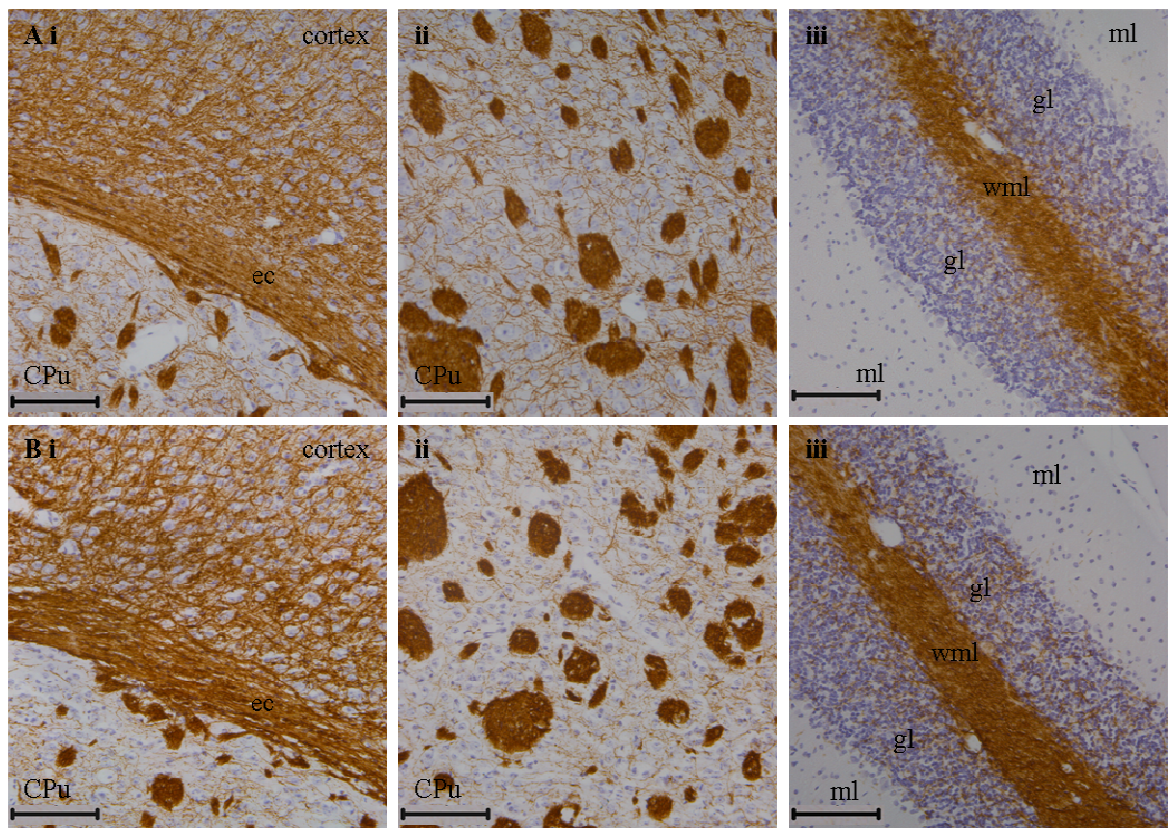
Figure 5.18. Immunohistochemical analysis of MBP in R6/2 tissue. Coronal brain sections from wt and tg animals were subjected to immunohistochemistry for detection of MBP immunoreactivity. No obvious changes in intensity as judged by relative staining or distribution of MBP were observed in tg animals (B) compared to wt (A) animals. (A) (i) MBP immunoreactivity was observed in the cortex, ec and striatum (CPu). (ii) Staining in the CPu was localized to white matter rich fiber bundles along with white matter processes forming a fine meshwork throughout the CPu. (iii) Immunoreactivity in the cerebellum was localized mainly to the wml with some processes extending into the granular cell layer. (B) (i) MBP immunoreactivity did not appear different in the cortex and ec of tg animals. (ii) MBP expression in the fiber bundles of the CPu did not show an obvious difference in staining. (iii) Staining of the cerebellum of tg animals appeared consistent with staining in wt animals. Images are representative of staining from 4 animals. External capsule (ec), caudate putmen (CPu), molecular layer (ml), granular layer (gl), white matter layer (wml). Magnifications: A/B (i-iii, x20), scale bar (i-iii, 100μm).

5.3.10.3.   Luxol fast blue staining in R6/2 tissue

Although there were no clear changes in CNP and MBP expression and/or staining, indicating other myelin specific proteins were not affected in R6/2 tg animals, to observe myelination in wt and tg animals, brain sections were analysed by Luxol fast blue (LFB) staining (Section 2.12). Tissue from tg and wt animals was processed in parallel. LFB showed staining of the corpus callosum and cingulate gyrus (Figure 5.19 A i). White matter fiber bundles were stained by luxol fast blue in the striatum (Figure 5.19 A ii),

staining of the white matter layer of the cerebellum with some staining in the granular layer (Figure 5.19 A iii). All white matter tracts were stained in both wt and tg animals. On a qualitative level, tg animals appeared to have lighter LFB staining compared to wt animals (Figure 5.19 B) however a difference in all animals could not be conclusively established. As suggested for MBP staining, quantification of the LFB staining would allow any changes in staining intensity to be resolved.
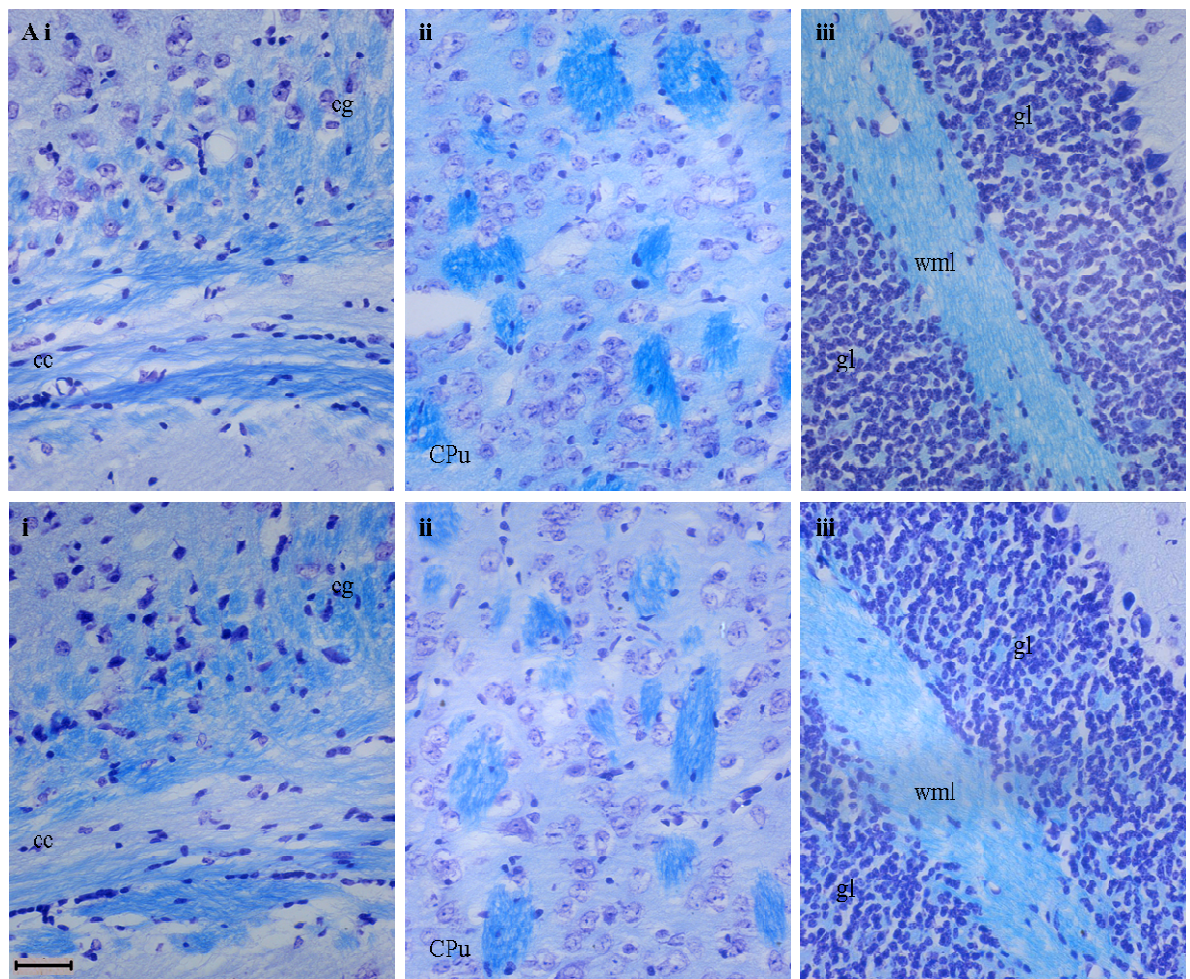
Figure 5.19. Luxol fast blue (LFB) staining in R6/2 tissue. Coronal brain sections from late stage (17 weeks) wt and tg animals were subjected to LFB staining for detection of white matter. All white matter structures were stained with LFB and no conclusive changes in the white matter of tg animals (B) compared to wt animals (A) were observed. (A) (i) The cc and cg were intensely stained by LFB. (ii) Staining in the CPu was localized to white matter rich fiber bundles. (iii) Staining in the cerebellum was localized mainly to the wml with some staining extending into the granular cell layer. (B) (i) There were no clear changes in the white matter structures of the cc and cg in tg animals. (ii) Staining of fiber bundles of the CPu did not appear different. (iii) White matter staining did not appear different in the cerebellum of tg animals. Images are representative of staining from 4 animals (17 weeks). Granular layer (gl), white matter layer (wml), caudate putmen (CPu), corpus callosum (cc), cingulated gyrus (cg). Scale bar, 50μm.

5.3.11. GFAP expression in R6/2 HD tissue

5.3.11.1.   Limited GFAP expression changes in brain homogenate samples

Induction of the sHsps was not observed in this disease context; however sHsp up-regulation in a number of neurodegenerative diseases has been associated with expression in astrocytes and astrogliosis, as describe in the general introduction (section 1.6.2.2). In order to investigate the level of astrogliosis in R6/2 animals, and see if this correlated with a lack of sHsp induction, GFAP expression was investigated biochemically at mid (9 weeks) and to late (17 weeks) stage of disease.

GFAP did not show any significant changes in protein expression at 9 weeks in the three brain regions (Figure 5.20 B). At 17 weeks, tg animals showed an increase in GFAP expression in the frontal cortex, but there were no changes in expression in the striatum and the cerebellum (Figure 5.20 B).
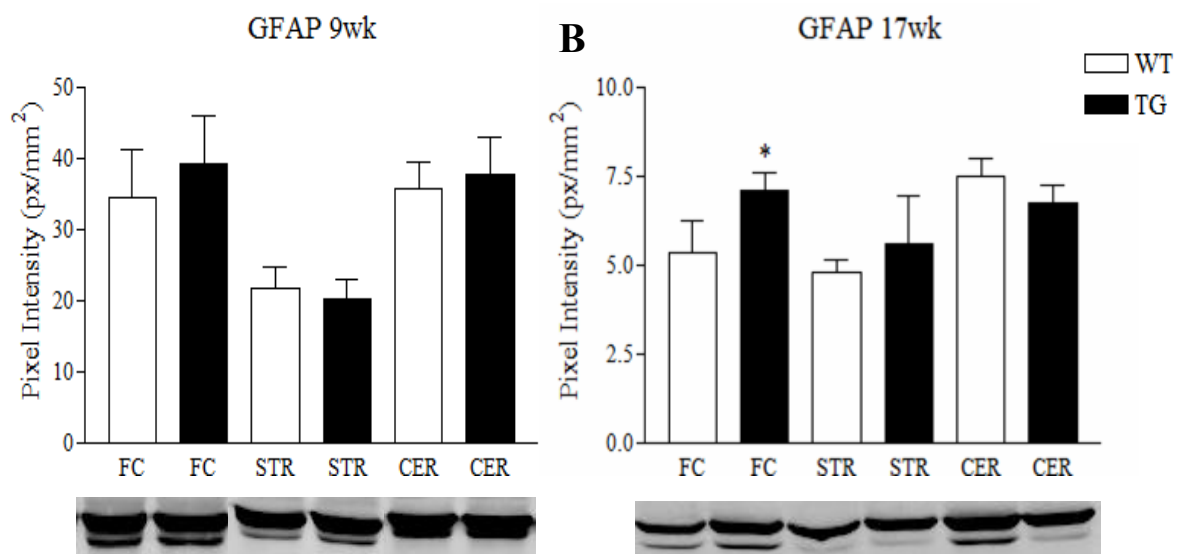
Figure 5.20. GFAP expression at mid and late stage of disease. 40µg of protein from the frontal cortex, striatum and the cerebellum were resolved by SDS-PAGE and expression of GFAP was detected by infrared fluorescence. Intensity values (pixels/ mm^2) were measured by Odyssey Infrared Scanner software. (A) No changes in GFAP expression were observed in tg animals in the three brain regions at 9 weeks. (B) GFAP levels were increased in tg animals in the frontal cortex, but no changes were observed in the striatum and cerebellum at 17 weeks. Representative blots are shown below corresponding graph (9wk, n = 3; 17wks, n = 4). Differences in pixel intensity at 9 and 17 weeks do not correspond to difference in protein levels between time points, but are reflective of differences in individual blots and normalization to protein loading. Student's t-test was used to determine significance (*p, <0.05), error bars represent SEM. FC (frontal cortex); STR (striatum); CER (cerebellum); WT (wild type); TG (transgenic).

5.3.11.2.　　　GFAP expression in R6/2 tissue sections

  GFAP expression analysis was extended by immunohistochemical analysis of late stage (17 week) tissue. GFAP staining in wt animals was observed in the cortex and the external capsule (Figure 5.21 A i). Astrocytes were present in the striatum and were mainly localized to the white matter fiber bundles (Figure 5.21 A ii). GFAP positive cells were distributed throughout the corpus callosum and cingulate gyrus (Figure 5.21 A iii) as well the hippocampus (Figure 5.21 A iv). GFAP immunoreactivity and astrocytic cell morphology in tg animals did not indicate a pronounced astrogliosis when compared to wt animals (Figure 5.21). However, close examination of some sections, such as the striatum (Figure 5.21 B ii.) suggest a modest increase in the number of astrocytes. In conjunction with up-regulation of GFAP in the frontal cortex (Figure 5.20 B) this suggests the possibility of a mild and limited astrogliosis.
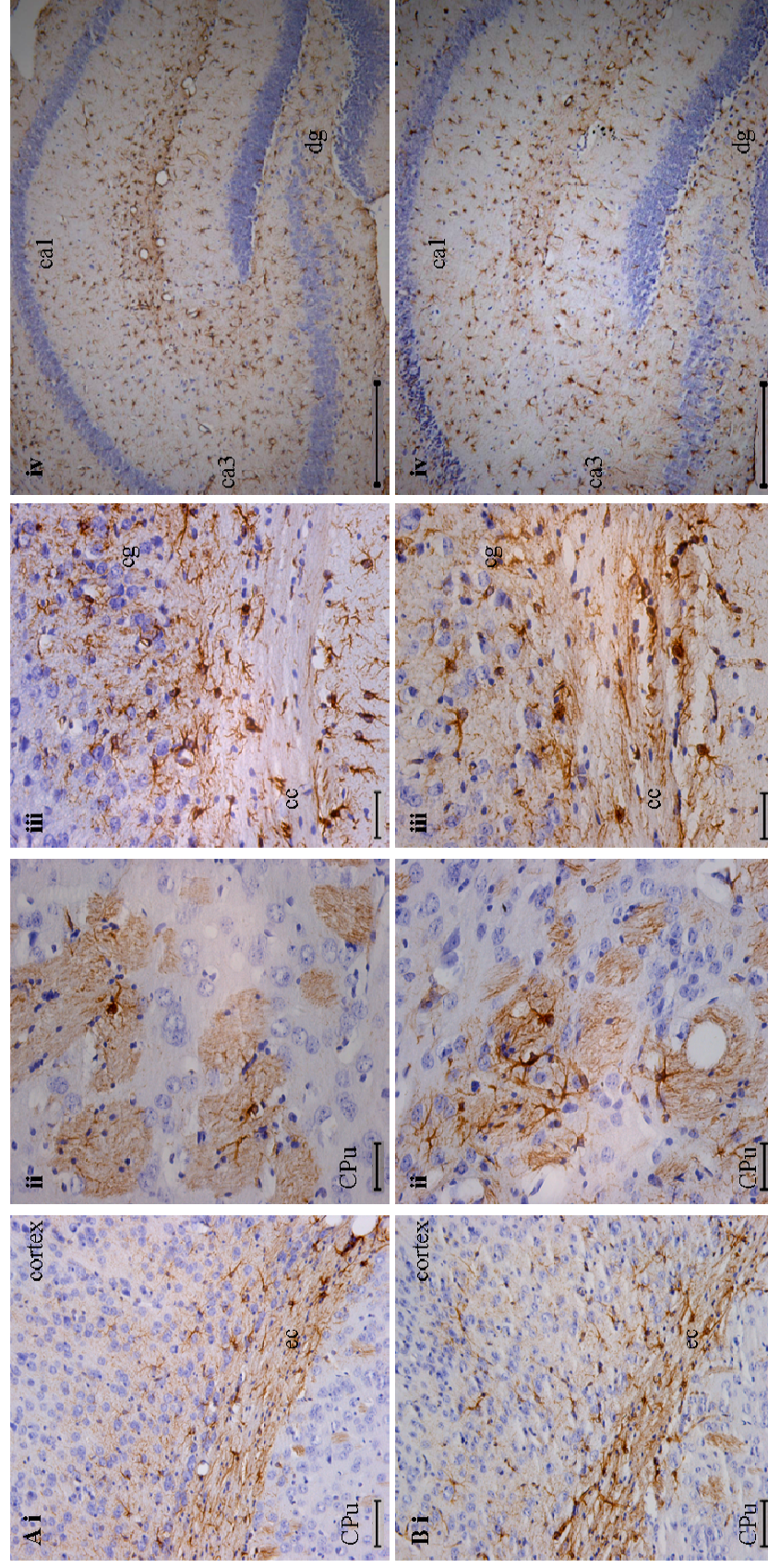
Figure 5.21. Immunohistochemical analysis of GFAP in R6/2 tissue. Coronal brain sections from late stage (17 weeks) wt and tg animals were subjected to immunohistochemistry for detection of GFAP immunoreactivity. No gross changes in GFAP immunoreactivity or astrocytic morphology were observed in tg animals (B) compared to wt animals (A). (A) (i) GFAP immunoreactivity was observed in the cortex, and ec. (ii) Astrocytic staining in the CPu was localized to white matter rich fiber bundles. (iii) Astrocytes were present throughout the cc and cg. (iv) Hippocampal sections also displayed widespread GFAP positive astrocytes. (B) (i). GFAP immunoreactivity did not appear different in the cortex and ec of tg animals. (ii) GFAP expression in the fiber bundles of the CPu did not appear different, although a modest increase in the number of GFAP positive astrocytes was observed. (iii) Immunoreactivity in the cc and cg remained similar to wt animals. (iv) There were no apparent changes in GFAP expression in hippocampal sections from tg animals. Images are representative of staining from 4 animals. External capsule (ec), caudate putmen (CPu), corpus callosum (cc), cingulate gyrus (cg), dentate gyrus (dg). Magnifications: A/B (i, x20; ii and iii, x40; iv, x10), scale bar (i, 100µm; ii and iii, 50µm; iv.200 µm).

194

5.3.12. mRNA expression of HspB5 is not decreased (QT-PCR)

HspB5 downregulation in the white matter of tg animals was not due to sequestration into Htt-Ex1 aggregates or due to overt changes in myelin structure and content. Htt-Ex1 is able to dysregulate many genes, raising the possibility of HspB5 being targeted in a similar way. HspB5 gene expression was therefore investigated. mRNA was extracted for QT-PCR analysis from the cortex and cerebellum of tg and wt animals at 9 weeks of age and from the cortex, striatum and the cerebellum at 17 weeks (section 2.5). HspB5 gene expression data was normalized to ATP5b expression. ATP5B was determined to be a suitable housekeeping gene based on its expressional stability in different brain regions (Benn et al., 2008). ATP5b primer specificity was confirmed by running 5μl of QT-PCR product on an agarose gel. A single band of the predicted size for cDNA amplification was observed (Figure 5.22 A). HspB5 primer specificity had previously been established in Chapter 3. HspB5 transcript levels did not change in the cortex and cerebellum at 9 weeks (Figure 5.22 B). There were no changes in expression in the cortex, striatum and cerebellum of tg animals at 17 weeks (Figure 5.22 C). The relative mRNA expression of HspB5 was consistent with high protein expression in the cerebellum (Figure 5.2/5.6) however this was not the case for the frontal cortex and striatum. At the protein level, HspB5 showed higher expression in the striatum compared to the frontal cortex; however at the mRNA level the reverse was observed (Figure 5.22 C).
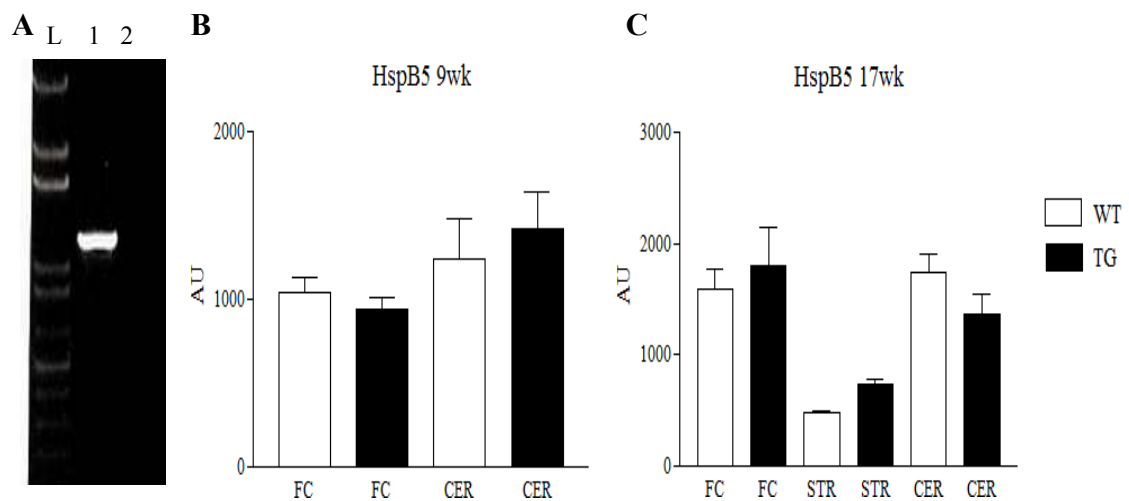
Figure 5.22. mRNA expression of HspB5 in HD tissue at 9 and 17 weeks (QT-PCR). Transcript analysis by QT-PCR of HspB5 in the cortex, striatum and cerebellum of wt and R6/2 tg animals was conducted. HspB5 data was normalised to ATP5b expression. (A) ATP5b primer specificity was confirmed by the presence of a single band (lane 1) of the predicted size for cDNA amplification. Negative control sample lacking cDNA template did not produce any bands (lane 2). (B) There were no significant changes in tg animals compared to wt animals at 9 weeks in the frontal cortex and cerebellum. (B) There were also no significant changes in tg animals compared to wt animals at 17 weeks in any of the three brain regions analysed. (n = 5; Student's t-test was used to determine significance (p, <0.05), error bars represent SEM).

5.4. Discussion

The aim of this chapter was to investigate the expression of the four sHsps that have shown to be constitutively expressed in the mouse CNS under normal conditions (Chapter 3), in a mouse model of chronic neurodegeneration. The R6/2 mouse model of HD, characterized by intracellular protein aggregates (Morton et al., 2000, Meade et al., 2002) was used, and chosen tissue from specific brain regions at different time points were investigated to reflect the different stages in disease progression (Carter et al., 1999, Morton et al., 2000) and compare anatomically susceptible brain regions.

In addition to providing insight into when a change occurs, the use of time points associated with distinct phases of disease also allows some speculation into the possible relevance of the changes during pathogenesis (Freeman and Morton, 2004).

5.4.1. Changes in sHsp protein expression

Protein expression of HspB1, HspB5, HspB6 and HspB8 was analysed at early (4wk) and mid (9wk) stage of disease in detergent extracted tissue, and at mid (9wk) and late (17wk) stage in non-detergent extracted homogenates. The striking observation from these results was the selective downregulation of the white matter specific HspB5 in all regions and time points analysed (Table 5.1). HspB5 loss was apparent at 4 weeks and showed a progressive almost 80% decline over the disease time course (Figure 5.12). The global changes in HspB5 expression suggest disease specific alterations that are brain region independent, but cell type (oligodendrocyte) specific. Because the pixel intensity for each blot is normalized to protein loading, the relative differences between brain regions could also be compared. The physiological (basal) levels of HspB5 in tissues of R6/2 wt animals appeared higher in the striatum and the cerebellum compared to the frontal cortex (Figure 5.6). This is indeed reflective of the higher levels of myelination in these regions compared to the frontal cortex, as shown by MBP expression (Figure 5.17) and is consistent with the white matter expression of HspB5 (see Chapter 4). Additionally HspB8 consistently showed higher levels of protein expression in the cerebellum of wt animals compared to the frontal cortex and striatum. Combined with the finding that HspB1 is induced at 9 weeks in the cerebellum it is possible that these sHsps contribute to the protection of the cerebellum from dysfunction in R6/2 animals (Mangiarini et al., 1996).

Interestingly, in a study comparing the gene expression profiles of 3 types of primary neurons expressing mutant htt or ataxin-1, it was found that Hsp70 protected neurons and was up-regulated selectively in the granule cells of the cerebellum. Insensitivity to degeneration of the cerebellum was lost by siRNA knockdown of Hsp70, whereas cortical neurons affected in human HD gained resistance by overexpressing Hsp70 (Tagawa et al., 2007). It was therefore concluded that Hsp70 levels are a critical factor for determining vulnerabilities to mutant htt among neuronal subtypes. This lends support to the potential protective role of the sHsps in the cerebellum, potentially involved in protein folding processes associated with the larger ATP dependent Hsp70 and Hsp40.

HspB1 and HspB8 form heterogeneous oligomeric complexes under physiological conditions (Sun et al., 2004) and show a great deal of overlap and similarity in expression

and cellular localization, as shown in Chapter 3. MRNA expression of both HspB1 and HspB8 was shown to localize to a subpopulation of motor neurons in the spinal cord (Chapter 3). HspB1 protein expression in other neuronal populations has also been extensively documented (Armstrong et al., 2001a), and given the overlapping expression of HspB8 with HspB1 suggests it is also expressed in similar cell types as HspB1. HspB1 expression in the cerebellum has allowed its use as a marker for Purkinje cells (Armstrong et al., 2009) and thus potentially places both of these sHsps in a suitable cell type to confer neuroprotection in the face of a pronounced white matter deficit which is likely to impinge on myelinated neuronal populations. Indeed, HspB1 has been shown to be protective in mice containing a mutation in HspB5 (R120G) (Ito et al., 2003).

In addition to HspB5, HspB6 is also enriched in the white matter (Chapter 3). However this sHsp does not show a change in expression levels in R6/2 compared to wt animals. Enrichment of both HspB5 and HspB6 in the white matter suggests important functions in this compartment. In the case of HspB5, although these functions have not yet been determined a number of potential functions have been proposed, such as cytoskeleton stabilization and lipid raft mediated signalling, by virtue of localization to the non-compact myelin in oligodendrocytes (Chapter 4). The selective and early downregulation of HspB5 suggests that the remaining protein may be directed towards general and essential functions such as maintaining myelin integrity and structure as shown for CNP (Yin et al., 1997) thus other potential functions may be negatively affected. If HspB5 is involved in signalling events by association with lipid rafts, the downregulation could have a direct impact on neuronal-glia cross talk, and may be a potential mechanism for neuronal dysfunction as a consequence of early myelin/oligodendrocyte dysfunction. Dysfunction could then be increased in regions such as the frontal cortex and striatum; with neuronal cells in these regions show more vulnerability (Sieradzan and Mann, 2001). The above suggests white matter dysfunction may contribute to early pathological events in R6/2 animals. It would therefore be of interest to analyse HspB5 expression in detergent extracted pellet samples in conjunction with supernatant samples to investigate if, in addition to the downregulation, a shift in compartment is also observed.

Additionally, unpublished preliminary data from our lab has also demonstrated a trend toward lower levels of HspB5 in the R6/1 mouse model of HD. Additionally preliminary

analysis of human Vonsattel stage II brain tissue suggest variable expression of HspB5 in HD tissue compared to controls (see Appendix 4).

5.4.2. HspB5 is not sequestered into mtHtt aggregates

Downregulation of a number of molecular chaperones (Hdj1, Hdj2, Hsp70, α-SGT (small glutamine-rich tetratricopeptide repeat containing proteins) and β-SGT) has previously been reported in the brains of R6/2 animals (Hay et al., 2004). Some of these chaperones, including Hsp70 were found to co-localise with intra-nuclear polyQ aggregates despite their predominately cytosolic localisation. The downregulation was proposed to occur via post-translational mechanisms, inducing sequestration into Htt-Ex1 aggregates or an increase in protein turn-over (Hay et al., 2004). This suggested the possibility that HspB5 was also being modulated by similar mechanisms in particular an association with aggregates as it was previously shown that sHsps promote removal of protein aggregates by incorporating into insoluble protein complexes and, with the assistance of large ATP dependent molecular chaperones such as Hsp100, promote refolding of substrates from such insoluble complexes (Haslbeck et al., 2005, Jiao et al., 2005).

However, dot blot analysis showed that HspB5 was not redistributed into the SDS insoluble htt aggregates (Figure 5.10). Nevertheless it appears that the downregulation was selective to the myelin compartment as determined in brain fractions, with an approximately 5-fold reduction in tg animals compared to wt animals (Figure 5.11 A). Although HspB5 did not associate with SDS insoluble Htt aggregates as determined by dot blot analysis, the distribution of endogenous htt protein and htt-Ex1 were investigated in brain and synaptosome sub-compartments to determine if these proteins were present in the same compartments as HspB5 as it would suggest that their interaction could contribute to the down regulation of HspB5, by the toxic loss of function of Htt and/or indeed gain of function of mtHtt. The distribution of htt and htt-Ex1 were very different to HspB5. Htt was mainly associated with the synaptosomal compartment and displayed a presynaptic protein profile, although our observations also support both a pre and post synaptic localization. This was consistent with its global expression and also its association with the presynaptic compartment shown previously (DiFiglia et al., 1995, Wood et al., 1996). However, some immunoreactivity was present the myelin fraction. Htt-Ex1 was enriched

in the P1 pellet, consistent with an intra-nuclear presence; though it did not show immunoreactivity in the myelin fraction, supporting the lack of association of HspB5 with htt aggregates. It is therefore unlikely that HspB5 directly interacts with htt-Ex1 and affects its misfolding and aggregation. This is also suggested by experiments performed by A. Wyttenbach and A. J. Morton who did not find co-localisation of HspB5 with htt-Ex1 inclusion bodies in R6/2 tg animals (A. Wyttenbach, personal communication).

The localization of inclusion bodies in tissue sections was investigated with an anti-ubiquitin antibody. In addition to intra-nuclear and cytoplasmic inclusions in neuronal cells of tg animals, some inclusion bodies in the white matter (cc) of tg animals were observed under high magnification. The immuno-positive cells were likely oligodendrocytes as they were part of a chain of cells forming tandem arrays, which typify these cells in the white matter. The inclusions present were small in comparison to neuronal inclusions in the same tissue. In a study by Shin et al. immunogold labelling of aggregates revealed nuclear htt aggregates in glial cells that were smaller than neuronal nuclear inclusions (Shin et al., 2005), consistent with our own observations at the light microscopic level. The ubiquitous expression of the Exon1 transgene in different brain regions (Mangiarini et al., 1996), indicates that the relative expression is likely similar in different cell types. The minor amount of inclusions in the white matter is therefore indicative of the intrinsic protection of this compartment against inclusion body formation.

Shin et al. (2005) also reported that only a few glial cells contained inclusions in R6/2 animals; however this increased with age and also correlated with disease progression. Indeed, wt glial cells were reported to protect neurons against mtHtt mediated toxicity in a co-culture system, whereas glia expressing mtHtt increased neuronal vulnerability (Shin et al., 2005). Transgenic mice generated to express mtHtt in astrocytes were shown to develop age-dependent neurological phenotype, motor function deficits and died earlier than wt and control tg mice (Bradford et al., 2009) implying an important role for astrocytes in HD pathology.

In the R6/2 mouse model, intra-nuclear inclusions and cytoplasmic aggregates are apparent at 4 weeks (Morton et al., 2000). This appearance of aggregates coincides with the decrease in expression of HspB5 at 4 weeks. As aggregate formation increases, HspB5 expression decreases, as we have shown at 9 weeks and 17 weeks. It may be speculated

that changes in normal neuronal-oligodendrocyte crosstalk (Simons and Trajkovic, 2006) could results in neuronal susceptibility to inclusion formation, or indeed the opposite may be the case whereby neuronal polyQ aggregation and inclusion formation impacts on oligodendrocyte function. Human glioblastoma and neuroblastoma co-cultures that were stably expressing mutant fALS-SOD1 were shown to demonstrate functional cross-talk by the production and molecular exchange of cytokines and subsequent induction of caspase pathways impacting on the function of both cell types (Ferri et al., 2004). This theme of glia/neuron cross-talk is increasingly established in many diseases (Marchetti et al., 2005, Rossi and Volterra, 2009).

5.4.3. White matter specific changes in HD

Involvement of the white matter in neurodegenerative disease is relatively understudied, despite indications that this compartment is affected in neurodegenerative diseases such as AD and PD (Duan et al., 2006). White matter abnormalities are being increasingly reported and studied in HD patients. A recent study examining changes in the corpus callosum (cc) by diffusion tensor imaging (DTI) revealed early microstructural changes indicative of white matter dysfunction, that occurred prior to measurable atrophy and more than a decade before onset of motor symptoms (Rosas et al., 2010). The cc is the primary cortical projection system and connects the two hemispheres. This study suggested a role for progressive white matter alterations for clinical symptoms to occur and a contribution to cognitive deficits by altered cortical circuitry (Rosas et al., 2010). Alterations in the cc have been reported in a number of neuro-psychiatric and neurological disorders including dementia (Stricker et al., 2009) and multiple sclerosis (MS) (Lowe et al., 2006) relating to altered cortical connectivity. Early white matter changes in HD patients were found to correlate with early neurological dysfunction and appear to precede striatal cell loss (Sapp et al., 1997)(Sapp et al., 1997). An increase in the number of degenerating myelinated fibers was observed in another study, although myelin thickness did not change (Wade et al., 2008)(Wade et al. 2008).

Additionally it has been reported that so-called "normal appearing white matter" (NAWM) as detected by magnetic resonance imaging (MRI) in MS patients, is in fact abnormal when imaged by non-conventional MRI techniques (Moore et al., 2008).

Increasing evidence for white matter damage and dysfunction is also observed in AD and has been correlated with cognitive decline (Duan et al., 2006). The early changes in HspB5 suggest HspB5 may be a good indicator or marker for white matter dysfunction in HD and perhaps other proteinopathies that show changes in the white matter associated with pathology, as discussed in section 4.1.2.

5.4.4. Myelin sub-compartment specific downregulation of HspB5

Immunohistochemical analysis also showed global downregulation of HspB5 in the white matter of tg animals. Additionally the staining pattern suggested that HspB5 expression was selectively reduced in the white matter fiber tracts even relative to cell bodies. As previously described in Chapter 4, HspB5 showed colocalisation with CNP a white matter specific protein selectively expressed in the non-compact myelin subdomain. We analysed expression of both proteins in the same tissue by double immunofluorescence to elucidate if HspB5 downregulation was due to a compartment effect. If so, a difference in CNP immunofluorescence would also be observed in tg animals compared to wt.

As expected, HspB5 showed reduced immunofluorescence staining in tg animals in all regions analysed. However, CNP staining did not appear any different in tg compared to wt animals, supporting the specific down regulation of HspB5 relative to a more general change in the non-compact myelin compartment.

Although there appeared to be no difference in HspB5 immunoreactivity in oligodendrocyte cell bodies of tg animals compared to wt, it was possible that the reduction in HspB5 expression was occurring as a result of a reduction in the number of oligodendrocytes. HspB5/CNP double stained, positive cells were counted in the hippocampus, as myelination in this region is relatively sparse in comparison to heavily myelinated structures such as the cc, thus allowing cell bodies to be distinguished. This analysis did not reveal any difference in CNP stained oligodendrocyte cell body number in tg animals compared to wt. The downregulation of HspB5 could not be attributed to a reduction in the number of the cells producing this protein, but was therefore likely to be due to a reduction in the number of myelin fibers/sheaths expressing HspB5. Although we did not observe any changes in the number of HspB5/CNP positive oligodendrocytes in the hippocampus, oligodendrocyte numbers have been shown to increase in HD in response to

myelin breakdown and dysfunction. No changes in CNP positive oligodendrocyte number in the hippocampus were observed, but increased numbers were observed in the striatum. The differences were correlated to when regions were myelinated in development, highlighting a susceptibility of regions myelinated early during development (striatum) (Bartzokis et al., 1999, Bartzokis et al., 2007). This suggests that the lack of change in HspB5/CNP positive cell number in the hippocampus may not reflect changes in other regions. We were unable to determine the number of HspB5/CNP positive cells in other brain regions due to masking of cell bodies by myelin fiber tracts.

MBP expression was also analysed to investigate whether other white matter proteins were altered. MBP is a major white matter protein expressed in the compact myelin sub compartment (Maier et al., 2008). Total protein and immunohistochemical analysis did not show any changes in tg animals compared to wt animals suggesting the compact myelin compartment was not affected. However, although this indicates normal MBP content and distribution, abnormalities cannot be ruled out. MBP is able to stain all myelinated structures in normal and multiple sclerosis tissue, however a rabbit antiserum (anti-EP) that recognized the synthetic peptide QDENPVV, which corresponds to human MBP residues 82-88 was shown to selectively immunostain abnormal appearing oligodendrocyte processes and cell bodies in areas associated with MS plaques and showed no immunoreactivity in normal tissue (Matsuo et al., 1997). The use of such antisera would indicate pathological changes in the white matter that otherwise appear normal.

Luxol fast blue (LFB) is a lipid binding dye, and due to the large proportion of lipids and lipoproteins in myelin membranes, it is able to differentiate the gray matter from the white matter. This dye is routinely used to investigate myelin loss/changes in acute and chronic conditions such as ischemia, AD and MS (Gilmore et al., 2009, Ihara et al., 2010). LFB staining did not detect any clear changes in white matter staining in tg animals, although there was an indication for lighter staining in tg animals. However to tease apart subtle changes quantification of the staining intensities is required (Ihara et al., 2010).

5.4.5. Potential contribution of HspB5 to inflammation and gliosis

Gliosis is not a prominent feature in the R6/2 mouse model, but this observation may be a result of limited studies in this area (Schwab et al., 2009). There are occasional reports

indicating gliosis (Reddy et al., 1998, Lin et al., 2001) in HD mouse models, but thorough studies are missing. The involvement of inflammation in HD had been documented showing increased activation of the complement system (a component of the innate immune system), microglial activity and up-regulation of inflammatory cytokines (Sapp et al., 2001, Dalrymple et al., 2007). In both HD patients and R6/2 mice expression of ferritin in microglia was reported to increase and microglial cells appeared dystrophic in that they had thick, twisted processes (Simmons et al., 2007). More recently, a study analysing cytokine levels in plasma samples from HD mutation carriers showed increases in IL-6 in pre-manifest HD carriers, and increased IL-6 and IL-8 expression in post-mortem striatal tissue of HD patients. In addition, IL-8, IL-4, IL-10, and TNF-α levels were also significantly increased with disease progression (Bjorkqvist et al., 2008). This study suggests the initial pro-inflammatory cytokine production as a consequence of the innate immune response is strongly linked to disease progression.

HspB5 has been implicated in the immune response. Loss of HspB5 (knockout) was shown to increase T-cell and macrophage secretion of Th1 pro-inflammatory cytokine production (IL-2, TNF-α, IL-12) (Ousman et al., 2007). It is plausible that a similar immune response as observed in human HD tissue and in HspB5 knockout mice could occur in R6/2 animals associated with the reduction of HspB5.

We investigated levels of the astrocytic protein GFAP, an indicator of gliosis and found no significant differences in GFAP expression at 9 weeks in the three brain regions analysed. At 17 weeks there was a significant, but modest up-regulation in the frontal cortex, but the striatum and the cerebellum did not show any changes. The modest up-regulation at late stage of disease suggests mild astrogliosis. The limited gliosis observed may be a consequence of the lack of induction of the sHsps, as the sHsps have been shown to be expressed and up-regulated in glial cells as part of an astrocytic response during neurodegenerative disease such as AD and Parkinson disease with dementia (PDD) (Renkawek et al., 1999). It must also be noted that the R6/2 model may not show all the pathologic phenotypes associated with HD. Several studies indicated that due to the fast and aggressive progression of polyQ pathology in this model, the CNS may compensate for the protein misfolding stress and even show resistance to external stress responses (Hansson et al., 2001a, Hansson et al., 2001b). For example, the striatal neurons of R6/2

mice that had been subjected to oxidative stress induced by dopamine, 6-
hydroxydopamine, or malonate were found to be more resistant to this insult in comparison
to age-matched wt littermates (Hansson et al., 2001a, Petersen et al., 2001).

5.4.6. Changes in sHsp mRNA expression

Changes in HspB5 expression could not be attributed to association with htt aggregates or
overt changes in myelin, so mRNA analysis was conducted to determine if the down
regulation was a consequence of transcriptional regulation. The promoter region of HspB5
contains a number of sites that bind transcription factors that have been shown to be
sequestered by mutant htt, reducing transcription of the genes (Figure 5.23). For example
mtHtt can dissociate Sp1 from specific gene promoters, decreasing transcription of Sp1
genes, but the overall levels of Sp1 do not change (Yu et al., 2002). The disruption to gene
expression by mtHtt is not general to all genes containing binding sites for affected
transcription factors, but appears to be selective to specific genes (Chen-Plotkin et al.,
2006).
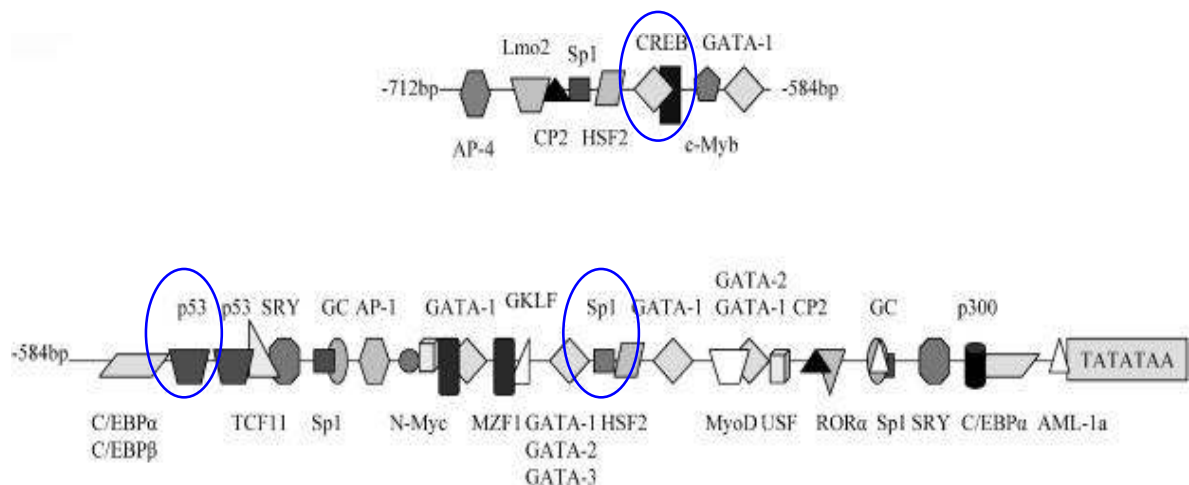
Figure 5.23. Transcription factor binding sites in the promoter region of HspB5.
The promoter of HspB5 contains binding sites for many transcription factors. Each
transcription factor responsive element is represented by an individual symbol in the
correct relative location to the TATA box. Transcription factor binding sites that are
potentially affected by mtHtt are circled in blue (Adapted from (Mineva et al., 2005).

HspB5 mRNA expression was normalized to ATP5B. There were no changes in HspB5 transcript levels in any of the brain regions analysed at mid and late stage of disease. This confirmed that down regulation was not due to transcriptional changes and suggests that HspB5 gene expression is not dysregulated by mtHtt. This leaves the possibility that the down regulation is a consequence of post-transcriptional and/or translational modifications.

Additionally, polyQ aggregation is known to alter transport events (Sinadinos et al., 2009). However, limited inclusion formation in oligodendrocytes argues against this point as the mechanism for HspB5 downregulation, suggesting alternative mechanisms are at play. Indeed, fast axonal transport is inhibited by nanomolar polyQ protein levels even when no aggregates are biochemically or microscopically detectable (Szebenyi et al., 2003).

In Chapter 4, it was suggested that HspB5 mRNA was transported to myelinating processes in a similar fashion to MBP. As it has been shown that mtHtt perturbs axonal transport in neurons (Morfini et al., 2005), and that such events can occur without the presence of aggregates, suggests this could also occur in oligodendrocytes as microtubule transport is an important process for targeting mRNA and proteins to the correct myelin compartments. This raises the possibility of HspB5 mRNA being transcribed and packaged into granules, but not targeted to its correct destination and thus remaining in a repressed state. This could be determined by carrying out dipped *in situ* hybridization experiments on wt and tg tissue sections to see if there is a difference in mRNA localization and potentially a retention to the cell bodies (Medrano and Steward, 2001). Altered transport could therefore explain the reduction of HspB5 staining in the myelin fiber tracts. Mechanistic experiments using oligodendrocyte cell cultures models with/out polyQ expression could also be used to address this hypothesis.

It is also likely that HspB5 is in fact being translated, but that there is an increase in turnover and degradation of this protein due to altered signalling events. Htt is localized to plasma membranes and has been described in lipid rafts. Additionally mtHtt has also been shown to associate more readily with neuronal lipid rafts. The critical role that lipid rafts have in cell signalling could mean that in HD there are multitudes of signalling changes emanating from lipid rafts that may alter cellular processes such as promoting turnover of

proteins (Valencia et al., 2010). Yet another possibility emanates from the finding that htt has been associated with Ago2 (Argonaute) and is localized to P-bodies (Savas et al., 2008). P-bodies are a class of somatic cytoplasmic RNP's, termed cytoplasmic RNA processing bodies that contain non-translated mRNAs and proteins involved in mRNA degradation and translational control (Barbee et al., 2006). MtHtt may perturb mRNA processing/trafficking or post-transcriptional regulation, or alterations in the normal function of htt may confer silencing or reduction of some genes at a translational level by associating with structures such as P-bodies.

Transient decreases of HspB5 have been reported in *in vivo* studies of mechanical stress (Mitton et al., 1997). The transient changes were suggested to occur as a result of increased degradation rather than transcriptional changes. The increase back to basal levels was suggested to be due to increasing levels of mRNA synthesis. It may be that the initial down regulation of HspB5 early in the disease is a white matter response to mtHtt, but the increased disease progression and the toxic functions of htt do not allow protein levels to return to normal, resulting in changes to the myelin compartment that likely impinge on neuronal function.

5.4.7. Potential implications of the selective loss of HspB5

The data so far is supportive of disease related changes of a white matter specific sHsp (HspB5), without overt changes to other white matter proteins and myelin. It is plausible that there are pathological changes occurring in the white matter that require ultrastructural analysis. However our findings suggest a possible myelin dysfunction and not loss that may contribute to R6/2 pathogenesis. The regional susceptibilities observed in HD correlate with brain regions that are myelinated early during development such as the striatum, whereas regions that are myelinated later in development are much less affected (e.g. the hippocampus). In HD the specific degeneration of myelinated projection neurons with sparing of interneurons gives weight to the involvement of myelin abnormalities in HD pathogenesis (Bartzokis et al., 2007). Myelin breakdown and homeostatic re-myelination events have been described in HD patients. A consequence of this is an increase in oligodendrocyte number and iron levels, which are thought to contribute to HD pathogenesis by production of ROS (Bartzokis et al., 2007). HspB5 has antioxidant

properties and is able to bind to Cu^{2+} with picomolar affinity, thus inhibiting Cu^{2+} induced oxidation and preventing ROS generation (Ahmad et al., 2008). Redox abnormalities and ROS damage in HD have been widely reported (reviewed in (Browne and Beal, 2006), thus it is plausible that loss of HspB5 could also contribute to increased oxidative stress.

A deviation of HspB5 from its suggested roles in the myelin compartment (Chapter 4) as a consequence of reduced expression, could impart dysfunction in oligodendrocytes and subsequent dysfunction in ensheathed axons via cross-talk between cell types. Cross-talk may not be restricted to intracellular events, as HspB5 has also been reported in the extracellular space (Wilhelmus et al., 2006c) which could also be important for signalling between cells. Additionally such a location could contribute to, or provide a route for modulation of an inflammatory response.

5.5. Summary

This chapter has described the expression profile of the sHsp family in the R6/2 mouse model of HD. A progressive and selective loss of HspB5 protein is observed in R6/2 tg animals in all brain regions. This white matter specific change occurs early in disease and suggests a key role for oligodendrocytes and the white matter in HD pathogenesis. Changes in the white matter are likely to impinge on the function of associated neuronal cells via cross talk and may trigger increased susceptibilities to damage and stress.

The loss of HspB5 protein is not a consequence of sequestration into SDS insoluble aggregates or due to a reduction in transcript levels. This suggests that post-transcriptional changes are the likely cause of the downregulation. Whether this occurs via disrupted mRNA targeting or increased protein degradation has yet to be determined. The schematic shown in Figure 5.24 summarizes a model on the potential roles of HspB5 function/dysfunction in the context of an intracellular proteinopathy (HD).
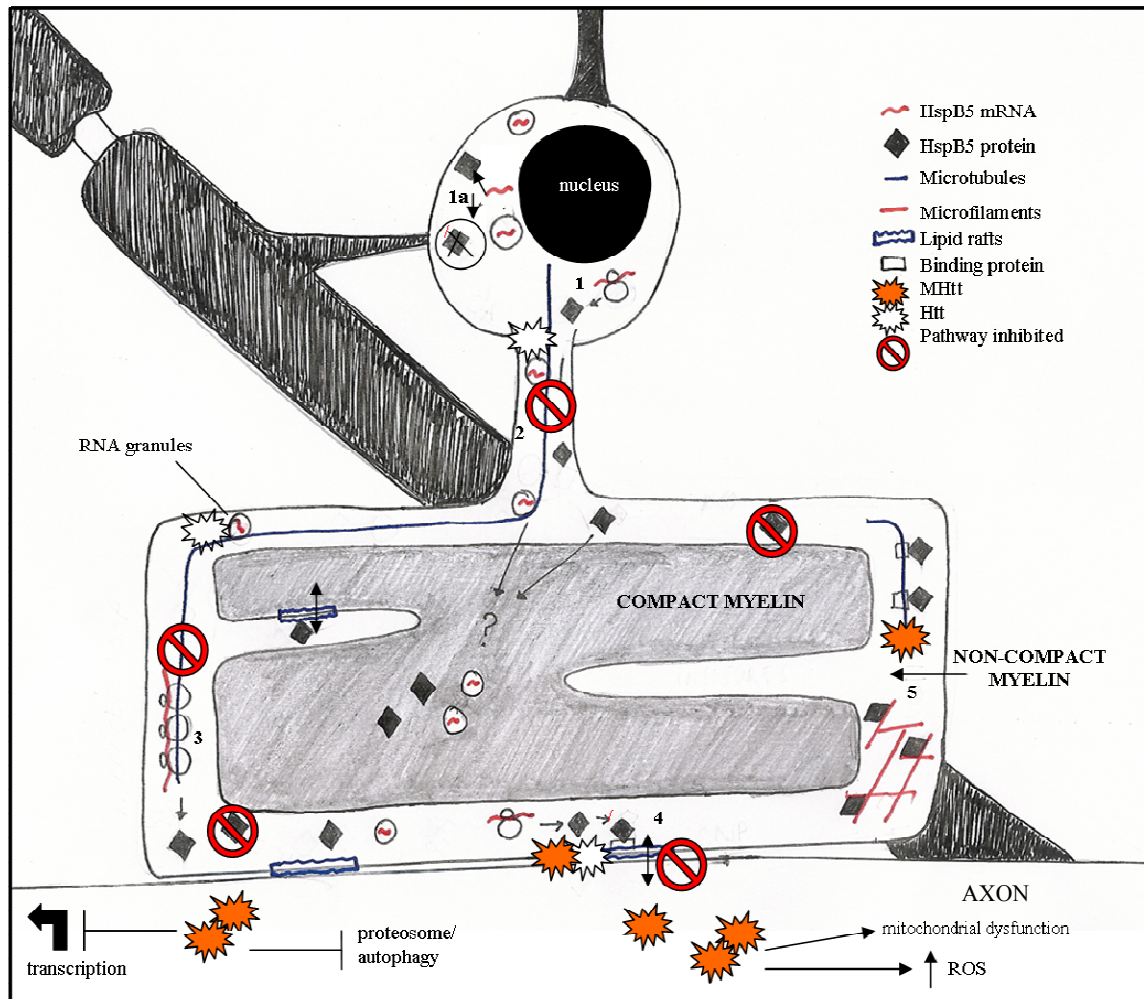
Figure 5.24. Proposed expression/function of HspB5 in the R6/2 model of HD. A schematic drawing which illustrates the expression of HspB5 in oligodendrocytes and shows the changes observed in the R6/2 mouse model of HD. (1) HspB5 mRNA is translated and the protein is targetted to the myelin sheath. (1a) Increased degradation of HspB5 may reduce HspB5 levels. (2) Htt loss of function may perturb transport of RNA granules and proteins. (3) Htt loss of function and association with RNA granules may disrupt tr anslational control resulting in a decrease in HspB5 mRNA that is transcribed by free ribosomes or polysomes at the site of function. (4) Reduced local synthesis or reduction in targetted proteins may change interactions with lipid rafts in regions where axo-glial crosstalk and signalling events can be initiated/regulated. Soluble mtHtt may alter signalling events by association with lipid rafts. Additionally perturbations in axonal frunction by mtHtt such as mitochondrial dysfunction, increase in oxidative stress (ROS), inhibition of proteosomal and autophagic pathways and transcriptional dysregulation could impact on oligodendrocyte/myelin function by altered cross/talk and induction of stress signals. (5) Reduction of HspB5 binding and association of soluble mtHtt with the cytoskeleton may disrupt membrane maintenance, synthesis, transport and signalling events. The decrease in HspB5 protein levels will impact on all the functions and processes that this sHsps is potentially involved in (as described in chapter 4).

Chapter 6: A coordinated and selective small heat shock protein response in non-neuronal cells in the ME7 model of Prion Disease

6.1. Introduction

The previous chapter investigated the expression of the sHsps in the R6/2 model of HD associated with intracellular protein misfolding. In order to investigate expression of the sHsps in a rodent model of extracellular protein deposition and to provide a comparison with responses seen in HD, the ME7 mouse model of Prion disease was used. The ME7 model has several features that are consistent with generic features associated with extracellular misfolding diseases such as deposition of abnormal protein deposits in the extracellular environment, gliosis, and inflammation (Jellinger, 2009). Intracerebral inoculation of ME7 brain homogenate into C57BL/6J mice leads to chronic neurodegeneration associated with progressive hippocampal pathology (Cunningham et al., 2003). Other brain regions, such as the thalamus are also affected during disease (Bruce et al., 1991, Kim et al., 1999, Cunningham et al., 2005). In addition to intracerebral inoculation, ME7 pathology can also be established by a number of routes, such as intraperitoneal (i.p.) and intravenous (i.v.) inoculation (Taylor et al., 1996). Infected animals have disease duration of approximately 24 weeks post infection and develop neurodegeneration over a defined timeline as described previously (section 1.9.3 a).

6.1.1. ME7 pathology

The ME7-model shows activated microglia, marked astrogliosis, vacuolation, spongiform degeneration and neuronal loss associated with the post-translational modification of cellular prion protein (PrP^c) leading to the conformationally altered isoform, PrP^{sc}. These pathological changes occur at distinct time points over the duration of disease. Three time points have been routinely used to dissect disease progression and investigate changes that occur early (8 weeks- pre-symptomatic), mid (13 weeks) and late (20 weeks -symptomatic) in disease. Much of this is based on behavioural dysfunction, in addition to changes associated with pathological events (Dell'Omo et al., 2002, Chiti et al., 2006, Gray et al., 2009).

ME7 induced infection is associated with hippocampal pathology, with gliosis, PrP^{sc} deposition, selective synaptic degeneration in the stratum radiatum and CA1 neuronal loss (Betmouni et al., 1996, Deacon et al., 2001, Cunningham et al., 2003). The selective cell loss of CA1 neurons in ME7 animals suggests susceptibility of certain hippocampal

regions to neurodegeneration and is indicative of cellular and regional differences that may confer vulnerabilities to pathological changes (Gray et al., 2009). The intrinsic susceptibility of CA1 pyramidal cells to pathological insult over and above the CA3 and DG is not selective to this model of prion disease and has been reported in a number of conditions such as ischemic insult (Schmidt-Kastner and Freund, 1991). The CA1 region has been reported to be one of the first regions to develop pathological markers of AD in human brains (West et al., 2000). Additionally *in vivo* models of tauopathy have correlated disease pathology to neuronal loss in the CA1 (Spires et al., 2006). CA1 vulnerabilities have also been linked with aging. Measurements of survival signalling mediated through AKT (protein kinase B) activation was found to be significantly reduced in CA1 nuclear regions compared to CA3 while expression of the pro-apoptotic transcription factor FOXO3a was increased in the CA1 compared to the CA3 (Jackson et al., 2009).

The defined anatomical pathways, neuronal circuitry and region susceptibilities of the hippocampus (see Figure 6.1) provides a tool for investigating ME7 induced hippocampal degeneration that lends itself to tractable dissection of roles played by molecules, cells and network connections (Lein et al., 2004, Thompson et al., 2008).

A major feature of prion diseases as well as in this model is the prominent astrocytic response (Kordek et al., 1997, Cunningham et al., 2003). As the sHsps have been shown to be up-regulated in astrocytes associated with disease responses in human tissue (Renkawek et al., 1999, Wilhelmus et al., 2006c), this would predict that HspB1, HspB5, HspB6 and HspB8 may also be up-regulated in prion the ME7 model.
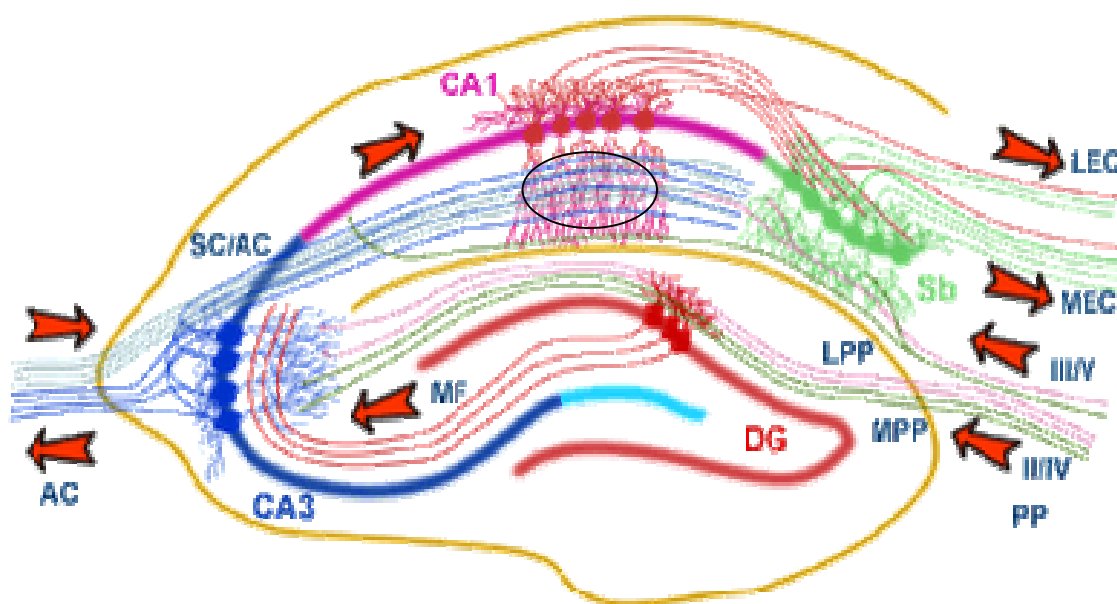
Figure 6.1. Illustration of the neuronal projections within the hippocampus: The Hippocampal Network. The hippocampus forms a uni-directional network. Inputs from the Entorhinal Cortex via the Perforant Path (PP –split into lateral and medial) form connections with the Dentate Gyrus (DG) and CA3 pyramidal neurons. CA3 neurons also receive input from the DG via the mossy fibers (MF) and send axons to CA1 pyramidal cells via the Schaffer Collateral Pathway (SC). Additionally, CA3 neurons project to CA1 cells in the contralateral hippocampus via the Associative Commissural pathway (AC). CA1 neurons send axons to the Subiculum (Sb). The synapses in the stratum radiatum (circle) formed of presynaptic inputs from CA3 Schaffer collateral and post-synapses of the apical dendrites of CA1 pyramidal neurons are vulnerable and degenerate in ME7 induced pathology.

6.2. Aims

The aim of this chapter is to analyse expression of the 4 sHsps constitutively expressed in the mouse CNS under physiological conditions (HspB1, HspB5, HspB6 and HspB8) in the ME7 mouse model of prion disease. Microdissected hippocampal tissue will be analysed at; early (8 weeks), mid (13 weeks), and late (20 weeks) stage of disease to reflect different stages of disease progression associated with distinct pathological events.

6.3. Results

6.3.1. Progressive changes in sHsp expression in ME7 prion disease.

Protein expression of the 4 sHsps expressed in the CNS was initially investigated at mid (13 weeks) and late (20 weeks) stage of disease, with a view to extend this to an earlier time point, if major changes were observed at mid stage of disease. 40μg of protein from each sample was resolved on SDS-PAGE and western blotting was used to analyse expression of the four sHsps expressed in the CNS. The pixel intensity values were normalized to protein loading (section 2.8.4) and the average intensity of the bands was plotted for the three brain regions. Differences in pixel intensity between time points do not correspond to differences in protein levels, but are reflective of differences in individual blots and subsequent normalization to protein loading.

6.3.1.1. HspB1

  There were no significant differences in the protein levels of HspB1 in ME7 compared to NBH animals in any of the hippocampal regions at 13 weeks (Figure 6.2 A). At 20 weeks HspB1 was up-regulated in the CA1 region of the hippocampus. A significant up-regulation was also observed in the DG, although the change was not as large as seen in the CA1 region (Figure 6.2 B).
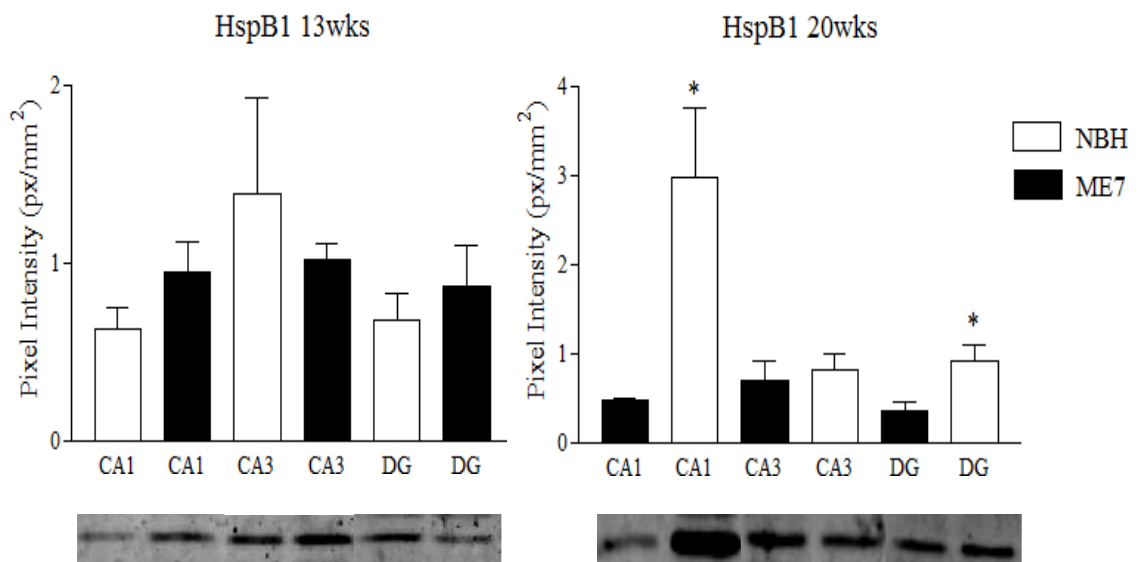
Figure 6.2. HspB1 protein expression in the hippocampus of NBH and ME7 animals at 13 and 20wks (pi). 40μg of protein from CA1, CA3 and DG homogenates were resolved by SDS-PAGE and the expression of HspB1 was measured by incubating membranes with an antibody against HspB1 followed by a fluorescently labelled secondary antibody which was detected by infrared fluorescence. Intensity values (pixels/mm^2) were measured using Odyssey Infrared Scanner software. Values were normalized to protein loading and expressed as pixels intensity per mm^2. Expression of HspB1 is shown in distinct hippocampal regions at A, 13 and B, 20 weeks. (A) No changes in HspB1 protein expression were observed in ME7 animals compared to NBH in the 3 hippocampal regions at 13 weeks. (B) HspB1 was significantly up-regulated in the CA1 and the DG at 20 weeks. Representative blots are shown below the corresponding graph (n = 4). Student's *t*-test was used to determine significance (*p, <0.05), error bars represent SEM.

6.3.1.2. HspB5

There were no significant differences in the protein expression of HspB5 in ME7 and NBH animals in all 3 regions of the hippocampus analysed at 13 weeks (Figure 6.3 A). At 20 weeks, the protein expression of HspB5 was up-regulated in the CA1 region of the hippocampus in ME7 animals; however the p value was 0.05 and therefore did not reach the threshold of significance (Figure 6.3 B).
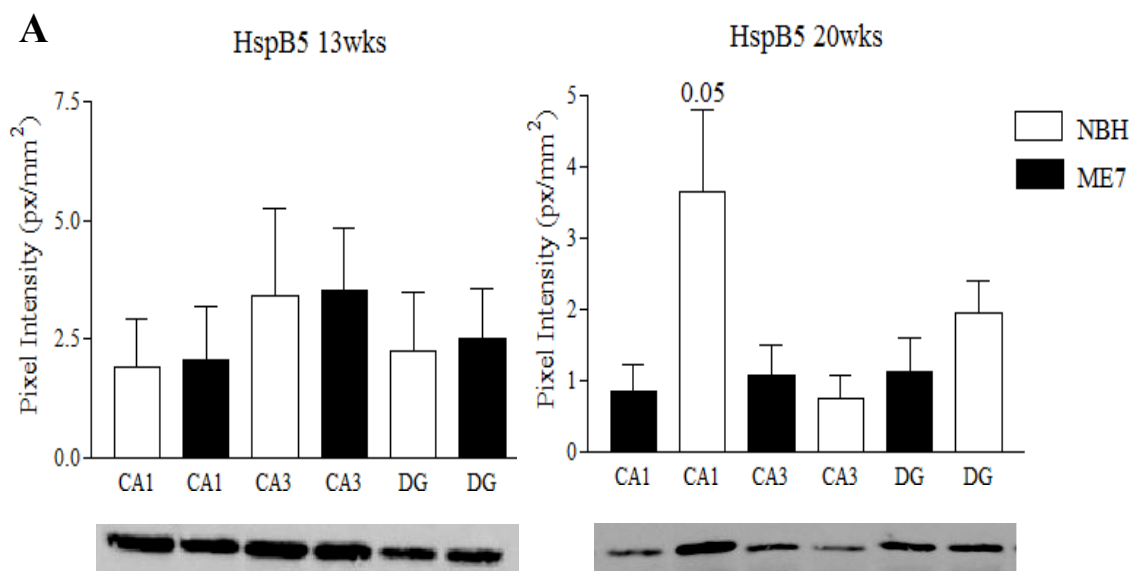
Figure 6.3. HspB5 protein expression in the hippocampus of NBH and ME7 animals at 13 and 20wks (pi). 40μg of protein from CA1, CA3 and DG homogenates were resolved by SDS-PAGE and protein expression of HspB5 was measured by incubating membranes with an antibody against HspB5 followed by a fluorescently labelled secondary antibody which was detected by infrared fluorescence. Intensity values were measured using Odyssey Infrared Scanner software and normalized to protein loading and expressed as pixel intensity per mm^2. Expression of HspB5 is shown in distinct hippocampal regions at A, 13 and B, 20 weeks. (A) No changes in HspB5 protein expression were observed in ME7 animals compared to NBH in the 3 hippocampal regions at 13 weeks. (B) At 20 weeks, HspB5 showed a trend towards up-regulation in the CA1 region, although this was not significant. Representative blots are shown below the corresponding graph (n = 4). Student's *t*-test was used to determine significance (p, <0.05), error bars represent SEM.

6.3.1.3. HspB6

There were no significant differences in HspB6 protein expression between ME7 and NBH animals in all regions of the hippocampus at 13 weeks and 20 weeks (Figure 6.4 A and B).
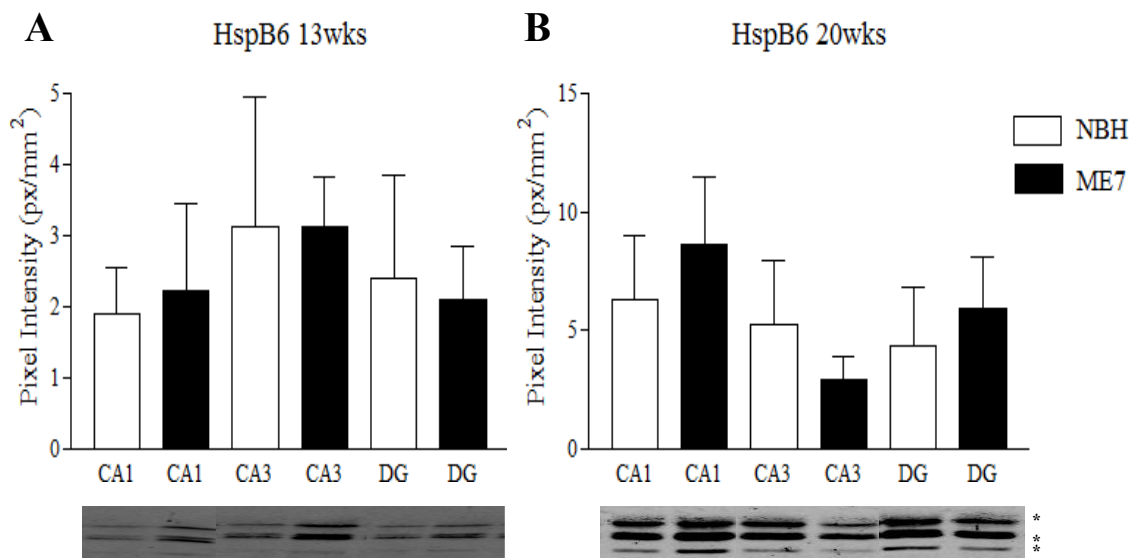
Figure 6.4. HspB6 protein expression in the hippocampus of NBH and ME7 animals at 13 and 20wks (pi). $40\mu g$ of protein from CA1, CA3 and DG homogenates were resolved by SDS-PAGE and protein expression of HspB6 was measured by incubating membranes with an antibody against HspB6 followed by a fluorescently labelled secondary antibody which was detected by infrared fluorescence. Intensity values (pixels/mm^2) were measured using Odyssey Infrared Scanner software. Values were normalized to protein loading and expressed as pixels intensity per mm^2. Expression of HspB6 is shown in distinct hippocampal regions at A, 13 and B, 20 weeks. As previously shown in Chapter 3 and 5, the 3 band (asterisks) represent isoforms of HspB6. (A) No changes in HspB6 protein expression were observed in ME7 animals compared to NBH in the 3 hippocampal regions at 13 weeks. (B) There were also no significant changes in expression at 20 weeks. Representative blots are shown below the corresponding graph (n = 4). Student's *t*-test was used to determine significance (p, <0.05), error bars represent SEM.

6.3.1.4. HspB8

HspB8 protein expression was significantly up-regulated in the CA1 at 13 week in ME7 animals compared to NBH (Figure 6.5 A). This change concurred with the hippocampal region and time point associated with synaptic degeneration in this model (Cunningham et al., 2003). At 20 weeks, HspB8 up-regulation in the CA1 was more pronounced and a statistically significant increase in HspB8 protein expression was also apparent in the DG of ME7 animals (Figure 6.5 B).
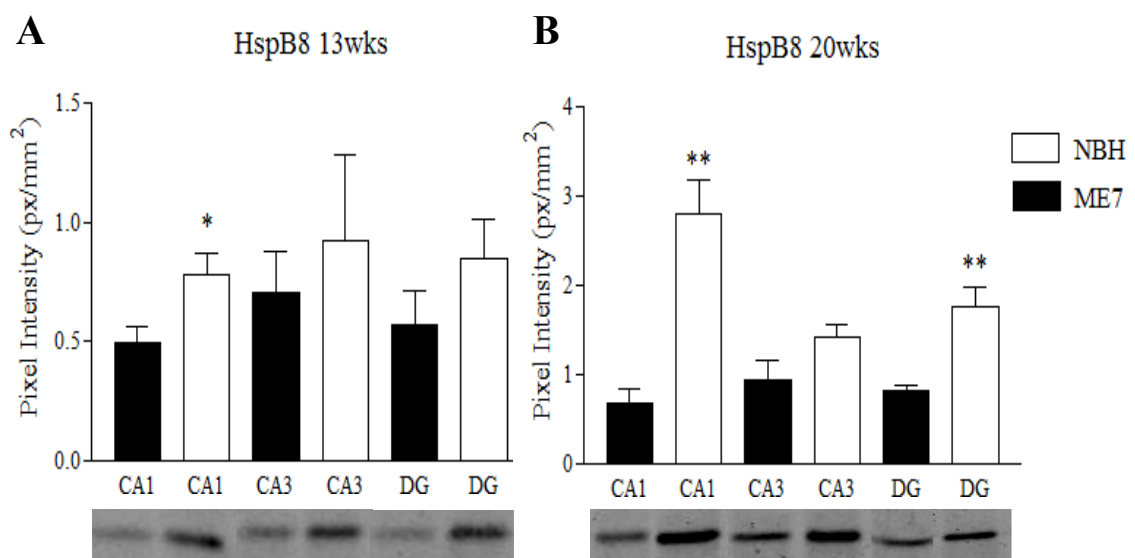
Figure 6.5. HspB8 protein expression in the hippocampus of NBH and ME7 animals at 13 and 20 wks (pi). 40µg of protein from CA1, CA3 and DG homogenates were resolved by SDS-PAGE and protein expression of HspB8 was measured by incubating membranes with an antibody against HspB8 followed by a fluorescently labelled secondary antibody which was detected by infrared fluorescence. Intensity values (pixels/mm^2) were measured using Odyssey Infrared Scanner software. Values were normalized to protein loading and expressed as pixels intensity per mm^2. Expression of HspB8 is shown in distinct hippocampal regions at A, 13 and B, 20 weeks. (A) HspB8 protein expression was up-regulated in the CA1 region of the hippocampus in ME7 animals compared to NBH at 13 weeks. (B) Additionally, HspB8 was also significantly up-regulated in the CA1 and the DG at 20 weeks. Representative blots are shown below the corresponding graph (n = 4). Student's *t*-test was used to determine significance (*p, <0.05; **p, <0.01), error bars represent SEM.

In summary, three out of four sHsps that are otherwise constitutively expressed in the brain were up-regulated in the hippocampus of ME7 animals at late stage of disease. HspB1 and HspB8 protein levels were up-regulated in the CA1 and DG and HspB5 showed a clear trend towards up-regulation in the CA1. HspB8 was also up-regulated in the CA1 at 13 weeks. These changes correlate with early synapse loss and neuronal death in the CA1 region. No change in protein expression was observed for HspB6.

6.3.2. mRNA expression of the sHsps (QT-PCR)

mRNA was extracted for QT-PCR analysis from the CA1, CA3 and DG of ME7 and NBH animals at 8, 13 and 20 weeks of age pi (section 2.5). sHsp gene expression data was normalized to the housekeeping gene, GAPDH (section 2.5.3). Additionally, mRNA expression of the other 6 members of the sHsp family that are not constitutively expressed in the CNS (Quraishe et al., 2008) showed no change in mRNA expression in ME7 animals compared to controls (data not shown).

There were no statistically significant changes in the mRNA expression of HspB1 and HspB5 at 8, 13 and 20 weeks in ME7 compared to NBH animals in the hippocampus (Figure 6.6 A & B). Interestingly, although there were no changes in the protein levels of HspB6 in ME7 animals, this sHsps showed a strong up-regulation of mRNA in the DG at 8 weeks. There were no changes at 13 weeks, however all regions of the hippocampus showed up-regulation of HspB6 mRNA at 20 weeks pi (Figure 6.6 C). HspB8 mRNA expression remained unchanged at 8 and 13 weeks, however, although not statistically significant, an upward trend in ME7 animals was apparent at 20 weeks (Figure 6.6 D). This disparity between protein and transcript expression highlights post-transcriptional regulation of the sHsps.
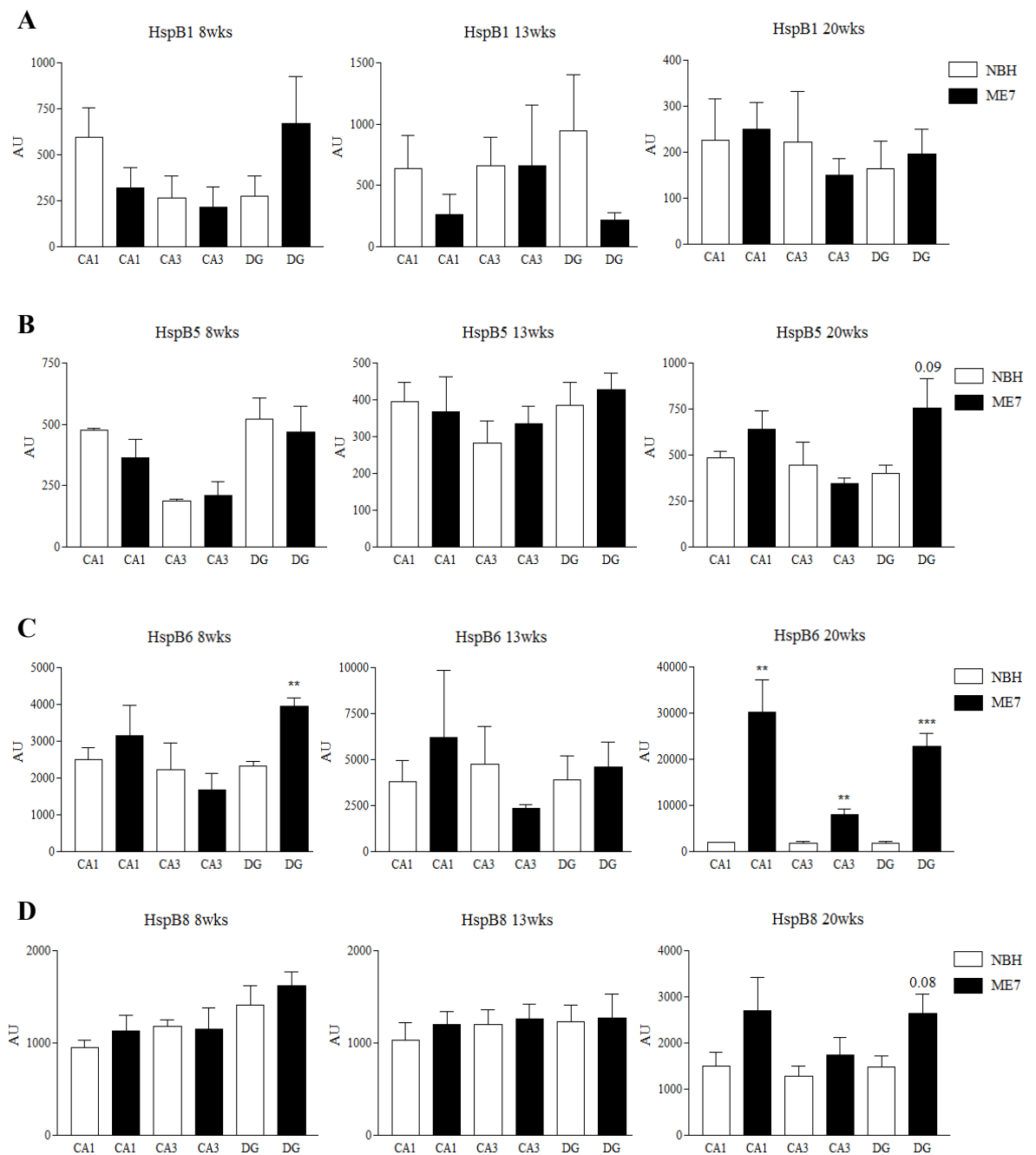
Figure 6.6. mRNA expression of the sHsps in microdissected hippocampal regions over a time course (QT-PCR). Transcript analysis by QT-PCR of the sHsp relative to GADH control in RNA extracted form distinct hippocampal regions (CA1, CA3 and DG). (A) There were no significant changes in the mRNA expression of HspB1 in ME7 animals compared to NBH animals at any of the time points analysed. (B) There were no significant changes in HspB5 mRNA expression in ME7 animals compared to NBH animals at any of the time points analysed. (C) HspB6 mRNA expression was up-regulated in the DG of ME7 animals at 8 weeks. There were no changes in any of the hippocampal regions at 13 weeks, however all three regions showed up-regulation of HspB6 mRNA at 20 weeks. (D) There were no significant changes in ME7 animals compared to NBH animals at any of the time points analysed. (8wks n = 3, 13/20wks n = 5/6). N numbers represent independent injection experiments. Student's *t*-test was used to determine significance, error bars represent SEM.

6.3.3. Specificity of HspB8 immunoreactivity determined by immunocytochemistry in cell culture

HspB8 protein analysis by western blotting was conducted using a non-commercial antibody (kindly provided by Dr. Wilbert Boelens). This antibody was reported to be unsuitable for immunohistochemical analysis. Therefore an alternative non-commercial HspB8 antibody (kindly provided by Dr. Mohan Roa) that was reported by the provider to be suitable for immunohistochemical analysis, but not western blotting was tested. Indeed, we did not observe immunoreactivity by western blotting (data not shown).

To determine specificity of this antibody, HeLa cells were transfected with constructs expressing human HspB1 (Hsp25), HspB6 (Hsp20) and HspB8 (Hsp22) (section 2.13). Cells overexpressing these sHsps were fixed on coverslips and processed for immunocytochemistry (section 2.13.). HspB8 immunoreactivity was absent in cells transfected with HspB1, HspB6 and untransfected cells. HspB8 immunoreactivity was selectively detectable in cells transfected with HspB8 using the non-commercial HspB8 antibody (obtained from Dr. Mohan Roa) (Figure 6.7). Of note was the appearance of bright immunoreactive dots reminiscent of aggregates in the perinuclear regions in some cells, only found in HspB8 transfected cells (see Figure 6.7 A and B). This antibody was subsequently used to analyse HspB8 expression immunohistochemically in mouse tissue.

.
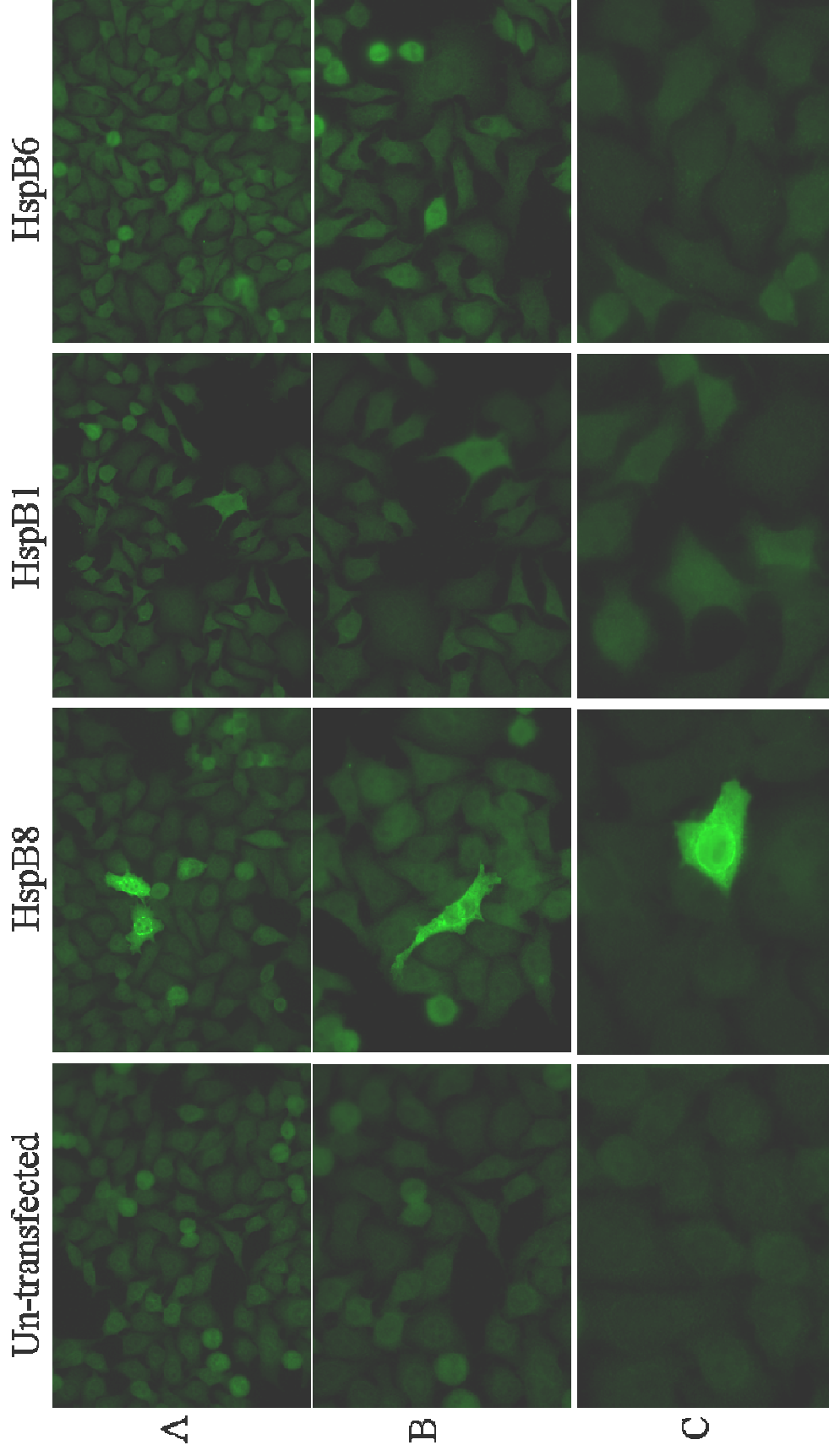
Figure 6.7. Immunocytochemical analysis of HspB8 in HeLa cells. HeLa cells were transfected with cDNA constructs encoding HspB8, HspB1 and HspB6. Cells were fixed 24 hours post-transfection and processed for immunocytochemistry. All coverslips were treated with a non-commercial anti-HspB8 antibody (Gifted by Dr. Mohan Roa). Specific HspB8 immunoreactivity was observed in cells transfected with the HspB8 construct that was clearly above background of cells transfected with HspB1 or HspB6. Cells transfected with HspB1, HspB6 and untransfected cells appeared not immunopositive for HspB8. Exposure times and settings in each picture were identical. Magnifications: A, x40; B, x63; C, x100.

6.3.4. Immunohistochemical analysis of sHsp expression in ME7 and NBH tissue

Hippocampal samples from ME7 infected animals showed a selective up-regulation of HspB1 and HspB8, and a trend towards up-regulation of HspB5 protein levels at late stage of disease. To substantiate this finding, tissue sections from ME7 and NBH animals were prepared and processed for immunohistochemical analysis as detailed in section 2.11. Coronal tissue sections between -1.22mm and -2.30mm relative to Bregma were used to analyse expression of HspB1, HspB5 and HspB8 in the hippocampus. Age matched tissue sections from ME7 and NBH animals were processed in parallel and developed in DAB solution.

HspB1, HspB5 and HspB8 all showed staining and up-regulation in the hippocampus in late stage ME7 tissue compared to NBH tissue (Figure 6.8 to 6.10). The cellular staining of these 3 sHsps displayed astrocytic morphology

6.3.4.1. Immunohistochemical analysis of HspB1 expression in ME7 and NBH tissue

HspB1 immunoreactivity in NBH animals (20wks) was readily detected in the hippocampus, and showed staining of the vasculature (Figure 6.8 A/C). This was marked by discrete staining of microvascular structures. As shown previously, *in situ* hybridization used to investigate HspB1 expression showed mRNA localization to the dorsal and lateral ventricles (Figure 3.4 a). These ventricles are lined by ependymal cells and the protein stain of HspB1 is suggestive of expression in this cell type. It is also possible that the staining reflects expression in astrocytic end feet that form connections with endothelial cells (Figure 6.8 A and C). Beyond this there was little or no other staining in the hippocampus and none attributable to neurons and glia.

In contrast, HspB1 immunoreactivity was greatly increased in the hippocampus of ME7 animals at 20 weeks (Figure 6.8 A and C). This increase was present in the CA1, CA3 and DG. The morphology of the stained cells was indicative of expression in astrocytes. HspB1 immunoreactivity was not uniformly distributed throughout the hippocampus, but HspB1 immunopositive cells formed a layer above (stratum oriens) and below (stratum radiatum) the CA1 pyramidal cell layer. A similar layer of HspB1 positive cells were present in the molecular layer of the dentate gyrus and also in the polymorphic layer of the dentate gyrus. The cellular staining was not discrete but showed diffuse localisation

around the cell body and main processes indicative of expression throughout the astrocytic cell into fine processes (Figure 6.8 C inset).
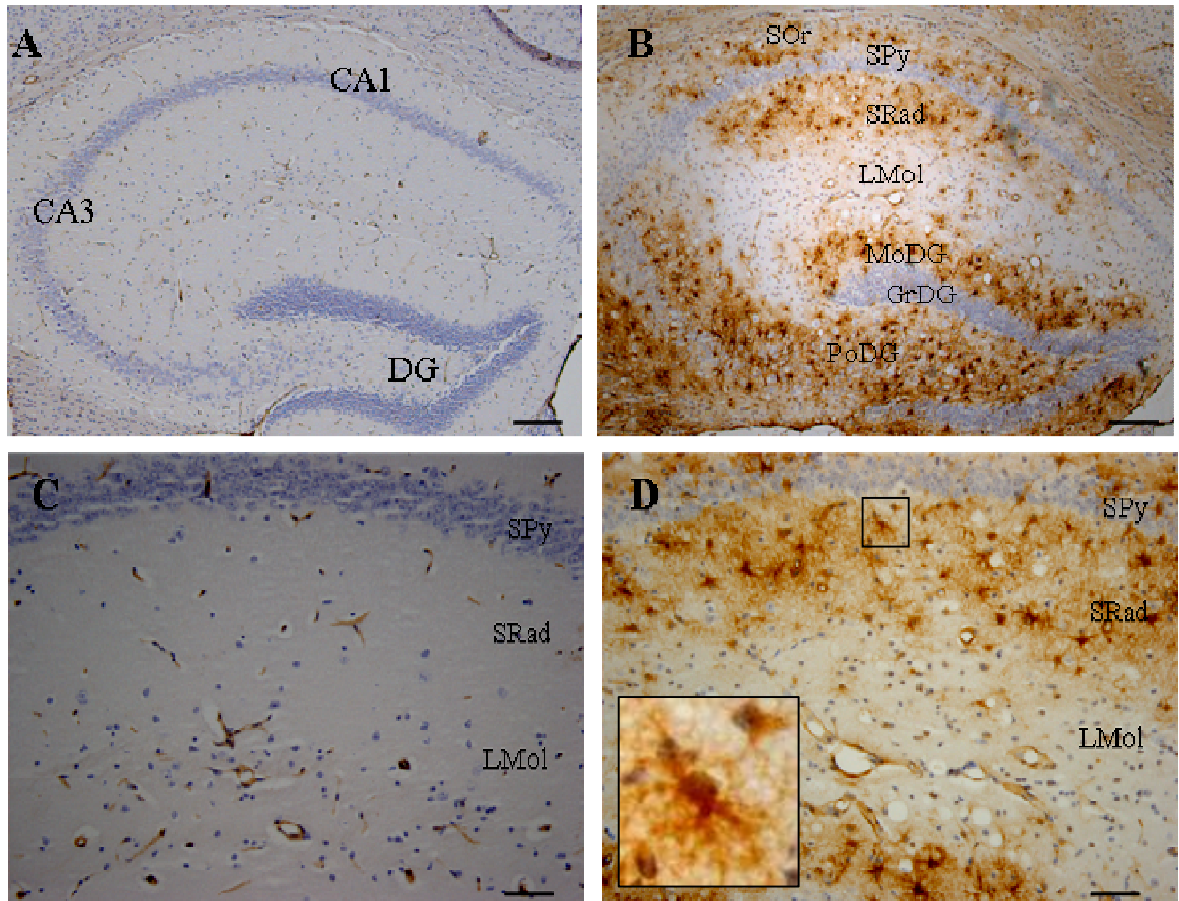
Figure 6.8. Immunohistochemical analysis of HspB1 in the hippocampus of 20 week NBH and ME7 animals. Coronal sections from NBH and ME7 animals at 20 weeks pi were processed for immunohistochemistry with an anti-HspB1 antibody. (A) HspB1 immunoreactivity was associated with the vasculature of NBH animals. (B) Increased immunoreactivity was observed in the hippocampus of ME7 animals. (C) Higher magnification images of the CA1 region of NBH animals showed HspB1 immunoreactivity associated with blood vessels. (D) HspB1 immunoreactivity was present in the SRad, with minimal staining of the LMol layer. Inset illustrates the diffuse nature of HspB1 staining in ME7 animals. The staining pattern was suggestive of expression in astrocytic cells. Images are representative of staining from 4 different animals. Hippocampal regions: stratum oriens (SOr), stratum pyramidal (Spy), stratum radiatum (SRad), lacunosum molecular (LMol), Molecular layer of Dentate Gyrus (MoDG), granular layer of Dentate Gyrus (GrDG), Polymorphic layer of Dentate Gyrus (PoDG). Scale bar: A/B, 100µm; C/D, 50µm.

6.3.4.2. Immunohistochemical analysis of HspB5 expression in ME7 and NBH tissue

HspB5 immunoreactivity in NBH animals was selective and limited to white matter structures such as the corpus callosum, as described in Chapter 5. Staining of the characteristic oligodendrocytes present in the lacunosum molecular layer were also observed (Figure 6.9 A and C). HspB5 immunostaining increased consistent with an increased expression in the hippocampus of ME7 animals (Figure 6.9 B and D). The cellular staining pattern was not as distinctive as the staining observed for HspB1, but similarly the morphology of the cells was suggestive of expression in astrocytes. Additionally, oligodendroglial staining in the lacunosum molecular did not appear any different in ME7 animals compared to NBH suggesting there were no overt white matter changes.
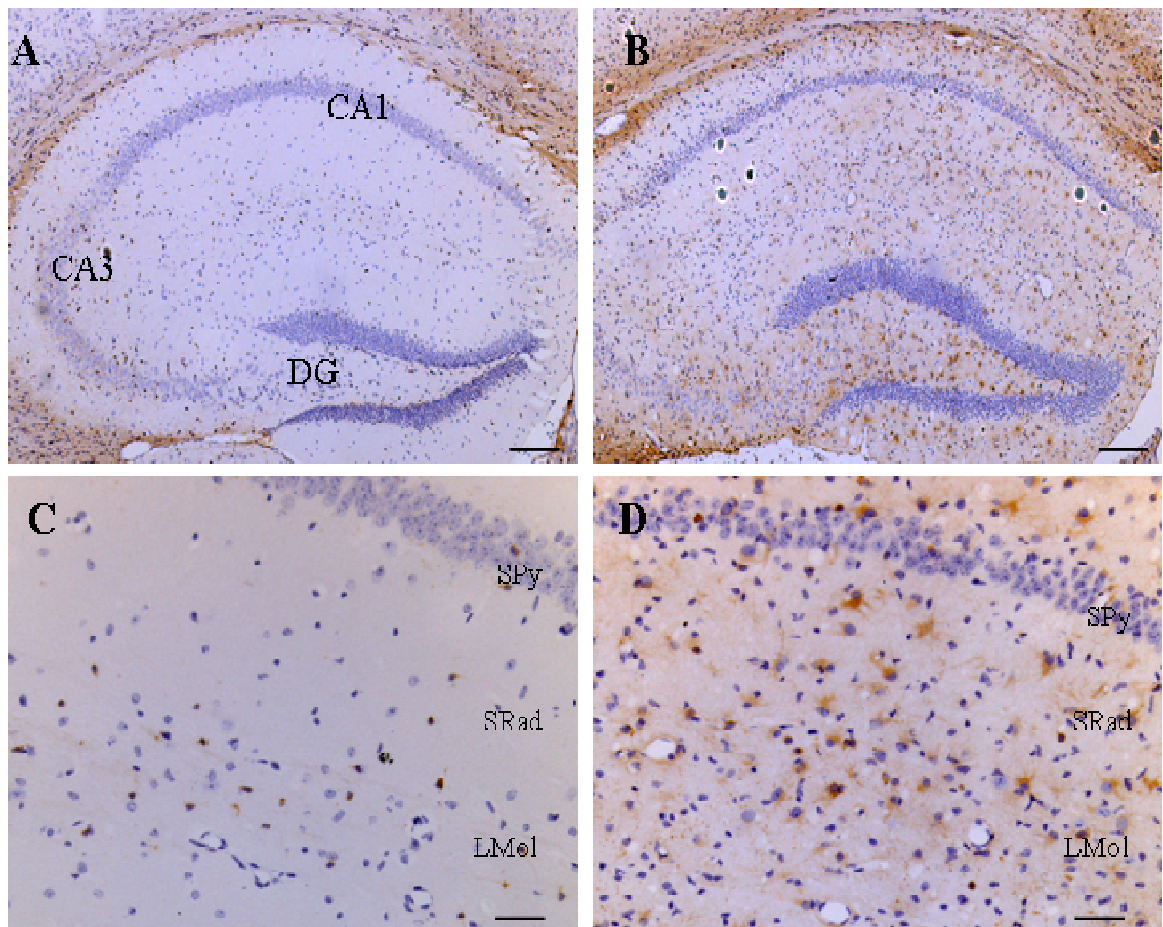
Figure 6.9. Immunohistochemical analysis of HspB5 in the hippocampus of 20 week NBH and ME7 animals. Coronal sections from NBH- and ME7-animals at 20 weeks pi were subjected to immunohistochemistry for detection of HspB5. (A) HspB5 immunoreactivity in NBH animals was associated with the corpus callosum. Staining was also observed in oligodendrocyte cell bodies decorating the hippocampus (See also Chapter 4). (B) Increased immunoreactivity in addition to oligodendrocytic staining which remained unchanged was present in the hippocampus of ME7-animals.
(C) Higher magnification images of the CA1 region of NBH animals showed HspB5 immunoreactivity in oligodendrocytes situated in the LMol. (D) HspB5 up-regulation in ME7 animals was suggestive of expression in astrocytic cells. Images are representative of staining from 4 different animals. Hippocampal regions: stratum pyramidal (Spy), stratum radiatum (SRad) and lacunosum molecular (LMol). Scale bar: A/B, 100μm; C/D, 50μm.

6.3.4.3. Immunohistochemical analysis of HspB8 expression in ME7 and NBH tissue

There was no specific HspB8 immunoreactivity in the hippocampus of NBH animals, a background staining of hue was apparent associated with the secondary antibody (Figure 6.10.A and C). However, HspB8 expression was up-regulated in the hippocampus in ME7 animals (Figure 6.10 B and D). The staining pattern was similar but more intense to that seen for HspB5 with immunoreactivity throughout the hippocampus. The cellular morphology of immunopositive cells also suggested expression of HspB8 in astrocytes.
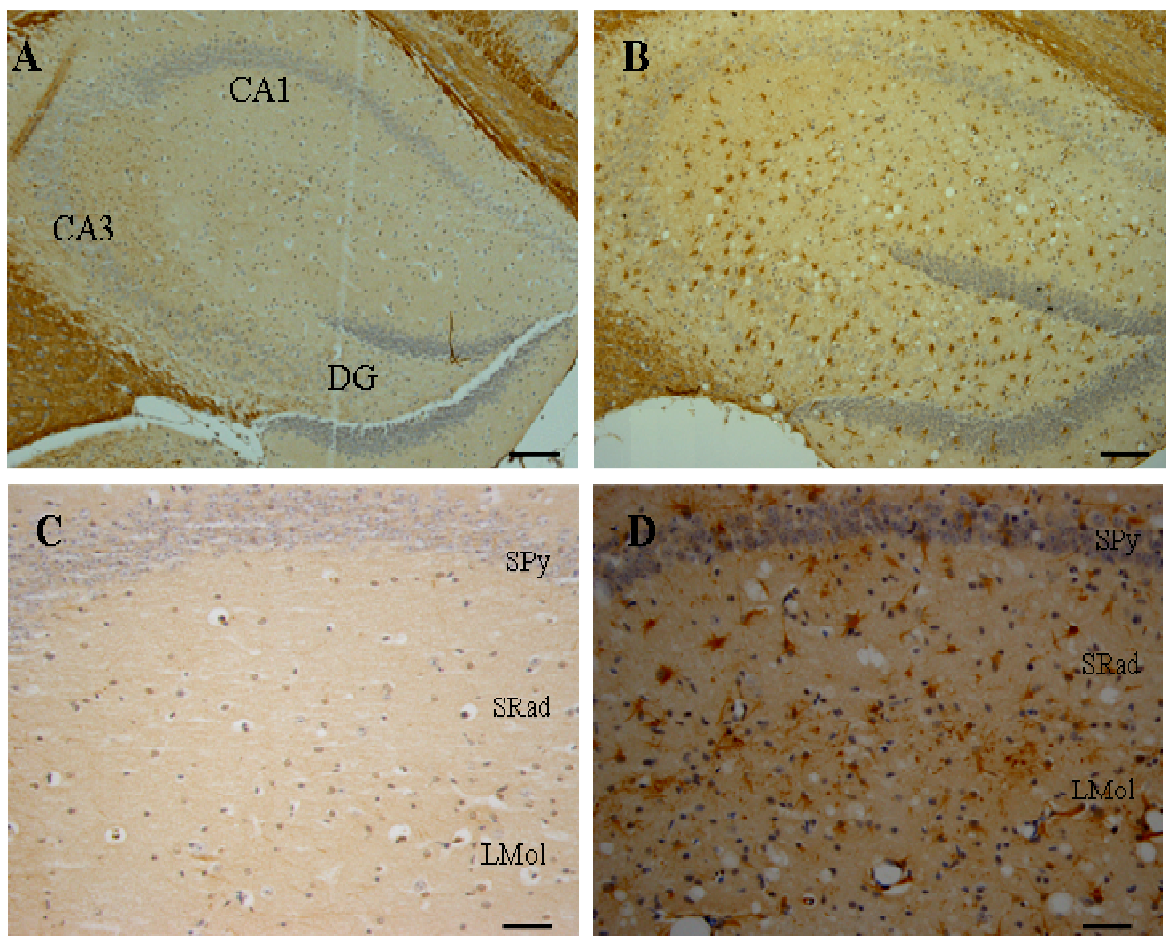
Figure 6.10. Immunohistochemical analysis of HspB8 in the hippocampus of 20 week NBH and ME7 animals. Coronal sections from NBH and ME7 animals at 20 weeks pi were subjected to immunohistochemistry for detection of HspB8. (A) and (C) Specific immunoreactivity was absent in the hippocampus of NBH animals. (B) HspB8 immunoreactivity was up-regulated in the hippocampus of ME7 animals. (D) Higher magnification images of the CA1 region showed up-regulation of HspB8 in cells with astrocytic morphology. Images are representative of staining from 4 different animals. Hippocampal regions: stratum pyramidal (Spy), stratum radiatum (SRad) and lacunosum molecular (LMol). Scale bar: A/B, 100µm; C/D, 50µm.

HspB6 expression was not analysed by immunohistochemistry as this sHsps did not show any change in protein expression by western blotting.

6.3.5. sHsp co-localization with GFAP (immunofluorescence)

To determine if the sHsp immunopositive cells were astrocytes, double immunofluorescence labelling of coronal brain sections was used to analyse the expression of the sHsps and GFAP, a robust astrocytic marker.

6.3.5.1. HspB1 expression in astrocytes

HspB1 expression was investigated at 13 weeks. Protein expression at this time point was no different in ME7 animals compared to NBH animals by western blotting, however 2 ME7 animals out of 4 displayed a modest increase in a restricted number of GFAP positive cells in ME7 animals at 13 weeks. These HspB1 positive cells were present in the molecular layer of the dentate gyrus with a few cells decorating the stratum radiatum (Figure 6.11 A ii). GFAP expression was compact within distinct thick astrocytic processes emanating from the cell body. HspB1 also showed expression and co-localisation with GFAP in these processes (Figure 6.11 B ii), but in addition a fine and diffuse decoration extending from these processes was also observed (Figure 6.12). This staining suggests expression of HspB1 throughout the astrocytic cell, extending into the extremities of astrocytic processes consistent with either expression of a soluble protein or one associated with cytoskeletal elements that define the cortical structure of the astrocyte.

HspB1 expression was also analysed at 20 weeks. Immunoreactivity in NBH animals showed staining of the vasculature that was not associated with GFAP. A background staining of hue was also observed which was associated with non specific secondary antibody immunoreactivity (Figure 6.13 Ai/ Bi). HspB1 immunoreactivity co-localised with GFAP in 20 week ME7 animals, consistent with the notion that the up-regulated staining was associated with astrocytes (Figure 6.13 Ai/ Bi). Expression was not homogeneous and displayed variability between astrocytic cells as well as being absent from astrocytes in the lacunosum molecular layer of the hippocampus. This was not reflected by GFAP staining which was consistent throughout the hippocampus. All HspB1 positive cells were GFAP positive, however all GFAP positive cells were not HspB1 positive.
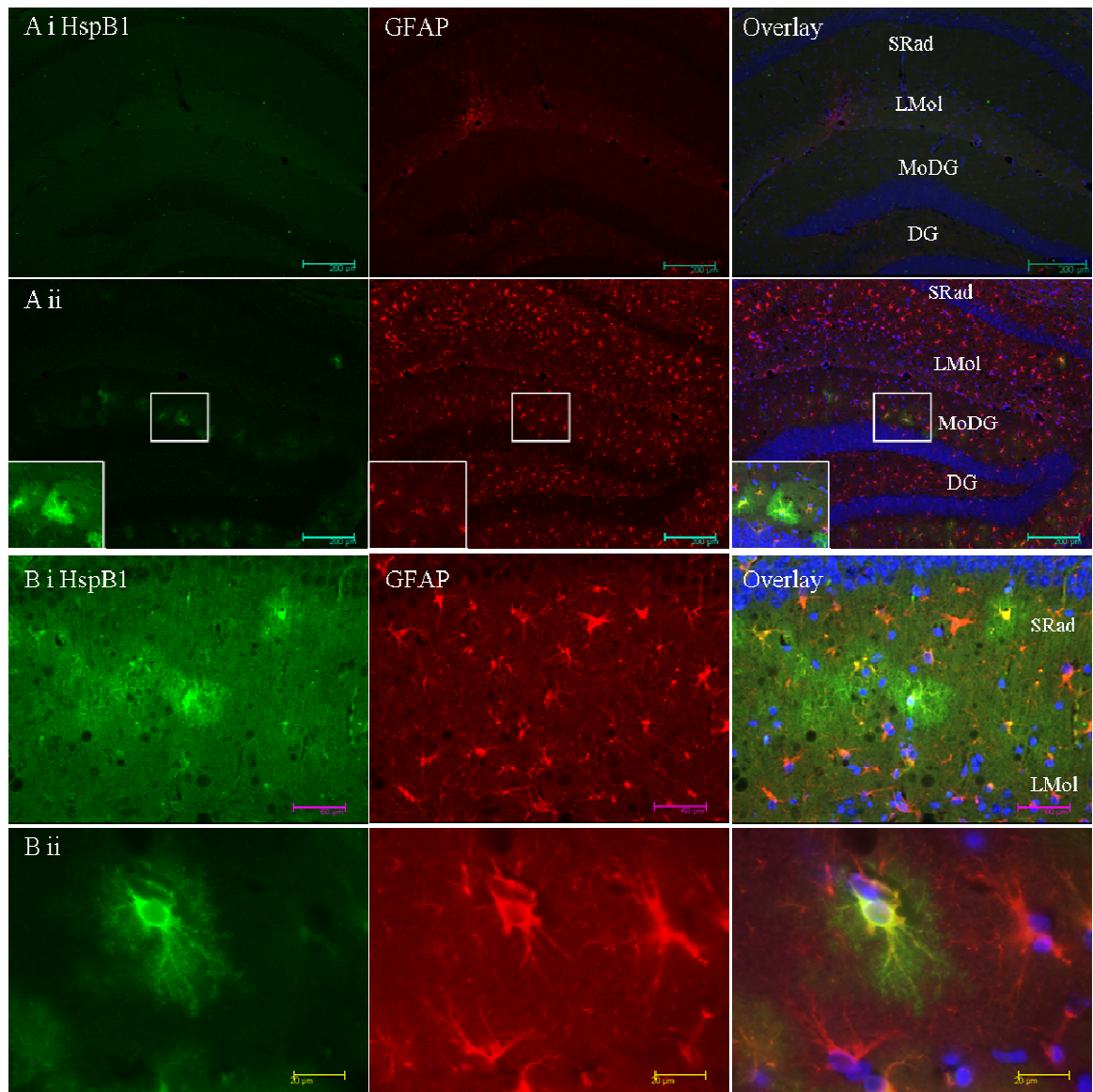
Figure 6.11. Double immunofluorescence staining of HspB1 and GFAP in 13 week NBH and ME7 animals. (Ai) HspB1 expression in the hippocampus of NBH animals. (Aii) HspB1 immunoreactivity was increased in a small number of GFAP positive cells in ME7 animals. These HspB1 positive cells decorated the MoDG, with some staining observed in the SRad. (Bi) HspB1 expression in the CA1 of ME7 animals was selective to a few GFAP positive cells. (Bii) Higher magnification images illustrate the diffuse and extended nature of the HspB1 staining in these astrocytes (B). Images are representative of staining from 2 out of 4 animals. Hippocampal regions: stratum pyramidal (Spy), stratum radiatum (SRad) and lacunosum molecular (LMol). Scale bar: A, 200µm; Bi, 50µm; Bii, 20µm.
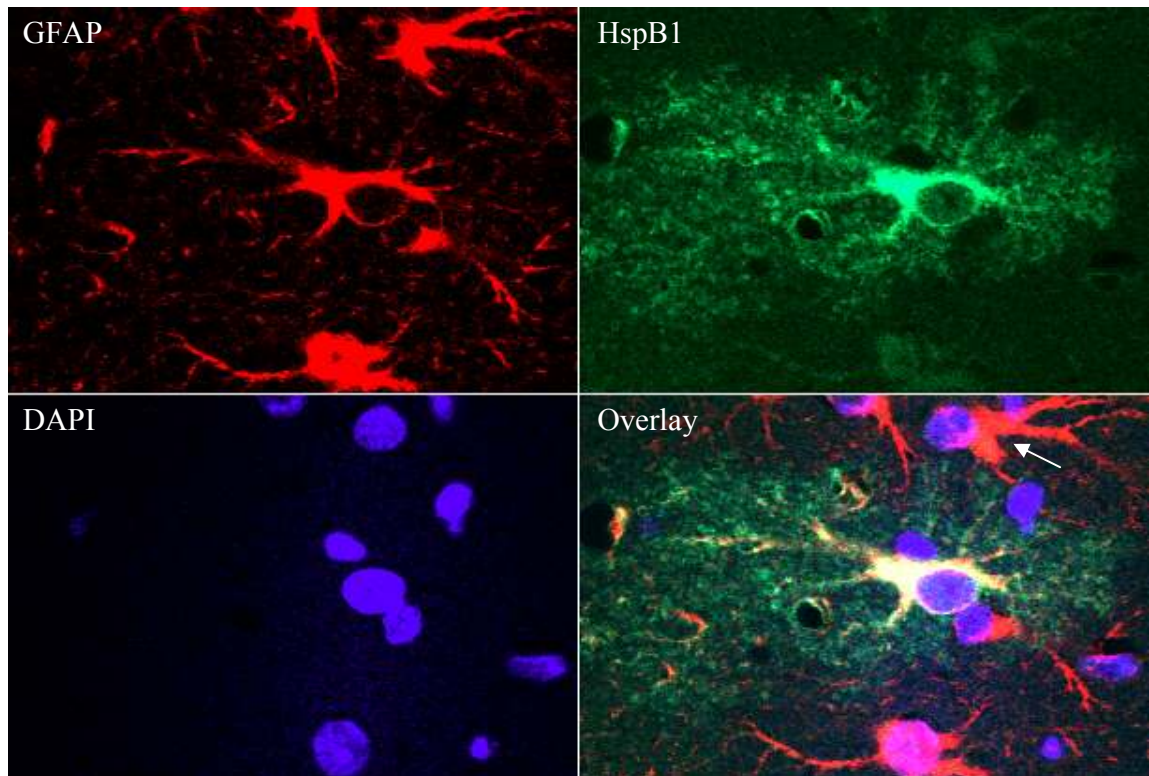
Figure 6.12. Localization of HspB1 and GFAP immunoreactivity in the CA1 of ME7 animals at 13 week. HspB1 co-localisation with GFAP was investigated by confocal microscopy analysis of immunostaining. HspB1 (green) immunopositive cell in the CA1 region of the hippocampus showed complete co-localisation (yellow) with GFAP staining (red). Additionally, HspB1 staining was shown to surround the main processes and cell body of the astrocyte displaying the distinctive bushy appearance of protoplasmic astrocytes. GFAP positive cells were also observed that showed no HspB1 immunoreactivity (arrow). Cell bodies were stained with DAPI (blue).
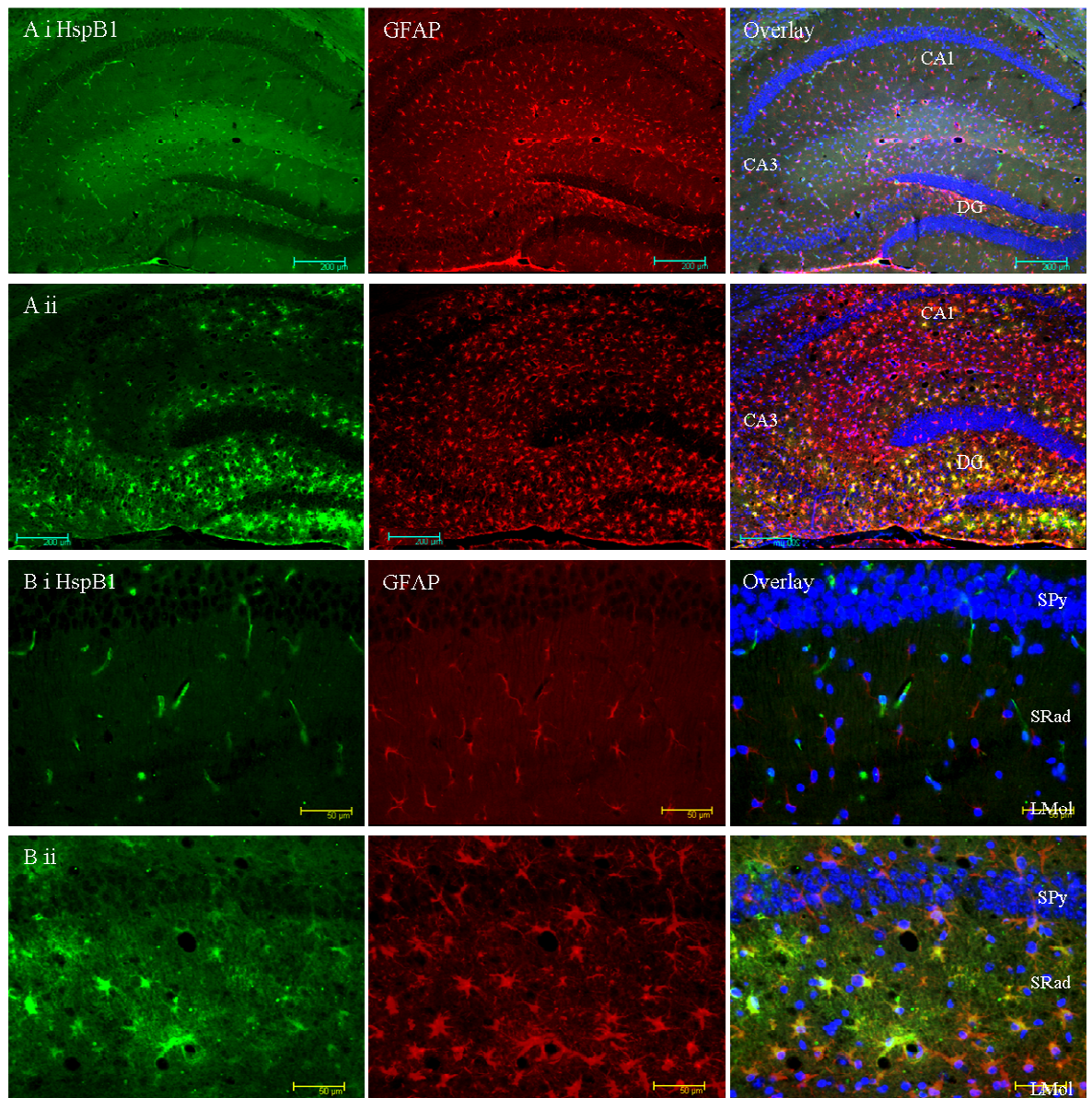
Figure 6.13. Double immunofluorescence staining of HspB1 and GFAP in the hippocampus of 20 week NBH and ME7 animals. (Ai/Bi) HspB1 expression in NBH animals was restricted to blood vessels and was distinct from GFAP staining. (Aii/Bii) Up-regulation in ME7 animals showed co-localisation with GFAP-positive cells. HspB1 staining is restricted away from the lacunosum moleculare. Representative staining in hippocampal sections (A) and CA1 (B) are shown for control (NBH) and ME7 animals. Images are representative of staining from 4 different animals. Hippocampal regions: stratum pyramidal (Spy), stratum radiatum (SRad) and lacunosum molecular (LMol). Scale bar: A, 200µm; B, 50µm.

6.3.5.2. HspB5 expression in astrocytes

  HspB5 expression was investigated immunohistochemically at 13 weeks. No changes in expression were observed (data not shown). HspB5 immunoreactivity in NBH animals was associated with oligodendrocytic cell bodies decorating the CA1, lacunosum moleculare, CA3 and dentate gyrus of the hippocampus. Oligodendrocytic expression is consistent with the expression observed in the R6/2 HD mouse model. Chapter 4 and 5 described HspB5 expression in oligodendrocytes in the hippocampus, thus this is an important stain to be considered. There was no co-localisation with GFAP staining in NBH animals and HspB5 expression was exclusively associated with the white matter (Figure 6.14 Ai/Bi). At 20 weeks HspB5 was up-regulated in the hippocampus of ME7 animals (Figure 6.14 A ii), however this was not associated with the cells that expressed HspB5 constitutively (oligodendrocytes), but a new set of cells namely astrocytes as shown by co-localisation with GFAP staining (Figure 6.14 B ii). Tomato lectin, a marker of microglial cells was used to investigate expression of HspB5 in microglia. HspB5 did not show co-localisation with tomato lectin staining in NBH or ME7 animals indicating that the increased immunostaining in ME7 was specific to astrocytes (Figure 6.15).
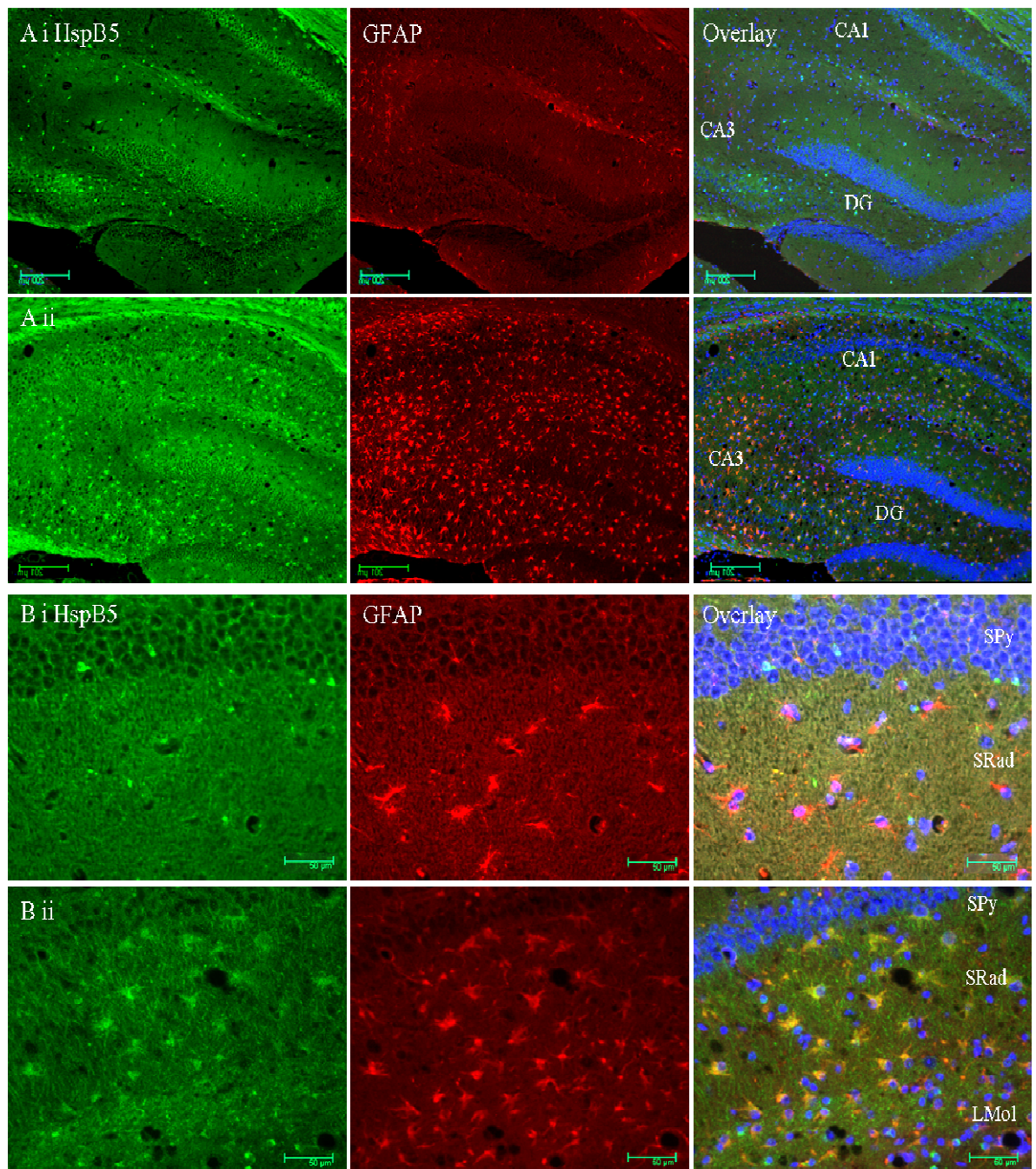
Figure 6.14. Double immunofluorescence staining of HspB5 and GFAP in the hippocampus of 20 week NBH and ME7 animals. (Ai/Bi) HspB5 expression in NBH animals was present in distinctive and intensely stained cell bodies distributed throughout the hippocampus, characteristic of oligodendrocytes. This staining did not co-localise with GFAP staining. (Aii) HspB5 immunostaining was increased in ME7 animals. (Bii) A strong oligodendrocytic background staining was present; however the signal was dominated by astrocytic staining in ME7 animals. The increased HspB5 staining seen in ME7 animals co-localised with GFAP-positive cells. Representative staining in hippocampal sections (A) and CA1 (B) are shown for control (NBH) and ME7-animals. Images are representative of staining from 4 animals. Hippocampal regions: stratum pyramidal (Spy), stratum radiatum (SRad) and lacunosum molecular (LMol). Scale bar: A, 200μm; B, 50μm.

233
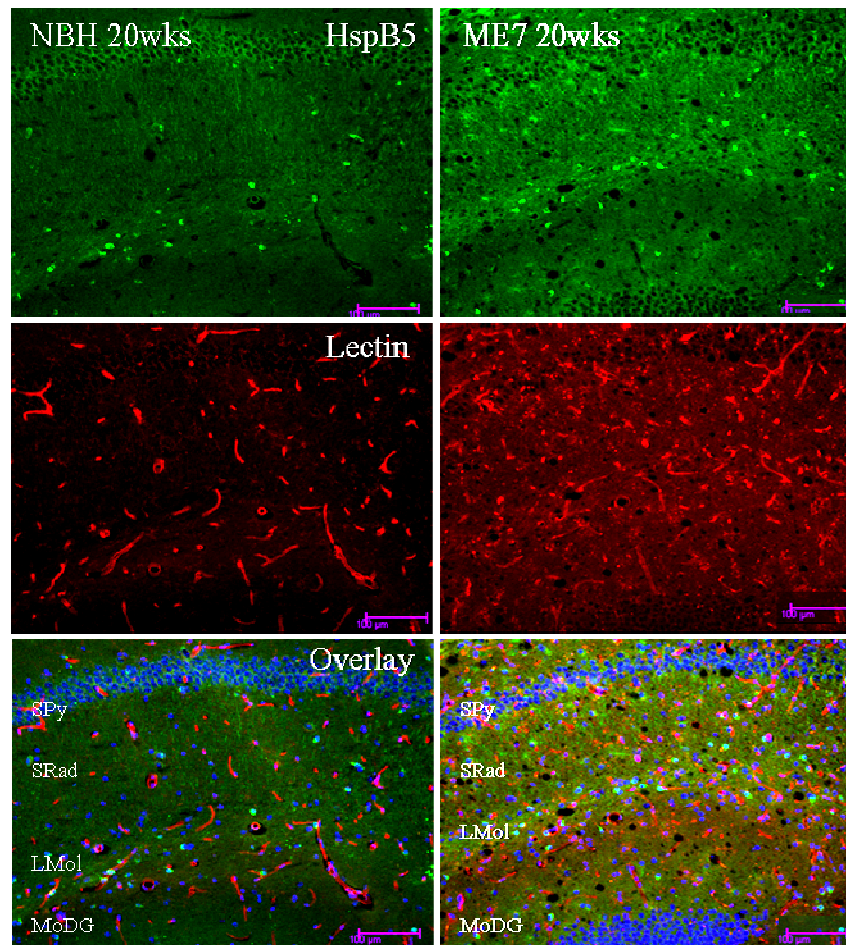
Figure 6.15. HspB5 up-regulation is not associated with microglial cells. HspB5 immunostaining in NBH shows tight staining of oligodendrocytes (see chapter 4). This staining that persists in the NBH hippocampus was distinct from increased staining in ME7 animals. Neither showed co-localisation with cells positive for tomato lectin. Images are representative of staining from 4 animals showing. Hippocampal regions: stratum pyramidal (Spy), stratum radiatum (SRad) and lacunosum molecular (LMol). Scale bar: CA1, 100µm; CA3, 50µm.

6.4.3.3. HspB8 expression in astrocytes

HspB8 expression was up-regulated in ME7 animals compared to NBH at 20 weeks and showed co-localisation with GFAP staining (Figure 6.16). Expression was increased in all regions of the hippocampus. The 13 week analysis remains to be done.
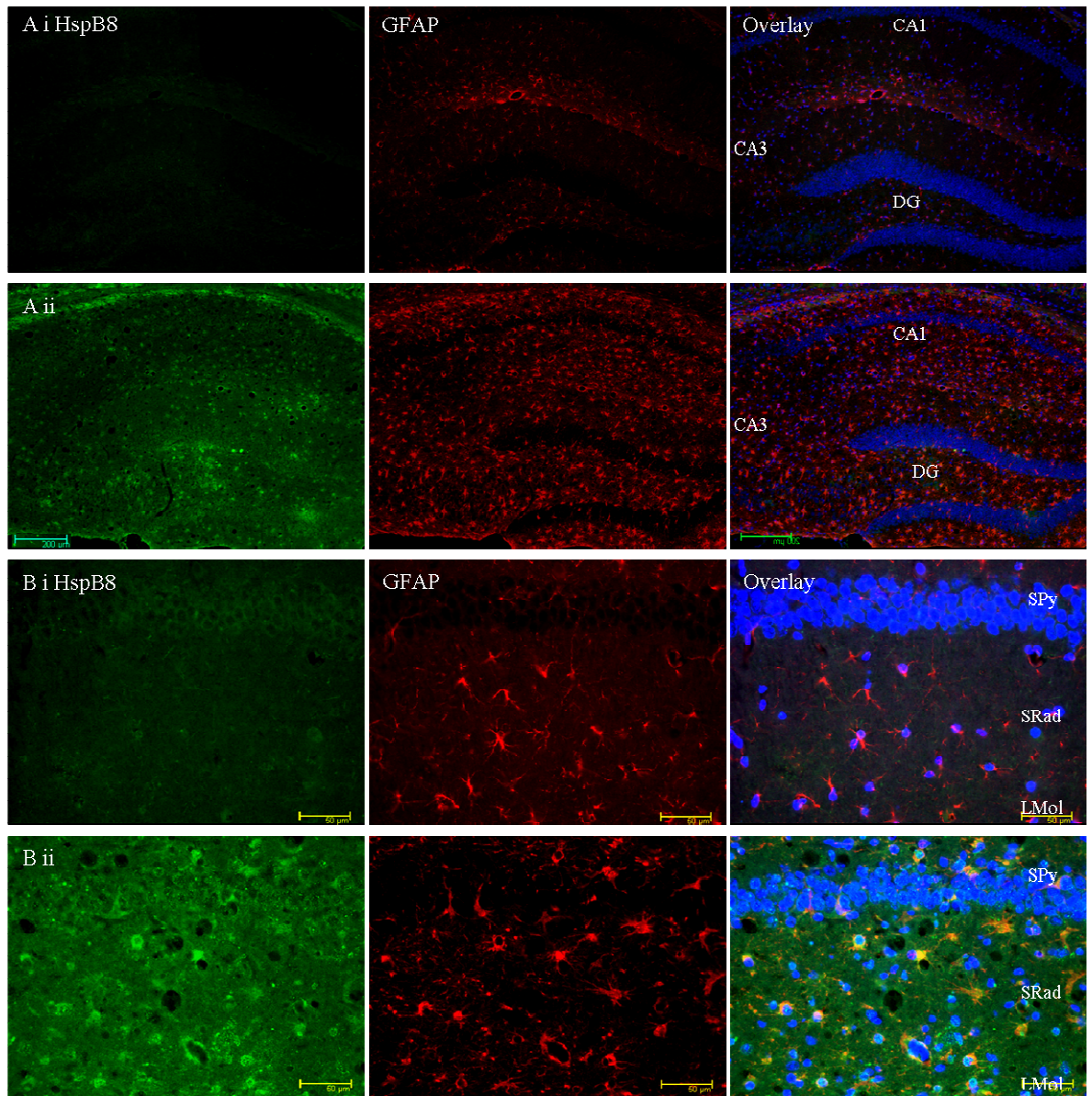
Figure 6.16. Double immunofluorescence staining of HspB8 and GFAP in the hippocampus of 20 week NBH and ME7 animals. (Ai/Bi) HspB8 expression in NBH animals was not associated with GFAP expression. (Aii) HspB8 showed up-regulation in ME7 animals. (Bii) The increased expression of immunoreactivity in ME7 animals displayed co-localisation with GFAP-positive cells. Representative staining in hippocampal sections (A) and CA1 (B) are shown for control (NBH) and ME7-animals. Images are representative of staining from 4 animals. Hippocampal regions: stratum pyramidal (Spy), stratum radiatum (SRad) and lacunosum molecular (LMol). Scale bar: A, 200µm; B, 50µm.

6.4.   Discussion

The ME7 mouse model of prion disease, characterized by extracellular PrP^{sc} protein aggregates was used to analyse expression of the sHsps. HspB1, HspB5 and HspB8 protein expression was up-regulated in the hippocampus of ME7 animals at late stage of disease, however there were no changes in HspB6 protein expression. The changes in protein expression were not regulated at the transcriptional level as the 3 sHsps that were up-regulated at the protein level showed no changes in mRNA expression. However HspB6 mRNA was significantly up-regulated in the hippocampus in ME7 animals at late stage. The disparity between protein and transcript suggests the up-regulation of the sHsps is a consequence of translational regulation or indeed reduced protein degradation to increase steady state protein levels.

It is unclear why HspB6 up-regulation of mRNA is observed in the absence of protein changes. However, stress induced HspB6 protein expression has been shown to be induced in a number of studies. HspB6 expression in AD tissue showed no change by western blotting, but elevated reactivity was found in astrocytes surrounding SPs, perhaps suggesting involvement or modulation of the disease process (Wilhelmus et al., 2006c). HspB6 was found to be up-regulated in the hippocampus of newborn piglets in response to hypoxia (David et al., 2006). It was also shown to be transiently up-regulated in two phases in a model of experimental ischemia-reperfusion injury. This was attributed to an initial glial response to ischemic insult, followed by CA1 neuronal apoptosis (Niwa et al., 2009). HspB6 protein staining was associated with the apical dendrites of CA1 pyramidal cells after ischemic insult. Phosphorylated HspB6 has been reported to be protective against apoptosis by direct interactions with Bax, a pro-apoptotic protein. It has been proposed that this interaction prevents Bax translocation from the cytosol to the mitochondria, preventing Cytochrome C release. However, in this study, phosphorylation of HspB6 was observed after CA1 pyramidal cell death as determined by TUNEL staining (Niwa et al., 2009). Although we have not investigated HspB6 expression immunohistochemically, in light of the above, it would be important to do so to understand HspB6 expression at a cellular level and potential changes in its distribution.

6.4.1. sHsp expression and astrogliosis

Immunohistochemical investigation supported the increased expression of 3 sHsps observed by western blotting. However, it has also highlighted a disparity between the two methods. The three sHsps showed no change in expression in the CA3 region by western blotting, but an up-regulation in the CA3 was shown immunohistochemically. This suggests the microdissection of the hippocampus may not accurately isolate the CA3 region and raises the possibility that contamination from other brain regions, such as the fimbria, which are closely associated with the hippocampal structure, mask the changes seen immunohistochemically. Indeed such a contamination, and the basal expression of HspB5 in the white matter may mask the subtle up-regulation of HspB5 as seen immunohistochemically (Figure 6.9) and would explain the trend towards up-regulation in ME7 animals, but the lack of significance.

Increased immunoreactivity of these sHsps was associated with expression in astrocytes as determined by co-localisation with GFAP. Immunohistochemical analysis of HspB1 revealed additional complexity to the up-regulation observed by western blotting. At 13 weeks HspB1 did not show any significant changes in protein expression. However immunohistochemical analysis revealed a very distinctive staining of a subset of astrocytes at this time point. HspB1 co-localised with GFAP, which was consistent with an association with the cytoskeleton, but this co-expression involved staining beyond the extremities of the GFAP immunoreactivity. This extended staining in the fine processes of a subset of astrocytes was reminiscent of staining of protoplasmic astrocytes, or experimentally dye filled astrocytes (Figure 6.11 and 6.12). Protoplasmic astrocytes have between 1000-10000 processes that make connections with synapses and blood vessels. Dye filled astrocytes were also shown to have bushy processes that occupied separate territories thus allowing the most efficient surveillance of the microenvironment (Bushong et al., 2004).

In addition to the elaborate morphology of these cells, the staining observed at 13 weeks was restricted to a few astrocytes that selectively expressed HspB1 in the molecular layer of the DG and the stratum radiatum of the CA1. At 20 weeks the staining of the HspB1 positive cells was not as elaborate as seen at 13 weeks, however was again restricted to a subpopulation of astrocytes displaying a similar extended staining pattern beyond GFAP

expression. This was perhaps a consequence of the increase in number of astrocytes at 20 weeks, reducing the territory of each cell. All HspB1 positive cells were GFAP positive, but only a subset of GFAP positive cells showed increased HspB1 immunoreactivity. The lacunosum molecular layer of the hippocampus containing distal dendrites was effectively devoid of HspB1 astrocytic staining, whereas the proximal dendrites of the stratum radiatum, where synapse loss is observed, showed abundant HspB1 staining. The pattern of staining is suggestive of a selective astrocytic response during disease associated with a compartment specific degeneration.

Expression of HspB8 in the CA1 subfield at 13 weeks by western blotting and the selective expression of HspB1 in this region in a few animals, suggest a potential involvement of these sHsps in cellular processes that may directly underlie the synaptic loss that precedes CA1 cell loss at this time point. In contrast, HspB1 positive astrocytes in the molecular layer of the DG may represent an astrocytic response to PrP^{sc} deposition in this region. HspB5 and HspB8 also showed co-localisation with GFAP at late stage of disease. HspB5 and HspB8 expression was very similar to GFAP expression and did not display the elaborate staining observed for HspB1. Additionally, HspB5 and HspB8 immunoreactivity was present throughout the hippocampus and was not associated with a subpopulation of astrocytes. HspB5 did not show any immunohistochemical changes in expression in ME7 animals at 13 weeks and HspB8 expression is yet to be determined.

The sHsp response and up-regulation in ME7 animals displays a distinct and staged response in astrocytes indicative of different phases of reactivity or astrocytosis. The selective up-regulation of HspB1 and HspB8 at an early time point may be a distinct response to the synaptic loss and degeneration that occurs at 13 weeks. It is very interesting that the few animals displaying HspB1 immunoreactivity at 13 weeks show differential expression in the CA1 region, which coincides with the area where synaptic loss occurs (stratum radiatum). The sHsp response at a late stage, when a concerted up-regulation of the sHsps is observed may be a co-coordinated continuation of the early response, or a cumulative astrocytic response as a consequence of astrogliosis.

Astrocytes are a heterogeneous population of cells with at least 9 morphological variants described (Matyash and Kettenmann, 2009). Early neuro-anatomists recognised two morphologically distinct glial cell populations in the white and gray matter, termed

protoplasmic and fibrous astrocytes. However astrocytes were further subdivided into 9 classes based on differential yet complementary labeling methods – mice expressing GFAP-GFP transgenically or astrocytes stained against GFAP and S100β (Matus and Mughal, 1975, Nolte et al., 2001, Emsley and Macklis, 2006). Therefore, in a given brain region, several types of astrocytes coexist together and cannot be simply classified as protoplasmic and fibrous astrocytes (Emsley and Macklis, 2006). Although astrocytes have been distinguished on a morphological basis, no thorough comparison of the physiological behaviour of these cells has been made (Matyash and Kettenmann, 2009). Morphologically undistinguishable astrocytes have also been found to exhibit different physiological behaviour (Houades et al., 2008). Interestingly the hippocampal CA1 layers display differences in morphology and orientation of astrocytes, which lends weight to the astrocytic subpopulation specific expression of HspB1. The astrocytes in the stratum lacunosum moleculare are small, with uniform radially orientated processes, astrocytes in the stratum radiatum are much bigger and polarised (Nixdorf-Bergweiler et al., 1994). The different populations of astrocytes that co-exist in the hippocampus have been shown to differ in their AMPA receptor subunit expression and show distinct coupling capabilities (Matthias et al., 2003, Wallraff et al., 2004).

 The selective neuronal death of CA1 neurons has been presumed to reflect the inherent vulnerability and connectivity of neuronal populations in this region (Ouyang et al., 2007). It has been reported that CA1 astrocytes were more sensitive to ischemia than DG astrocytes. Oxidative stress was suggested to contribute to selective changes in CA1, because CA1 astrocytes show early increases in mitochondrial free radicals and reduced mitochondrial membrane potential. These changes were not seen in the DG astrocytes (Ouyang et al., 2007). It is clear that distinct subpopulations of astrocytes co-exist in the brain and the functional implications of the regional and local heterogeneity is displayed by the sensitivity or contribution of some subpopulations such as those in the CA1 to disease processes (Hewett, 2009). These observations suggest that the selective sHsp response in astrocytes, particularly in relation to HspB1 expression, could represent a distinct population that may be responding to early pathological changes, and the combined sHsp response in late stage of disease is a coordinated regional astrocytic response.

Interestingly, an increase in μ-calpain activation in astrocytes of late stage prion disease has been reported (Gray et al., 2006). It has also been shown that calpain inhibitors of μ- and m-calpain increase HspB5 phosphorylation via p38-MAP and intracellular calcium signalling. Phosphorylation of Ser-59 seems to be crucial for its cytoprotective effects (Aggeli et al., 2008). This suggests that the astrocytic changes at late stage of disease would indeed impact on the phosphorylation of the sHsps and likely promote large sHsp homo- and heter-oligomeric complex formation, supporting a chaperoning role in this disease context potentially as a distinct event from the selective up-regulation at 13 weeks.

6.4.2. Biological significance of astrocytic expression

Expression and up-regulation of the sHsps in glial cells, particularly in the context of disease settings have been reported in a number of studies (Dabir et al., 2004, van Noort, 2008). Activation of astrocytes may be involved in up-regulating expression of the sHsps in an attempt to prevent or deal with the deposition of protein aggregates (Renkawek et al., 1999, Wilhelmus et al., 2006c), or it may be an intrinsic defence mechanism used by the astrocytes to protect them, or indeed other cells such as neurons, from pathological insult.

HspB5 has been identified as a major component of Rosenthal fibers (RF), intra-cytoplasmic inclusions within astrocytes. In human brains, reactive astrocytes around infarcts were GFAP and HspB5 positive. It was also noted that the population of HspB5 positive cells were heterogeneous, in that more astrocytes were GFAP positive than HspB5 positive (Iwaki et al., 1992). This suggested that there may be many different adaptive responses in astrocytes during pathology and 'reactive' astrocytes are clearly not homogenous. This observation indicates that the selective expression of HspB1 in a subpopulation of astrocytes may represent a different class of 'reactive' astrocytes in the hippocampus in addition to the astrocytes that express HspB5 and HspB8. It may also reflect a response to PrP^{sc} deposition, which accumulates in the hilus of the dentate gyrus, followed by the CA3 and CA1. It is also likely that the local microenvironment is different between the hippocampal regions and therefore triggers changes in some astrocytes, but not all. Gliosis, as mentioned previously coincides with aggregate deposition in ME7 animals. This suggests that the presence of extracellular aggregates and/or membrane bound PrP^{sc} triggers a glial response as these cells are constantly in surveillance of their

local microenvironment and up-regulation of sHsps would be consistent with a protective role.

Another interesting avenue arises from the potential for astrocytes to process and assist in the generation of the PrP^{sc} species. The potential for astrocytic contribution to the PrP^{sc} load comes from a number of studies. PrP^{c} expression is required for the conversion to PrP^{sc} (Bueler et al., 1993, Sailer et al., 1994). PrP mRNA is present in high amounts in neurons (Harris et al., 1993), but has also been reported in astrocytes and oligodendrocytes in the brains of postnatal hamsters and rats (Moser et al., 1995) suggesting involvement of glial cells in prion replication. Transgenic mice devoid of murine PrP^{c} were generated to express hamster PrP^{c} transgenes driven by the GFAP promoter. These mice developed severe disease and accumulated high levels of PrP^{sc} after inoculation with hamster scrapie (Raeber et al., 1997). As astrocytes are involved in neuronal maintenance (Mucke and Eddleston, 1993), astrocytic dysfunction could result in neuronal dysfunction and toxicity. In view of the misfolding event involved in PrP^{c} conversion to PrP^{sc}, such an involvement of astrocytes could be the basis for sHsp up-regulation. Interestingly HspB5 was shown to be a potent copper chelator, binding with picomolar affinity. This was associated with a decrease in the production of ROS (Ahmad et al., 2008). PrP^{c} is a copper binding protein and it is likely involved in protecting against oxidative stress or acting as a copper buffer (Davies and Brown, 2008). The up-regulation of sHsps may be a general response to the increased burden of such metals and oxidative stress in an attempt to maintain the normal homeostatic balance or in the case of prion disease a compensatory role due to the loss of PrP^{c} function. Interestingly, increased expression of HspB1 has been shown to reduce iron levels and increase the reduced (antioxidant) form of glutathione (Arrigo et al., 2005b).

6.4.3. An extracellular presence of the sHsps?

The sHsps have been associated with extracellular functions such as regulating the inflammatory response and they have been associated with protein aggregates and plaques in the extracellular environment (Wilhelmus et al., 2006c). The evidence although limited, supports an extracellular presence and function of the sHsps that is associated with a pathological context.

HspB1 is a circulating protein marker of increased malignancy in breast cancer and has been found in the serum of cancer patients (Fanelli et al., 1998). HspB5 and HspB1 expression has also been shown to occur close to PrP^{sc} plaques in astrocytes and microglia (Renkawek et al., 1992). Due to the lack of a signal sequence targeting sHsps to the extracellular space, it has been proposed that sHsps may be released into the extracellular environment by non-conventional means, such as by exosomes or via the lysosomal pathway (Graner et al., 2007) as they have been found extracellularly in the absence of cell lysis/necrosis (Fanelli et al., 1998). This supports the idea that non-neuronal cells may liberate sHsps in a targeted and selective manner. The presence of sHsp positive astrocytes that potentially secrete HspB1 and other sHsps into the extracellular environment is an interesting concept and would provide a mechanism to confer neuroprotection via chaperone functions associated with sHsps or indeed modulation of an inflammatory response. Although the halo-like expression of HspB1 in astrocytes initially suggested the possibility of an extracellular presence, it is clear that this morphology is characteristic of protoplasmic astrocytes and indeed represents the spatial field a single astrocyte can encompass (Bushong et al., 2004).

6.4.4. sHsps and the inflammatory response

The sHsps have been shown to be involved in regulating the inflammatory response (Roelofs et al., 2006, van Noort, 2008). The inflammatory response in autoimmune de-myelination was shown to be exacerbated in HspB5 knock-out mice. This sHsp was demonstrated to be a potent negative regulator of the inflammatory response, acting as a brake on several inflammatory pathways in the CNS and immune system. Knockout mice showed higher levels of pro-inflammatory cytokine secretion leading to intense CNS inflammation (Ousman et al., 2007). Thus HspB5 may modulate the inflammatory response during prion disease and sensitise the cells against further insults. Extracellular HspB8 has also been shown to bind to TLR4 (Toll-like receptor 4) (Roelofs et al., 2006). This again is supportive of a role in the inflammatory process and also gives weight to the extracellular presence of the sHsps.

Il-10 has been shown to play a prominent role in prion disease regulation. Il-10 deficient mice were found to be highly susceptible to developing prion disease after inoculation with

RML or ME7 brain homogenate and showed a marked shortening of the incubation time in both strains. Lack of Il-10 led to an early expression of TNF-α, sensitising mice to prion pathology (Thackray et al., 2004). Although microglia are primarily thought to be involved in the inflammatory response, astrocytes and oligodendrocytes are also a source of inflammatory mediators and may contribute to inflammation during disease (McKinnon et al., 1993, Omari et al., 2005, Fernandez et al., 2007). Indeed, HspB1 can induce IL-10 in human monocytes; this was dependent on the activation of the p38 MAPK pathway. Activation of other kinase pathways by HspB1 such as ERK1/2 (extracellular signal-related kinase) and JNK1/2 (c-Jun N-terminal kinase) resulted in inflammatory cytokine production (TNF-α) (Fanelli et al., 1998).

The inflammatory response seen during ME7-induced prion disease is atypical in nature with a predominantly anti-inflammatory cytokine profile (see general introduction). Given the implications of the sHsps in modulation of inflammatory processes outlined above, it is possible to suggest that the sHsps may contribute to and maintain the atypical anti-inflammatory response in this model of neurodegeneration.

6.4.5. Potential negative consequences of sHsps up-regulation

The results indicate that the sHsps are responding to a disease with extracellular aggregates in a different way to a disease with intracellular aggregates. The precise roles of these sHsps is not clear and although it is likely that the up-regulation is beneficial and slows disease progression due to the functions attributed to this group of molecular chaperones, this does not exclude the possibility of a detrimental effect in this disease context. It was recently shown that extracellular HspB5 was involved in the fragmentation of amyloid fibrils. This role was thought to enhance production of further fibrils by providing a mechanism for seed formation and nucleation (Raman et al., 2005). The decrease in fibrils resulted in increased toxicity, consistent with small oligomeric species being more toxic (Stege et al., 1999, Raman et al., 2005). This raises the possibility that the up-regulation of the sHsps, particularly HspB5 at late stage of disease may enhance the neurodegenerative process by inducing the formation of toxic PrP^{sc} species. Liberation of such species could tip the scale in favour of neuronal cell death.

Mutations in the sHsps (B1, B5 and B8) that result in hereditary neurodegenerative diseases result in compromised structural stability resulting in the aggregation of these sHsps. It is unclear whether the disease phenotype is due to gain of function induced by aggregate toxicity, or a loss of chaperone capacity (Carra et al., 2005). However it is evident that the basal levels of the sHsps are important for normal protein homeostasis and up-regulation is potentially important to restore or reduce the imbalance under conditions of stress. Oligodendrocytes are also able to mount a stress response and HspB1 and HspB5 have been shown to be up-regulated in oligodendrocytic cells in addition to astrocytes in a number of disease/stress contexts (Aquino et al., 1997, Duvanel et al., 2004). Although there were no overt changes in HspB5 staining of oligodendrocyte cell bodies and myelin in the hippocampus, it is likely that there is some contribution of this cell type in neuroprotection via axonal support and cross talk with axons and astrocytes. An interesting possibility that may confer neuroprotection to some hippocampal regions is the varying levels of myelination. The DG, CA3 and lacunosum molecular layer of the hippocampus show greater MBP, CNP and HspB5 staining in comparison to the CA1 region.

6.5. Summary

This chapter has described the expression profile of the sHsp family in the ME7 mouse model of prion disease that is characterized by extracellular protein deposits. HspB1, HspB5 and HspB8 were up-regulated in the hippocampus of late stage ME7 animals. Additionally HspB1 (although not significant) and HspB8 were up-regulated in the CA1 region at 13 weeks. The sHsps response was attributable to the selective expression in astrocytes, likely driven via a reactive response in these glial cells. This up-regulation was not transcriptionally regulated, suggesting translational mechanism were modulating the sHsps levels. The consequence of the induced astrocyte expression of sHsps during disease progression remains unclear. However the sHsps may play roles both intra-and extracellularly in modulating neuro-inflammation and neuro-protection/degeneration via cell-cell communication. To test more specific hypothesis in relation to the protective effects of sHsps in the future, ME7 homogenate could be injected into HspB1, B5 or B8 knockout (that are available) or double knockout mice, and disease outcomes could be tested. The hypothetical functions of sHsps in the prion model are summarized in Figure 6.17.
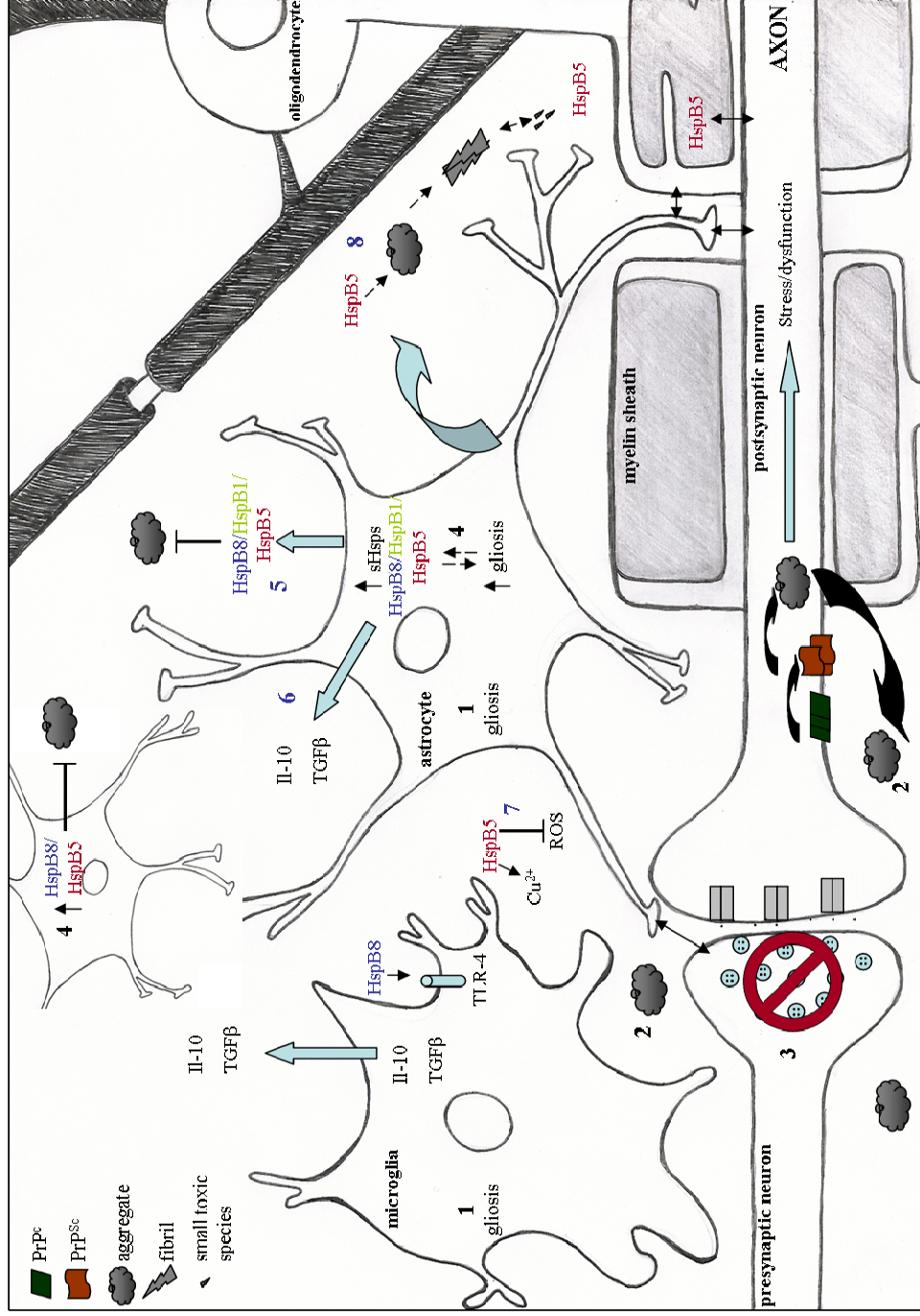
Figure 6.17. Proposed expression/function of the sHsps in the ME7 model of Prion Disease. The schematic illustrates the induced expression of the sHps in astrocytes and shows the proposed modulatory functions in the ME7 mouse model of Prion Disease. Gliosis is observed at 8 weeks (1). PrP^{Sc} aggregates are deposited in the extracellular environment (2). The associated stress may induce upregulation of HspB1 and HspB8 at 13 weeks and HspB5 at 20 weeks (4) in astrocytes. Additionally HspB1 expression is selective to a subpopulation of astrocytes. sHsps may be secreted into the extracellular environment to respond to abnormal protein deposition (5), to regulate the inflammatory response by promoting anti-inflammatory cytokine production (6) and counteract ROS production (7). HspB5 may also promote toxicity by promoting production of small oligomeric species/fragments (8). The precise contribution of the sHsp remains unclear, however the response may be important in modulating disease progression and outcomes.

Chapter 7: General discussion

Prior to this study the expression of the sHsps had not been systematically studied in the mouse CNS. The importance of understanding the physiological expression of this family of molecular chaperones in the CNS arises from mutations in a few members that perturb motor neuron function and an association of the sHsps with neurodegenerative diseases. Therefore, the expression of the 10 members of the sHsp family was first systematically and comparatively characterised under physiological (non-disease) conditions in the mouse CNS. This work established a baseline of expression and as described in Chapter 3, four members of the sHsp protein family (HspB1, HspB5, HspB6 and HspB8) were found to be constitutively expressed in the CNS (Quraishe et al., 2008). The observations in this systematic study support reports in the literature, in which expression of the sHsps under non-stress/disease conditions was predominantly associated with non-neuronal cell types (Table 3.4) (Renkawek et al., 1992, Plumier et al., 1997). HspB5 and HspB6 expression was predominantly localised to the white matter under physiological conditions. Enrichment of HspB5 in the white matter and potential expression in the non-compact myelin compartment as described in Chapter 4, suggests a number of possible functions in this cell type. Perturbations of these functions could contribute to dysfunction of the white matter/oligodendrocytes and impinge on neuronal cell function via alterations in the normal crosstalk between these cell types.

Our analysis does not preclude expression in neurons in the CNS and indeed HspB1 and HspB8 were selectively expressed in the large motor neurons in the ventral horn of the spinal cord, consistent with a role of HspB1 and HspB8 in these cells, which when perturbed due to mutations result in specific motor neuropathies (Evgrafov et al., 2004, Irobi et al., 2004). Limited HspB1 expression has been reported in other neuronal populations in the CNS (Plumier et al., 1997, Armstrong et al., 2001a), however the constitutively higher and selective expression of HspB1 and HspB8, in a subset of motor neurons in the spinal cord as shown in Chapter 3 and other studies (Plumier et al., 1997, Irobi et al., 2004) may reflect a need of these neurons for additional chaperone capacity or associated sHsp functions such as redox regulation. Indeed motor neurons in the ventral horns have been suggested to be more sensitive to oxidative stress associated with ischemia/reperfusion than neurons localised to other spinal cord regions (Kolesar et al., 2009). Furthermore, a region specific response of the spinal cord to oxidative stress has

previously been reported in a model of transient ischemia followed by short periods of reperfusion (1 and 3 h) (Kolesarova et al., 2006) and in a model of repeated spinal cord ischemia (Pavel et al., 2001). Additionally, oligodendrocytes have also been shown to be more susceptible to oxidative stress in comparison to astrocytes (Husain and Juurlink, 1995). The intrinsic vulnerabilities of these cell types to stress/injury suggest that higher basal levels of sHsps maybe required to buffer normal cellular mechanisms and maintain homeostasis. Indeed, higher levels of constitutively expressed Hsc70 and HspB1 have previously been correlated with a higher defense capacity against chronic misfolding stress in motor neurons of the spinal cord compared to other neuronal populations such as the neurons of the substantia nigra and entorhinal cortex (Chen and Brown, 2007).

Expression of the sHsps are not only associated with oxidative stress and ischemia but also heat stress and osmotic stress. Little is known about sHsp expression during conditions of chronic stress driven by intra/extracellular protein misfolding occurring during proteinopathies. Hence to understand the involvement of the sHsps in both intra/extracellular protein misfolding contexts, we investigated the expression of the sHsps in a HD and a prion model of protein misfolding.

As both models are characterized by protein misfolding and aggregation it was hypothesized that there would potentially be convergent cellular mechanisms involving the sHsps at play during pathogenesis. However, the different sHsp signatures as determined in Chapter 3 argue against this point and indeed, the data revealed opposing results in these two models.

As described in chapter 5, in the R6/2 mouse model of HD, characterised by intracellular aggregates, a selective and progressive downregulation of the white matter specific HspB5 protein was observed in tg animals in all white matter compartments of the brain (Chapter 5). Although obvious white matter changes were not observed, the early and selective changes in HspB5 expression suggest a possible contribution of oligodendrocytes during HD pathogenesis. The proposed localization of HspB5 in the non-compact myelin compartment additionally places this sHsps in a key location for involvement in neuronal-glial cross-talk. Indeed white matter abnormalities are routinely observed in HD patients (Jernigan et al., 1991).

In the ME7 mouse model of prion disease HspB1, HspB5 and HspB8 protein expression was up-regulated in astrocytes. For HspB1 this was associated with a subpopulation of astrocytes in the hippocampus detectable at an early time point. HspB5 and HspB8 expression was observed in all GFAP positive astrocytes.

The changes observed in each model and potential implications for sHsp function were discussed in Chapters 5 and 6. However the disease specific sHsp responses raise some interesting questions and correlate with some key differences in these models i.e. the location of aggregates, astrogliosis and the inflammatory response.

7.1.　　Protein aggregation and astrogliosis

sHsp expression changes could be due to protein misfolding itself, and its localization. The presence of extracellular aggregates in ME7 animals may be "sensed" by glial cells resulting in gliosis and up-regulation of the sHsps. However the selective expression of HspB8 in the CA1 at 13 weeks and expression of HspB1 in a subpopulation of astrocytes restricted to the stratum radiatum suggests this early astrocytic response is unlikely to be a consequence of extracellular deposition as PrP^{sc} deposition in this region of the hippocampus is sparse at this time point (Cunningham et al., 2003). It is more likely a result of the early synaptic dysfunction and loss that occurs in the CA1 region at this time point (Cunningham et al., 2003).

Interestingly, the differential astrocytic response in the stratum radiatum and lacunosum moleculare layers of the CA1 could be associated with the distinct innervations of these layers in the hippocampal formation. The stratum radiatum receives inputs from CA3 pyramidal neurons; these synapses are selectively lost during ME7 induced pathology. The entorhinal cortex projects to the subiculum and to both the CA1 and CA3 and the terminals of these fibers projecting to CA1 and CA3 are present in the stratum lacunosum moleculare (van Groen et al., 2003). Group II metabotropic glutamate receptors (mGluRs) which modulate neuronal excitability and synaptic transmission are highly expressed in the terminal field of inputs from the entorhinal cortex in the stratum lacunosum moleculare of the CA1 compared to other regions (Ohishi et al., 1998). The distinct nature of these inputs compared to the stratum radiatum, may indicate that a distinct set of astrocytes are involved in their surveillance. Indeed, astrocytes in this region of the hippocampus are

morphologically different from the astrocytes in the stratum radiatum (Nixdorf-Bergweiler et al., 1994; Ogata and Kosaka, 2002) which would support the potential for differential induction of the sHsps and other response depending on the affected synapses.

It can be speculated that up-regulation of sHsps in the CA1 is associated with possible changes in the microenvironment, synaptic dysfunction and degeneration in the CA1 in particular the stratum radiatum and may mean a protective response is induced to protect against the cell loss that occurs there at late stage of disease. Indeed, in ALS astrocytes are thought to interact with motor neurons in a complex manner. Tg mice expressing mutant SOD-1 (a model of ALS) were shown to release fibroblast growth factor-1 (FGF-1) to induce local astrocyte activation by signalling through the FGF-1 receptor leading to the expression of antioxidant and cytoprotective enzymes such as heme-oxygenase-1 to prevent motor neuron degeneration (Pehar et al., 2005, Vargas et al., 2005). However FGF-1 activation of astrocytes has also been reported to promote motor neuron apoptosis (Cassina et al., 2005). Further, in the brains of AD patients, reactive astrocytes selectively expressing nitric oxide synthase (NOS) were found at the place of clear and overt neuronal loss, particularly in the entorhinal cortex layer II and CA4 (Simic et al., 2000).

The sHsp induction at the late stage of disease may represent a distinct astrocytic response during disease, separate to that seen at earlier time points, and is perhaps due to the accumulation of PrP^{sc} which is deposited throughout the hippocampus at late stage (Cunningham et al., 2003). The heterogeneity of astrocytes in the hippocampus as discussed in chapter 6 would support such a differential response associated with different stages and events during pathogenesis.

An astrogliosis associated with synaptic/cell loss and extracellular misfolding in the ME7 model suggests that in a model where there is very limited cell loss, as in the R6/2 model (Turmaine et al., 2000) astrogliosis may not be a prominent feature. Indeed in the R6/2 animals we did not observe an astrogliosis to the same extent as in the ME7 model. However the limited astrogliosis in the frontal cortex as shown by western blotting suggests cortical astrocytes may be more sensitive to disease related changes in the cortex.

Protein aggregation within neuronal cells in R6/2 animals could mean that astrocytes are unable to 'sense' these aggregates and therefore do not response by way of astrogliosis. Additionally the limited number of aggregates in glial cells suggests they are able to deal

with misfolding events much more efficiently than neurons and therefore do not become activated. This would be consistent with the limited astrogliosis we observe in R6/2 animals, with up-regulation at late stage of disease only in the frontal cortex.

7.2. Inflammation

Our studies show changes of sHsp expression in non-neuronal cells that are potentially an important source of aspects of the innate immunity (McKinnon et al., 1993, Omari et al., 2005). As suggested in previous chapters the astrocytic up-regulation of the sHsps in the ME7 animals and downregulation of HspB5 in R6/2 tg animals may contribute to and modulate the inflammatory response in either disease. Overall an anti-inflammatory response is observed in the ME7 model (Cunningham et al., 2005). Increased expression of the sHsps could act as an inflammatory "break" by promoting the production of anti-inflammatory cytokines such as IL-10 as discussed in chapter 6.

The contribution and nature of an inflammatory response in R6/2 animals is not clear as a number of studies show differing reports with opposing changes in gliosis associated with R6/2 tg animals (Ma et al., 2003, Simmons et al., 2007). In a recent study, stimulation by LPA of isolated macrophages or microglia from mouse models of HD including R6/2 has been shown to induce the production of pro-inflammatory cytokine IL-6. The serum levels of cytokines in end stage R6/2 animals have been reported to be elevated, included Il-6, IL-10, and IL-1β (Bjorkqvist et al., 2008). The mouse model data was show to be consistent with cytokine production in human serum samples in the same study. Opposed to this, no changes in the levels of pro-inflammatory cytokines were observed in end stage R6/2 tg animals (A. Wyttenbach, personal communication).

However, in view of the anti-inflammatory response potentially associated with up-regulation of the sHsps in the ME7 model, it can be postulated that R6/2 tg animals may produce a pro-inflammatory cytokine profile. HspB5 involvement in modulating inflammatory pathways also points towards a potential pro-inflammatory profile, particularly as loss of this protein was found to exacerbate the pro-inflammatory response in a mouse model of EAE (Ousman et al., 2007). Thus it will be important to elucidate the nature of the inflammatory profile in R6/2 animals, or indeed the way in which they respond to additional insults (e.g. peripheral infection).

7.3.   Potential mechanisms for sHsp regulation

Although the sHsp response in intra vs. extracellular proteinopathies is distinct, both models show a common convergent feature in that mRNA expression does not underpin changes in protein expression. Transcript analysis of the sHsps in R6/2 and ME7 animals showed that this was not the mechanism regulating the changes in expression. These observations raise the question; how is sHsp expression modulated in R6/2 and ME7 animals? It is most probable that post-translational regulation such as increased or decreased protein turnover, underpin the changes observed. To address the likelihood of increased/decreased sHsp degradation, in-vitro culture systems could be utilised. Cell models of prion (Gu et al., 2002) and HD (Wyttenbach et al., 2001) have been used to investigate disease related changes and such models could be used to analyze changes in the sHsps e.g. pulse chase experiments under conditions of UPP/autophagy inhibition. Interestingly decreased expression of HspB1 has been suggested to contribute to Machado-Joseph disease (MJD), an autosomal dominant spinocerebellar degenerative disease caused by expanded polyQ tract within the ataxin-3 gene (Wen et al., 2003). This led to analysis of the mechanisms involved in downregulation of HspB1 expression. In cell models of MJD expressing mutant ataxin-3, HspB1 levels were found to be significantly reduced compared to cells expressing normal ataxin-3 (Wen et al., 2003). The changes in protein expression were not associated with transcriptional changes as determined by PCR. Therefore ^{35}S-methionine pulse-chase labeling was used to label newly synthesized proteins. This data revealed reduced levels of ^{35}S labelled HspB1 in mutant cells compared to control cells indicating alterations in protein synthesis which were also not affected by HspB1 degradation by the UPP (Chang et al., 2009). The authors noted that alterations in HspB1 expression were not reflective of general changes in protein synthesis and degradation as other proteins (Bcl-2 and Hsp70) did not show similar reduction in protein expression and were accumulated in the cell after proteasomal inhibition (Chang et al., 2009).

This study indicates that sHsps levels may be modulated by alterations in degradative pathways, likely mediated by the autophagy-lysosomal pathway. Indeed protein degradation pathways are altered during both prion disease and HD as described in the general introduction. Htt aggregates in cell and mouse models have been suggested to

induce autophagy (Ravikumar et al., 2004). In prion pathology, neurons in the vicinity of tissue damage were found to contain PrP^{sc} in lysosomes, indicating that overloading endosomal/lysosomal function may correlate with regional pathology (Kovacs et al., 2007). Additionally PrP^{sc} has been shown to inhibit and impair the UPP in a number of cell lines (Kristiansen et al., 2007). These observations suggest the potential for reduction of sHsp degradation in ME7 animals by impaired UPP. The situation in the R6/2 model in this respect is less clear as the role of the UPP in HD is controversial. However, it may be speculated that HspB5 degradation is increased via the UPP in R6/2 animals.

Another post-translational modification that may be important for protein stability is phosphorylation. The phosphorylation state of the sHsps is important in modulating their functional role. The sHsps are rapidly induced at the transcriptional level following stress, but also undergo several post-translational modifications that alter their functional roles for use as immediate response elements (Stetler et al., 2009).

As proposed for HspB5, induction of μ-calpain in late stage ME7 animals may decrease sHsp phosphorylation thereby altering oligomeric status and promoting a chaperone function. It may be that the phosphorylation state of HspB1 and HspB8 at 13 weeks is different to HspB5 at late stage supporting a differential response. Interestingly changes in the ERK/MAPK signalling pathways have been observed in a study analyzing the gene expression changes in mice infected with scrapie strains 22A, ME7 or 79a (Sorensen et al., 2008). An increase in MAPK signaling could promote the phosphorylation of the sHsps as they are downstream targets and would support a role in cytoskeletal regulation. The need for cytoskeletal regulation and support is suggested by a study demonstrating colocalisation of PrP^{c} and PrP^{sc} with GFAP in brain homogenates from healthy and scrapie (263 K) infected hamsters respectively (Dong et al., 2008), suggesting the PrP^{sc} species could alter cytoskeletal dynamics in prion infected animals resulting in GFAP up-regulation. GFAP up-regulation in astrocytes is followed by changes in other cytoskeletal components such as vimentin and vinculin, resulting in remodeling of the actin cytoskeleton (Ostrow and Sachs, 2005). Determining the phosphorylation and oligomeric state of the sHsps would further help discern their potential role during disease.

7.4.   Potential for modulating sHsp levels

One of the key questions arising form this study is whether the sHsp are protective in these disease contexts? A number of studies have investigated regulation of the sHsps during insults such as ischemia and excitotoxicity suggesting that the sHsps play a protective role (An et al., 2008, Stetler et al., 2008). For example, transgenic mice overexpressing HspB1 that were subjected to kainate induced neurotoxicity were found to have reduced lesion size, less seizures and neuronal death in comparison to wild-type controls (Akbar et al., 2003).

However, studies that have involved overexpression of the sHsps under chronic neurodegenerative conditions have not shown a similar protective effect. For example, tg mice overexpressing HspB1 when crossed with R6/2 mice, showed no improvements in the R6/2 phenotype. Additionally, HspB1 was unable to reduce oxidative stress and the lack of protection was associated with the presence of low molecular weight species and not large oligomeric species that were shown to be present in heat shocked brain lysates (Zourlidou et al., 2007), suggesting the importance of post-translational regulation of the sHsps. Overexpression of the large Hsps has similarly not led to neuroprotection. For example Hsp70 mice were crossed into R6/2, resulting in only modest effects on disease progression (Hansson et al., 2003). In contrast, the loss of Hsp70 by gene knockout was shown to exacerbate pathogenesis and reduce survival of R6/2 tg animals (Wacker et al., 2009) clearly implicating this chaperone as a protective factor. Interestingly Hsp70 knockout mice did not produce an exacerbation of disease in the RML mouse model of prion disease, suggesting Hsp70 knockout mice were not responding generally to protein misfolding diseases but the response was selective to the HD context (Wacker et al., 2009).

Although the overexpression studies have not been able to show an improvement in neurodegenerative outcomes by overexpression of Hsps, it may be that the key Hsp has not been targeted or that indeed several Hsps need to be targeted (Sajjad et al., 2010). Based on our data, and the proposal that white matter specific downregulation of HspB5 is a potential contributor to the HD pathology observed in R6/2 animals, it may be proposed that up-regulation of HspB5 could have beneficial effects and alleviate the symptoms and potentially extend the life span of R6/2 animals. Indeed loss of sHsps has important implications for normal cellular functions as illustrated by the study on heat shock factor-1

(Hsf-1) knockout mice. These mice have been shown to develop many of the characteristic symptoms of neurodegenerative diseases, such as severe astrogliosis, activated microglia, impaired UPP, oxidative stress and progressive myelin loss (Homma et al., 2007).

Genetically engineered knockout mice have been established for HspB1 (Huang et al., 2007) and HspB5 (Brady et al., 2001). HspB1 KO mice do not display morphological abnormalities; however HspB5 KO mice have muscle degeneration selective to the tongue and soleus (Brady et al., 2001; Huang et al., 2007). These mice also display a modest ageing phenotype (personal communication, A Wyttenbach). Such models could be used to answer the question whether the induction of the sHsps in ME7 animals is protective. If so, an exacerbation and enhanced progression of disease is likely to be observed in sHsp knockout mice inoculated with ME7 brain homogenate. Similarly crossing HspB5 knockout mice with R6/2 tg animals will provide indications to the role of HspB5 in this disease. The potential for further exacerbation of pathology in R6/2 animals and an induced inflammatory response is supported by HspB5 knockout studies in an EAE model as discussed in Chapter 5 (Ousman et al., 2007).

An important consideration arising from our observations is the potential that the selective downregulation of HspB5 in oligodendrocytes, although very interesting may be an artifact of this disease model, for this reason it will be necessary to establish possible changes in HspB5 expression in other mouse models of HD. Indeed, our preliminary results suggest a similar decrease in the R6/1 model of HD, however, analysis of human Vonsattel stage II brain tissue suggest variable expression of HspB5 in HD tissue compared to controls and no apparent loss of expression (M, U, Sajjad, unpublished data). This may reflect the distinctly higher levels of white matter in humans compared to rodents (Zhang and Sejnowski, 2000). Analysis of more end stage human tissue and other HD mouse models is currently under way.

The striking sHsps signature suggests an important and differential effect in distinct proteinopathies. This should be extended to systematically study the sHsp signature in PD, ALS and AD. The emerging potential significance of non-neuronal cells during chronic neurodegeneration is supported by this study. The multitude of activities of the sHsps suggests that they could play various roles in the complexity of intra- and extracellular

proteinopathies. It is likely that misfolding events drive an induction or indeed a reduction of sHsp protein expression which may then modulate inflammatory pathways. Or, misfolding events may lead to gliosis and inflammation which may trigger a sHsp response (Figure 7.1).

A

B
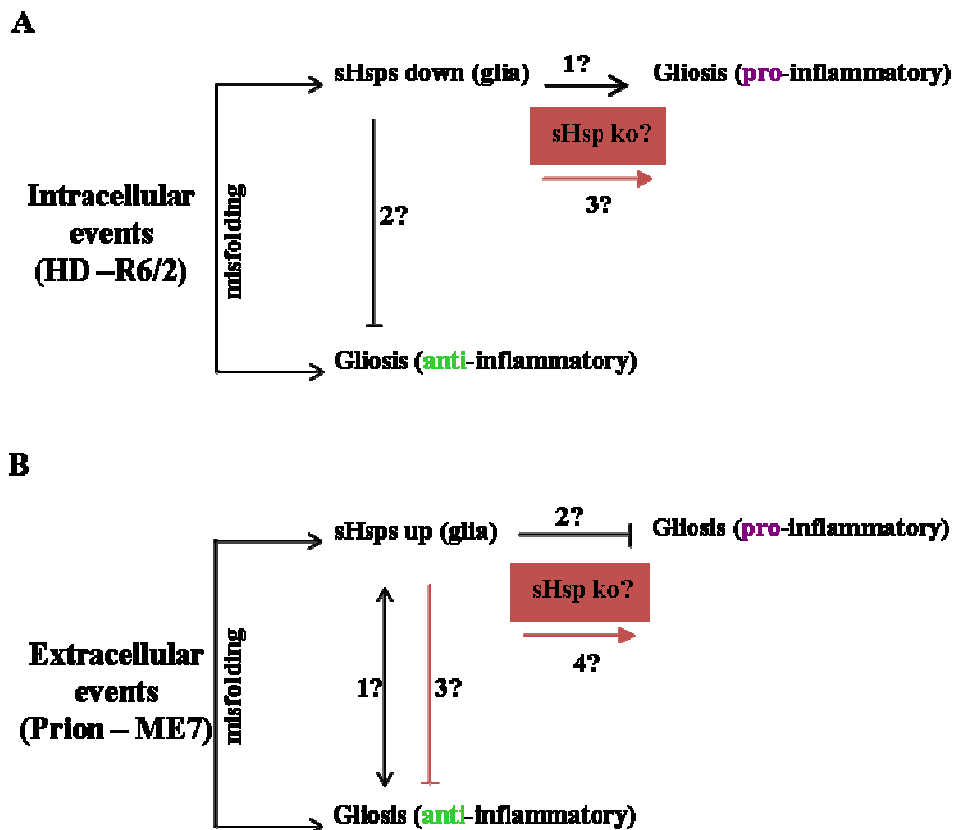
Figure 7.1. Modulation of cellular processes by the sHsps in extra vs. intracellular proteinopathies. Misfolding events may drive changes in sHsp expression in both extracellular and intracellular proteinopathies. These changes may modulate gliosis and inflammation. Or, indeed misfolding may drive gliosis which in turn may modulate sHsp expression. (A) In the R6/2 model, HspB5 downregulation may promote a pro-inflammatory response (1) and inhibit an anti-inflammatory response (2). R6/2 phenotype and potential gliosis (pro-inflammatory) may potentially be exacerbated in knockout animals crossed with R6/2 animals (3). (B)Up-regulation of sHsps in the ME7 model may promote an anti-inflammatory response, or gliosis may modulate sHsp levels (1). Induction of sHsps may in-turn inhibit or dampen a pro-inflammatory response (2). sHsp knockout models inoculated with ME7 may alter the inflammatory response by potentially inhibiting the anti-inflammatory response (3) and removing the inhibition on the pro-inflammatory pathway leading to exacerbation of pathology (4).

Appendices
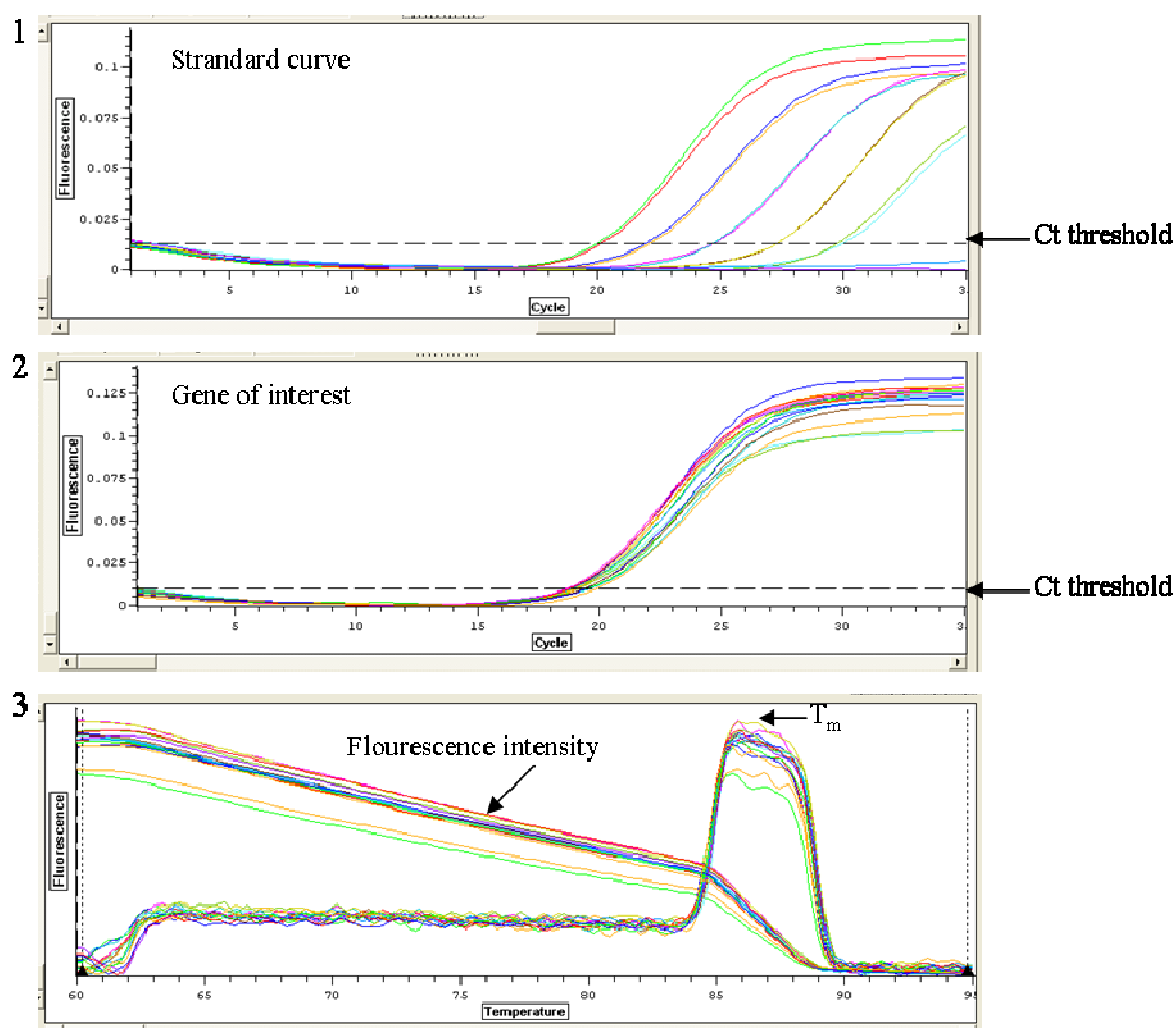
Figure A1. Example of standard curves from a QT-PCR experiment. Standard curves were made using cDNA from naïve tissue and were constructed from 5-fold serial dilutions (undiluted – 1:625) Duplicate reactions were performed at each starting concentration. Ct threshold were automatically set at x1.0 standard deviation over cycle range.

Figure A2. Example of a gene specific QT-PCR experiment. A gene specific reaction showing the Ct values at which a fluorescence signal becomes detectable. Ct values for each sample are recorded as the Ct at which the fluorescence signal crosses the threshold.

Figure A3. Example of melting curves from a QT-PCR experiment. Melting curves are shown from one experiment, depicting the fluorescence intensity and the melting point (T_m) of the amplicon. The presence of a single peak at the same T_m seen in the standards (standard melting curve not shown) supports specific amplification. Additional peaks would suggest non-specific priming and potential primer dimer formation.

Appendix 2
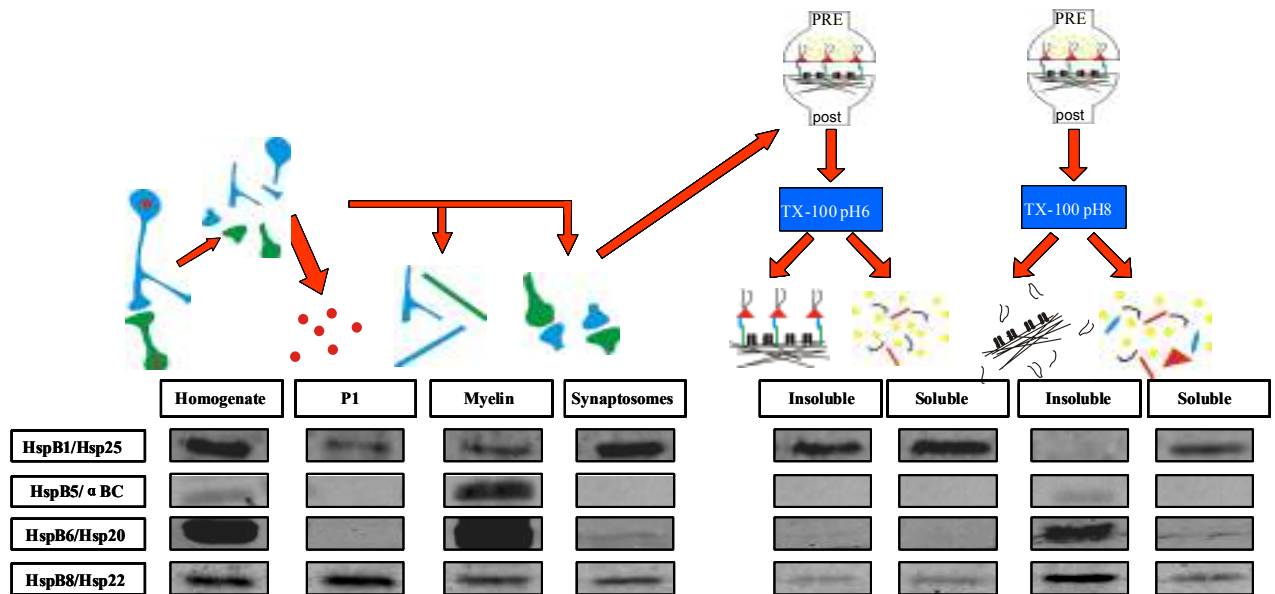
Figure A4. Brain and synaptosome fractions (n=2)

Appendix 3

Detergent extractability of the sHsps in brain homogenate.

A simple fractionation protocol was adopted to investigate the detergent extractability of the sHsps in whole brain tissue. This involved treating two halves of the same brain with different protocols. A physiological buffer (100mM KCL, 20mM Hepes, plus compete protease inhibitor) was used to homogenize one half of the brain. The other half of the brain was then homogenized in lysis buffer containing 1% NP-40 in order to mimic the protocol used for the 4 week and 9 week samples analysed in section 5.3.1. The detergent extracted homogenate was centrifuged to produce a pellet (P1) and supernatant (S1) fraction. S1 was further centrifuged to give a P2 and S2 fraction. The S2 fraction was the equivalent of the samples analysed in section 5.3.1. 50μg of protein from each sample was resolved on SDS-PAGE and western blotting was used to analyse expression of the sHsps (Figure A5).

  The sHsps display differential detergent extractabilities in whole brain tissue (Figure A5). HspB1 is completely solubilised, and the majority of the protein is present in the S1 supernatant fraction. HspB5 is equally distributed between pellet and supernatant fractions

from the first spin (P1 and S1), and is mostly present in the S2 fraction after the second spin. HspB6 is triton insoluble and remains exclusively in the pellet (P1). HspB8 is also equally distributed between the pellet and supernatant fraction after the first spin (P1 and S1), and is almost exclusively present in the S2 fraction after the second spin.
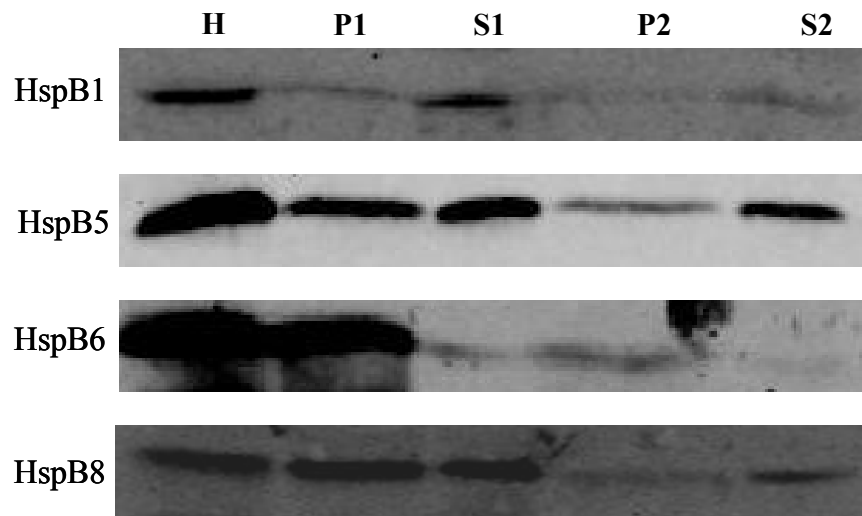
Figure A5. Detergent extractability of the sHsps. 50μg of protein were resolved by SDS-PAGE and expression of the 4 sHsps was observed using a fluorescently labelled secondary antibody. The sHsps display differential detergent extractabilities. HspB1 is almost completely solubilised by NP-40, and is present in the initial supernatant fractions. HspB5 is distributed between pellet and supernatant fractions (P1 and S1), and is mostly present in S2 fraction after the second spin. HspB6 is detergent insoluble and remains in the P1 pellet. HspB8 is also distributed between the pellet and supernatant fractions (P1 and S1), and in mostly present in S2 after the second low speed spin. H (total brain homogenate in Hepes/KCL); P1 (1% NP-40 pellet 1); S1 (1% NP-40 supernatant 1); P2 (1% NP-40 pellet 2); S2 (1% Triton supernatant 2).

Appendix 4

Preliminary analysis of HspB5 protein expression in human Vonsattel stage II HD brain tissue. Tissue was kindly provided by Dr. Richard Faull (University of Auckland, New Zealand) and Dr. Lesley Jones (University of Cardiff, UK). The tissue samples were processed by A. Wyttenbach and Western Blots run by M. U. Sajjad.
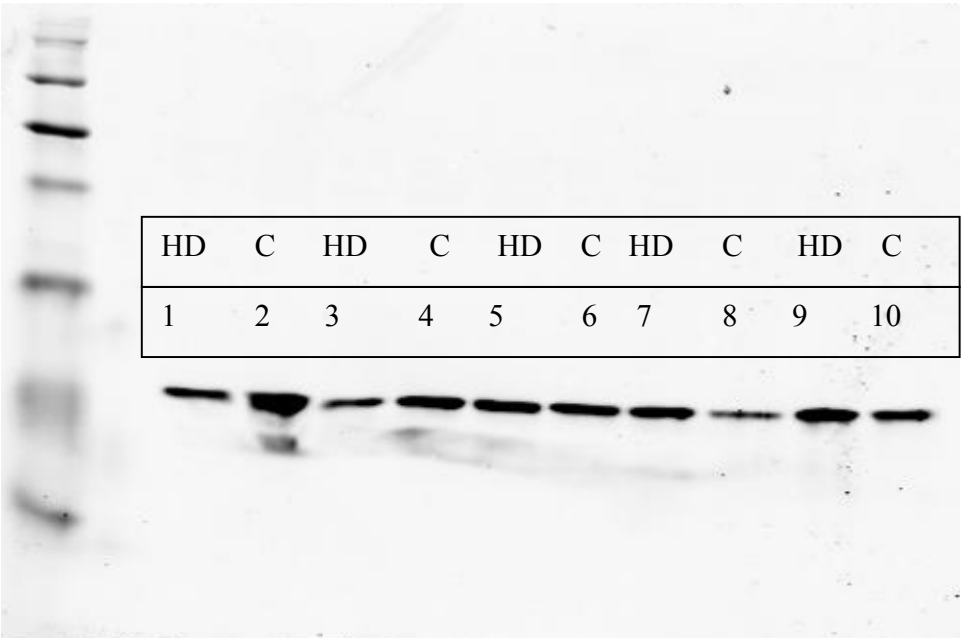
Figure A6. Human frontal cortex- monoclonal HspB5 antibody. C = control, HD: Huntington's Disease brain tissue.
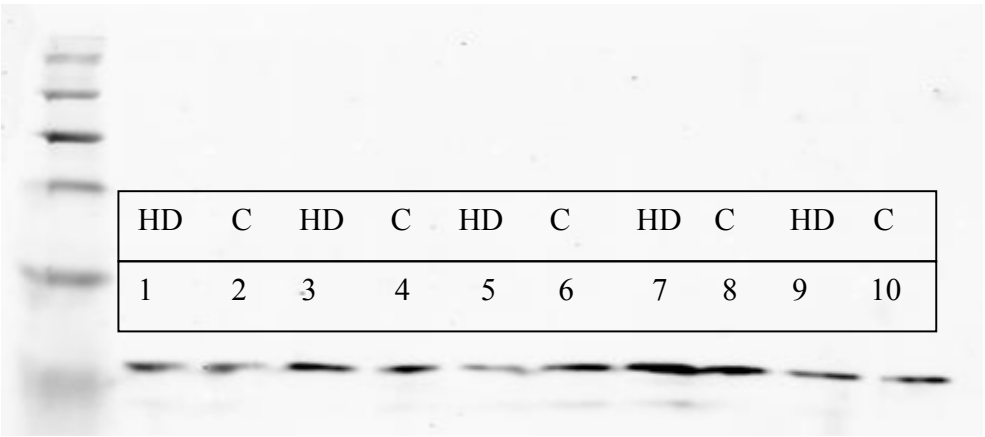
Figure A7. Human cerebellum - monoclonal HspB5 antibody. C = control, HD: Huntington's Disease brain tissue.
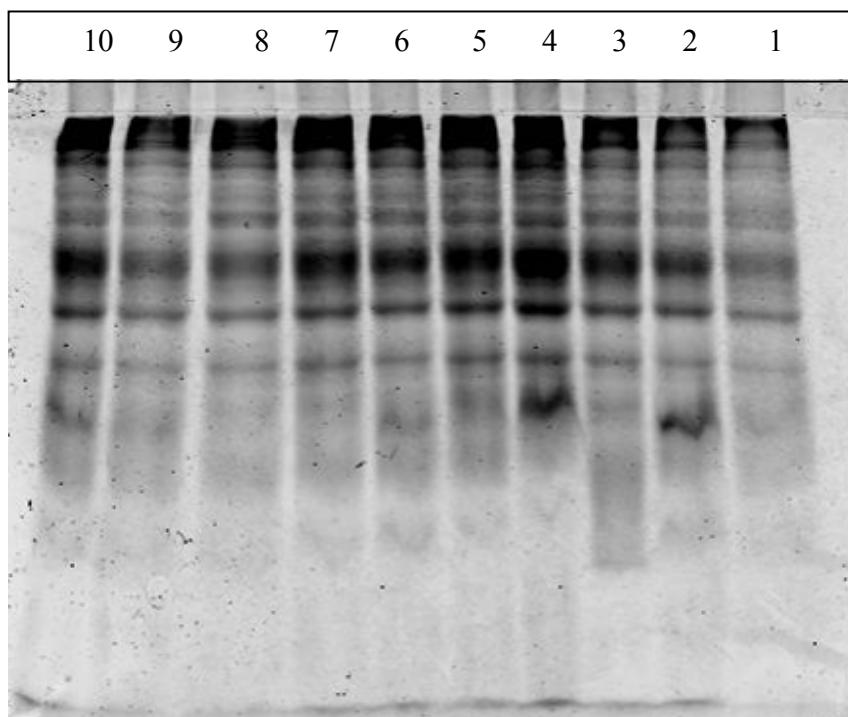
Figure A8. Loading control coomassie gel run in parallel for Figure A6 (human frontal cortex tissue).
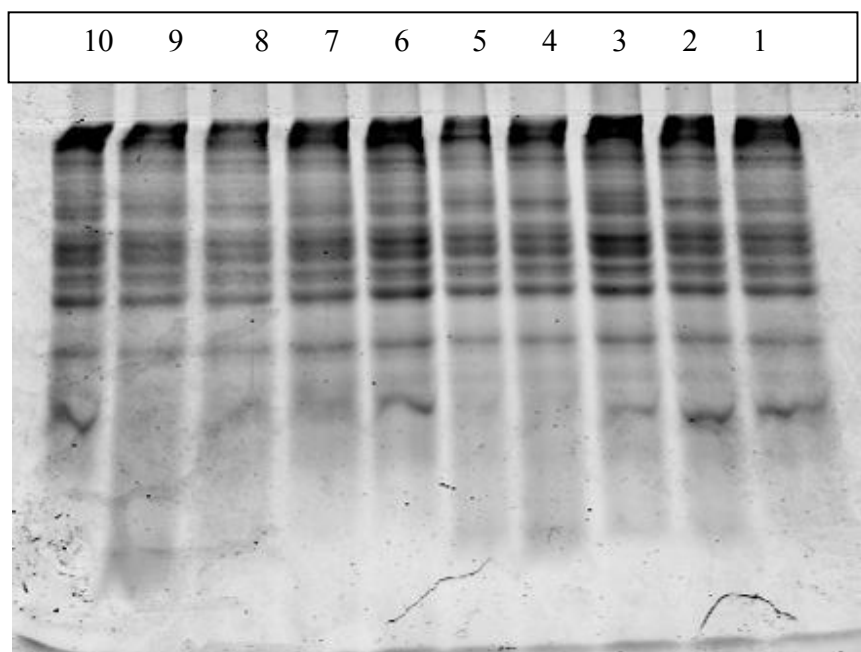
Figure A9. Loading control coomassie gel run in parallel for Figure A7 (human frontal cerebellum tissue).
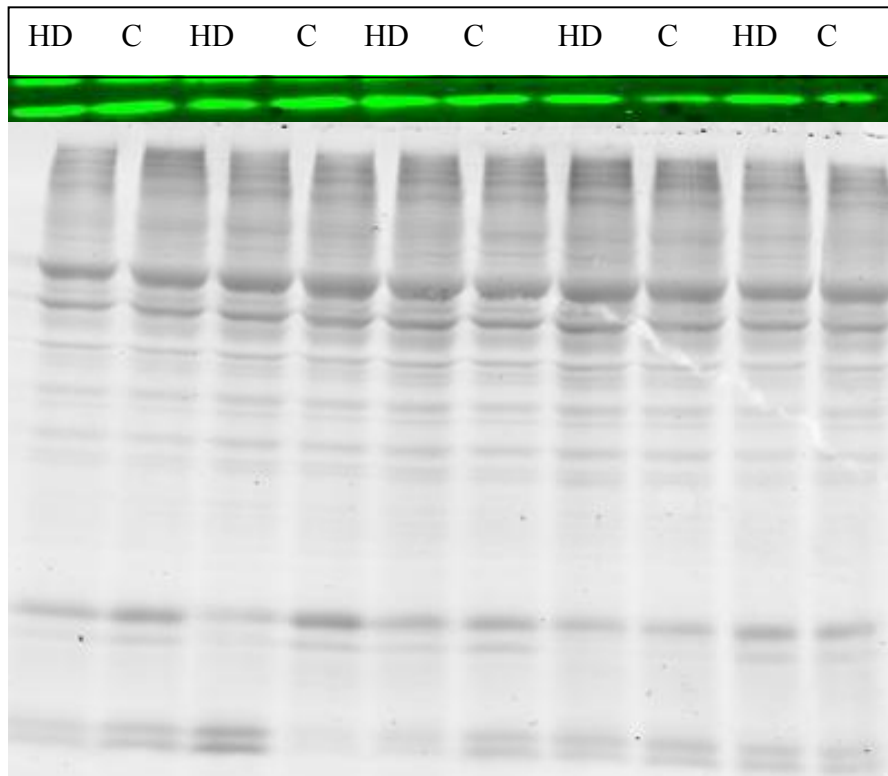
Figure A10. Human frontal cortex - immunofluorescence (green) for polyclonal HspB5 antibody. Corresponding coomassie is shown below.
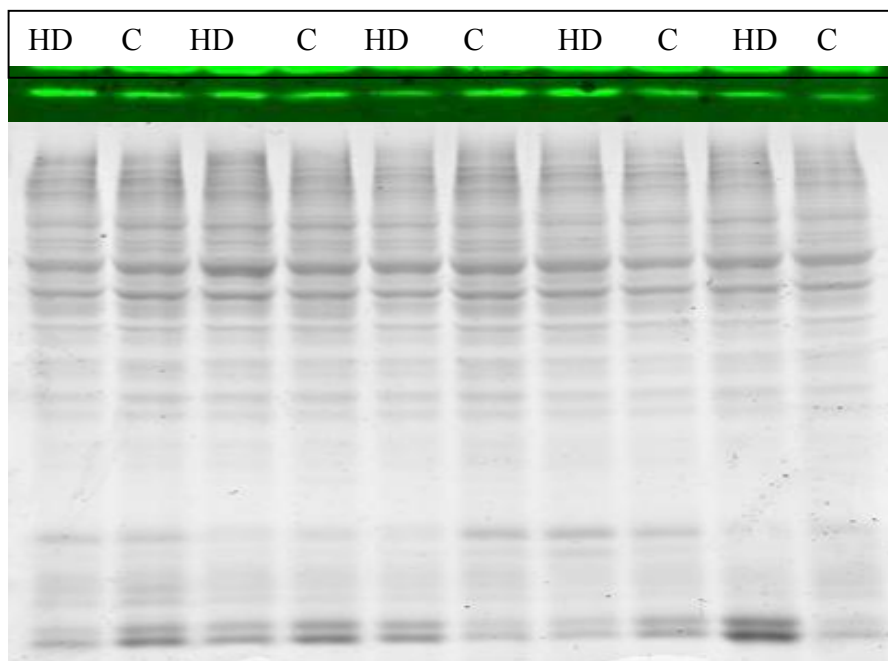
Figure A11. Human cerebellum - immunofluorescence (green) for polyclonal HspB5 antibody. Corresponding coomassie is shown below.

References

Ackerley S, James PA, Kalli A, French S, Davies KE, Talbot K (A mutation in the small heat-shock protein HSPB1 leading to distal hereditary motor neuronopathy disrupts neurofilament assembly and the axonal transport of specific cellular cargoes. Hum Mol Genet 15:347-354.2006).

Adori C, Kovacs GG, Low P, Molnar K, Gorbea C, Fellinger E, Budka H, Mayer RJ, Laszlo L (The ubiquitin-proteasome system in Creutzfeldt-Jakob and Alzheimer disease: intracellular redistribution of components correlates with neuronal vulnerability. Neurobiol Dis 19:427-435.2005).

Aggeli IK, Beis I, Gaitanaki C (Oxidative stress and calpain inhibition induce alpha B-crystallin phosphorylation via p38-MAPK and calcium signalling pathways in H9c2 cells. Cell Signal 20:1292-1302.2008).

Aguirre AA, Chittajallu R, Belachew S, Gallo V (NG2-expressing cells in the subventricular zone are type C-like cells and contribute to interneuron generation in the postnatal hippocampus. J Cell Biol 165:575-589.2004).

Ahmad MF, Singh D, Taiyab A, Ramakrishna T, Raman B, Rao Ch M (Selective Cu2+ binding, redox silencing, and cytoprotective effects of the small heat shock proteins alphaA- and alphaB-crystallin. J Mol Biol 382:812-824.2008).

Ahmed MA, Bamm VV, Shi L, Steiner-Mosonyi M, Dawson JF, Brown L, Harauz G, Ladizhansky V (Induced secondary structure and polymorphism in an intrinsically disordered structural linker of the CNS: solid-state NMR and FTIR spectroscopy of myelin basic protein bound to actin. Biophys J 96:180-191.2009).

Ainger K, Avossa D, Diana AS, Barry C, Barbarese E, Carson JH (Transport and localization elements in myelin basic protein mRNA. J Cell Biol 138:1077-1087.1997).

Akbar MT, Lundberg AM, Liu K, Vidyadaran S, Wells KE, Dolatshad H, Wynn S, Wells DJ, Latchman DS, de Belleroche J (The neuroprotective effects of heat shock protein 27 overexpression in transgenic animals against kainate-induced seizures and hippocampal cell death. J Biol Chem 278:19956-19965.2003).

Albin RL, Reiner A, Anderson KD, Penney JB, Young AB (Striatal and nigral neuron subpopulations in rigid Huntington's disease: implications for the functional anatomy of chorea and rigidity-akinesia. Ann Neurol 27:357-365.1990).

Alford KA, Glennie S, Turrell BR, Rawlinson L, Saklatvala J, Dean JL (Heat shock protein 27 functions in inflammatory gene expression and transforming growth factor-beta-activated kinase-1 (TAK1)-mediated signaling. J Biol Chem 282:6232-6241.2007).

An JJ, Lee YP, Kim SY, Lee SH, Lee MJ, Jeong MS, Kim DW, Jang SH, Yoo KY, Won MH, Kang TC, Kwon OS, Cho SW, Lee KS, Park J, Eum WS, Choi SY (Transduced human PEP-1-heat shock protein 27 efficiently protects against brain ischemic insult. FEBS J 275:1296-1308.2008).

Aquino DA, Capello E, Weisstein J, Sanders V, Lopez C, Tourtellotte WW, Brosnan CF, Raine CS, Norton WT (Multiple sclerosis: altered expression of 70- and 27-kDa heat shock proteins in lesions and myelin. J Neuropathol Exp Neurol 56:664-672.1997).

Armstrong CL, Chung SH, Armstrong JN, Hochgeschwender U, Jeong YG, Hawkes R (A novel somatostatin-immunoreactive mossy fiber pathway associated with HSP25-immunoreactive purkinje cell stripes in the mouse cerebellum. J Comp Neurol 517:524-538.2009).

Armstrong CL, Krueger-Naug AM, Currie RW, Hawkes R (Constitutive expression of heat shock protein HSP25 in the central nervous system of the developing and adult mouse. J Comp Neurol 434:262-274.2001a).

Armstrong RA, Lantos PL, Cairns NJ (Spatial correlations between the vacuolation, prion protein deposits, and surviving neurons in the cerebral cortex in sporadic Creutzfeldt-Jakob disease. Neuropathology 21:266-271.2001b).

Aron AR, Schlaghecken F, Fletcher PC, Bullmore ET, Eimer M, Barker R, Sahakian BJ, Robbins TW (Inhibition of subliminally primed responses is mediated by the caudate and thalamus: evidence from functional MRI and Huntington's disease. Brain 126:713-723.2003).

Arrasate M, Mitra S, Schweitzer ES, Segal MR, Finkbeiner S (Inclusion body formation reduces levels of mutant huntingtin and the risk of neuronal death. Nature 431:805-810.2004).

Arrigo AP, Firdaus WJ, Mellier G, Moulin M, Paul C, Diaz-latoud C, Kretz-remy C (Cytotoxic effects induced by oxidative stress in cultured mammalian cells and protection provided by Hsp27 expression. Methods 35:126-138.2005a).

Arrigo AP, Simon S, Gibert B, Kretz-Remy C, Nivon M, Czekalla A, Guillet D, Moulin M, Diaz-Latoud C, Vicart P (Hsp27 (HspB1) and alphaB-crystallin (HspB5) as therapeutic targets. FEBS Lett 581:3665-3674.2007).

Arrigo AP, Virot S, Chaufour S, Firdaus W, Kretz-Remy C, Diaz-Latoud C (Hsp27 consolidates intracellular redox homeostasis by upholding glutathione in its reduced form and by decreasing iron intracellular levels. Antioxid Redox Signal 7:414-422.2005b).

Ashkar S, Weber GF, Panoutsakopoulou V, Sanchirico ME, Jansson M, Zawaideh S, Rittling SR, Denhardt DT, Glimcher MJ, Cantor H (Eta-1 (osteopontin): an early component of type-1 (cell-mediated) immunity. Science 287:860-864.2000).

Asuni AA, Hilton K, Siskova Z, Lunnon K, Reynolds R, Perry VH, O'Connor V (Alpha-synuclein deficiency in the C57BL/6JOlaHsd strain does not modify disease progression in the ME7-model of prion disease. Neuroscience 165:662-674.2010).

Bains JS, Oliet SH (Glia: they make your memories stick! Trends Neurosci 30:417-424.2007).

Banik NL, Smith ME (Protein determinants of myelination in different regions of developing rat central nervous system. Biochem J 162:247-255.1977).

Barbarese E, Koppel DE, Deutscher MP, Smith CL, Ainger K, Morgan F, Carson JH (Protein translation components are colocalized in granules in oligodendrocytes. J Cell Sci 108 (Pt 8):2781-2790.1995).

Barbee SA, Estes PS, Cziko AM, Hillebrand J, Luedeman RA, Coller JM, Johnson N, Howlett IC, Geng C, Ueda R, Brand AH, Newbury SF, Wilhelm JE, Levine RB, Nakamura A, Parker R, Ramaswami M (Staufen- and FMRP-containing neuronal RNPs are structurally and functionally related to somatic P bodies. Neuron 52:997-1009.2006).

Barres BA, Barde Y (Neuronal and glial cell biology. Curr Opin Neurobiol 10:642-648.2000).

Bartsch U, Kirchhoff F, Schachner M (Immunohistological localization of the adhesion molecules L1, N-CAM, and MAG in the developing and adult optic nerve of mice. J Comp Neurol 284:451-462.1989).

Bartzokis G, Cummings J, Perlman S, Hance DB, Mintz J (Increased basal ganglia iron levels in Huntington disease. Arch Neurol 56:569-574.1999).

Bartzokis G, Lu PH, Tishler TA, Fong SM, Oluwadara B, Finn JP, Huang D, Bordelon Y, Mintz J, Perlman S (Myelin breakdown and iron changes in Huntington's disease: pathogenesis and treatment implications. Neurochem Res 32:1655-1664.2007).

Basha E, Friedrich KL, Vierling E (The N-terminal arm of small heat shock proteins is important for both chaperone activity and substrate specificity. J Biol Chem 281:39943-39952.2006).

Basha E, Lee GJ, Breci LA, Hausrath AC, Buan NR, Giese KC, Vierling E (The identity of proteins associated with a small heat shock protein during heat stress in vivo indicates that these chaperones protect a wide range of cellular functions. J Biol Chem 279:7566-7575.2004).

Bates GP, Mangiarini L, Mahal A, Davies SW (Transgenic models of Huntington's disease. Hum Mol Genet 6:1633-1637.1997).

Bauer NG, Richter-Landsberg C (The dynamic instability of microtubules is required for aggresome formation in oligodendroglial cells after proteolytic stress. J Mol Neurosci 29:153-168.2006).

Baumann N, Pham-Dinh D (Biology of oligodendrocyte and myelin in the mammalian central nervous system. Physiol Rev 81:871-927.2001).

Beall A, Bagwell D, Woodrum D, Stoming TA, Kato K, Suzuki A, Rasmussen H, Brophy CM (The small heat shock-related protein, HSP20, is phosphorylated on serine 16 during cyclic nucleotide-dependent relaxation. J Biol Chem 274:11344-11351.1999).

Belachew S, Chittajallu R, Aguirre AA, Yuan X, Kirby M, Anderson S, Gallo V (Postnatal NG2 proteoglycan-expressing progenitor cells are intrinsically multipotent and generate functional neurons. J Cell Biol 161:169-186.2003).

Benn CL, Fox H, Bates GP (Optimisation of region-specific reference gene selection and relative gene expression analysis methods for pre-clinical trials of Huntington's disease. Mol Neurodegener 3:17.2008).

Benndorf R, Hayess K, Ryazantsev S, Wieske M, Behlke J, Lutsch G (Phosphorylation and supramolecular organization of murine small heat shock protein HSP25 abolish its actin polymerization-inhibiting activity. J Biol Chem 269:20780-20784.1994).

Bennett EJ, Bence NF, Jayakumar R, Kopito RR (Global impairment of the ubiquitin-proteasome system by nuclear or cytoplasmic protein aggregates precedes inclusion body formation. Mol Cell 17:351-365.2005).

Bergman A, Siegal ML (Evolutionary capacitance as a general feature of complex gene networks. Nature 424:549-552.2003).

Berry V, Francis P, Reddy MA, Collyer D, Vithana E, MacKay I, Dawson G, Carey AH, Moore A, Bhattacharya SS, Quinlan RA (Alpha-B crystallin gene (CRYAB) mutation causes dominant congenital posterior polar cataract in humans. Am J Hum Genet 69:1141-1145.2001).

Bessert DA, Skoff RP (High-resolution in situ hybridization and TUNEL staining with free-floating brain sections. J Histochem Cytochem 47:693-702.1999).

Betmouni S, Perry VH, Gordon JL (Evidence for an early inflammatory response in the central nervous system of mice with scrapie. Neuroscience 74:1-5.1996).

Bifulco M, Laezza C, Stingo S, Wolff J (2',3'-Cyclic nucleotide 3'-phosphodiesterase: a membrane-bound, microtubule-associated protein and membrane anchor for tubulin. Proc Natl Acad Sci U S A 99:1807-1812.2002).

Bjorkdahl C, Sjogren MJ, Zhou X, Concha H, Avila J, Winblad B, Pei JJ (Small heat shock proteins Hsp27 or alphaB-crystallin and the protein components of neurofibrillary tangles: tau and neurofilaments. J Neurosci Res 86:1343-1352.2008).

Bjorkqvist M, Wild EJ, Thiele J, Silvestroni A, Andre R, Lahiri N, Raibon E, Lee RV, Benn CL, Soulet D, Magnusson A, Woodman B, Landles C, Pouladi MA, Hayden MR, Khalili-Shirazi A, Lowdell MW, Brundin P, Bates GP, Leavitt BR, Moller T, Tabrizi SJ (A novel pathogenic pathway of immune activation detectable before clinical onset in Huntington's disease. J Exp Med 205:1869-1877.2008).

Boespflug-Tanguy O, Labauge P, Fogli A, Vaurs-Barriere C (Genes involved in leukodystrophies: a glance at glial functions. Curr Neurol Neurosci Rep 8:217-229.2008).

Boggs JM (Myelin basic protein: a multifunctional protein. Cell Mol Life Sci 63:1945-1961.2006).

Boot-Handford RP, Briggs MD (The unfolded protein response and its relevance to connective tissue diseases. Cell Tissue Res 339:197-211.2010).

Bova MP, McHaourab HS, Han Y, Fung BK (Subunit exchange of small heat shock proteins. Analysis of oligomer formation of alphaA-crystallin and Hsp27 by fluorescence resonance energy transfer and site-directed truncations. J Biol Chem 275:1035-1042.2000).

Braak H, Del Tredici K, Sandmann-Kiel D, Rub U, Schultz C (Nerve cells expressing heat-shock proteins in Parkinson's disease. Acta Neuropathol 102:449-454.2001).

Bradford J, Shin JY, Roberts M, Wang CE, Li XJ, Li S (Expression of mutant huntingtin in mouse brain astrocytes causes age-dependent neurological symptoms. Proc Natl Acad Sci U S A 106:22480-22485.2009).

Brady JP, Garland D, Duglas-Tabor Y, Robison WG, Jr., Groome A, Wawrousek EF (Targeted disruption of the mouse alpha A-crystallin gene induces cataract and cytoplasmic inclusion bodies containing the small heat shock protein alpha B-crystallin. Proc Natl Acad Sci U S A 94:884-889.1997).

Brady JP, Garland DL, Green DE, Tamm ER, Giblin FJ, Wawrousek EF (AlphaB-crystallin in lens development and muscle integrity: a gene knockout approach. Invest Ophthalmol Vis Sci 42:2924-2934.2001).

Brocke S, Piercy C, Steinman L, Weissman IL, Veromaa T (Antibodies to CD44 and integrin alpha4, but not L-selectin, prevent central nervous system inflammation and experimental encephalomyelitis by blocking secondary leukocyte recruitment. Proc Natl Acad Sci U S A 96:6896-6901.1999).

Brophy CM, Beall A, Lamb S, Dickinson M, Ware DJ (Small heat shock proteins and vasospasm in human umbilical artery smooth muscle. Biol Reprod 57:1354-1359.1997).

Brouns R, De Deyn PP (The complexity of neurobiological processes in acute ischemic stroke. Clin Neurol Neurosurg 111:483-495.2009).

Brown DR, Schmidt B, Groschup MH, Kretzschmar HA (Prion protein expression in muscle cells and toxicity of a prion protein fragment. Eur J Cell Biol 75:29-37.1998).

Brown DR, Schmidt B, Kretzschmar HA (Role of microglia and host prion protein in neurotoxicity of a prion protein fragment. Nature 380:345-347.1996).

Brown DR, Schmidt B, Kretzschmar HA (Effects of oxidative stress on prion protein expression in PC12 cells. Int J Dev Neurosci 15:961-972.1997).

Brown DR, Wong BS, Hafiz F, Clive C, Haswell SJ, Jones IM (Normal prion protein has an activity like that of superoxide dismutase. Biochem J 344 Pt 1:1-5.1999).

Brown PD, Davies SL, Speake T, Millar ID (Molecular mechanisms of cerebrospinal fluid production. Neuroscience 129:957-970.2004).

Brown Z, Ponce A, Lampi K, Hancock L, Takemoto L (Differential binding of mutant (R116C) and wildtype alphaA crystallin to actin. Curr Eye Res 32:1051-1054.2007).

Browne SE, Beal MF (The energetics of Huntington's disease. Neurochem Res 29:531-546.2004).

Browne SE, Beal MF (Oxidative damage in Huntington's disease pathogenesis. Antioxid Redox Signal 8:2061-2073.2006).

Bruce ME (TSE strain variation. Br Med Bull 66:99-108.2003).

Bruce ME, McConnell I, Fraser H, Dickinson AG (The disease characteristics of different strains of scrapie in Sinc congenic mouse lines: implications for the nature of the agent and host control of pathogenesis. J Gen Virol 72 (Pt 3):595-603.1991).

Brunner C, Lassmann H, Waehneldt TV, Matthieu JM, Linington C (Differential ultrastructural localization of myelin basic protein, myelin/oligodendroglial glycoprotein, and 2',3'-cyclic nucleotide 3'-phosphodiesterase in the CNS of adult rats. J Neurochem 52:296-304.1989).

Bryantsev AL, Kurchashova SY, Golyshev SA, Polyakov VY, Wunderink HF, Kanon B, Budagova KR, Kabakov AE, Kampinga HH (Regulation of stress-induced intracellular sorting and chaperone function of Hsp27 (HspB1) in mammalian cells. Biochem J 407:407-417.2007).

Bucciantini M, Giannoni E, Chiti F, Baroni F, Formigli L, Zurdo J, Taddei N, Ramponi G, Dobson CM, Stefani M (Inherent toxicity of aggregates implies a common mechanism for protein misfolding diseases. Nature 416:507-511.2002).

Budka H (Neuropathology of prion diseases. Br Med Bull 66:121-130.2003).

Bueler H, Aguzzi A, Sailer A, Greiner RA, Autenried P, Aguet M, Weissmann C (Mice devoid of PrP are resistant to scrapie. Cell 73:1339-1347.1993).

Bueler H, Fischer M, Lang Y, Bluethmann H, Lipp HP, DeArmond SJ, Prusiner SB, Aguet M, Weissmann C (Normal development and behaviour of mice lacking the neuronal cell-surface PrP protein. Nature 356:577-582.1992).

Bukach OV, Glukhova AE, Seit-Nebi AS, Gusev NB (Heterooligomeric complexes formed by human small heat shock proteins HspB1 (Hsp27) and HspB6 (Hsp20). Biochim Biophys Acta 1794:486-495.2009).

Bukach OV, Seit-Nebi AS, Marston SB, Gusev NB (Some properties of human small heat shock protein Hsp20 (HspB6). Eur J Biochem 271:291-302.2004).

Burger AM, Seth AK (The ubiquitin-mediated protein degradation pathway in cancer: therapeutic implications. Eur J Cancer 40:2217-2229.2004).

Bushong EA, Martone ME, Ellisman MH (Maturation of astrocyte morphology and the establishment of astrocyte domains during postnatal hippocampal development. Int J Dev Neurosci 22:73-86.2004).

Calabrese V, Guagliano E, Sapienza M, Panebianco M, Calafato S, Puleo E, Pennisi G, Mancuso C, Butterfield DA, Stella AG (Redox regulation of cellular stress response in aging and neurodegenerative disorders: role of vitagenes. Neurochem Res 32:757-773.2007).

Carmen J, Magnus T, Cassiani-Ingoni R, Sherman L, Rao MS, Mattson MP (Revisiting the astrocyte-oligodendrocyte relationship in the adult CNS. Prog Neurobiol 82:151-162.2007).

Carra S, Seguin SJ, Lambert H, Landry J (HspB8 chaperone activity toward poly(Q)-containing proteins depends its association with Bag3, a stimulator of macroautophagy. J Biol Chem 283:1437-1444.2008).

Carra S, Sivilotti M, Chavez Zobel AT, Lambert H, Landry J (HspB8, a small heat shock protein mutated in human neuromuscular disorders, has in vivo chaperone activity in cultured cells. Hum Mol Genet 14:1659-1669.2005).

Carson JH, Worboys K, Ainger K, Barbarese E (Translocation of myelin basic protein mRNA in oligodendrocytes requires microtubules and kinesin. Cell Motil Cytoskeleton 38:318-328.1997).

Carter RJ, Lione LA, Humby T, Mangiarini L, Mahal A, Bates GP, Dunnett SB, Morton AJ (Characterization of progressive motor deficits in mice transgenic for the human Huntington's disease mutation. J Neurosci 19:3248-3257.1999).

Cash TP, Pan Y, Simon MC (Reactive oxygen species and cellular oxygen sensing. Free Radic Biol Med 43:1219-1225.2007).

Cashikar AG, Duennwald M, Lindquist SL (A chaperone pathway in protein disaggregation. Hsp26 alters the nature of protein aggregates to facilitate reactivation by Hsp104. J Biol Chem 280:23869-23875.2005).

Cassina P, Pehar M, Vargas MR, Castellanos R, Barbeito AG, Estevez AG, Thompson JA, Beckman JS, Barbeito L (Astrocyte activation by fibroblast growth factor-1 and motor neuron apoptosis: implications for amyotrophic lateral sclerosis. J Neurochem 93:38-46.2005).

Cattaneo E, Rigamonti D, Goffredo D, Zuccato C, Squitieri F, Sipione S (Loss of normal huntingtin function: new developments in Huntington's disease research. Trends Neurosci 24:182-188.2001).

Cha JH, Kosinski CM, Kerner JA, Alsdorf SA, Mangiarini L, Davies SW, Penney JB, Bates GP, Young AB (Altered brain neurotransmitter receptors in transgenic mice expressing a portion of an abnormal human huntington disease gene. Proc Natl Acad Sci U S A 95:6480-6485.1998).

Chabas D, Baranzini SE, Mitchell D, Bernard CC, Rittling SR, Denhardt DT, Sobel RA, Lock C, Karpuj M, Pedotti R, Heller R, Oksenberg JR, Steinman L (The influence of the proinflammatory cytokine, osteopontin, on autoimmune demyelinating disease. Science 294:1731-1735.2001).

Chan EY, Luthi-Carter R, Strand A, Solano SM, Hanson SA, DeJohn MM, Kooperberg C, Chase KO, DiFiglia M, Young AB, Leavitt BR, Cha JH, Aronin N, Hayden MR,

Olson JM (Increased huntingtin protein length reduces the number of polyglutamine-induced gene expression changes in mouse models of Huntington's disease. Hum Mol Genet 11:1939-1951.2002).

Chan WY, Kohsaka S, Rezaie P (The origin and cell lineage of microglia: new concepts. Brain Res Rev 53:344-354.2007).

Chang WH, Cemal CK, Hsu YH, Kuo CL, Nukina N, Chang MH, Hu HT, Li C, Hsieh M (Dynamic expression of Hsp27 in the presence of mutant ataxin-3. Biochem Biophys Res Commun 336:258-267.2005).

Chen-Plotkin AS, Sadri-Vakili G, Yohrling GJ, Braveman MW, Benn CL, Glajch KE, DiRocco DP, Farrell LA, Krainc D, Gines S, MacDonald ME, Cha JH (Decreased association of the transcription factor Sp1 with genes downregulated in Huntington's disease. Neurobiol Dis 22:233-241.2006).

Chen B, Piel WH, Gui L, Bruford E, Monteiro A (The HSP90 family of genes in the human genome: insights into their divergence and evolution. Genomics 86:627-637.2005).

Chen S, Brown IR (Neuronal expression of constitutive heat shock proteins: implications for neurodegenerative diseases. Cell Stress Chaperones 12:51-58.2007).

Chicurel ME, Terrian DM, Potter H (mRNA at the synapse: analysis of a synaptosomal preparation enriched in hippocampal dendritic spines. J Neurosci 13:4054-4063.1993).

Chiti F, Bucciantini M, Capanni C, Taddei N, Dobson CM, Stefani M (Solution conditions can promote formation of either amyloid protofilaments or mature fibrils from the HypF N-terminal domain. Protein Sci 10:2541-2547.2001).

Chiti Z, Knutsen OM, Betmouni S, Greene JR (An integrated, temporal study of the behavioural, electrophysiological and neuropathological consequences of murine prion disease. Neurobiol Dis 22:363-373.2006).

Choi SI, Ju WK, Choi EK, Kim J, Lea HZ, Carp RI, Wisniewski HM, Kim YS (Mitochondrial dysfunction induced by oxidative stress in the brains of hamsters infected with the 263 K scrapie agent. Acta Neuropathol 96:279-286.1998).

Choi YG, Kim JI, Lee HP, Jin JK, Choi EK, Carp RI, Kim YS (Induction of heme oxygenase-1 in the brains of scrapie-infected mice. Neurosci Lett 289:173-176.2000).

Chung KK, Dawson TM, Dawson VL (Nitric oxide, S-nitrosylation and neurodegeneration. Cell Mol Biol (Noisy-le-grand) 51:247-254.2005).

Ciarmiello A, Cannella M, Lastoria S, Simonelli M, Frati L, Rubinsztein DC, Squitieri F (Brain white-matter volume loss and glucose hypometabolism precede the clinical symptoms of Huntington's disease. J Nucl Med 47:215-222.2006).

Clark HB, Burright EN, Yunis WS, Larson S, Wilcox C, Hartman B, Matilla A, Zoghbi HY, Orr HT (Purkinje cell expression of a mutant allele of SCA1 in transgenic mice leads to disparate effects on motor behaviors, followed by a progressive cerebellar dysfunction and histological alterations. J Neurosci 17:7385-7395.1997).

Cobb BA, Petrash JM (Characterization of alpha-crystallin-plasma membrane binding. J Biol Chem 275:6664-6672.2000).

Cohen RS, Blomberg F, Berzins K, Siekevitz P (The structure of postsynaptic densities isolated from dog cerebral cortex. I. Overall morphology and protein composition. J Cell Biol 74:181-203.1977).

Coi A, Bianucci AM, Bonomi F, Rasmussen P, Mura GM, Ganadu ML (Structural perturbation of alphaB-crystallin by zinc and temperature related to its chaperone-like activity. Int J Biol Macromol 42:229-234.2008).

Compston A, Coles A (Multiple sclerosis. Lancet 359:1221-1231.2002).

Connor JR (Iron regulation in the brain at the cell and molecular level. Adv Exp Med Biol 356:229-238.1994).

Cornford EM, Varesi JB, Hyman S, Damian RT, Raleigh MJ (Mitochondrial content of choroid plexus epithelium. Exp Brain Res 116:399-405.1997).

Correa-Cerro LS, Mandell JW (Molecular mechanisms of astrogliosis: new approaches with mouse genetics. J Neuropathol Exp Neurol 66:169-176.2007).

Cowan CM, Raymond LA (Selective neuronal degeneration in Huntington's disease. Curr Top Dev Biol 75:25-71.2006).

Criado JR, Sanchez-Alavez M, Conti B, Giacchino JL, Wills DN, Henriksen SJ, Race R, Manson JC, Chesebro B, Oldstone MB (Mice devoid of prion protein have cognitive deficits that are rescued by reconstitution of PrP in neurons. Neurobiol Dis 19:255-265.2005).

Crotzer VL, Blum JS (Autophagy and intracellular surveillance: Modulating MHC class II antigen presentation with stress. Proc Natl Acad Sci U S A 102:7779-7780.2005).

Csermely P, Schnaider T, Soti C, Prohaszka Z, Nardai G (The 90-kDa molecular chaperone family: structure, function, and clinical applications. A comprehensive review. Pharmacol Ther 79:129-168.1998).

Cunningham C, Boche D, Perry VH (Transforming growth factor beta1, the dominant cytokine in murine prion disease: influence on inflammatory cytokine synthesis and alteration of vascular extracellular matrix. Neuropathol Appl Neurobiol 28:107-119.2002).

Cunningham C, Deacon R, Wells H, Boche D, Waters S, Diniz CP, Scott H, Rawlins JN, Perry VH (Synaptic changes characterize early behavioural signs in the ME7 model of murine prion disease. Eur J Neurosci 17:2147-2155.2003).

Cunningham C, Deacon RM, Chan K, Boche D, Rawlins JN, Perry VH (Neuropathologically distinct prion strains give rise to similar temporal profiles of behavioral deficits. Neurobiol Dis 18:258-269.2005).

D'Antonio M, Michalovich D, Paterson M, Droggiti A, Woodhoo A, Mirsky R, Jessen KR (Gene profiling and bioinformatic analysis of Schwann cell embryonic development and myelination. Glia 53:501-515.2006).

Dabir DV, Trojanowski JQ, Richter-Landsberg C, Lee VM, Forman MS (Expression of the small heat-shock protein alphaB-crystallin in tauopathies with glial pathology. Am J Pathol 164:155-166.2004).

Dalrymple A, Wild EJ, Joubert R, Sathasivam K, Bjorkqvist M, Petersen A, Jackson GS, Isaacs JD, Kristiansen M, Bates GP, Leavitt BR, Keir G, Ward M, Tabrizi SJ (Proteomic profiling of plasma in Huntington's disease reveals neuroinflammatory activation and biomarker candidates. J Proteome Res 6:2833-2840.2007).

David JC, Boelens WC, Grongnet JF (Up-regulation of heat shock protein HSP 20 in the hippocampus as an early response to hypoxia of the newborn. J Neurochem 99:570-581.2006).

Davies P, Brown DR (The chemistry of copper binding to PrP: is there sufficient evidence to elucidate a role for copper in protein function? Biochem J 410:237-244.2008).

De Angelis DA, Braun PE (2',3'-Cyclic nucleotide 3'-phosphodiesterase binds to actin-based cytoskeletal elements in an isoprenylation-independent manner. J Neurochem 67:943-951.1996).

de Wit NJ, Verschuure P, Kappe G, King SM, de Jong WW, van Muijen GN, Boelens WC (Testis-specific human small heat shock protein HSPB9 is a cancer/testis antigen, and potentially interacts with the dynein subunit TCTEL1. Eur J Cell Biol 83:337-345.2004).

Deacon RM, Raley JM, Perry VH, Rawlins JN (Burrowing into prion disease. Neuroreport 12:2053-2057.2001).

DeArmond SJ, Yang SL, Cayetano-Canlas J, Groth D, Prusiner SB (The neuropathological phenotype in transgenic mice expressing different prion protein constructs. Philos Trans R Soc Lond B Biol Sci 343:415-423.1994).

Deber CM, Reynolds SJ (Central nervous system myelin: structure, function, and pathology. Clin Biochem 24:113-134.1991).

Deby C, Goutier R (New perspectives on the biochemistry of superoxide anion and the efficiency of superoxide dismutases. Biochem Pharmacol 39:399-405.1990).

Dell'Omo G, Vannoni E, Vyssotski AL, Di Bari MA, Nonno R, Agrimi U, Lipp HP (Early behavioural changes in mice infected with BSE and scrapie: automated home cage monitoring reveals prion strain differences. Eur J Neurosci 16:735-742.2002).

den Engelsman J, Keijsers V, de Jong WW, Boelens WC (The small heat-shock protein alpha B-crystallin promotes FBX4-dependent ubiquitination. J Biol Chem 278:4699-4704.2003).

Der Perng M, Quinlan RA (Neuronal diseases: small heat shock proteins calm your nerves. Curr Biol 14:R625-626.2004).

Diaz-Hernandez M, Valera AG, Moran MA, Gomez-Ramos P, Alvarez-Castelao B, Castano JG, Hernandez F, Lucas JJ (Inhibition of 26S proteasome activity by huntingtin filaments but not inclusion bodies isolated from mouse and human brain. J Neurochem 98:1585-1596.2006).

Dierick I, Irobi J, De Jonghe P, Timmerman V (Small heat shock proteins in inherited peripheral neuropathies. Ann Med 37:413-422.2005).

DiFiglia M, Sapp E, Chase K, Schwarz C, Meloni A, Young C, Martin E, Vonsattel JP, Carraway R, Reeves SA, et al. (Huntingtin is a cytoplasmic protein associated with vesicles in human and rat brain neurons. Neuron 14:1075-1081.1995).

DiFiglia M, Sapp E, Chase KO, Davies SW, Bates GP, Vonsattel JP, Aronin N (Aggregation of huntingtin in neuronal intranuclear inclusions and dystrophic neurites in brain. Science 277:1990-1993.1997).

Dobson CM (The structural basis of protein folding and its links with human disease. Philos Trans R Soc Lond B Biol Sci 356:133-145.2001).

Doerwald L, van Rheede T, Dirks RP, Madsen O, Rexwinkel R, van Genesen ST, Martens GJ, de Jong WW, Lubsen NH (Sequence and functional conservation of the intergenic region between the head-to-head genes encoding the small heat shock proteins alphaB-crystallin and HspB2 in the mammalian lineage. J Mol Evol 59:674-686.2004).

Dreiza CM, Brophy CM, Komalavilas P, Furnish EJ, Joshi L, Pallero MA, Murphy-Ullrich JE, von Rechenberg M, Ho YS, Richardson B, Xu N, Zhen Y, Peltier JM, Panitch

A (Transducible heat shock protein 20 (HSP20) phosphopeptide alters cytoskeletal dynamics. FASEB J 19:261-263.2005).

Duan JH, Wang HQ, Xu J, Lin X, Chen SQ, Kang Z, Yao ZB (White matter damage of patients with Alzheimer's disease correlated with the decreased cognitive function. Surg Radiol Anat 28:150-156.2006).

Dunker AK, Obradovic Z (The protein trinity--linking function and disorder. Nat Biotechnol 19:805-806.2001).

Duvanel CB, Monnet-Tschudi F, Braissant O, Matthieu JM, Honegger P (Tumor necrosis factor-alpha and alphaB-crystallin up-regulation during antibody-mediated demyelination in vitro: a putative protective mechanism in oligodendrocytes. J Neurosci Res 78:711-722.2004).

Dyer CA, Philibotte TM, Billings-Gagliardi S, Wolf MK (Cytoskeleton in myelin-basic-protein-deficient shiverer oligodendrocytes. Dev Neurosci 17:53-62.1995).

Einheber S, Zanazzi G, Ching W, Scherer S, Milner TA, Peles E, Salzer JL (The axonal membrane protein Caspr, a homologue of neurexin IV, is a component of the septate-like paranodal junctions that assemble during myelination. J Cell Biol 139:1495-1506.1997).

Ellis RJ (Macromolecular crowding: obvious but underappreciated. Trends Biochem Sci 26:597-604.2001).

Emsley JG, Macklis JD (Astroglial heterogeneity closely reflects the neuronal-defined anatomy of the adult murine CNS. Neuron Glia Biol 2:175-186.2006).

Esser C, Alberti S, Hohfeld J (Cooperation of molecular chaperones with the ubiquitin/proteasome system. Biochim Biophys Acta 1695:171-188.2004).

Estrada Sanchez AM, Mejia-Toiber J, Massieu L (Excitotoxic neuronal death and the pathogenesis of Huntington's disease. Arch Med Res 39:265-276.2008).

Evgrafov OV, Mersiyanova I, Irobi J, Van Den Bosch L, Dierick I, Leung CL, Schagina O, Verpoorten N, Van Impe K, Fedotov V, Dadali E, Auer-Grumbach M, Windpassinger C, Wagner K, Mitrovic Z, Hilton-Jones D, Talbot K, Martin JJ, Vasserman N, Tverskaya S, Polyakov A, Liem RK, Gettemans J, Robberecht W, De Jonghe P, Timmerman V (Mutant small heat-shock protein 27 causes axonal Charcot-Marie-Tooth disease and distal hereditary motor neuropathy. Nat Genet 36:602-606.2004).

Fabrizi C, Kelly BM, Gillespie CS, Schlaepfer WW, Scherer SS, Brophy PJ (Transient expression of the neurofilament proteins NF-L and NF-M by Schwann cells is regulated by axonal contact. J Neurosci Res 50:291-299.1997).

Fadok VA, Bratton DL, Guthrie L, Henson PM (Differential effects of apoptotic versus lysed cells on macrophage production of cytokines: role of proteases. J Immunol 166:6847-6854.2001).

Fan CY, Lee S, Ren HY, Cyr DM (Exchangeable chaperone modules contribute to specification of type I and type II Hsp40 cellular function. Mol Biol Cell 15:761-773.2004).

Fan GC, Chu G, Kranias EG (Hsp20 and its cardioprotection. Trends Cardiovasc Med 15:138-141.2005).

Fan GC, Zhou X, Wang X, Song G, Qian J, Nicolaou P, Chen G, Ren X, Kranias EG (Heat shock protein 20 interacting with phosphorylated Akt reduces doxorubicin-triggered oxidative stress and cardiotoxicity. Circ Res 103:1270-1279.2008).

Fanarraga ML, Griffiths IR, Zhao M, Duncan ID (Oligodendrocytes are not inherently programmed to myelinate a specific size of axon. J Comp Neurol 399:94-100.1998).

Fandrich M, Fletcher MA, Dobson CM (Amyloid fibrils from muscle myoglobin. Nature 410:165-166.2001).

Fanelli MA, Cuello Carrion FD, Dekker J, Schoemaker J, Ciocca DR (Serological detection of heat shock protein hsp27 in normal and breast cancer patients. Cancer Epidemiol Biomarkers Prev 7:791-795.1998).

Farrer LA, Cupples LA, Kiely DK, Conneally PM, Myers RH (Inverse relationship between age at onset of Huntington disease and paternal age suggests involvement of genetic imprinting. Am J Hum Genet 50:528-535.1992).

Fennema-Notestine C, Archibald SL, Jacobson MW, Corey-Bloom J, Paulsen JS, Peavy GM, Gamst AC, Hamilton JM, Salmon DP, Jernigan TL (In vivo evidence of cerebellar atrophy and cerebral white matter loss in Huntington disease. Neurology 63:989-995.2004).

Fernandez-Funez P, Nino-Rosales ML, de Gouyon B, She WC, Luchak JM, Martinez P, Turiegano E, Benito J, Capovilla M, Skinner PJ, McCall A, Canal I, Orr HT, Zoghbi HY, Botas J (Identification of genes that modify ataxin-1-induced neurodegeneration. Nature 408:101-106.2000).

Fernandez AM, Fernandez S, Carrero P, Garcia-Garcia M, Torres-Aleman I (Calcineurin in reactive astrocytes plays a key role in the interplay between proinflammatory and anti-inflammatory signals. J Neurosci 27:8745-8756.2007).

Ferreiro E, Oliveira CR, Pereira CM (The release of calcium from the endoplasmic reticulum induced by amyloid-beta and prion peptides activates the mitochondrial apoptotic pathway. Neurobiol Dis 30:331-342.2008).

Ferri A, Nencini M, Casciati A, Cozzolino M, Angelini DF, Longone P, Spalloni A, Rotilio G, Carri MT (Cell death in amyotrophic lateral sclerosis: interplay between neuronal and glial cells. FASEB J 18:1261-1263.2004).

Fewell SW, Smith CM, Lyon MA, Dumitrescu TP, Wipf P, Day BW, Brodsky JL (Small molecule modulators of endogenous and co-chaperone-stimulated Hsp70 ATPase activity. J Biol Chem 279:51131-51140.2004).

Fitzner D, Schneider A, Kippert A, Mobius W, Willig KI, Hell SW, Bunt G, Gaus K, Simons M (Myelin basic protein-dependent plasma membrane reorganization in the formation of myelin. EMBO J 25:5037-5048.2006).

Fontaine JM, Rest JS, Welsh MJ, Benndorf R (The sperm outer dense fiber protein is the 10th member of the superfamily of mammalian small stress proteins. Cell Stress Chaperones 8:62-69.2003).

Fontaine JM, Sun X, Benndorf R, Welsh MJ (Interactions of HSP22 (HSPB8) with HSP20, alphaB-crystallin, and HSPB3. Biochem Biophys Res Commun 337:1006-1011.2005).

Frank M, van der Haar ME, Schaeren-Wiemers N, Schwab ME (rMAL is a glycosphingolipid-associated protein of myelin and apical membranes of epithelial cells in kidney and stomach. J Neurosci 18:4901-4913.1998).

Freeman W, Morton AJ (Regional and progressive changes in brain expression of complexin II in a mouse transgenic for the Huntington's disease mutation. Brain Res Bull 63:45-55.2004).

Friedman MJ, Shah AG, Fang ZH, Ward EG, Warren ST, Li S, Li XJ (Polyglutamine domain modulates the TBP-TFIIB interaction: implications for its normal function and neurodegeneration. Nat Neurosci 10:1519-1528.2007).

Fujita Y, Ohto E, Katayama E, Atomi Y (alphaB-Crystallin-coated MAP microtubule resists nocodazole and calcium-induced disassembly. J Cell Sci 117:1719-1726.2004).

Gabreels-Festen AA, Bolhuis PA, Hoogendijk JE, Valentijn LJ, Eshuis EJ, Gabreels FJ (Charcot-Marie-Tooth disease type 1A: morphological phenotype of the 17p duplication versus PMP22 point mutations. Acta Neuropathol 90:645-649.1995).

Gafni J, Ellerby LM (Calpain activation in Huntington's disease. J Neurosci 22:4842-4849.2002).

Ganea E (Chaperone-like activity of alpha-crystallin and other small heat shock proteins. Curr Protein Pept Sci 2:205-225.2001).

Garcia-Marin V, Garcia-Lopez P, Freire M (Cajal's contributions to glia research. Trends Neurosci 30:479-487.2007).

Gasser T (Molecular pathogenesis of Parkinson disease: insights from genetic studies. Expert Rev Mol Med 11:e22.2009).

Gauthier LR, Charrin BC, Borrell-Pages M, Dompierre JP, Rangone H, Cordelieres FP, De Mey J, MacDonald ME, Lessmann V, Humbert S, Saudou F (Huntingtin controls neurotrophic support and survival of neurons by enhancing BDNF vesicular transport along microtubules. Cell 118:127-138.2004).

Ghosh JG, Houck SA, Clark JI (Interactive sequences in the stress protein and molecular chaperone human alphaB crystallin recognize and modulate the assembly of filaments. Int J Biochem Cell Biol 39:1804-1815.2007).

Giasson BI, Ischiropoulos H, Lee VM, Trojanowski JQ (The relationship between oxidative/nitrative stress and pathological inclusions in Alzheimer's and Parkinson's diseases. Free Radic Biol Med 32:1264-1275.2002).

Giese A, Brown DR, Groschup MH, Feldmann C, Haist I, Kretzschmar HA (Role of microglia in neuronal cell death in prion disease. Brain Pathol 8:449-457.1998).

Gil JM, Rego AC (Mechanisms of neurodegeneration in Huntington's disease. Eur J Neurosci 27:2803-2820.2008).

Gilmore CP, DeLuca GC, Bo L, Owens T, Lowe J, Esiri MM, Evangelou N (Spinal cord neuronal pathology in multiple sclerosis. Brain Pathol 19:642-649.2009).

Giuditta A, Chun JT, Eyman M, Cefaliello C, Bruno AP, Crispino M (Local gene expression in axons and nerve endings: the glia-neuron unit. Physiol Rev 88:515-555.2008).

Glickman MH, Maytal V (Regulating the 26S proteasome. Curr Top Microbiol Immunol 268:43-72.2002).

Goldbaum O, Richter-Landsberg C (Stress proteins in oligodendrocytes: differential effects of heat shock and oxidative stress. J Neurochem 78:1233-1242.2001).

Goldberg AL (Protein degradation and protection against misfolded or damaged proteins. Nature 426:895-899.2003).

Golenhofen N, Perng MD, Quinlan RA, Drenckhahn D (Comparison of the small heat shock proteins alphaB-crystallin, MKBP, HSP25, HSP20, and cvHSP in heart and skeletal muscle. Histochem Cell Biol 122:415-425.2004).

Gonzalez L, Martin S, Begara-McGorum I, Hunter N, Houston F, Simmons M, Jeffrey M (Effects of agent strain and host genotype on PrP accumulation in the brain of sheep naturally and experimentally affected with scrapie. J Comp Pathol 126:17-29.2002).

Gow A, Southwood CM, Li JS, Pariali M, Riordan GP, Brodie SE, Danias J, Bronstein JM, Kachar B, Lazzarini RA (CNS myelin and sertoli cell tight junction strands are absent in Osp/claudin-11 null mice. Cell 99:649-659.1999).

Grami V, Marrero Y, Huang L, Tang D, Yappert MC, Borchman D (alpha-Crystallin binding in vitro to lipids from clear human lenses. Exp Eye Res 81:138-146.2005).

Graner MW, Cumming RI, Bigner DD (The heat shock response and chaperones/heat shock proteins in brain tumors: surface expression, release, and possible immune consequences. J Neurosci 27:11214-11227.2007).

Gravel M, Peterson J, Yong VW, Kottis V, Trapp B, Braun PE (Overexpression of 2',3'-cyclic nucleotide 3'-phosphodiesterase in transgenic mice alters oligodendrocyte development and produces aberrant myelination. Mol Cell Neurosci 7:453-466.1996).

Gray BC, Siskova Z, Perry VH, O'Connor V (Selective presynaptic degeneration in the synaptopathy associated with ME7-induced hippocampal pathology. Neurobiol Dis 35:63-74.2009).

Gray BC, Skipp P, O'Connor VM, Perry VH (Increased expression of glial fibrillary acidic protein fragments and mu-calpain activation within the hippocampus of prion-infected mice. Biochem Soc Trans 34:51-54.2006).

Griffiths I, Klugmann M, Anderson T, Thomson C, Vouyiouklis D, Nave KA (Current concepts of PLP and its role in the nervous system. Microsc Res Tech 41:344-358.1998).

Gu F, Luo W, Li X, Wang Z, Lu S, Zhang M, Zhao B, Zhu S, Feng S, Yan YB, Huang S, Ma X (A novel mutation in AlphaA-crystallin (CRYAA) caused autosomal dominant congenital cataract in a large Chinese family. Hum Mutat 29:769.2008).

Gu Y, Fujioka H, Mishra RS, Li R, Singh N (Prion peptide 106-126 modulates the aggregation of cellular prion protein and induces the synthesis of potentially neurotoxic transmembrane PrP. J Biol Chem 277:2275-2286.2002).

Guentchev M, Voigtlander T, Haberler C, Groschup MH, Budka H (Evidence for oxidative stress in experimental prion disease. Neurobiol Dis 7:270-273.2000).

Guidot DM, McCord JM, Wright RM, Repine JE (Absence of electron transport (Rho 0 state) restores growth of a manganese-superoxide dismutase-deficient Saccharomyces cerevisiae in hyperoxia. Evidence for electron transport as a major source of superoxide generation in vivo. J Biol Chem 268:26699-26703.1993).

Guijarro JI, Sunde M, Jones JA, Campbell ID, Dobson CM (Amyloid fibril formation by an SH3 domain. Proc Natl Acad Sci U S A 95:4224-4228.1998).

Gunawardena S, Her LS, Brusch RG, Laymon RA, Niesman IR, Gordesky-Gold B, Sintasath L, Bonini NM, Goldstein LS (Disruption of axonal transport by loss of huntingtin or expression of pathogenic polyQ proteins in Drosophila. Neuron 40:25-40.2003).

Haak J, Kregel KC (1962-2007: a cell stress odyssey. Novartis Found Symp 291:3-15; discussion 15-22, 137-140.2008).

Hagemann TL, Boelens WC, Wawrousek EF, Messing A (Suppression of GFAP toxicity by alphaB-crystallin in mouse models of Alexander disease. Hum Mol Genet 18:1190-1199.2009).

Haley DA, Horwitz J, Stewart PL (The small heat-shock protein, alphaB-crystallin, has a variable quaternary structure. J Mol Biol 277:27-35.1998).

Hampel H, Teipel SJ, Alexander GE, Pogarell O, Rapoport SI, Moller HJ (In vivo imaging of region and cell type specific neocortical neurodegeneration in Alzheimer's disease. Perspectives of MRI derived corpus callosum measurement for mapping disease progression and effects of therapy. Evidence from studies with MRI, EEG and PET. J Neural Transm 109:837-855.2002).

Hansson O, Castilho RF, Korhonen L, Lindholm D, Bates GP, Brundin P (Partial resistance to malonate-induced striatal cell death in transgenic mouse models of Huntington's disease is dependent on age and CAG repeat length. J Neurochem 78:694-703.2001a).

Hansson O, Guatteo E, Mercuri NB, Bernardi G, Li XJ, Castilho RF, Brundin P (Resistance to NMDA toxicity correlates with appearance of nuclear inclusions, behavioural deficits and changes in calcium homeostasis in mice transgenic for exon 1 of the huntington gene. Eur J Neurosci 14:1492-1504.2001b).

Harris DA, Lele P, Snider WD (Localization of the mRNA for a chicken prion protein by in situ hybridization. Proc Natl Acad Sci U S A 90:4309-4313.1993).

Haslbeck M (sHsps and their role in the chaperone network. Cell Mol Life Sci 59:1649-1657.2002).

Haslbeck M, Buchner J (Chaperone function of sHsps. Prog Mol Subcell Biol 28:37-59.2002).

Haslbeck M, Franzmann T, Weinfurtner D, Buchner J (Some like it hot: the structure and function of small heat-shock proteins. Nat Struct Mol Biol 12:842-846.2005).

Haslbeck M, Kastenmuller A, Buchner J, Weinkauf S, Braun N (Structural dynamics of archaeal small heat shock proteins. J Mol Biol 378:362-374.2008).

Haslbeck M, Walke S, Stromer T, Ehrnsperger M, White HE, Chen S, Saibil HR, Buchner J (Hsp26: a temperature-regulated chaperone. EMBO J 18:6744-6751.1999).

Havasi A, Li Z, Wang Z, Martin JL, Botla V, Ruchalski K, Schwartz JH, Borkan SC (Hsp27 inhibits Bax activation and apoptosis via a phosphatidylinositol 3-kinase-dependent mechanism. J Biol Chem 283:12305-12313.2008).

Hay DG, Sathasivam K, Tobaben S, Stahl B, Marber M, Mestril R, Mahal A, Smith DL, Woodman B, Bates GP (Progressive decrease in chaperone protein levels in a mouse model of Huntington's disease and induction of stress proteins as a therapeutic approach. Hum Mol Genet 13:1389-1405.2004).

Heath AR, Hindman HM (CNPase activity in the vertebrate retina, retinal pigmented epithelium, and choroid. J Exp Zool 238:183-191.1986).

Hermel E, Gafni J, Propp SS, Leavitt BR, Wellington CL, Young JE, Hackam AS, Logvinova AV, Peel AL, Chen SF, Hook V, Singaraja R, Krajewski S, Goldsmith PC, Ellerby HM, Hayden MR, Bredesen DE, Ellerby LM (Specific caspase interactions and amplification are involved in selective neuronal vulnerability in Huntington's disease. Cell Death Differ 11:424-438.2004).

Hewett JA (Determinants of regional and local diversity within the astroglial lineage of the normal central nervous system. J Neurochem 110:1717-1736.2009).

Hill CP, Masters EI, Whitby FG (The 11S regulators of 20S proteasome activity. Curr Top Microbiol Immunol 268:73-89.2002).

Hinman JD, Chen CD, Oh SY, Hollander W, Abraham CR (Age-dependent accumulation of ubiquitinated 2',3'-cyclic nucleotide 3'-phosphodiesterase in myelin lipid rafts. Glia 56:118-133.2008).

Hodges A, Strand AD, Aragaki AK, Kuhn A, Sengstag T, Hughes G, Elliston LA, Hartog C, Goldstein DR, Thu D, Hollingsworth ZR, Collin F, Synek B, Holmans PA, Young AB, Wexler NS, Delorenzi M, Kooperberg C, Augood SJ, Faull RL, Olson JM, Jones L, Luthi-Carter R (Regional and cellular gene expression changes in human Huntington's disease brain. Hum Mol Genet 15:965-977.2006).

Hodgson JG, Agopyan N, Gutekunst CA, Leavitt BR, LePiane F, Singaraja R, Smith DJ, Bissada N, McCutcheon K, Nasir J, Jamot L, Li XJ, Stevens ME, Rosemond E, Roder JC, Phillips AG, Rubin EM, Hersch SM, Hayden MR (A YAC mouse model for Huntington's disease with full-length mutant huntingtin, cytoplasmic toxicity, and selective striatal neurodegeneration. Neuron 23:181-192.1999).

Holley JE, Gveric D, Newcombe J, Cuzner ML, Gutowski NJ (Astrocyte characterization in the multiple sclerosis glial scar. Neuropathol Appl Neurobiol 29:434-444.2003).

Homma S, Jin X, Wang G, Tu N, Min J, Yanasak N, Mivechi NF (Demyelination, astrogliosis, and accumulation of ubiquitinated proteins, hallmarks of CNS disease in hsf1-deficient mice. J Neurosci 27:7974-7986.2007).

Horwich AL, Fenton WA, Chapman E, Farr GW (Two families of chaperonin: physiology and mechanism. Annu Rev Cell Dev Biol 23:115-145.2007).

Houades V, Koulakoff A, Ezan P, Seif I, Giaume C (Gap junction-mediated astrocytic networks in the mouse barrel cortex. J Neurosci 28:5207-5217.2008).

Hu W, Rosenberg RN, Stuve O (Prion proteins: a biological role beyond prion diseases. Acta Neurol Scand 116:75-82.2007).

Hur EM, Youssef S, Haws ME, Zhang SY, Sobel RA, Steinman L (Osteopontin-induced relapse and progression of autoimmune brain disease through enhanced survival of activated T cells. Nat Immunol 8:74-83.2007).

Husain J, Juurlink BH (Oligodendroglial precursor cell susceptibility to hypoxia is related to poor ability to cope with reactive oxygen species. Brain Res 698:86-94.1995).

Hylander BL, Chen X, Graf PC, Subjeck JR (The distribution and localization of hsp110 in brain. Brain Res 869:49-55.2000).

Ihara M, Polvikoski TM, Hall R, Slade JY, Perry RH, Oakley AE, Englund E, O'Brien JT, Ince PG, Kalaria RN (Quantification of myelin loss in frontal lobe white matter in vascular dementia, Alzheimer's disease, and dementia with Lewy bodies. Acta Neuropathol.2010).

Imarisio S, Carmichael J, Korolchuk V, Chen CW, Saiki S, Rose C, Krishna G, Davies JE, Ttofi E, Underwood BR, Rubinsztein DC (Huntington's disease: from pathology and genetics to potential therapies. Biochem J 412:191-209.2008).

Inagaki N, Hayashi T, Arimura T, Koga Y, Takahashi M, Shibata H, Teraoka K, Chikamori T, Yamashina A, Kimura A (Alpha B-crystallin mutation in dilated cardiomyopathy. Biochem Biophys Res Commun 342:379-386.2006).

Irobi J, Van Impe K, Seeman P, Jordanova A, Dierick I, Verpoorten N, Michalik A, De Vriendt E, Jacobs A, Van Gerwen V, Vennekens K, Mazanec R, Tournev I, Hilton-Jones D, Talbot K, Kremensky I, Van Den Bosch L, Robberecht W, Van

Vandekerckhove J, Van Broeckhoven C, Gettemans J, De Jonghe P, Timmerman V (Hot-spot residue in small heat-shock protein 22 causes distal motor neuropathy. Nat Genet 36:597-601.2004).

Ishibashi T, Ding L, Ikenaka K, Inoue Y, Miyado K, Mekada E, Baba H (Tetraspanin protein CD9 is a novel paranodal component regulating paranodal junctional formation. J Neurosci 24:96-102.2004).

Ito H, Kamei K, Iwamoto I, Inaguma Y, Tsuzuki M, Kishikawa M, Shimada A, Hosokawa M, Kato K (Hsp27 suppresses the formation of inclusion bodies induced by expression of R120G alpha B-crystallin, a cause of desmin-related myopathy. Cell Mol Life Sci 60:1217-1223.2003).

Iwaki T, Wisniewski T, Iwaki A, Corbin E, Tomokane N, Tateishi J, Goldman JE (Accumulation of alpha B-crystallin in central nervous system glia and neurons in pathologic conditions. Am J Pathol 140:345-356.1992).

Jackson TC, Rani A, Kumar A, Foster TC (Regional hippocampal differences in AKT survival signaling across the lifespan: implications for CA1 vulnerability with aging. Cell Death Differ 16:439-448.2009).

Jacobsen JC, Bawden CS, Rudiger SR, McLaughlan CJ, Reid SJ, Waldvogel HJ, Macdonald ME, Gusella JF, Walker SK, Kelly JM, Webb GC, Faull RL, Rees MI, Snell RG (An ovine transgenic Huntington's disease model. Hum Mol Genet.2010).

Jahn O, Tenzer S, Werner HB (Myelin proteomics: molecular anatomy of an insulating sheath. Mol Neurobiol 40:55-72.2009).

Jakob U, Gaestel M, Engel K, Buchner J (Small heat shock proteins are molecular chaperones. J Biol Chem 268:1517-1520.1993).

Jamieson E, Jeffrey M, Ironside JW, Fraser JR (Apoptosis and dendritic dysfunction precede prion protein accumulation in 87V scrapie. Neuroreport 12:2147-2153.2001).

Jana NR, Nukina N (Recent advances in understanding the pathogenesis of polyglutamine diseases: involvement of molecular chaperones and ubiquitin-proteasome pathway. J Chem Neuroanat 26:95-101.2003).

Jansson M, Panoutsakopoulou V, Baker J, Klein L, Cantor H (Cutting edge: Attenuated experimental autoimmune encephalomyelitis in eta-1/osteopontin-deficient mice. J Immunol 168:2096-2099.2002).

Jean YY, Lercher LD, Dreyfus CF (Glutamate elicits release of BDNF from basal forebrain astrocytes in a process dependent on metabotropic receptors and the PLC pathway. Neuron Glia Biol 4:35-42.2008).

Jeffrey M, Goodsir CM, Bruce ME, McBride PA, Fowler N, Scott JR (Murine scrapie-infected neurons in vivo release excess prion protein into the extracellular space. Neurosci Lett 174:39-42.1994).

Jeffrey M, Halliday WG, Bell J, Johnston AR, MacLeod NK, Ingham C, Sayers AR, Brown DA, Fraser JR (Synapse loss associated with abnormal PrP precedes neuronal degeneration in the scrapie-infected murine hippocampus. Neuropathol Appl Neurobiol 26:41-54.2000).

Jellinger KA (Recent advances in our understanding of neurodegeneration. J Neural Transm 116:1111-1162.2009).

Jendroska K, Heinzel FP, Torchia M, Stowring L, Kretzschmar HA, Kon A, Stern A, Prusiner SB, DeArmond SJ (Proteinase-resistant prion protein accumulation in

Syrian hamster brain correlates with regional pathology and scrapie infectivity. Neurology 41:1482-1490.1991).

Jernigan TL, Salmon DP, Butters N, Hesselink JR (Cerebral structure on MRI, Part II: Specific changes in Alzheimer's and Huntington's diseases. Biol Psychiatry 29:68-81.1991).

Jiao W, Li P, Zhang J, Zhang H, Chang Z (Small heat-shock proteins function in the insoluble protein complex. Biochem Biophys Res Commun 335:227-231.2005).

Johnson RT (Prion diseases. Lancet Neurol 4:635-642.2005).

Juurlink BH (Response of glial cells to ischemia: roles of reactive oxygen species and glutathione. Neurosci Biobehav Rev 21:151-166.1997).

Kabashi E, Durham HD (Failure of protein quality control in amyotrophic lateral sclerosis. Biochim Biophys Acta 1762:1038-1050.2006).

Kachar B, Behar T, Dubois-Dalcq M (Cell shape and motility of oligodendrocytes cultured without neurons. Cell Tissue Res 244:27-38.1986).

Kampinga HH, Hageman J, Vos MJ, Kubota H, Tanguay RM, Bruford EA, Cheetham ME, Chen B, Hightower LE (Guidelines for the nomenclature of the human heat shock proteins. Cell Stress Chaperones 14:105-111.2009).

Kamradt MC, Chen F, Sam S, Cryns VL (The small heat shock protein alpha B-crystallin negatively regulates apoptosis during myogenic differentiation by inhibiting caspase-3 activation. J Biol Chem 277:38731-38736.2002).

Kamradt MC, Lu M, Werner ME, Kwan T, Chen F, Strohecker A, Oshita S, Wilkinson JC, Yu C, Oliver PG, Duckett CS, Buchsbaum DJ, LoBuglio AF, Jordan VC, Cryns VL (The small heat shock protein alpha B-crystallin is a novel inhibitor of TRAIL-induced apoptosis that suppresses the activation of caspase-3. J Biol Chem 280:11059-11066.2005).

Kappe G, Franck E, Verschuure P, Boelens WC, Leunissen JA, de Jong WW (The human genome encodes 10 alpha-crystallin-related small heat shock proteins: HspB1-10. Cell Stress Chaperones 8:53-61.2003).

Kappe G, Verschuure P, Philipsen RL, Staalduinen AA, Van de Boogaart P, Boelens WC, De Jong WW (Characterization of two novel human small heat shock proteins: protein kinase-related HspB8 and testis-specific HspB9. Biochim Biophys Acta 1520:1-6.2001).

Kassubek J, Bernhard Landwehrmeyer G, Ecker D, Juengling FD, Muche R, Schuller S, Weindl A, Peinemann A (Global cerebral atrophy in early stages of Huntington's disease: quantitative MRI study. Neuroreport 15:363-365.2004).

Kato H, Kogure K, Liu XH, Araki T, Kato K, Itoyama Y (Immunohistochemical localization of the low molecular weight stress protein HSP27 following focal cerebral ischemia in the rat. Brain Res 679:1-7.1995).

Kato K, Shinohara H, Kurobe N, Goto S, Inaguma Y, Ohshima K (Immunoreactive alpha A crystallin in rat non-lenticular tissues detected with a sensitive immunoassay method. Biochim Biophys Acta 1080:173-180.1991).

Katona I, Sperlagh B, Sik A, Kafalvi A, Vizi ES, Mackie K, Freund TF (Presynaptically located CB1 cannabinoid receptors regulate GABA release from axon terminals of specific hippocampal interneurons. J Neurosci 19:4544-4558.1999).

Kaye EM (Update on genetic disorders affecting white matter. Pediatr Neurol 24:11-24.2001).

Kelly BM, Gillespie CS, Sherman DL, Brophy PJ (Schwann cells of the myelin-forming phenotype express neurofilament protein NF-M. J Cell Biol 118:397-410.1992).

Khosravani H, Zhang Y, Tsutsui S, Hameed S, Altier C, Hamid J, Chen L, Villemaire M, Ali Z, Jirik FR, Zamponi GW (Prion protein attenuates excitotoxicity by inhibiting NMDA receptors. J Cell Biol 181:551-565.2008).

Kijima K, Numakura C, Goto T, Takahashi T, Otagiri T, Umetsu K, Hayasaka K (Small heat shock protein 27 mutation in a Japanese patient with distal hereditary motor neuropathy. J Hum Genet 50:473-476.2005).

Kim JI, Ju WK, Choi JH, Choi E, Carp RI, Wisniewski HM, Kim YS (Expression of cytokine genes and increased nuclear factor-kappa B activity in the brains of scrapie-infected mice. Brain Res Mol Brain Res 73:17-27.1999).

Kim KK, Kim R, Kim SH (Crystal structure of a small heat-shock protein. Nature 394:595-599.1998).

Kim MV, Seit-Nebi AS, Gusev NB (The problem of protein kinase activity of small heat shock protein Hsp22 (H11 or HspB8). Biochem Biophys Res Commun 325:649-652.2004).

Kim R, Lai L, Lee HH, Cheong GW, Kim KK, Wu Z, Yokota H, Marqusee S, Kim SH (On the mechanism of chaperone activity of the small heat-shock protein of Methanococcus jannaschii. Proc Natl Acad Sci U S A 100:8151-8155.2003).

Kim T, Pfeiffer SE (Myelin glycosphingolipid/cholesterol-enriched microdomains selectively sequester the non-compact myelin proteins CNP and MOG. J Neurocytol 28:281-293.1999).

King MA, Hands S, Hafiz F, Mizushima N, Tolkovsky AM, Wyttenbach A (Rapamycin inhibits polyglutamine aggregation independently of autophagy by reducing protein synthesis. Mol Pharmacol 73:1052-1063.2008).

Kippert A, Trajkovic K, Rajendran L, Ries J, Simons M (Rho regulates membrane transport in the endocytic pathway to control plasma membrane specialization in oligodendroglial cells. J Neurosci 27:3560-3570.2007).

Klamt F, Dal-Pizzol F, Conte da Frota MJ, Walz R, Andrades ME, da Silva EG, Brentani RR, Izquierdo I, Fonseca Moreira JC (Imbalance of antioxidant defense in mice lacking cellular prion protein. Free Radic Biol Med 30:1137-1144.2001).

Klapstein GJ, Fisher RS, Zanjani H, Cepeda C, Jokel ES, Chesselet MF, Levine MS (Electrophysiological and morphological changes in striatal spiny neurons in R6/2 Huntington's disease transgenic mice. J Neurophysiol 86:2667-2677.2001).

Klemenz R, Andres AC, Frohli E, Schafer R, Aoyama A (Expression of the murine small heat shock proteins hsp 25 and alpha B crystallin in the absence of stress. J Cell Biol 120:639-645.1993).

Kobayashi Y, Kume A, Li M, Doyu M, Hata M, Ohtsuka K, Sobue G (Chaperones Hsp70 and Hsp40 suppress aggregate formation and apoptosis in cultured neuronal cells expressing truncated androgen receptor protein with expanded polyglutamine tract. J Biol Chem 275:8772-8778.2000).

Kolesar D, Kolesarova M, Pavel J, Davidova A, Marsala J, Lukacova N (Region-specific sensitivity of the spinal cord to ischemia/reperfusion: the dynamic of changes in catalytic NOS activity. J Physiol Sci 59:97-103.2009).

Kolesarova M, Pavel J, Lukacova N, Kolesar D, Marsala J (Effect of ischemia in vivo and oxygen-glucose deprivation in vitro on NOS pools in the spinal cord: comparative study. Cell Mol Neurobiol 26:1281-1294.2006).

Komalavilas P, Penn RB, Flynn CR, Thresher J, Lopes LB, Furnish EJ, Guo M, Pallero MA, Murphy-Ullrich JE, Brophy CM (The small heat shock-related protein, HSP20, is a cAMP-dependent protein kinase substrate that is involved in airway smooth muscle relaxation. Am J Physiol Lung Cell Mol Physiol 294:L69-78.2008).

Kopito RR (Aggresomes, inclusion bodies and protein aggregation. Trends Cell Biol 10:524-530.2000).

Kordek R, Hainfellner JA, Liberski PP, Budka H (Deposition of the prion protein (PrP) during the evolution of experimental Creutzfeldt-Jakob disease. Acta Neuropathol 98:597-602.1999).

Kordek R, Liberski PP, Yanagihara R, Isaacson S, Gajdusek DC (Molecular analysis of prion protein (PrP) and glial fibrillary acidic protein (GFAP) transcripts in experimental Creutzfeldt-Jakob disease in mice. Acta Neurobiol Exp (Wars) 57:85-90.1997).

Korhonen L, Lindholm D (The ubiquitin proteasome system in synaptic and axonal degeneration: a new twist to an old cycle. J Cell Biol 165:27-30.2004).

Kovacs GG, Budka H (Prion diseases: from protein to cell pathology. Am J Pathol 172:555-565.2008).

Kovacs GG, Gelpi E, Strobel T, Ricken G, Nyengaard JR, Bernheimer H, Budka H (Involvement of the endosomal-lysosomal system correlates with regional pathology in Creutzfeldt-Jakob disease. J Neuropathol Exp Neurol 66:628-636.2007).

Kowaltowski AJ, de Souza-Pinto NC, Castilho RF, Vercesi AE (Mitochondria and reactive oxygen species. Free Radic Biol Med 47:333-343.2009).

Kramer EM, Schardt A, Nave KA (Membrane traffic in myelinating oligodendrocytes. Microsc Res Tech 52:656-671.2001).

Krief S, Faivre JF, Robert P, Le Douarin B, Brument-Larignon N, Lefrere I, Bouzyk MM, Anderson KM, Greller LD, Tobin FL, Souchet M, Bril A (Identification and characterization of cvHsp. A novel human small stress protein selectively expressed in cardiovascular and insulin-sensitive tissues. J Biol Chem 274:36592-36600.1999).

Krishna P, Gloor G (The Hsp90 family of proteins in Arabidopsis thaliana. Cell Stress Chaperones 6:238-246.2001).

Kristiansen M, Deriziotis P, Dimcheff DE, Jackson GS, Ovaa H, Naumann H, Clarke AR, van Leeuwen FW, Menendez-Benito V, Dantuma NP, Portis JL, Collinge J, Tabrizi SJ (Disease-associated prion protein oligomers inhibit the 26S proteasome. Mol Cell 26:175-188.2007).

Kuhl D, Skehel P (Dendritic localization of mRNAs. Curr Opin Neurobiol 8:600-606.1998).

Kurihara T, Tsukada Y (The regional and subcellular distribution of 2',3'-cyclic nucleotide 3'-phosphohydrolase in the central nervous system. J Neurochem 14:1167-1174.1967).

Kursula P (Structural properties of proteins specific to the myelin sheath. Amino Acids 34:175-185.2008).

Larocca JN, Rodriguez-Gabin AG (Myelin biogenesis: vesicle transport in oligodendrocytes. Neurochem Res 27:1313-1329.2002).

Lassmann H, Lucchinetti CF (Cortical demyelination in CNS inflammatory demyelinating diseases. Neurology 70:332-333.2008).

Lee DW, Sohn HO, Lim HB, Lee YG, Kim YS, Carp RI, Wisniewski HM (Alteration of free radical metabolism in the brain of mice infected with scrapie agent. Free Radic Res 30:499-507.1999).

Lee HP, Jun YC, Choi JK, Kim JI, Carp RI, Kim YS (Activation of mitogen-activated protein kinases in hamster brains infected with 263K scrapie agent. J Neurochem 95:584-593.2005a).

Lee J, Gravel M, Zhang R, Thibault P, Braun PE (Process outgrowth in oligodendrocytes is mediated by CNP, a novel microtubule assembly myelin protein. J Cell Biol 170:661-673.2005b).

Lee MK, Stirling W, Xu Y, Xu X, Qui D, Mandir AS, Dawson TM, Copeland NG, Jenkins NA, Price DL (Human alpha-synuclein-harboring familial Parkinson's disease-linked Ala-53 --> Thr mutation causes neurodegenerative disease with alpha-synuclein aggregation in transgenic mice. Proc Natl Acad Sci U S A 99:8968-8973.2002).

Lee WC, Yoshihara M, Littleton JT (Cytoplasmic aggregates trap polyglutamine-containing proteins and block axonal transport in a Drosophila model of Huntington's disease. Proc Natl Acad Sci U S A 101:3224-3229.2004).

Lein ES, Hawrylycz MJ, Ao N, Ayres M, Bensinger A, Bernard A, Boe AF, Boguski MS, Brockway KS, Byrnes EJ, Chen L, Chen TM, Chin MC, Chong J, Crook BE, Czaplinska A, Dang CN, Datta S, Dee NR, Desaki AL, Desta T, Diep E, Dolbeare TA, Donelan MJ, Dong HW, Dougherty JG, Duncan BJ, Ebbert AJ, Eichele G, Estin LK, Faber C, Facer BA, Fields R, Fischer SR, Fliss TP, Frensley C, Gates SN, Glattfelder KJ, Halverson KR, Hart MR, Hohmann JG, Howell MP, Jeung DP, Johnson RA, Karr PT, Kawal R, Kidney JM, Knapik RH, Kuan CL, Lake JH, Laramee AR, Larsen KD, Lau C, Lemon TA, Liang AJ, Liu Y, Luong LT, Michaels J, Morgan JJ, Morgan RJ, Mortrud MT, Mosqueda NF, Ng LL, Ng R, Orta GJ, Overly CC, Pak TH, Parry SE, Pathak SD, Pearson OC, Puchalski RB, Riley ZL, Rockett HR, Rowland SA, Royall JJ, Ruiz MJ, Sarno NR, Schaffnit K, Shapovalova NV, Sivisay T, Slaughterbeck CR, Smith SC, Smith KA, Smith BI, Sodt AJ, Stewart NN, Stumpf KR, Sunkin SM, Sutram M, Tam A, Teemer CD, Thaller C, Thompson CL, Varnam LR, Visel A, Whitlock RM, Wohnoutka PE, Wolkey CK, Wong VY, Wood M, Yaylaoglu MB, Young RC, Youngstrom BL, Yuan XF, Zhang B, Zwingman TA, Jones AR (Genome-wide atlas of gene expression in the adult mouse brain. Nature 445:168-176.2007).

Lein ES, Zhao X, Gage FH (Defining a molecular atlas of the hippocampus using DNA microarrays and high-throughput in situ hybridization. J Neurosci 24:3879-3889.2004).

Levchenko I, Yamauchi M, Baker TA (ClpX and MuB interact with overlapping regions of Mu transposase: implications for control of the transposition pathway. Genes Dev 11:1561-1572.1997).

Li JY, Plomann M, Brundin P (Huntington's disease: a synaptopathy? Trends Mol Med 9:414-420.2003).

Li SH, Li XJ (Huntingtin and its role in neuronal degeneration. Neuroscientist 10:467-475.2004).

Li X, Standley C, Sapp E, Valencia A, Qin ZH, Kegel KB, Yoder J, Comer-Tierney LA, Esteves M, Chase K, Alexander J, Masso N, Sobin L, Bellve K, Tuft R, Lifshitz L, Fogarty K, Aronin N, DiFiglia M (Mutant huntingtin impairs vesicle formation from recycling endosomes by interfering with Rab11 activity. Mol Cell Biol 29:6106-6116.2009).

Liberski PP, Ironside JW (An outline of the neuropathology of transmissible spongiform encephalopathies (prion diseases). Folia Neuropathol 42 Suppl B:39-58.2004).

Lin CH, Tallaksen-Greene S, Chien WM, Cearley JA, Jackson WS, Crouse AB, Ren S, Li XJ, Albin RL, Detloff PJ (Neurological abnormalities in a knock-in mouse model of Huntington's disease. Hum Mol Genet 10:137-144.2001).

Lin SC, Bergles DE (Physiological characteristics of NG2-expressing glial cells. J Neurocytol 31:537-549.2002).

Lindquist S (The heat-shock response. Annu Rev Biochem 55:1151-1191.1986).

Lione LA, Carter RJ, Hunt MJ, Bates GP, Morton AJ, Dunnett SB (Selective discrimination learning impairments in mice expressing the human Huntington's disease mutation. J Neurosci 19:10428-10437.1999).

Litt M, Kramer P, LaMorticella DM, Murphey W, Lovrien EW, Weleber RG (Autosomal dominant congenital cataract associated with a missense mutation in the human alpha crystallin gene CRYAA. Hum Mol Genet 7:471-474.1998).

Liu M, Ke T, Wang Z, Yang Q, Chang W, Jiang F, Tang Z, Li H, Ren X, Wang X, Wang T, Li Q, Yang J, Liu J, Wang QK (Identification of a CRYAB mutation associated with autosomal dominant posterior polar cataract in a Chinese family. Invest Ophthalmol Vis Sci 47:3461-3466.2006).

Liu S, Li J, Tao Y, Xiao X (Small heat shock protein alphaB-crystallin binds to p53 to sequester its translocation to mitochondria during hydrogen peroxide-induced apoptosis. Biochem Biophys Res Commun 354:109-114.2007).

Lorenzetti D, Watase K, Xu B, Matzuk MM, Orr HT, Zoghbi HY (Repeat instability and motor incoordination in mice with a targeted expanded CAG repeat in the Sca1 locus. Hum Mol Genet 9:779-785.2000).

Lowe J, Errington DR, Lennox G, Pike I, Spendlove I, Landon M, Mayer RJ (Ballooned neurons in several neurodegenerative diseases and stroke contain alpha B crystallin. Neuropathol Appl Neurobiol 18:341-350.1992).

Lowe MJ, Horenstein C, Hirsch JG, Marrie RA, Stone L, Bhattacharyya PK, Gass A, Phillips MD (Functional pathway-defined MRI diffusion measures reveal increased transverse diffusivity of water in multiple sclerosis. Neuroimage 32:1127-1133.2006).

Ludwin SK, Bakker DA (Can oligodendrocytes attached to myelin proliferate? J Neurosci 8:1239-1244.1988).

Lunn KF, Baas PW, Duncan ID (Microtubule organization and stability in the oligodendrocyte. J Neurosci 17:4921-4932.1997).

Luo S, Vacher C, Davies JE, Rubinsztein DC (Cdk5 phosphorylation of huntingtin reduces its cleavage by caspases: implications for mutant huntingtin toxicity. J Cell Biol 169:647-656.2005).

Luthi-Carter R, Strand A, Peters NL, Solano SM, Hollingsworth ZR, Menon AS, Frey AS, Spektor BS, Penney EB, Schilling G, Ross CA, Borchelt DR, Tapscott SJ, Young AB, Cha JH, Olson JM (Decreased expression of striatal signaling genes in a mouse model of Huntington's disease. Hum Mol Genet 9:1259-1271.2000).

Lynch MA (The multifaceted profile of activated microglia. Mol Neurobiol 40:139-156.2009).

Ma L, Morton AJ, Nicholson LF (Microglia density decreases with age in a mouse model of Huntington's disease. Glia 43:274-280.2003).

Mabbott NA, Williams A, Farquhar CF, Pasparakis M, Kollias G, Bruce ME (Tumor necrosis factor alpha-deficient, but not interleukin-6-deficient, mice resist peripheral infection with scrapie. J Virol 74:3338-3344.2000).

Macara IG, Iioka H, Mili S (Axon growth-stimulus package includes local translation. Nat Cell Biol 11:919-921.2009).

Mackay DS, Boskovska OB, Knopf HL, Lampi KJ, Shiels A (A nonsense mutation in CRYBB1 associated with autosomal dominant cataract linked to human chromosome 22q. Am J Hum Genet 71:1216-1221.2002).

Maglio LE, Perez MF, Martins VR, Brentani RR, Ramirez OA (Hippocampal synaptic plasticity in mice devoid of cellular prion protein. Brain Res Mol Brain Res 131:58-64.2004).

Maier O, Hoekstra D, Baron W (Polarity development in oligodendrocytes: sorting and trafficking of myelin components. J Mol Neurosci 35:35-53.2008).

Majeski AE, Dice JF (Mechanisms of chaperone-mediated autophagy. Int J Biochem Cell Biol 36:2435-2444.2004).

Mallucci GR, Ratte S, Asante EA, Linehan J, Gowland I, Jefferys JG, Collinge J (Post-natal knockout of prion protein alters hippocampal CA1 properties, but does not result in neurodegeneration. EMBO J 21:202-210.2002).

Mangiarini L, Sathasivam K, Seller M, Cozens B, Harper A, Hetherington C, Lawton M, Trottier Y, Lehrach H, Davies SW, Bates GP (Exon 1 of the HD gene with an expanded CAG repeat is sufficient to cause a progressive neurological phenotype in transgenic mice. Cell 87:493-506.1996).

Mangin JM, Kunze A, Chittajallu R, Gallo V (Satellite NG2 progenitor cells share common glutamatergic inputs with associated interneurons in the mouse dentate gyrus. J Neurosci 28:7610-7623.2008).

Maragakis NJ, Rothstein JD (Mechanisms of Disease: astrocytes in neurodegenerative disease. Nat Clin Pract Neurol 2:679-689.2006).

Marchetti B, Serra PA, Tirolo C, L'Episcopo F, Caniglia S, Gennuso F, Testa N, Miele E, Desole S, Barden N, Morale MC (Glucocorticoid receptor-nitric oxide crosstalk and vulnerability to experimental parkinsonism: pivotal role for glia-neuron interactions. Brain Res Brain Res Rev 48:302-321.2005).

Martini R, Mohajeri MH, Kasper S, Giese KP, Schachner M (Mice doubly deficient in the genes for P0 and myelin basic protein show that both proteins contribute to the formation of the major dense line in peripheral nerve myelin. J Neurosci 15:4488-4495.1995).

Matsuo A, Lee GC, Terai K, Takami K, Hickey WF, McGeer EG, McGeer PL (Unmasking of an unusual myelin basic protein epitope during the process of

myelin degeneration in humans: a potential mechanism for the generation of autoantigens. Am J Pathol 150:1253-1266.1997).

Matthias K, Kirchhoff F, Seifert G, Huttmann K, Matyash M, Kettenmann H, Steinhauser C (Segregated expression of AMPA-type glutamate receptors and glutamate transporters defines distinct astrocyte populations in the mouse hippocampus. J Neurosci 23:1750-1758.2003).

Matus A, Mughal S (Immunohistochemical localisation of S-100 protein in brain. Nature 258:746-748.1975).

Matyash V, Kettenmann H (Heterogeneity in astrocyte morphology and physiology. Brain Res Rev.2009).

McKinnon RD, Piras G, Ida JA, Jr., Dubois-Dalcq M (A role for TGF-beta in oligodendrocyte differentiation. J Cell Biol 121:1397-1407.1993).

Meade CA, Deng YP, Fusco FR, Del Mar N, Hersch S, Goldowitz D, Reiner A (Cellular localization and development of neuronal intranuclear inclusions in striatal and cortical neurons in R6/2 transgenic mice. J Comp Neurol 449:241-269.2002).

Medrano S, Steward O (Differential mRNA localization in astroglial cells in culture. J Comp Neurol 430:56-71.2001).

Menalled LB (Knock-in mouse models of Huntington's disease. NeuroRx 2:465-470.2005).

Menalled LB, Chesselet MF (Mouse models of Huntington's disease. Trends Pharmacol Sci 23:32-39.2002).

Milnerwood AJ, Cummings DM, Dallerac GM, Brown JY, Vatsavayai SC, Hirst MC, Rezaie P, Murphy KP (Early development of aberrant synaptic plasticity in a mouse model of Huntington's disease. Hum Mol Genet 15:1690-1703.2006).

Mineva I, Gartner W, Hauser P, Kainz A, Loffler M, Wolf G, Oberbauer R, Weissel M, Wagner L (Differential expression of alphaB-crystallin and Hsp27-1 in anaplastic thyroid carcinomas because of tumor-specific alphaB-crystallin gene (CRYAB) silencing. Cell Stress Chaperones 10:171-184.2005).

Minton AP (The effect of volume occupancy upon the thermodynamic activity of proteins: some biochemical consequences. Mol Cell Biochem 55:119-140.1983).

Mitew S, Kirkcaldie MT, Halliday GM, Shepherd CE, Vickers JC, Dickson TC (Focal demyelination in Alzheimer's disease and transgenic mouse models. Acta Neuropathol.2010).

Mitteregger G, Vosko M, Krebs B, Xiang W, Kohlmannsperger V, Nolting S, Hamann GF, Kretzschmar HA (The role of the octarepeat region in neuroprotective function of the cellular prion protein. Brain Pathol 17:174-183.2007).

Mitton KP, Tumminia SJ, Arora J, Zelenka P, Epstein DL, Russell P (Transient loss of alphaB-crystallin: an early cellular response to mechanical stretch. Biochem Biophys Res Commun 235:69-73.1997).

Mogk A, Haslberger T, Tessarz P, Bukau B (Common and specific mechanisms of AAA+ proteins involved in protein quality control. Biochem Soc Trans 36:120-125.2008).

Mogk A, Mayer MP, Deuerling E (Mechanisms of protein folding: molecular chaperones and their application in biotechnology. Chembiochem 3:807-814.2002).

Moore GR, Laule C, Mackay A, Leung E, Li DK, Zhao G, Traboulsee AL, Paty DW (Dirty-appearing white matter in multiple sclerosis: preliminary observations of

myelin phospholipid and axonal loss. J Neurol 255:1802-1811, discussion 1812.2008).

Morange M (The protein side of the central dogma: permanence and change. Hist Philos Life Sci 28:513-524.2006).

Morell P, Greenfield S, Costantino-Ceccarini E, Wisniewski H (Changes in the protein composition of mouse brain myelin during development. J Neurochem 19:2545-2554.1972).

Morfini G, Pigino G, Brady ST (Polyglutamine expansion diseases: failing to deliver. Trends Mol Med 11:64-70.2005).

Morozov V, Wawrousek EF (Caspase-dependent secondary lens fiber cell disintegration in alphaA-/alphaB-crystallin double-knockout mice. Development 133:813-821.2006).

Morton AJ, Glynn D, Leavens W, Zheng Z, Faull RL, Skepper JN, Wight JM (Paradoxical delay in the onset of disease caused by super-long CAG repeat expansions in R6/2 mice. Neurobiol Dis 33:331-341.2009).

Morton AJ, Lagan MA, Skepper JN, Dunnett SB (Progressive formation of inclusions in the striatum and hippocampus of mice transgenic for the human Huntington's disease mutation. J Neurocytol 29:679-702.2000).

Morton AJ, Leavens W (Mice transgenic for the human Huntington's disease mutation have reduced sensitivity to kainic acid toxicity. Brain Res Bull 52:51-59.2000).

Moser M, Colello RJ, Pott U, Oesch B (Developmental expression of the prion protein gene in glial cells. Neuron 14:509-517.1995).

Muchowski PJ (Protein misfolding, amyloid formation, and neurodegeneration: a critical role for molecular chaperones? Neuron 35:9-12.2002).

Mucke L, Eddleston M (Astrocytes in infectious and immune-mediated diseases of the central nervous system. FASEB J 7:1226-1232.1993).

Murphy KP, Carter RJ, Lione LA, Mangiarini L, Mahal A, Bates GP, Dunnett SB, Morton AJ (Abnormal synaptic plasticity and impaired spatial cognition in mice transgenic for exon 1 of the human Huntington's disease mutation. J Neurosci 20:5115-5123.2000).

Nakagawa M, Tsujimoto N, Nakagawa H, Iwaki T, Fukumaki Y, Iwaki A (Association of HSPB2, a member of the small heat shock protein family, with mitochondria. Exp Cell Res 271:161-168.2001).

Nance MA, Myers RH (Juvenile onset Huntington's disease--clinical and research perspectives. Ment Retard Dev Disabil Res Rev 7:153-157.2001).

Napoli I, Neumann H (Microglial clearance function in health and disease. Neuroscience 158:1030-1038.2009).

Nelis E, Warner LE, Vriendt ED, Chance PF, Lupski JR, Van Broeckhoven C (Comparison of single-strand conformation polymorphism and heteroduplex analysis for detection of mutations in Charcot-Marie-Tooth type 1 disease and related peripheral neuropathies. Eur J Hum Genet 4:329-333.1996).

Neuwald AF, Aravind L, Spouge JL, Koonin EV (AAA+: A class of chaperone-like ATPases associated with the assembly, operation, and disassembly of protein complexes. Genome Res 9:27-43.1999).

Nicholl ID, Quinlan RA (Chaperone activity of alpha-crystallins modulates intermediate filament assembly. EMBO J 13:945-953.1994).

Nimmrich V, Ebert U (Is Alzheimer's disease a result of presynaptic failure? Synaptic dysfunctions induced by oligomeric beta-amyloid. Rev Neurosci 20:1-12.2009).

Niwa M, Hara A, Taguchi A, Aoki H, Kozawa O, Mori H (Spatiotemporal expression of Hsp20 and its phosphorylation in hippocampal CA1 pyramidal neurons after transient forebrain ischemia. Neurol Res 31:721-727.2009).

Nixdorf-Bergweiler BE, Albrecht D, Heinemann U (Developmental changes in the number, size, and orientation of GFAP-positive cells in the CA1 region of rat hippocampus. Glia 12:180-195.1994).

Nolte C, Matyash M, Pivneva T, Schipke CG, Ohlemeyer C, Hanisch UK, Kirchhoff F, Kettenmann H (GFAP promoter-controlled EGFP-expressing transgenic mice: a tool to visualize astrocytes and astrogliosis in living brain tissue. Glia 33:72-86.2001).

Norton WT, Poduslo SE (Myelination in rat brain: changes in myelin composition during brain maturation. J Neurochem 21:759-773.1973).

Nucifora FC, Jr., Sasaki M, Peters MF, Huang H, Cooper JK, Yamada M, Takahashi H, Tsuji S, Troncoso J, Dawson VL, Dawson TM, Ross CA (Interference by huntingtin and atrophin-1 with cbp-mediated transcription leading to cellular toxicity. Science 291:2423-2428.2001).

Oesch B, Westaway D, Walchli M, McKinley MP, Kent SB, Aebersold R, Barry RA, Tempst P, Teplow DB, Hood LE, et al. (A cellular gene encodes scrapie PrP 27-30 protein. Cell 40:735-746.1985).

Ohishi H, Neki A, Mizuno N (Distribution of a metabotropic glutamate receptor, mGluR2, in the central nervous system of the rat and mouse: an immunohistochemical study with a monoclonal antibody. Neurosci Res 30:65-82.1998).

Ohto-Fujita E, Fujita Y, Atomi Y (Analysis of the alphaB-crystallin domain responsible for inhibiting tubulin aggregation. Cell Stress Chaperones 12:163-171.2007).

Olafson RW, Drummond GI, Lee JF (Studies on 2',3'-cyclic nucleotide-3'-phosphohydrolase from brain. Can J Biochem 47:961-966.1969).

Omari KM, John GR, Sealfon SC, Raine CS (CXC chemokine receptors on human oligodendrocytes: implications for multiple sclerosis. Brain 128:1003-1015.2005).

Orth M, Schapira AH (Mitochondria and degenerative disorders. Am J Med Genet 106:27-36.2001).

Oshita SE, Chen F, Kwan T, Yehiely F, Cryns VL (The small heat shock protein HspB2 is a novel anti-apoptotic protein that inhibits apical caspase activation in the extrinsic apoptotic pathway. Breast Cancer Res Treat.2010).

Ostrow LW, Sachs F (Mechanosensation and endothelin in astrocytes--hypothetical roles in CNS pathophysiology. Brain Res Brain Res Rev 48:488-508.2005).

Ousman SS, Tomooka BH, van Noort JM, Wawrousek EF, O'Connor KC, Hafler DA, Sobel RA, Robinson WH, Steinman L (Protective and therapeutic role for alphaB-crystallin in autoimmune demyelination. Nature 448:474-479.2007).

Outeiro TF, Klucken J, Strathearn KE, Liu F, Nguyen P, Rochet JC, Hyman BT, McLean PJ (Small heat shock proteins protect against alpha-synuclein-induced toxicity and aggregation. Biochem Biophys Res Commun 351:631-638.2006).

Ouyang YB, Voloboueva LA, Xu LJ, Giffard RG (Selective dysfunction of hippocampal CA1 astrocytes contributes to delayed neuronal damage after transient forebrain ischemia. J Neurosci 27:4253-4260.2007).

Pamplona R, Naudi A, Gavin R, Pastrana MA, Sajnani G, Ilieva EV, Del Rio JA, Portero-Otin M, Ferrer I, Requena JR (Increased oxidation, glycoxidation, and lipoxidation of brain proteins in prion disease. Free Radic Biol Med 45:1159-1166.2008).

Pande VS, Rokhsar DS (Folding pathway of a lattice model for proteins. Proc Natl Acad Sci U S A 96:1273-1278.1999).

Patel PI, Roa BB, Welcher AA, Schoener-Scott R, Trask BJ, Pentao L, Snipes GJ, Garcia CA, Francke U, Shooter EM, Lupski JR, Suter U (The gene for the peripheral myelin protein PMP-22 is a candidate for Charcot-Marie-Tooth disease type 1A. Nat Genet 1:159-165.1992).

Pavel J, Lukacova N, Marsala J, Marsala M (The regional changes of the catalytic NOS activity in the spinal cord of the rabbit after repeated sublethal ischemia. Neurochem Res 26:833-839.2001).

Pehar M, Vargas MR, Cassina P, Barbeito AG, Beckman JS, Barbeito L (Complexity of astrocyte-motor neuron interactions in amyotrophic lateral sclerosis. Neurodegener Dis 2:139-146.2005).

Perea J, Robertson A, Tolmachova T, Muddle J, King RH, Ponsford S, Thomas PK, Huxley C (Induced myelination and demyelination in a conditional mouse model of Charcot-Marie-Tooth disease type 1A. Hum Mol Genet 10:1007-1018.2001).

Perng MD, Cairns L, van den IP, Prescott A, Hutcheson AM, Quinlan RA (Intermediate filament interactions can be altered by HSP27 and alphaB-crystallin. J Cell Sci 112 (Pt 13):2099-2112.1999).

Perry VH, Cunningham C, Boche D (Atypical inflammation in the central nervous system in prion disease. Curr Opin Neurol 15:349-354.2002).

Perutz MF, Johnson T, Suzuki M, Finch JT (Glutamine repeats as polar zippers: their possible role in inherited neurodegenerative diseases. Proc Natl Acad Sci U S A 91:5355-5358.1994).

Petersen A, Gil J, Maat-Schieman ML, Bjorkqvist M, Tanila H, Araujo IM, Smith R, Popovic N, Wierup N, Norlen P, Li JY, Roos RA, Sundler F, Mulder H, Brundin P (Orexin loss in Huntington's disease. Hum Mol Genet 14:39-47.2005).

Petersen A, Hansson O, Puschban Z, Sapp E, Romero N, Castilho RF, Sulzer D, Rice M, DiFiglia M, Przedborski S, Brundin P (Mice transgenic for exon 1 of the Huntington's disease gene display reduced striatal sensitivity to neurotoxicity induced by dopamine and 6-hydroxydopamine. Eur J Neurosci 14:1425-1435.2001).

Petersen C, Fuzesi L, Hoyer-Fender S (Outer dense fibre proteins from human sperm tail: molecular cloning and expression analyses of two cDNA transcripts encoding proteins of approximately 70 kDa. Mol Hum Reprod 5:627-635.1999).

Peterson J, Radke G, Takemoto L (Interaction of lens alpha and gamma crystallins during aging of the bovine lens. Exp Eye Res 81:680-689.2005).

Phillips GR, Huang JK, Wang Y, Tanaka H, Shapiro L, Zhang W, Shan WS, Arndt K, Frank M, Gordon RE, Gawinowicz MA, Zhao Y, Colman DR (The presynaptic particle web: ultrastructure, composition, dissolution, and reconstitution. Neuron 32:63-77.2001).

Piao CS, Kim SW, Kim JB, Lee JK (Co-induction of alphaB-crystallin and MAPKAPK-2 in astrocytes in the penumbra after transient focal cerebral ischemia. Exp Brain Res 163:421-429.2005).

Plumier JC, Hopkins DA, Robertson HA, Currie RW (Constitutive expression of the 27-kDa heat shock protein (Hsp27) in sensory and motor neurons of the rat nervous system. J Comp Neurol 384:409-428.1997).

Pocock JM, Kettenmann H (Neurotransmitter receptors on microglia. Trends Neurosci 30:527-535.2007).

Poliak S, Peles E (The local differentiation of myelinated axons at nodes of Ranvier. Nat Rev Neurosci 4:968-980.2003).

Pras E, Frydman M, Levy-Nissenbaum E, Bakhan T, Raz J, Assia EI, Goldman B (A nonsense mutation (W9X) in CRYAA causes autosomal recessive cataract in an inbred Jewish Persian family. Invest Ophthalmol Vis Sci 41:3511-3515.2000).

Preville X, Salvemini F, Giraud S, Chaufour S, Paul C, Stepien G, Ursini MV, Arrigo AP (Mammalian small stress proteins protect against oxidative stress through their ability to increase glucose-6-phosphate dehydrogenase activity and by maintaining optimal cellular detoxifying machinery. Exp Cell Res 247:61-78.1999).

Prusiner SB (Molecular biology of prion diseases. Science 252:1515-1522.1991).

Prusiner SB (Molecular biology and pathogenesis of prion diseases. Trends Biochem Sci 21:482-487.1996).

Prusiner SB (Prions. Proc Natl Acad Sci U S A 95:13363-13383.1998).

Prusiner SB, Bolton DC, Groth DF, Bowman KA, Cochran SP, McKinley MP (Further purification and characterization of scrapie prions. Biochemistry 21:6942-6950.1982).

Prusiner SB, Groth D, Serban A, Koehler R, Foster D, Torchia M, Burton D, Yang SL, DeArmond SJ (Ablation of the prion protein (PrP) gene in mice prevents scrapie and facilitates production of anti-PrP antibodies. Proc Natl Acad Sci U S A 90:10608-10612.1993).

Quraishe S, Asuni A, Boelens WC, O'Connor V, Wyttenbach A (Expression of the small heat shock protein family in the mouse CNS: differential anatomical and biochemical compartmentalization. Neuroscience 153:483-491.2008).

Rachidi W, Vilette D, Guiraud P, Arlotto M, Riondel J, Laude H, Lehmann S, Favier A (Expression of prion protein increases cellular copper binding and antioxidant enzyme activities but not copper delivery. J Biol Chem 278:9064-9072.2003).

Radford SE, Dobson CM (From computer simulations to human disease: emerging themes in protein folding. Cell 97:291-298.1999).

Raeber AJ, Race RE, Brandner S, Priola SA, Sailer A, Bessen RA, Mucke L, Manson J, Aguzzi A, Oldstone MB, Weissmann C, Chesebro B (Astrocyte-specific expression of hamster prion protein (PrP) renders PrP knockout mice susceptible to hamster scrapie. EMBO J 16:6057-6065.1997).

Raman B, Ban T, Sakai M, Pasta SY, Ramakrishna T, Naiki H, Goto Y, Rao Ch M (AlphaB-crystallin, a small heat-shock protein, prevents the amyloid fibril growth of an amyloid beta-peptide and beta2-microglobulin. Biochem J 392:573-581.2005).

Rangone H, Poizat G, Troncoso J, Ross CA, MacDonald ME, Saudou F, Humbert S (The serum- and glucocorticoid-induced kinase SGK inhibits mutant huntingtin-induced toxicity by phosphorylating serine 421 of huntingtin. Eur J Neurosci 19:273-279.2004).

Rasband MN, Tayler J, Kaga Y, Yang Y, Lappe-Siefke C, Nave KA, Bansal R (CNP is required for maintenance of axon-glia interactions at nodes of Ranvier in the CNS. Glia 50:86-90.2005).

Ravikumar B, Vacher C, Berger Z, Davies JE, Luo S, Oroz LG, Scaravilli F, Easton DF, Duden R, O'Kane CJ, Rubinsztein DC (Inhibition of mTOR induces autophagy and reduces toxicity of polyglutamine expansions in fly and mouse models of Huntington disease. Nat Genet 36:585-595.2004).

Reddy PH, Williams M, Charles V, Garrett L, Pike-Buchanan L, Whetsell WO, Jr., Miller G, Tagle DA (Behavioural abnormalities and selective neuronal loss in HD transgenic mice expressing mutated full-length HD cDNA. Nat Genet 20:198-202.1998).

Reichenbach A, Derouiche A, Kirchhoff F (Morphology and dynamics of perisynaptic glia. Brain Res Rev.2010).

Renkawek K, Bosman GJ, de Jong WW (Expression of small heat-shock protein hsp 27 in reactive gliosis in Alzheimer disease and other types of dementia. Acta Neuropathol 87:511-519.1994).

Renkawek K, de Jong WW, Merck KB, Frenken CW, van Workum FP, Bosman GJ (alpha B-crystallin is present in reactive glia in Creutzfeldt-Jakob disease. Acta Neuropathol 83:324-327.1992).

Renkawek K, Stege GJ, Bosman GJ (Dementia, gliosis and expression of the small heat shock proteins hsp27 and alpha B-crystallin in Parkinson's disease. Neuroreport 10:2273-2276.1999).

Rezaie P, Lantos PL (Microglia and the pathogenesis of spongiform encephalopathies. Brain Res Brain Res Rev 35:55-72.2001).

Riccio P, Giovannelli S, Bobba A, Romito E, Fasano A, Bleve-Zacheo T, Favilla R, Quagliariello E, Cavatorta P (Specificity of zinc binding to myelin basic protein. Neurochem Res 20:1107-1113.1995).

Richter-Landsberg C (The oligodendroglia cytoskeleton in health and disease. J Neurosci Res 59:11-18.2000).

Richter-Landsberg C, Goldbaum O (Stress proteins in neural cells: functional roles in health and disease. Cell Mol Life Sci 60:337-349.2003).

Rios JC, Melendez-Vasquez CV, Einheber S, Lustig M, Grumet M, Hemperly J, Peles E, Salzer JL (Contactin-associated protein (Caspr) and contactin form a complex that is targeted to the paranodal junctions during myelination. J Neurosci 20:8354-8364.2000).

Roelofs MF, Boelens WC, Joosten LA, Abdollahi-Roodsaz S, Geurts J, Wunderink LU, Schreurs BW, van den Berg WB, Radstake TR (Identification of small heat shock protein B8 (HSP22) as a novel TLR4 ligand and potential involvement in the pathogenesis of rheumatoid arthritis. J Immunol 176:7021-7027.2006).

Rogalla T, Ehrnsperger M, Preville X, Kotlyarov A, Lutsch G, Ducasse C, Paul C, Wieske M, Arrigo AP, Buchner J, Gaestel M (Regulation of Hsp27 oligomerization, chaperone function, and protective activity against oxidative stress/tumor necrosis factor alpha by phosphorylation. J Biol Chem 274:18947-18956.1999).

Rosas HD, Lee SY, Bender AC, Zaleta AK, Vangel M, Yu P, Fischl B, Pappu V, Onorato C, Cha JH, Salat DH, Hersch SM (Altered white matter microstructure in the

corpus callosum in Huntington's disease: implications for cortical "disconnection". Neuroimage 49:2995-3004.2010).

Rosas HD, Tuch DS, Hevelone ND, Zaleta AK, Vangel M, Hersch SM, Salat DH (Diffusion tensor imaging in presymptomatic and early Huntington's disease: Selective white matter pathology and its relationship to clinical measures. Mov Disord 21:1317-1325.2006).

Rossi D, Volterra A (Astrocytic dysfunction: insights on the role in neurodegeneration. Brain Res Bull 80:224-232.2009).

Rouse J, Cohen P, Trigon S, Morange M, Alonso-Llamazares A, Zamanillo D, Hunt T, Nebreda AR (A novel kinase cascade triggered by stress and heat shock that stimulates MAPKAP kinase-2 and phosphorylation of the small heat shock proteins. Cell 78:1027-1037.1994).

Rubinsztein DC (Lessons from animal models of Huntington's disease. Trends Genet 18:202-209.2002).

Rubinsztein DC (The roles of intracellular protein-degradation pathways in neurodegeneration. Nature 443:780-786.2006).

Rudiger S, Buchberger A, Bukau B (Interaction of Hsp70 chaperones with substrates. Nat Struct Biol 4:342-349.1997).

Rutherford S, Hirate Y, Swalla BJ (The Hsp90 capacitor, developmental remodeling, and evolution: the robustness of gene networks and the curious evolvability of metamorphosis. Crit Rev Biochem Mol Biol 42:355-372.2007).

Sabri MI, Bone AH, Davison AN (Turnover of myelin and other structural proteins in the developing rat brain. Biochem J 142:499-507.1974).

Saft C, Zange J, Andrich J, Muller K, Lindenberg K, Landwehrmeyer B, Vorgerd M, Kraus PH, Przuntek H, Schols L (Mitochondrial impairment in patients and asymptomatic mutation carriers of Huntington's disease. Mov Disord 20:674-679.2005).

Saibil H (Molecular chaperones: containers and surfaces for folding, stabilising or unfolding proteins. Curr Opin Struct Biol 10:251-258.2000).

Sailer A, Bueler H, Fischer M, Aguzzi A, Weissmann C (No propagation of prions in mice devoid of PrP. Cell 77:967-968.1994).

Sajjad MU, Samson B, Wyttenbach A (Heat Shock Proteins: Therapeutic Drug Targets for Chronic Neurodegeneration? Curr Pharm Biotechnol.2010).

Sakahira H, Breuer P, Hayer-Hartl MK, Hartl FU (Molecular chaperones as modulators of polyglutamine protein aggregation and toxicity. Proc Natl Acad Sci U S A 99 Suppl 4:16412-16418.2002).

Sakurai T, Fujita Y, Ohto E, Oguro A, Atomi Y (The decrease of the cytoskeleton tubulin follows the decrease of the associating molecular chaperone alphaB-crystallin in unloaded soleus muscle atrophy without stretch. FASEB J 19:1199-1201.2005).

Sanbe A, Yamauchi J, Miyamoto Y, Fujiwara Y, Murabe M, Tanoue A (Interruption of CryAB-amyloid oligomer formation by HSP22. J Biol Chem 282:555-563.2007).

Santhiya ST, Manisastry SM, Rawlley D, Malathi R, Anishetty S, Gopinath PM, Vijayalakshmi P, Namperumalsamy P, Adamski J, Graw J (Mutation analysis of congenital cataracts in Indian families: identification of SNPS and a new causative allele in CRYBB2 gene. Invest Ophthalmol Vis Sci 45:3599-3607.2004).

Sapp E, Kegel KB, Aronin N, Hashikawa T, Uchiyama Y, Tohyama K, Bhide PG, Vonsattel JP, DiFiglia M (Early and progressive accumulation of reactive microglia in the Huntington disease brain. J Neuropathol Exp Neurol 60:161-172.2001).

Sapp E, Schwarz C, Chase K, Bhide PG, Young AB, Penney J, Vonsattel JP, Aronin N, DiFiglia M (Huntingtin localization in brains of normal and Huntington's disease patients. Ann Neurol 42:604-612.1997).

Sasaki A, Hirato J, Nakazato Y (Immunohistochemical study of microglia in the Creutzfeldt-Jakob diseased brain. Acta Neuropathol 86:337-344.1993).

Sathasivam K, Hobbs C, Turmaine M, Mangiarini L, Mahal A, Bertaux F, Wanker EE, Doherty P, Davies SW, Bates GP (Formation of polyglutamine inclusions in non-CNS tissue. Hum Mol Genet 8:813-822.1999).

Savas JN, Makusky A, Ottosen S, Baillat D, Then F, Krainc D, Shiekhattar R, Markey SP, Tanese N (Huntington's disease protein contributes to RNA-mediated gene silencing through association with Argonaute and P bodies. Proc Natl Acad Sci U S A 105:10820-10825.2008).

Sawaishi Y (Review of Alexander disease: beyond the classical concept of leukodystrophy. Brain Dev 31:493-498.2009).

Schachner M, Bartsch U (Multiple functions of the myelin-associated glycoprotein MAG (siglec-4a) in formation and maintenance of myelin. Glia 29:154-165.2000).

Schaeren-Wiemers N, Valenzuela DM, Frank M, Schwab ME (Characterization of a rat gene, rMAL, encoding a protein with four hydrophobic domains in central and peripheral myelin. J Neurosci 15:5753-5764.1995).

Scherer SS, Arroyo EJ (Recent progress on the molecular organization of myelinated axons. J Peripher Nerv Syst 7:1-12.2002).

Schirmer EC, Glover JR, Singer MA, Lindquist S (HSP100/Clp proteins: a common mechanism explains diverse functions. Trends Biochem Sci 21:289-296.1996).

Schmidt-Kastner R, Freund TF (Selective vulnerability of the hippocampus in brain ischemia. Neuroscience 40:599-636.1991).

Schwab C, Klegeris A, McGeer PL (Inflammation in transgenic mouse models of neurodegenerative disorders. Biochim Biophys Acta.2009).

Schwarz L, Vollmer G, Richter-Landsberg C (The Small Heat Shock Protein HSP25/27 (HspB1) Is Abundant in Cultured Astrocytes and Associated with Astrocytic Pathology in Progressive Supranuclear Palsy and Corticobasal Degeneration. Int J Cell Biol 2010:717520.2010).

Selcen D, Engel AG (Myofibrillar myopathy caused by novel dominant negative alpha B-crystallin mutations. Ann Neurol 54:804-810.2003).

Selkoe DJ (Aging, amyloid, and Alzheimer's disease: a perspective in honor of Carl Cotman. Neurochem Res 28:1705-1713.2003).

Sghaier H, Le Ai TH, Horiike T, Shinozawa T (Molecular chaperones: proposal of a systematic computer-oriented nomenclature and construction of a centralized database. In Silico Biol 4:311-322.2004).

Shaner L, Sousa R, Morano KA (Characterization of Hsp70 binding and nucleotide exchange by the yeast Hsp110 chaperone Sse1. Biochemistry 45:15075-15084.2006).

Sharp PS, Akbar MT, Bouri S, Senda A, Joshi K, Chen HJ, Latchman DS, Wells DJ, de Belleroche J (Protective effects of heat shock protein 27 in a model of ALS occur in the early stages of disease progression. Neurobiol Dis 30:42-55.2008).

Shin JH, Kim SW, Lim CM, Jeong JY, Piao CS, Lee JK (alphaB-crystallin suppresses oxidative stress-induced astrocyte apoptosis by inhibiting caspase-3 activation. Neurosci Res 64:355-361.2009).

Shin JY, Fang ZH, Yu ZX, Wang CE, Li SH, Li XJ (Expression of mutant huntingtin in glial cells contributes to neuronal excitotoxicity. J Cell Biol 171:1001-1012.2005).

Siddique M, Gernhard S, von Koskull-Doring P, Vierling E, Scharf KD (The plant sHSP superfamily: five new members in Arabidopsis thaliana with unexpected properties. Cell Stress Chaperones 13:183-197.2008).

Sieradzan KA, Mann DM (The selective vulnerability of nerve cells in Huntington's disease. Neuropathol Appl Neurobiol 27:1-21.2001).

Simic G, Lucassen PJ, Krsnik Z, Kruslin B, Kostovic I, Winblad B, Bogdanovi (nNOS expression in reactive astrocytes correlates with increased cell death related DNA damage in the hippocampus and entorhinal cortex in Alzheimer's disease. Exp Neurol 165:12-26.2000).

Simmons DA, Casale M, Alcon B, Pham N, Narayan N, Lynch G (Ferritin accumulation in dystrophic microglia is an early event in the development of Huntington's disease. Glia 55:1074-1084.2007).

Simons M, Kramer EM, Thiele C, Stoffel W, Trotter J (Assembly of myelin by association of proteolipid protein with cholesterol- and galactosylceramide-rich membrane domains. J Cell Biol 151:143-154.2000).

Simons M, Trajkovic K (Neuron-glia communication in the control of oligodendrocyte function and myelin biogenesis. J Cell Sci 119:4381-4389.2006).

Sinadinos C, Burbidge-King T, Soh D, Thompson LM, Marsh JL, Wyttenbach A, Mudher AK (Live axonal transport disruption by mutant huntingtin fragments in Drosophila motor neuron axons. Neurobiol Dis 34:389-395.2009).

Singh BN, Rao KS, Ramakrishna T, Rangaraj N, Rao Ch M (Association of alphaB-crystallin, a small heat shock protein, with actin: role in modulating actin filament dynamics in vivo. J Mol Biol 366:756-767.2007).

Siskova Z, Baron W, de Vries H, Hoekstra D (Fibronectin impedes "myelin" sheet-directed flow in oligodendrocytes: a role for a beta 1 integrin-mediated PKC signaling pathway in vesicular trafficking. Mol Cell Neurosci 33:150-159.2006).

Siskova Z, Page A, O'Connor V, Perry VH (Degenerating synaptic boutons in prion disease: microglia activation without synaptic stripping. Am J Pathol 175:1610-1621.2009).

Siso S, Puig B, Varea R, Vidal E, Acin C, Prinz M, Montrasio F, Badiola J, Aguzzi A, Pumarola M, Ferrer I (Abnormal synaptic protein expression and cell death in murine scrapie. Acta Neuropathol 103:615-626.2002).

Sitia R, Braakman I (Quality control in the endoplasmic reticulum protein factory. Nature 426:891-894.2003).

Skinner PJ, Abbassi H, Chesebro B, Race RE, Reilly C, Haase AT (Gene expression alterations in brains of mice infected with three strains of scrapie. BMC Genomics 7:114.2006).

Sohal RS (Oxidative stress hypothesis of aging. Free Radic Biol Med 33:573-574.2002).

Somogyi P, Tamas G, Lujan R, Buhl EH (Salient features of synaptic organisation in the cerebral cortex. Brain Res Brain Res Rev 26:113-135.1998).

Spillantini MG, Schmidt ML, Lee VM, Trojanowski JQ, Jakes R, Goedert M (Alpha-synuclein in Lewy bodies. Nature 388:839-840.1997).

Spires TL, Orne JD, SantaCruz K, Pitstick R, Carlson GA, Ashe KH, Hyman BT (Region-specific dissociation of neuronal loss and neurofibrillary pathology in a mouse model of tauopathy. Am J Pathol 168:1598-1607.2006).

Sprinkle TJ (2',3'-cyclic nucleotide 3'-phosphodiesterase, an oligodendrocyte-Schwann cell and myelin-associated enzyme of the nervous system. Crit Rev Neurobiol 4:235-301.1989).

Stack EC, Kubilus JK, Smith K, Cormier K, Del Signore SJ, Guelin E, Ryu H, Hersch SM, Ferrante RJ (Chronology of behavioral symptoms and neuropathological sequela in R6/2 Huntington's disease transgenic mice. J Comp Neurol 490:354-370.2005).

Stamler R, Kappe G, Boelens W, Slingsby C (Wrapping the alpha-crystallin domain fold in a chaperone assembly. J Mol Biol 353:68-79.2005).

Steele AD, Lindquist S, Aguzzi A (The prion protein knockout mouse: a phenotype under challenge. Prion 1:83-93.2007).

Stefani M, Dobson CM (Protein aggregation and aggregate toxicity: new insights into protein folding, misfolding diseases and biological evolution. J Mol Med 81:678-699.2003).

Steffan JS, Agrawal N, Pallos J, Rockabrand E, Trotman LC, Slepko N, Illes K, Lukacsovich T, Zhu YZ, Cattaneo E, Pandolfi PP, Thompson LM, Marsh JL (SUMO modification of Huntingtin and Huntington's disease pathology. Science 304:100-104.2004).

Steffan JS, Kazantsev A, Spasic-Boskovic O, Greenwald M, Zhu YZ, Gohler H, Wanker EE, Bates GP, Housman DE, Thompson LM (The Huntington's disease protein interacts with p53 and CREB-binding protein and represses transcription. Proc Natl Acad Sci U S A 97:6763-6768.2000).

Stege GJ, Renkawek K, Overkamp PS, Verschuure P, van Rijk AF, Reijnen-Aalbers A, Boelens WC, Bosman GJ, de Jong WW (The molecular chaperone alphaB-crystallin enhances amyloid beta neurotoxicity. Biochem Biophys Res Commun 262:152-156.1999).

Steinman L (A molecular trio in relapse and remission in multiple sclerosis. Nat Rev Immunol 9:440-447.2009).

Stenoien DL, Cummings CJ, Adams HP, Mancini MG, Patel K, DeMartino GN, Marcelli M, Weigel NL, Mancini MA (Polyglutamine-expanded androgen receptors form aggregates that sequester heat shock proteins, proteasome components and SRC-1, and are suppressed by the HDJ-2 chaperone. Hum Mol Genet 8:731-741.1999).

Stetler RA, Cao G, Gao Y, Zhang F, Wang S, Weng Z, Vosler P, Zhang L, Signore A, Graham SH, Chen J (Hsp27 protects against ischemic brain injury via attenuation of a novel stress-response cascade upstream of mitochondrial cell death signaling. J Neurosci 28:13038-13055.2008).

Stetler RA, Gao Y, Signore AP, Cao G, Chen J (HSP27: mechanisms of cellular protection against neuronal injury. Curr Mol Med 9:863-872.2009).

Storey E, Beal MF (Neurochemical substrates of rigidity and chorea in Huntington's disease. Brain 116 (Pt 5):1201-1222.1993).

Streit WJ, Walter SA, Pennell NA (Reactive microgliosis. Prog Neurobiol 57:563-581.1999).

Stricker NH, Schweinsburg BC, Delano-Wood L, Wierenga CE, Bangen KJ, Haaland KY, Frank LR, Salmon DP, Bondi MW (Decreased white matter integrity in late-myelinating fiber pathways in Alzheimer's disease supports retrogenesis. Neuroimage 45:10-16.2009).

Sugars KL, Brown R, Cook LJ, Swartz J, Rubinsztein DC (Decreased cAMP response element-mediated transcription: an early event in exon 1 and full-length cell models of Huntington's disease that contributes to polyglutamine pathogenesis. J Biol Chem 279:4988-4999.2004).

Sugiyama Y, Suzuki A, Kishikawa M, Akutsu R, Hirose T, Waye MM, Tsui SK, Yoshida S, Ohno S (Muscle develops a specific form of small heat shock protein complex composed of MKBP/HSPB2 and HSPB3 during myogenic differentiation. J Biol Chem 275:1095-1104.2000).

Sui X, Li D, Qiu H, Gaussin V, Depre C (Activation of the bone morphogenetic protein receptor by H11kinase/Hsp22 promotes cardiac cell growth and survival. Circ Res 104:887-895.2009).

Summers DW, Douglas PM, Cyr DM (Prion propagation by Hsp40 molecular chaperones. Prion 3:59-64.2009).

Sun X, Fontaine JM, Rest JS, Shelden EA, Welsh MJ, Benndorf R (Interaction of human HSP22 (HSPB8) with other small heat shock proteins. J Biol Chem 279:2394-2402.2004).

Sun Y, MacRae TH (The small heat shock proteins and their role in human disease. FEBS J 272:2613-2627.2005a).

Sun Y, MacRae TH (Small heat shock proteins: molecular structure and chaperone function. Cell Mol Life Sci 62:2460-2476.2005b).

Sur R, Lyte PA, Southall MD (Hsp27 regulates pro-inflammatory mediator release in keratinocytes by modulating NF-kappaB signaling. J Invest Dermatol 128:1116-1122.2008).

Suter U, Snipes GJ (Peripheral myelin protein 22: facts and hypotheses. J Neurosci Res 40:145-151.1995).

Suzuki A, Sugiyama Y, Hayashi Y, Nyu-i N, Yoshida M, Nonaka I, Ishiura S, Arahata K, Ohno S (MKBP, a novel member of the small heat shock protein family, binds and activates the myotonic dystrophy protein kinase. J Cell Biol 140:1113-1124.1998).

Swamynathan SK, Piatigorsky J (Regulation of the mouse alphaB-crystallin and MKBP/HspB2 promoter activities by shared and gene specific intergenic elements: the importance of context dependency. Int J Dev Biol 51:689-700.2007).

Szebenyi G, Morfini GA, Babcock A, Gould M, Selkoe K, Stenoien DL, Young M, Faber PW, MacDonald ME, McPhaul MJ, Brady ST (Neuropathogenic forms of huntingtin and androgen receptor inhibit fast axonal transport. Neuron 40:41-52.2003).

Tagawa K, Marubuchi S, Qi ML, Enokido Y, Tamura T, Inagaki R, Murata M, Kanazawa I, Wanker EE, Okazawa H (The induction levels of heat shock protein 70 differentiate the vulnerabilities to mutant huntingtin among neuronal subtypes. J Neurosci 27:868-880.2007).

Tait S, Gunn-Moore F, Collinson JM, Huang J, Lubetzki C, Pedraza L, Sherman DL, Colman DR, Brophy PJ (An oligodendrocyte cell adhesion molecule at the site of assembly of the paranodal axo-glial junction. J Cell Biol 150:657-666.2000).

Takahashi T, Mihara H (Peptide and protein mimetics inhibiting amyloid beta-peptide aggregation. Acc Chem Res 41:1309-1318.2008).

Tallot P, Grongnet JF, David JC (Dual perinatal and developmental expression of the small heat shock proteins [FC12]aB-crystallin and Hsp27 in different tissues of the developing piglet. Biol Neonate 83:281-288.2003).

Tang B, Liu X, Zhao G, Luo W, Xia K, Pan Q, Cai F, Hu Z, Zhang C, Chen B, Zhang F, Shen L, Zhang R, Jiang H (Mutation analysis of the small heat shock protein 27 gene in chinese patients with Charcot-Marie-Tooth disease. Arch Neurol 62:1201-1207.2005a).

Tang BS, Zhao GH, Luo W, Xia K, Cai F, Pan Q, Zhang RX, Zhang FF, Liu XM, Chen B, Zhang C, Shen L, Jiang H, Long ZG, Dai HP (Small heat-shock protein 22 mutated in autosomal dominant Charcot-Marie-Tooth disease type 2L. Hum Genet 116:222-224.2005b).

Tang TS, Tu H, Orban PC, Chan EY, Hayden MR, Bezprozvanny I (HAP1 facilitates effects of mutant huntingtin on inositol 1,4,5-trisphosphate-induced Ca release in primary culture of striatal medium spiny neurons. Eur J Neurosci 20:1779-1787.2004).

Taylor DM, McConnell I, Fraser H (Scrapie infection can be established readily through skin scarification in immunocompetent but not immunodeficient mice. J Gen Virol 77 (Pt 7):1595-1599.1996).

Taylor JP, Hardy J, Fischbeck KH (Toxic proteins in neurodegenerative disease. Science 296:1991-1995.2002).

Taylor RP, Benjamin IJ (Small heat shock proteins: a new classification scheme in mammals. J Mol Cell Cardiol 38:433-444.2005).

Thackray AM, McKenzie AN, Klein MA, Lauder A, Bujdoso R (Accelerated prion disease in the absence of interleukin-10. J Virol 78:13697-13707.2004).

Theriault JR, Lambert H, Chavez-Zobel AT, Charest G, Lavigne P, Landry J (Essential role of the NH2-terminal WD/EPF motif in the phosphorylation-activated protective function of mammalian Hsp27. J Biol Chem 279:23463-23471.2004).

Thompson CL, Pathak SD, Jeromin A, Ng LL, MacPherson CR, Mortrud MT, Cusick A, Riley ZL, Sunkin SM, Bernard A, Puchalski RB, Gage FH, Jones AR, Bajic VB, Hawrylycz MJ, Lein ES (Genomic anatomy of the hippocampus. Neuron 60:1010-1021.2008).

Thorburne SK, Juurlink BH (Low glutathione and high iron govern the susceptibility of oligodendroglial precursors to oxidative stress. J Neurochem 67:1014-1022.1996).

Thulasiraman V, Yang CF, Frydman J (In vivo newly translated polypeptides are sequestered in a protected folding environment. EMBO J 18:85-95.1999).

Tobaben S, Thakur P, Fernandez-Chacon R, Sudhof TC, Rettig J, Stahl B (A trimeric protein complex functions as a synaptic chaperone machine. Neuron 31:987-999.2001).

Todd KJ, Serrano A, Lacaille JC, Robitaille R (Glial cells in synaptic plasticity. J Physiol Paris 99:75-83.2006).

Trajkovic K, Dhaunchak AS, Goncalves JT, Wenzel D, Schneider A, Bunt G, Nave KA, Simons M (Neuron to glia signaling triggers myelin membrane exocytosis from endosomal storage sites. J Cell Biol 172:937-948.2006).

Trapp BD, Andrews SB, Cootauco C, Quarles R (The myelin-associated glycoprotein is enriched in multivesicular bodies and periaxonal membranes of actively myelinating oligodendrocytes. J Cell Biol 109:2417-2426.1989).

Trapp BD, Bernier L, Andrews SB, Colman DR (Cellular and subcellular distribution of 2',3'-cyclic nucleotide 3'-phosphodiesterase and its mRNA in the rat central nervous system. J Neurochem 51:859-868.1988).

Trapp BD, Moench T, Pulley M, Barbosa E, Tennekoon G, Griffin J (Spatial segregation of mRNA encoding myelin-specific proteins. Proc Natl Acad Sci U S A 84:7773-7777.1987).

Truant R, Atwal RS, Burtnik A (Nucleocytoplasmic trafficking and transcription effects of huntingtin in Huntington's disease. Prog Neurobiol 83:211-227.2007).

Tsai HF, Lin SJ, Li C, Hsieh M (Decreased expression of Hsp27 and Hsp70 in transformed lymphoblastoid cells from patients with spinocerebellar ataxia type 7. Biochem Biophys Res Commun 334:1279-1286.2005).

Tsang D, Tsang YS, Ho WK, Wong RN (Myelin basic protein is a zinc-binding protein in brain: possible role in myelin compaction. Neurochem Res 22:811-819.1997).

Turmaine M, Raza A, Mahal A, Mangiarini L, Bates GP, Davies SW (Nonapoptotic neurodegeneration in a transgenic mouse model of Huntington's disease. Proc Natl Acad Sci U S A 97:8093-8097.2000).

Tydlacka S, Wang CE, Wang X, Li S, Li XJ (Differential activities of the ubiquitin-proteasome system in neurons versus glia may account for the preferential accumulation of misfolded proteins in neurons. J Neurosci 28:13285-13295.2008).

Unterberger U, Voigtlander T, Budka H (Pathogenesis of prion diseases. Acta Neuropathol 109:32-48.2005).

Valencia A, Reeves PB, Sapp E, Li X, Alexander J, Kegel KB, Chase K, Aronin N, DiFiglia M (Mutant huntingtin and glycogen synthase kinase 3-beta accumulate in neuronal lipid rafts of a presymptomatic knock-in mouse model of Huntington's disease. J Neurosci Res 88:179-190.2010).

Valko M, Leibfritz D, Moncol J, Cronin MT, Mazur M, Telser J (Free radicals and antioxidants in normal physiological functions and human disease. Int J Biochem Cell Biol 39:44-84.2007).

van de Klundert FA, Smulders RH, Gijsen ML, Lindner RA, Jaenicke R, Carver JA, de Jong WW (The mammalian small heat-shock protein Hsp20 forms dimers and is a poor chaperone. Eur J Biochem 258:1014-1021.1998).

van den IP, Wheelock R, Prescott A, Russell P, Quinlan RA (Nuclear speckle localisation of the small heat shock protein alpha B-crystallin and its inhibition by the R120G cardiomyopathy-linked mutation. Exp Cell Res 287:249-261.2003).

van der Burg JM, Bacos K, Wood NI, Lindqvist A, Wierup N, Woodman B, Wamsteeker JI, Smith R, Deierborg T, Kuhar MJ, Bates GP, Mulder H, Erlanson-Albertsson C, Morton AJ, Brundin P, Petersen A, Bjorkqvist M (Increased metabolism in the R6/2 mouse model of Huntington's disease. Neurobiol Dis 29:41-51.2008).

van der Knaap MS, Naidu S, Breiter SN, Blaser S, Stroink H, Springer S, Begeer JC, van Coster R, Barth PG, Thomas NH, Valk J, Powers JM (Alexander disease: diagnosis with MR imaging. AJNR Am J Neuroradiol 22:541-552.2001).

van Groen T, Miettinen P, Kadish I (The entorhinal cortex of the mouse: organization of the projection to the hippocampal formation. Hippocampus 13:133-149.2003).

Van Montfort R, Slingsby C, Vierling E (Structure and function of the small heat shock protein/alpha-crystallin family of molecular chaperones. Adv Protein Chem 59:105-156.2001).

van Noort JM (Stress proteins in CNS inflammation. J Pathol 214:267-275.2008).

van Noort JM, van Sechel AC, Bajramovic JJ, el Ouagmiri M, Polman CH, Lassmann H, Ravid R (The small heat-shock protein alpha B-crystallin as candidate autoantigen in multiple sclerosis. Nature 375:798-801.1995).

Vargas MR, Pehar M, Cassina P, Martinez-Palma L, Thompson JA, Beckman JS, Barbeito L (Fibroblast growth factor-1 induces heme oxygenase-1 via nuclear factor erythroid 2-related factor 2 (Nrf2) in spinal cord astrocytes: consequences for motor neuron survival. J Biol Chem 280:25571-25579.2005).

Verschuure P, Croes Y, van den IPR, Quinlan RA, de Jong WW, Boelens WC (Translocation of small heat shock proteins to the actin cytoskeleton upon proteasomal inhibition. J Mol Cell Cardiol 34:117-128.2002).

Verschuure P, Tatard C, Boelens WC, Grongnet JF, David JC (Expression of small heat shock proteins HspB2, HspB8, Hsp20 and cvHsp in different tissues of the perinatal developing pig. Eur J Cell Biol 82:523-530.2003).

Vicart P, Caron A, Guicheney P, Li Z, Prevost MC, Faure A, Chateau D, Chapon F, Tome F, Dupret JM, Paulin D, Fardeau M (A missense mutation in the alphaB-crystallin chaperone gene causes a desmin-related myopathy. Nat Genet 20:92-95.1998).

Vinet J, Lemieux P, Tamburri A, Tiesinga P, Scafidi J, Gallo V, Sik A (Subclasses of oligodendrocytes populate the mouse hippocampus. Eur J Neurosci 31:425-438.2010).

Volker C, Lupas AN (Molecular evolution of proteasomes. Curr Top Microbiol Immunol 268:1-22.2002).

Volkov RA, Panchuk, II, Mullineaux PM, Schoffl F (Heat stress-induced H(2)O (2) is required for effective expression of heat shock genes in Arabidopsis. Plant Mol Biol 61:733-746.2006).

Vonsattel JP, Myers RH, Stevens TJ, Ferrante RJ, Bird ED, Richardson EP, Jr. (Neuropathological classification of Huntington's disease. J Neuropathol Exp Neurol 44:559-577.1985).

Wacker JL, Huang SY, Steele AD, Aron R, Lotz GP, Nguyen Q, Giorgini F, Roberson ED, Lindquist S, Masliah E, Muchowski PJ (Loss of Hsp70 exacerbates pathogenesis but not levels of fibrillar aggregates in a mouse model of Huntington's disease. J Neurosci 29:9104-9114.2009).

Wacker JL, Zareie MH, Fong H, Sarikaya M, Muchowski PJ (Hsp70 and Hsp40 attenuate formation of spherical and annular polyglutamine oligomers by partitioning monomer. Nat Struct Mol Biol 11:1215-1222.2004).

Wade A, Jacobs P, Morton AJ (Atrophy and degeneration in sciatic nerve of presymptomatic mice carrying the Huntington's disease mutation. Brain Res 1188:61-68.2008).

Waelter S, Boeddrich A, Lurz R, Scherzinger E, Lueder G, Lehrach H, Wanker EE (Accumulation of mutant huntingtin fragments in aggresome-like inclusion bodies as a result of insufficient protein degradation. Mol Biol Cell 12:1393-1407.2001).

Walker FO (Huntington's disease. Lancet 369:218-228.2007).

Walling HW, Baldassare JJ, Westfall TC (Molecular aspects of Huntington's disease. J Neurosci Res 54:301-308.1998).

Wallraff A, Odermatt B, Willecke K, Steinhauser C (Distinct types of astroglial cells in the hippocampus differ in gap junction coupling. Glia 48:36-43.2004).

Walsh DM, Klyubin I, Fadeeva JV, Cullen WK, Anwyl R, Wolfe MS, Rowan MJ, Selkoe DJ (Naturally secreted oligomers of amyloid beta protein potently inhibit hippocampal long-term potentiation in vivo. Nature 416:535-539.2002).

Walsh DT, Betmouni S, Perry VH (Absence of detectable IL-1beta production in murine prion disease: a model of chronic neurodegeneration. J Neuropathol Exp Neurol 60:173-182.2001).

Walz R, Amaral OB, Rockenbach IC, Roesler R, Izquierdo I, Cavalheiro EA, Martins VR, Brentani RR (Increased sensitivity to seizures in mice lacking cellular prion protein. Epilepsia 40:1679-1682.1999).

Wang CE, Tydlacka S, Orr AL, Yang SH, Graham RK, Hayden MR, Li S, Chan AW, Li XJ (Accumulation of N-terminal mutant huntingtin in mouse and monkey models implicated as a pathogenic mechanism in Huntington's disease. Hum Mol Genet 17:2738-2751.2008).

Wang J, Song JJ, Franklin MC, Kamtekar S, Im YJ, Rho SH, Seong IS, Lee CS, Chung CH, Eom SH (Crystal structures of the HslVU peptidase-ATPase complex reveal an ATP-dependent proteolysis mechanism. Structure 9:177-184.2001).

Wang X, Klevitsky R, Huang W, Glasford J, Li F, Robbins J (AlphaB-crystallin modulates protein aggregation of abnormal desmin. Circ Res 93:998-1005.2003).

Warrick JM, Paulson HL, Gray-Board GL, Bui QT, Fischbeck KH, Pittman RN, Bonini NM (Expanded polyglutamine protein forms nuclear inclusions and causes neural degeneration in Drosophila. Cell 93:939-949.1998).

Waters ER, Rioflorido I (Evolutionary analysis of the small heat shock proteins in five complete algal genomes. J Mol Evol 65:162-174.2007).

Waxman SG, Ritchie JM (Molecular dissection of the myelinated axon. Ann Neurol 33:121-136.1993).

Wen FC, Li YH, Tsai HF, Lin CH, Li C, Liu CS, Lii CK, Nukina N, Hsieh M (Down-regulation of heat shock protein 27 in neuronal cells and non-neuronal cells expressing mutant ataxin-3. FEBS Lett 546:307-314.2003).

West MJ, Kawas CH, Martin LJ, Troncoso JC (The CA1 region of the human hippocampus is a hot spot in Alzheimer's disease. Ann N Y Acad Sci 908:255-259.2000).

Wheeler DL, Barrett T, Benson DA, Bryant SH, Canese K, Chetvernin V, Church DM, Dicuccio M, Edgar R, Federhen S, Feolo M, Geer LY, Helmberg W, Kapustin Y, Khovayko O, Landsman D, Lipman DJ, Madden TL, Maglott DR, Miller V, Ostell J, Pruitt KD, Schuler GD, Shumway M, Sequeira E, Sherry ST, Sirotkin K, Souvorov A, Starchenko G, Tatusov RL, Tatusova TA, Wagner L, Yaschenko E (Database resources of the National Center for Biotechnology Information. Nucleic Acids Res 36:D13-21.2008).

White AR, Collins SJ, Maher F, Jobling MF, Stewart LR, Thyer JM, Beyreuther K, Masters CL, Cappai R (Prion protein-deficient neurons reveal lower glutathione reductase activity and increased susceptibility to hydrogen peroxide toxicity. Am J Pathol 155:1723-1730.1999).

Whitley D, Goldberg SP, Jordan WD (Heat shock proteins: a review of the molecular chaperones. J Vasc Surg 29:748-751.1999).

Wilhelmus MM, Boelens WC, Otte-Holler I, Kamps B, de Waal RM, Verbeek MM (Small heat shock proteins inhibit amyloid-beta protein aggregation and cerebrovascular amyloid-beta protein toxicity. Brain Res 1089:67-78.2006a).

Wilhelmus MM, Boelens WC, Otte-Holler I, Kamps B, Kusters B, Maat-Schieman ML, de Waal RM, Verbeek MM (Small heat shock protein HspB8: its distribution in Alzheimer's disease brains and its inhibition of amyloid-beta protein aggregation and cerebrovascular amyloid-beta toxicity. Acta Neuropathol 111:139-149.2006b).

Wilhelmus MM, Otte-Holler I, Wesseling P, de Waal RM, Boelens WC, Verbeek MM (Specific association of small heat shock proteins with the pathological hallmarks of Alzheimer's disease brains. Neuropathol Appl Neurobiol 32:119-130.2006c).

Williams AE, Lawson LJ, Perry VH, Fraser H (Characterization of the microglial response in murine scrapie. Neuropathol Appl Neurobiol 20:47-55.1994).

Williams KL, Rahimtula M, Mearow KM (Hsp27 and axonal growth in adult sensory neurons in vitro. BMC Neurosci 6:24.2005).

Willis D, Li KW, Zheng JQ, Chang JH, Smit A, Kelly T, Merianda TT, Sylvester J, van Minnen J, Twiss JL (Differential transport and local translation of cytoskeletal, injury-response, and neurodegeneration protein mRNAs in axons. J Neurosci 25:778-791.2005).

Wittmann CW, Wszolek MF, Shulman JM, Salvaterra PM, Lewis J, Hutton M, Feany MB (Tauopathy in Drosophila: neurodegeneration without neurofibrillary tangles. Science 293:711-714.2001).

Wood JD, MacMillan JC, Harper PS, Lowenstein PR, Jones AL (Partial characterisation of murine huntingtin and apparent variations in the subcellular localisation of huntingtin in human, mouse and rat brain. Hum Mol Genet 5:481-487.1996).

Wyttenbach A, Carmichael J, Swartz J, Furlong RA, Narain Y, Rankin J, Rubinsztein DC (Effects of heat shock, heat shock protein 40 (HDJ-2), and proteasome inhibition on protein aggregation in cellular models of Huntington's disease. Proc Natl Acad Sci U S A 97:2898-2903.2000).

Wyttenbach A, Sauvageot O, Carmichael J, Diaz-Latoud C, Arrigo AP, Rubinsztein DC (Heat shock protein 27 prevents cellular polyglutamine toxicity and suppresses the increase of reactive oxygen species caused by huntingtin. Hum Mol Genet 11:1137-1151.2002).

Wyttenbach A, Swartz J, Kita H, Thykjaer T, Carmichael J, Bradley J, Brown R, Maxwell M, Schapira A, Orntoft TF, Kato K, Rubinsztein DC (Polyglutamine expansions cause decreased CRE-mediated transcription and early gene expression changes prior to cell death in an inducible cell model of Huntington's disease. Hum Mol Genet 10:1829-1845.2001).

Xi JH, Bai F, McGaha R, Andley UP (Alpha-crystallin expression affects microtubule assembly and prevents their aggregation. FASEB J 20:846-857.2006).

Yamamoto Y, Mizuno R, Nishimura T, Ogawa Y, Yoshikawa H, Fujimura H, Adachi E, Kishimoto T, Yanagihara T, Sakoda S (Cloning and expression of myelin-associated oligodendrocytic basic protein. A novel basic protein constituting the central nervous system myelin. J Biol Chem 269:31725-31730.1994).

Yamamoto Y, Yoshikawa H, Nagano S, Kondoh G, Sadahiro S, Gotow T, Yanagihara T, Sakoda S (Myelin-associated oligodendrocytic basic protein is essential for normal arrangement of the radial component in central nervous system myelin. Eur J Neurosci 11:847-855.1999).

Yan H, Hui Y ([The recent progress on the role of alpha-crystallin as a molecular chaperone in cataractogenesis]. Yan Ke Xue Bao 16:91-96.2000).

Yang SH, Cheng PH, Banta H, Piotrowska-Nitsche K, Yang JJ, Cheng EC, Snyder B, Larkin K, Liu J, Orkin J, Fang ZH, Smith Y, Bachevalier J, Zola SM, Li SH, Li XJ, Chan AW (Towards a transgenic model of Huntington's disease in a non-human primate. Nature 453:921-924.2008).

Yang Y, Cvekl A (Tissue-specific regulation of the mouse alphaA-crystallin gene in lens via recruitment of Pax6 and c-Maf to its promoter. J Mol Biol 351:453-469.2005).

Yaung J, Jin M, Barron E, Spee C, Wawrousek EF, Kannan R, Hinton DR (alpha-Crystallin distribution in retinal pigment epithelium and effect of gene knockouts on sensitivity to oxidative stress. Mol Vis 13:566-577.2007).

Yin X, Peterson J, Gravel M, Braun PE, Trapp BD (CNP overexpression induces aberrant oligodendrocyte membranes and inhibits MBP accumulation and myelin compaction. J Neurosci Res 50:238-247.1997).

Yorimitsu T, Klionsky DJ (Autophagy: molecular machinery for self-eating. Cell Death Differ 12 Suppl 2:1542-1552.2005).

Young JC, Moarefi I, Hartl FU (Hsp90: a specialized but essential protein-folding tool. J Cell Biol 154:267-273.2001).

Yu LM, Goda Y (Dendritic signalling and homeostatic adaptation. Curr Opin Neurobiol 19:327-335.2009).

Yu ZX, Li SH, Nguyen HP, Li XJ (Huntingtin inclusions do not deplete polyglutamine-containing transcription factors in HD mice. Hum Mol Genet 11:905-914.2002).

Zala D, Colin E, Rangone H, Liot G, Humbert S, Saudou F (Phosphorylation of mutant huntingtin at S421 restores anterograde and retrograde transport in neurons. Hum Mol Genet 17:3837-3846.2008).

Zhang K, Sejnowski TJ (A universal scaling law between gray matter and white matter of cerebral cortex. Proc Natl Acad Sci U S A 97:5621-5626.2000).

Zhou D, Li P, Lin Y, Lott JM, Hislop AD, Canaday DH, Brutkiewicz RR, Blum JS (Lamp-2a facilitates MHC class II presentation of cytoplasmic antigens. Immunity 22:571-581.2005).

Zigmond SH (Signal transduction and actin filament organization. Curr Opin Cell Biol 8:66-73.1996).

Zourlidou A, Gidalevitz T, Kristiansen M, Landles C, Woodman B, Wells DJ, Latchman DS, de Belleroche J, Tabrizi SJ, Morimoto RI, Bates GP (Hsp27 overexpression in the R6/2 mouse model of Huntington's disease: chronic neurodegeneration does not induce Hsp27 activation. Hum Mol Genet 16:1078-1090.2007).

Zucker B, Luthi-Carter R, Kama JA, Dunah AW, Stern EA, Fox JH, Standaert DG, Young AB, Augood SJ (Transcriptional dysregulation in striatal projection- and

interneurons in a mouse model of Huntington's disease: neuronal selectivity and potential neuroprotective role of HAP1. Hum Mol Genet 14:179-189.2005).

Zwickl P, Seemuller E, Kapelari B, Baumeister W (The proteasome: a supramolecular assembly designed for controlled proteolysis. Adv Protein Chem 59:187-222.2001).